UNIVERSIDAD NACIONAL AUTÓNOMA DE MÉXICO

POSGRADO EN CIENCIAS FÍSICAS

MULTIQUARK SYSTEMS WITH HEAVY QUARKS

TESIS

QUE PARA OPTAR POR EL GRADO DE :

DOCTOR EN CIENCIAS (FÍSICA)

PRESENTA:

M. EN C. EMMANUEL ORTIZ PACHECO

TUTOR PRINCIPAL
DR. ROELOF BIJKER BIJKER
INSTITUTO DE CIENCIAS NUCLEARES, UNAM

COMITÉ TUTOR
DR. CÉSAR FERNÁNDEZ RAMÍREZ
INSTITUTO DE CIENCIAS NUCLEARES, UNAM

DRA. MYRIAM MONDRAGÓN CEBALLOS
INSTITUTO DE FÍSICA, UNAM

CIUDAD DE MÉXICO, ABRIL 2021

Abstract

In this work a study of the qqQ baryons and $qqqQ\bar{Q}$ pentaquarks is presented, where q represents the light quarks and Q the heavy quarks:

In the first part, a study of the strong and radiative decays for singly heavy baryons, in the deformed quark model, is presented. The treatment is for both, the S- and P-wave states. In particular, for the electromagnetic case one can focus on the two independent decays widths $\Sigma_Q^{*+}(uuQ) \to \Sigma_Q(uuQ)+\gamma$ and $\Lambda_Q^*(udQ) \to \Lambda_Q(udQ)+\gamma$, the generalization to the rest is obtained immediately by flavor symmetry properties. On the other hand, the strong decay widths are calculated by means of the Elementary-Meson Emission Model, where each of the contributions owing to individual isospin channels are also obtained. The results of both types of processes are reported and compared with the current experimental data and with other works.

In the second part, a classification of ground and one orbital excited states for the hidden charm pentaquark with total angular momentum $J^P = 3/2^-$ is made, and for configurations with flavor content $uudc\bar{c}$. From a large number of states, 5 for ground states and 19 for radially excited states, it is found that only 3 can contribute to the photoproduction of pentaquarks. Finally in order to obtain their decay widths , whose current interest is relevant for confirmation in new experiments, the orbital contribution to the photoproduction of these pentaquark states is calculated. The analysis is through two approximations: the harmonic oscillator and the hyper-Coulomb potentials. At the end, the photoproduction channel $p(uud) + \gamma \to P_c(uudc\bar{c})$ is found to be highly suppressed, either in ground or excited pentaquark states, and calculated with both the harmonic oscillator and the hypercentral models.

Resumen

En este trabajo se presenta un estudio de qqQ bariones y $qqqQ\bar{Q}$ pentaquarks donde q representa los quarks ligeros y Q los quarks pesados:

En la primera parte, se presenta un estudio de los decaimientos electromagnéticos y fuertes de bariones con un quark pesado, en el modelo de quarks deformado. El tratamiento es tanto para los estados de onda S como P. En particular, para el caso electromagnético uno puede enfocarse en dos decaimientos independientes $\Sigma_Q^{*+}(uuQ) \to \Sigma_Q(uuQ) + \gamma$ y $\Lambda_Q^*(udQ) \to \Lambda_Q(udQ) + \gamma$, donde la generalización al resto se obtiene directamente debido a las propiedades de simetría de sabor. Por otro lado, se calculan las anchuras de decaimientos fuertes por medio del Elementary-Meson Emission Model, donde también se obtienen cada una de las contribuciones debidas a los canales individuales de isoespín permitidas por las reglas de selección. Se reportan los resultados de ambos tipos de procesos y se comparan tanto con los datos experimentales como con otros trabajos actuales.

En la segunda parte, se muestra una clasificación de los estados base y estados con un cuanto de excitación orbital de los pentaquarks, con momento angular total $J^P = 3/2^-$ y contenido de sabor $uudc\bar{c}$. Se encuentra que, de un gran número de estados, 5 para estados base y 19 para estados radialmente excitados, sólo 3 de estos pueden contribuir a la fotoproducción del pentaquark. Finalmente, con el fin de obtener las anchuras de decaimiento de la fotoproducción de los estados pentaquark, cuyo interés es relevante para la confirmación en nuevos experimentos, se calcula la contribución orbital de este proceso. Para este fin se utilizan dos aproximaciones: un potencial tipo oscilador armónico y un hiperpotencial tipo Coulomb. Se encuentra que el canal de fotoproducción del pentauquark $p(uud) + \gamma \to P_c(uudc\bar{c})$ está altamente suprimido, ya sea en los estados base o excitados y calculado con ambos modelos, el del oscilador armónico y el hipercentral.

Contents

Introduction

In the quark model hadrons are described as composite particles consisting of quarks and antiquarks. The minimal quark content is a quark-antiquark pair for mesons and a three-quark configuration for baryons. In the original version of the quark model there were three possible quark flavors, up, down and strange, together called the light quarks. Later, evidence was found for the existence of three other quark flavors, charm, bottom and top, called the heavy quarks. In recent years, the LHCb, Belle, BaBar and BESIII collaborations have discovered a large amount of new hadrons with heavy quark flavors. The LHCb Collaboration has announced the observation of new baryon resonances, particularly singly charm and singly bottom baryons. For example, in 2019 LHCb reported the observation of new ground states $\Sigma_b^{\pm}$ with spin-parity $J^P = 1/2^+$ and $\Sigma_b^{*\pm}$ with $3/2^+$ as well as the resonance $\Sigma_b(6097)^{\pm}$, all were found in the $\Lambda_b^0\pi^{\pm}$ channels using pp collision data [1]. For the case of the $\Xi_{c/b}$ and $\Xi'_{c/b}$ baryons there has been a lot of information provided not only by LHCb, but also by Belle and BaBar. For the charm sector, the following resonances have been well established: $\Xi_c(2645)$, $\Xi_c(2790)$, $\Xi_c(2815)$, $\Xi_c(2930)$, $\Xi_c(2970)$, $\Xi_c(3055)$, $\Xi_c(3080)$ and $\Xi_c(3123)$. There are further resonances just discovered by LHCb, the new single charm resonances $\Xi_c^0(2923)$ and $\Xi_c^0(2939)$ observed in the channel $\Lambda_c^+K^-$ [2]. Not to forget the bottom sector, where since 2015 LHCb observed $\Xi_b^-(5935)$ and $\Xi_b^-(5955)$ resonances close to the threshold $\Xi_b\pi$ [3], and the resonances Ξ_b and Ξ_b^* [4, 5]. The resonance $\Xi_b^0(5945)$ was reported decaying to $\Xi_b\pi$ [6], while $\Xi_b^-(6227)$ was observed in 2018 in both Λ_bK and $\Xi_b\pi$ channels [7]. Additional to these long list of heavy baryons, in 2017 the LHCb Collaboration found, the following five narrow states $\Omega_c(3000), \Omega_c(3050), \Omega_c(3066), \Omega_c(3090)$ and $\Omega_c(3117)$ in the $\Xi_c^+K^-$ decay channel [8, 9]. Very recently the knowledge of Ω_b has been expanded with the discovery of more resonances, because the LHCb collaboration reported 4 signals in $\Omega_b(6316)$, $\Omega_b(6330)$, $\Omega_b(6340)$ and $\Omega_b(6350)$ in the $\Xi_b^0K^-$ mass spectrum [10].

In 2015, for the first time. LHCb observed two signals in the $J/\psi\, p$ channel of the $\Lambda_b^0 \to J/\psi\, p\, K^-$ decay, consistent with a charmonium-pentaquark state with minimal quark content $uudc\bar{c}$ [11, 12]. The measured masses of these resonances were $4380\pm8\pm29$ MeV and $4449.8\pm1.7\pm2.5$ MeV, and the pentaquarks were denoted as $P_c(4380)$ and $P_c(4450)$, respectively. The preferred assignments J^P were suggested with opposite parity, and with one state having spin $3/2$, while the other $5/2$. More recently, in 2019 with more data and statistics the LHCb collaboration discovered a new narrow pentaquark state $P_c(4312)^+$, with a mass of $4311.9 \pm 0.7^{+6.8}_{-0.6}$ MeV [13] and in the same channel than previously observed. Additionally, they confirmed not only the pentaquark signal $P_c(4450)^+$, but also it was observed to consist of two narrow peaks $P_c(4440)^+$ with a mass of $4440.3\pm1.3^{+4.1}_{-4.7}$ MeV and $P_c(4457)^+$ with $4457.3 \pm 0.6^{+4.1}_{-1.7}$ MeV. Currently, there are several interpretations trying to provide an explanation for all these detected signals. Some works find them to be kinematical effects [14], or anomalous triangle singularities [15]. Others interpret them as molecular states [16, 17, 18, 19, 20], and others, like the present, guide their study with compact five quark states [21, 22, 23, 24, 25]. One of the main motivations to carry out an analysis of these pentaquark states $qqqc\bar{c}$ is precisely to identify the multiplet to which they belong, in order to be able to describe their decay widths and thus obtain a direct connection to the experiment. There is not just theoretical work to interpret and comprehend the pentaquark signals, but also experimental efforts trying to confirm them. The GlueX experiment located in Hall D at Jefferson Lab has had, as one of its main purposes, the search and confirmation of the announced pentaquark states by LHCb, through electron scattering experiments based on J/ψ photoproduction [26, 27, 28, 29, 30]. In 2019, The GlueX Collaboration published the first results of the collected data by 2016 and 2017, where in the conclusions of their

analysis they did not see evidence, to date, of the pentaquark signals by this mechanism [31].

The aim of this thesis is to present a study of the heavy baryons and pentaquarks in the framework of the quark model, in particular, masses, electromagnetic and strong decays widths. This thesis is organized as follows: In Chapter 1, the Constituent Quark Model is reviewed focusing on the baryons with flavor content u, d and s. Later, in Chapter 2 an extension to four flavors, u, d, s and Q is presented, where Q represents, either charm c, or bottom b heavy quarks. Within this classification, the deformed quark model is introduced in which we distinguish the light from the heavy quarks masses, in order to construct the S- and P-wave states of all singly heavy baryons. Through a mass rule which takes into account spin-orbit, isospin and flavor dependent contributions, the mass spectra are derived. In Chapters 3 and 4, the strong and electromagnetic couplings of baryons are discussed, in order to obtain the corresponding decay widths. At the end of this chapter, all the results are presented and discussed, where they are also compared with other works. In Chapter 5, the orbital, spin, color and flavor wave functions of the pentaquarks are obtained based on the permutation symmetry under the three light quarks and distinguishing the charm and the anti-charm from the other flavors. In addition, a classification of the pentaquarks is derived for the ground-state and the one orbital excited states. Once constructed all the pentaquark wave functions, then is discussed in Chapter 6 the photoproduction of the hidden-charm pentaquarks by a pair annihilation process, not only for the color-spin-flavor matrix elements, but also the orbital contribution to the photoproduction of pentaquark as a form factor that contains all the information of the orbital part. In Chapters 7 and 8, this orbital part is calculated in terms of two approximations: with an harmonic oscillator and a hyper-Coulomb potentials. The results are presented and discussed at the end of the chapter. I present the summary and the main conclusions of the complete work in Chapter 9. The technical details about reductions in the calculations along the work, as well as the non-relativistic limit and some useful formulas are provided in the Appendices. Finally, at the end of this text three articles are added, two of which were already published in The Journal of Physics G: Nuclear and Particle Physics [32] and The European Physical Journal C [33]. The last article was already sent to be considered for publication in Physical Review D [34]. The first work includes the analysis and classification of the hidden-charm pentaquark from the ground state as $qqqq\bar{q}$ configurations, where the mass spectrum and the magnetic moments of these pentaquarks are also calculated. The second focuses on the identification and classification of the Ω_c baryons discovered by the LHCb [8], as well as the the strong decay widths. At the end of this work are presented some predictions for the Ω_b states that later were confirmed from the LHCb Collaboration [10]. The last paper contains new information in the spectrum and strong decay widths for the recently detected $\Xi_{c/b}$ and $\Xi'_{c/b}$ baryons states.

Chapter 1

qqq Baryons

1.1 Quark Model

Hadrons are systems of strongly interacting particles corresponding to bound states of quarks and gluon fields. The multiquark systems depend on the internal degrees of freedom like color, flavor and spin, as well as the spatial degrees of freedom due to relative motion of the constituent quarks. In particular, baryons are fermions with baryon number $\mathcal{B} = 1$. In the most general case, they are composed of three quarks. (i) *The color part of their states functions is an* $SU(3)$ *singlet, a completely antisymmetric state of three colors.* (ii) *Since quarks are fermions, the total wave function must be antisymmetric under interchange of any two equal-mass quarks.* These two principles provide the necessary elements to classify multiquark states.

It is important to emphasize the fact that the only three flavors considered in this section are u, d and s. Besides spin $S = \frac{1}{2}$ for each flavor, we have other internal degrees of freedom. They are the three colors r, g and b. The algebraic structure of the constituent states of quarks will be formed by the spin-flavor (sf) and color (c) groups

$$\mathcal{G}_{sfc} = SU_{sf}(6) \otimes SU_c(3), \tag{1.1}$$

where $SU_{sf}(6)$ represents the group of unitary transformations for spin and flavor as coupled states, and group $SU_c(3)$ the unitary transformations among the three colors. The spin-flavor algebra can be divided into groups

$$SU_{sf}(6) \supset SU_f(3) \otimes SU_s(2). \tag{1.2}$$

In the same way we can decompose the flavor algebra as

$$SU_f(3) \supset SU_I(2) \otimes U_Y(1), \tag{1.3}$$

with label I denoting the isospin and Y the hypercharge of quarks. These quantum numbers can be expressed in terms of the charge Q of quarks, through the Gell-Mann–Nishijima relation,

$$\mathsf{Q} = I_3 + \frac{Y}{2} = I_3 + \frac{\mathcal{B} + \mathcal{S}}{2}, \tag{1.4}$$

where the hypercharge is defined as the sum of baryon number $\mathcal{B}$ plus the strangeness $\mathcal{S}$ of quarks and I_3 denotes the projection of isospin I,

$$Y \equiv \mathcal{B} + \mathcal{S}. \tag{1.5}$$

In Table 1.1, I present the quantum numbers of quarks and antiquarks. Quarks have baryon number $\mathcal{B} = \frac{1}{3}$, spin $S = \frac{1}{2}$ and positive parity, whereas antiquarks have $\mathcal{B} = -\frac{1}{3}$, $S = \frac{1}{2}$ and negative parity.

The technique of Young diagrams is very useful to classify multiquark states.

Table 1.1: Quantum numbers of quarks and antiquarks. Here, S denotes spin, $\mathcal{S}$ strangeness, I isospin and I_3 isospin projection.

	$\mathcal{B}$	S^P	I	I_3	$\mathcal{S}$	Y	Q
u	$\frac{1}{3}$	$\frac{1}{2}^+$	$\frac{1}{2}$	$\frac{1}{2}$	0	$\frac{1}{3}$	$\frac{2}{3}$
d	$\frac{1}{3}$	$\frac{1}{2}^+$	$\frac{1}{2}$	$-\frac{1}{2}$	0	$\frac{1}{3}$	$-\frac{1}{3}$
s	$\frac{1}{3}$	$\frac{1}{2}^+$	0	0	-1	$-\frac{2}{3}$	$-\frac{1}{3}$
$\bar{u}$	$-\frac{1}{3}$	$\frac{1}{2}^-$	$\frac{1}{2}$	$-\frac{1}{2}$	0	$-\frac{1}{3}$	$-\frac{2}{3}$
$\bar{d}$	$-\frac{1}{3}$	$\frac{1}{2}^-$	$\frac{1}{2}$	$\frac{1}{2}$	0	$-\frac{1}{3}$	$\frac{1}{3}$
$\bar{s}$	$-\frac{1}{3}$	$\frac{1}{2}^-$	0	0	1	$\frac{2}{3}$	$\frac{1}{3}$

Young Diagrams

Making use of the Young diagrams technique and the multiplet labels of $SU(n)$, it is possible to:

1. Construct the allowed representations of $SU(n)$ for the multiquark system with $n = 2$, 3 and 6 degrees of freedom for the spin, flavor (or color) and spin-flavor respectively. That is, determine the structure of the complete multiplet.

2. Identify and label the particle multiplets of $SU(n)$.

3. Find the number of particles of a multiplet by its label.

The $U(n)$ Young tableaux is labeled by a string of numbers $[f_1, f_2, ..., f_n]$ with the restriction that $f_1 \geq f_2 \geq ... \geq f_n$, where f_i denotes the number of the i-th row. Under $SU(n)$ the Young tableau $[f_1 f_2, ..., f_n]$ is equivalent to $[f_1 - f_n, f_2 - f_n, ..., f_1 - f_n]$, *i.e.*, there is one label less in this representation. Quarks transform as the fundamental representation [1] under $SU(n)$. However, antiquarks transform according to the conjugate representation $[1^{n-1}]$ under $SU(n)$. As a result, the three quarks belong to a flavor triplet [1] of $SU_f(3)$, and the three antiquarks to an flavor anti-triplet [11].

Labels of *SU(3)* multiplets

Usually, multiplets are identified by their dimension, but in general this classification is not unique. For example, quarks and antiquarks have the same dimension. For the particular case of $SU(3)$ we have the labels (λ, μ), which are related to the Young diagrams by $(\lambda, \mu) = (f_1 - f_2, f_2 - f_3)$. The dimension of a given representation can be calculated in a closed formula, for this case $dim_{(\lambda,\mu)} = (\lambda + 1)(\mu + 1)(\lambda + \mu + 2)/2$. This shows that the quarks belong to $(\lambda, \mu) = (1, 0)$ with dimension $dim_{(1,0)} = 3$, and the antiquarks to $(\lambda, \mu) = (0, 1)$ with dimension $dim_{(0,1)} = 3$ each with three flavors outlined in the plane weight diagram $I_3 - Y$ as can be seen in Table 1.1 and Fig. 1.1. Consequently, it is better to introduce this notation to identify states.

The spin of quarks and antiquarks is determined by the representation $[f_1, f_2] \equiv [f_1 - f_2]$ of $SU_s(2)$

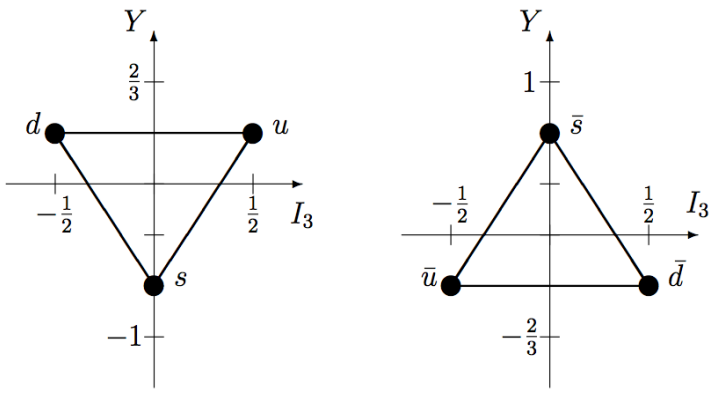

Fig. 1.1: Triplet of quarks with $[1] \equiv (\lambda, \mu) = (1, 0)$ and the antiquarks $[11] \equiv (\lambda, \mu) = (0, 1)$

as $S = \frac{f_1 - f_2}{2}$. The spin-flavor classification of a single quark and antiquark is given by

$$\begin{array}{lccccc} & SU_{sf}(6) & \supset & SU_f(3) & \otimes & SU_s(2) \\ quark & [1] & \supset & [1] & \otimes & [1] \\ & \square & \supset & \square & \otimes & \square \\ antiquark & [11111] & \supset & [11] & \otimes & [1] \\ & \begin{array}{c}\square\\\square\\\square\\\square\\\square\end{array} & \supset & \begin{array}{c}\square\\\square\end{array} & \otimes & \square\,. \end{array} \tag{1.6}$$

1.1.1 Multiquark States

The restriction that physical states are color singlets, makes quarks or anti-quarks grouped into multiplets with states of only three quarks (q^3 baryons), or quark antiquark pairs (mesons $q\bar{q}$), or products of these. That is, individual quark states do not exist in isolation. In general, the multiquark configurations can be expressed as

$$q^{3m+n}\bar{q}^{3k+n} \ , \tag{1.7}$$

which can be reduced to qqq *baryons* for $m = 1$ and $k = n = 0$, or we can obtain $\bar{q}\bar{q}\bar{q}$ anti-baryons for $m = n = 0$, $k = 1$, and $q\bar{q}$ mesons for $m = k = 0$ y $n = 1$. Moreover, we can have tetraquark states $qq\bar{q}\bar{q}$ with $n = 2$, $m = k = 0$, and *pentaquarks states* $qqqq\bar{q}$ with $m = n = 1$ and $k = 0$.

1.1.2 Baryon states in $SU(3)$ with flavors u, d, s.

Baryons are configurations of three quarks $qqq \equiv q^3$ which interact with each other through gluonic exchange. The color part of its wave function is a color singlet state of $SU(3)$. Since quarks are fermions their wave function must be completely antisymmetric under exchange of any two quarks

Table 1.2: Baryon states of color, flavor and spin-flavor allowed

	q^3	*Dimension*
color	[111]	singlet
spin	[3]	4
	[21]	2
flavor	[3]	decuplet
	[21]	octet
	[111]	singlet
spin-flavor	[3]	56
	[21]	70
	[111]	20

of equal masses (u and d in the limit of isospin symmetry). In general spin, flavor and spin-flavor states for a system with q^3 are obtained by taking the product

$$[1] \otimes [1] \otimes [1] = [3] \oplus 2\,[21] \oplus [111] \tag{1.8}$$

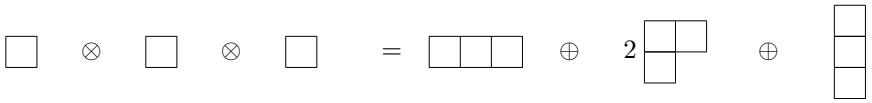

The symmetry of permutation for q^3 system is characterized then by Young diagram [3] (symmetric), [21] (mixed symmetry) and [111] (antisymmetric). In flavor space, these representations are usually denoted by their dimensions, as **10** (decuplet), **8** (octet) and **1** (singlet), respectively.
The total angular momentum of baryon is given by the coupling of spins, since we do not consider relative orbital angular momentum. Because the representation of $SU(2)$ can have at most two rows, this means that the spin of the three quarks can have at least two values $S = \frac{f_1 - f_2}{2} = \frac{3}{2}$ which corresponds to the Young diagram [3], or $S = \frac{1}{2}$ from the Young tableaux [21]. In this case the antisymmetric representation [111] does not occur. The dimension of spin is given by $2S + 1$, and the color, spin, flavor and spin-flavor states are listed in the Table 1.2.

The spin and flavor content for each multiplet of spin-flavor is given by decomposition of $SU_{sf}(6)$ representations into $SU_f(3) \otimes SU_s(2)$ according to the Young diagrams technique

$$SU_{sf}(6) \supset SU_f(3) \otimes SU_s(2)$$

$$\begin{aligned} [56] &\supset {}^2 8 \oplus {}^4 10, \\ [70] &\supset {}^2 8 \oplus {}^4 8 \oplus {}^2 10 \oplus {}^2 1, \\ [20] &\supset {}^2 8 \oplus {}^4 1, \end{aligned}$$

where the superscript index denotes $2S + 1$. For example, the symmetric representation [56] contains a flavor octet with $S = \frac{1}{2}$ characterized by $(\lambda, \mu) = (1, 1)$, and a flavor decuplet with $S = \frac{3}{2}$ by $(\lambda, \mu) = (3, 0)$. In the absence of orbital excitations the parity of the qqq baryons is positive $P(qqq) = (+)(+)(+)(-)^l = +$.

In Table 1.3 the flavor classification of the octet and the decuplet are presented, in terms of isospin I and hypercharge Y according to the decomposition of flavor symmetry $SU_f(3)$ in $SU_I(2) \otimes U_Y(1)$. Nucleon and Delta are non strange baryons with strangeness $\mathcal{S} = 0$, while the hyperons Σ, Λ, Ξ

Table 1.3: Baryon classification of ground state according to $SU_f(3) \supset SU_I(2) \otimes U_Y(1)$

			I	Y	Q
$J^P = \frac{1}{2}^+ octet$	Nucleon	N	$\frac{1}{2}$	1	0,1
	Sigma	Σ	1	0	-1,0,1
	Lambda	Λ	0	0	0
	Xi	Ξ	$\frac{1}{2}$	-1	-1,0
$J^P = \frac{3}{2}^+ decuplet$	Delta	Δ	$\frac{3}{2}$	1	-1,0,1,2
	Sigma	Σ^*	1	0	-1,0,1
	Xi	Ξ^*	$\frac{1}{2}$	-1	-1,0
	Omega	Ω	0	-2	-1

and Ω carry strangeness $\mathcal{S} = -1, -1, -2$ y -3, respectively. The flavor singlet [111] corresponds to an electromagnetic orbitally excited baryon Λ which has isospin $I = 0$ and hypercharge $Y = 0$ (strangeness $\mathcal{S} = -1$).

The weight diagram of the octet and decuplet can be seen in the Fig. 1.2. The generators of three-flavor $SU(3)$ quark model are given in terms of 8 Gell-Mann 3×3 λ matrices, where these matrices are traceless $Tr(\lambda_a) = 0$ and hermitian [35]. The 8 generators of $SU(3)$ can be divided into two weight operators

$$\begin{aligned} \hat{I}_3 &= \frac{1}{2}\lambda_3 = \frac{1}{2}(u^\dagger u - d^\dagger d) \\ \hat{Y} &= \frac{1}{\sqrt{3}}\lambda_8 = \frac{1}{2}(u^\dagger u + d^\dagger d - 2s^\dagger s), \end{aligned} \tag{1.9}$$

and also three raising and three lowering operators

$$\begin{aligned} I_+ &= \frac{1}{2}(\lambda_1 + i\lambda_2) = u^\dagger d & I_- &= \frac{1}{2}(\lambda_1 - i\lambda_2) = d^\dagger u \\ U_+ &= \frac{1}{2}(\lambda_6 + i\lambda_7) = d^\dagger s & U_- &= \frac{1}{2}(\lambda_1 - i\lambda_2) = s^\dagger d \\ V_+ &= \frac{1}{2}(\lambda_4 + i\lambda_5) = u^\dagger s & V_- &= \frac{1}{2}(\lambda_1 - i\lambda_2) = s^\dagger u. \end{aligned} \tag{1.10}$$

The step operators connect different states within a $SU(3)$ flavor multiplet, on the other hand, the weight operators gives the eigenvalues of isospin and hypercharge.

1.2 The wave functions of three-flavor baryons

The complete wave function for baryons can be obtained under the two principles with which the chapter was started, *i.e.*, since the three quarks should satisfy the Pauli exclusion principle, the total wave function must be *antisymmetric* under any permutation of three quarks. On the other hand, physical states are scalars in color space, which means that the color part is an *antisymmetric* $SU(3)$ singlet

$$\psi = \psi^{\mathrm{o}}\phi^{\mathrm{f}}\chi^{\mathrm{s}}\psi^{\mathrm{c}}, \tag{1.11}$$

The last condition implies that spin-flavor and orbital parts must have the same symmetry; the options for both are symmetric, mixed symmetry, or antisymmetric. Since we are not considering orbital excitations (in particular just baryons in the ground state), the orbital wave function ψ^{o} is *symmetric*, and therefore the spin-flavor part has to be *symmetric* too.

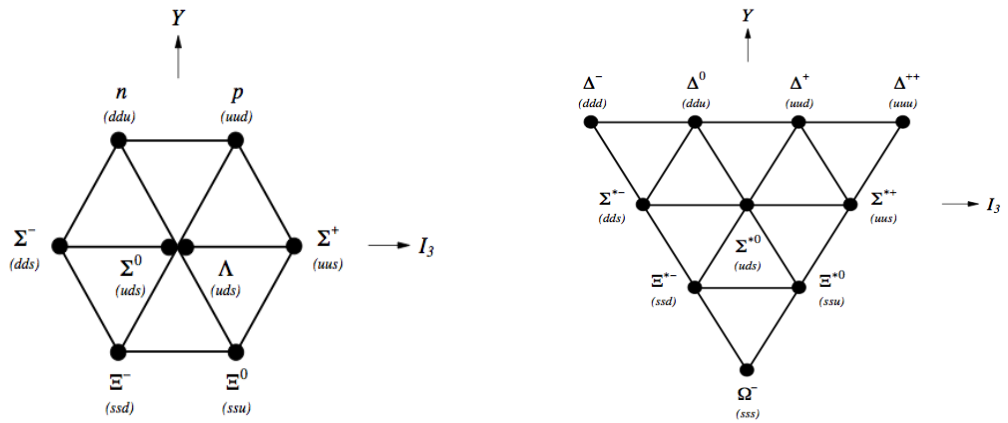

(a) (b)

Fig. 1.2: Baryon octet $J^P = \frac{1}{2}^+$ and baryon decuplet $J^P = \frac{3}{2}^+$

1.2.1 Color wave function

The basic properties defining this degree of freedom are:

1. Any quark u, d, s,... can exist in three different color states, which are called r, g and b, and of course these labels are associated with to 'red', 'green' and 'blue', respectively.

2. Each one of those states are characterized by two conserved *color charges*, I_3^C and Y^C, which are similar to electric charge in the electromagnetic case. These charges depend only on the states of color r, g, b and not on the flavors $u, d, s, ...$

3. only states with zero value for color charges are observables like free particles, and they are called *color singlets*. This property is known as *color confinement*.

Now, since the wave function of **color singlet** should be antisymmetric, the only combination for the three degrees of freedom is

$$|\psi^c\rangle = \frac{1}{\sqrt{6}}|rgb - grb + brg - rbg + gbr - bgr\rangle, \tag{1.12}$$

and it has the six possible combinations of colors r, g and b.

1.2.2 Orbital wave function

In order to understand the structure of orbital wave function, the relative motion between the three quarks is taken into account. This dynamics is studied through the quark harmonic oscillator model, that proposes a Hamiltonian responsible for confinement of three effective quarks 1, 2 and 3 taken with equal masses ($m_1 = m_2 = m_3$)

$$H = \frac{{p_1}^2}{2m} + \frac{{p_2}^2}{2m} + \frac{{p_3}^2}{2m} + \frac{1}{2}C\sum_{i<j}^{3}|\vec{r_i} - \vec{r_j}|^2, \tag{1.13}$$

where it is assumed that the interaction comes from a harmonic oscillator potential. The case with unequal quark masses will be discussed in Section 2.

The analytical solutions for the eigenstates are well known, and to get them it is customary to use a change of coordinates in order to decouple the Hamiltonian into several oscillators. This work is carried out by the Jacobi coordinates, which are defined for equal masses as

$$\begin{cases} \vec{\rho} \equiv \frac{1}{\sqrt{2}}(\vec{r_1} - \vec{r_2}) \\ \vec{\lambda} \equiv \frac{1}{\sqrt{6}}(\vec{r_1} + \vec{r_2} - 2\vec{r_3}) \\ \vec{R} \equiv \frac{1}{3}(\vec{r_1} + \vec{r_2} + \vec{r_3}) \end{cases} \Rightarrow \begin{cases} \vec{r_1} = \vec{R} + \frac{1}{\sqrt{2}}\vec{\rho} + \frac{1}{\sqrt{6}}\vec{\lambda} \\ \vec{r_2} = \vec{R} - \frac{1}{\sqrt{2}}\vec{\rho} + \frac{1}{\sqrt{6}}\vec{\lambda} \\ \vec{r_3} = \vec{R} - \sqrt{\frac{2}{3}}\vec{\lambda}, \end{cases} \tag{1.14}$$

where the Jacobian corresponding to this change of coordinates into Cartesian ones, turns out to be

$$\prod_{i=1}^{3} d^3 r_i = 3\sqrt{3} d^3\rho d^3\lambda d^3 R. \tag{1.15}$$

With these new coordinates the Hamiltonian can be rewritten as

$$H = \frac{{P_{CM}}^2}{2M} + \frac{{p_\rho}^2}{2m_\rho} + \frac{{p_\lambda}^2}{2m_\lambda} + \frac{3}{2}C\rho^2 + \frac{3}{2}C\lambda^2, \tag{1.16}$$

so that this Hamiltonian now includes the center of mass motion with $M = 3m$, plus two harmonic oscillators ρ and λ with the same spring constant C and the same effective mass $m_\rho = m_\lambda = m$. In this case since all three quarks have the same mass, both oscillators have the same frequency, hence this system is degenerate. The associated momenta to these coordinates are

$$\vec{P} = M\frac{d\vec{R}}{dt}, \qquad \vec{p_\rho} = m_\rho \frac{d\vec{\rho}}{dt}, \qquad \vec{p_\lambda} = m_\lambda \frac{d\vec{\lambda}}{dt}, \tag{1.17}$$

or in form of coordinated system is

$$\begin{cases} \vec{p_\rho} = \frac{1}{\sqrt{2}}(\vec{p_1} - \vec{p_2}), \\ \vec{p_\lambda} = \frac{1}{\sqrt{6}}(\vec{p_1} + \vec{p_2} - 2\vec{p_3}), \\ \vec{P} = \vec{p_1} + \vec{p_2} + \vec{p_3} \end{cases} \Rightarrow \begin{cases} \vec{p_1} = \frac{1}{3}\vec{P} + \frac{1}{\sqrt{2}}\vec{p}_\rho + \frac{1}{\sqrt{6}}\vec{p}_\lambda \\ \vec{p_2} = \frac{1}{3}\vec{P} - \frac{1}{\sqrt{2}}\vec{p}_\rho + \frac{1}{\sqrt{6}}\vec{p}_\lambda \\ \vec{p_3} = \frac{1}{3}\vec{P} - \sqrt{\frac{2}{3}}\vec{p_\lambda}, \end{cases}$$

and in analogy to the cartesian coordinates here we have the Jacobian

$$\prod_{i=1}^{3} d^3 p_i = \frac{1}{3\sqrt{3}} d^3 p_\rho d^3 p_\lambda d^3 P. \tag{1.18}$$

With the above change of coordinates, the orbital baryon wave function $\psi_B^o(\vec{r}_1, \vec{r}_2, \vec{r}_3)$ is given by

$$\psi_B^o(\vec{r}_1, \vec{r}_2, \vec{r}_3) = \frac{1}{(2\pi)^{3/2}} e^{\vec{P}_{CM}\cdot\vec{R}} \psi^{rel}(\vec{\rho}, \vec{\lambda}), \tag{1.19}$$

where the relative wave functions are expressed in terms of coupled harmonic oscillator wave functions, as

$$\psi^{rel}(\vec{\rho}, \vec{\lambda}) = \frac{1}{\sqrt{3\sqrt{3}}} \sum_{m_\rho m_\lambda} \langle l_\rho m_\rho l_\lambda m_\lambda | LM\rangle \psi_{n_\rho l_\rho m_\rho}(\vec{\rho}) \psi_{n_\lambda l_\lambda m_\lambda}(\vec{\lambda}). \tag{1.20}$$

All things considered, **the ground state** for the relative motion in coordinate space is given by

$$\psi_0^{rel}(\vec{\rho}, \vec{\lambda}) = \frac{1}{\sqrt{3\sqrt{3}}} \frac{\alpha^3}{\pi^{\frac{3}{2}}} e^{-\alpha^2(\rho^2+\lambda^2)/2}, \tag{1.21}$$

while for states with one quantum of radial excitation in the λ-mode and ρ-mode, one has

$$\psi_{\lambda}^{rel}(\vec{\rho},\vec{\lambda}) = \frac{1}{\sqrt{3\sqrt{3}}}\frac{\alpha^{3/2}}{\pi^{\frac{3}{4}}}e^{-\alpha^2\rho^2/2}\sqrt{\frac{8}{3\sqrt{\pi}}}\lambda\alpha^{5/2}e^{-\alpha^2\lambda^2/2}Y_{1,m_{l_\lambda}}(\hat{\lambda}), \tag{1.22}$$

and

$$\psi_{\rho}^{rel}(\vec{\rho},\vec{\lambda}) = \frac{1}{\sqrt{3\sqrt{3}}}\frac{\alpha^{3/2}}{\pi^{\frac{3}{4}}}e^{-\alpha^2\lambda^2/2}\sqrt{\frac{8}{3\sqrt{\pi}}}\rho\alpha^{5/2}e^{-\alpha^2\rho^2/2}Y_{1,m_{l_\rho}}(\hat{\rho}), \tag{1.23}$$

respectively. The above expressions are given in terms of the spherical harmonics, and also with the harmonic oscillator constant and frequency

$$\alpha^2 = (3Cm)^{\frac{1}{2}}, \qquad \omega = \sqrt{\frac{3C}{m}}. \tag{1.24}$$

Making a Fourier transform it is easy to obtain the wave function in momentum space, for example, for the ground state one obtain

$$\psi_{B}^{rel}(\vec{p_\rho},\vec{p_\lambda}) = \sqrt{3\sqrt{3}}\frac{1}{\pi^{\frac{3}{2}}\alpha^3}e^{-(p_\rho^2+p_\lambda^2)/2\alpha^2}. \tag{1.25}$$

1.2.3 Spin wave function

In this section the spin wave functions for baryon configurations are obtained. For this purpose let us start considering just **one quark**. The spin wave function in the notation $|[f],S,M_S\rangle$ is given for the representation [1] of Young tableaux. The only two states associated with the spin are:

$$|[1],1/2,1/2\rangle = |\uparrow\rangle \qquad \text{and} \qquad |[1],1/2,-1/2\rangle = |\downarrow\rangle. \tag{1.26}$$

The allowed spin wave function for **two quarks** are given by the Young tableaux: [2] for $S=1$ (symmetric), and [11] for $S=0$ (antisymmetric). The spin is given by a closed formula $S=(f_1-f_2)/2$. Hence the states associated with this configuration are

$$|[2],1,1\rangle = |\uparrow\uparrow\rangle \qquad \text{and} \qquad |[11],0,0\rangle = \frac{1}{\sqrt{2}}(|\uparrow\downarrow\rangle - |\downarrow\uparrow\rangle). \tag{1.27}$$

If we use the spin ladder operator for two particles $S_- = S_{1-} + S_{2-}$ over the state $|[2],1,1\rangle$, we can get the remaining projections:

$$|[2],1,0\rangle = \frac{1}{\sqrt{2}}(|\uparrow\downarrow\rangle + |\downarrow\uparrow\rangle) \qquad \text{and} \qquad |[2],1,-1\rangle = |\downarrow\downarrow\rangle. \tag{1.28}$$

In the same way, for **three quarks** the spin wave functions are given by the following Young tableaux: [3] for $S=3/2$, and [21] for $S=1/2$. The explicit relations can be obtained by coupling the third quark to the basis of the first two quarks, and adding the respective Clebsh Gordan coefficient

$$|(S_{12},S_3)SM_S\rangle = \sum_{M_{12},M_3}\langle S_{12}M_{12},S_3M_3|S,M_S\rangle|S_{12}M_{12}\rangle|S_3M_3\rangle. \tag{1.29}$$

In this way, the totally symmetric A_1 wave function is

$$|[3],3/2,3/2\rangle_{A_1} = |(1,1/2)3/2,3/2\rangle = \langle 1,1,1/2,1/2|3/2,3/2\rangle|[2]1,1\rangle|[1]1/2,1/2\rangle = |\uparrow\uparrow\uparrow\rangle, \tag{1.30}$$

for the states with symmetry E_λ and E_ρ we have

$$\begin{aligned}|[21],1/2,1/2\rangle_{E_\lambda} &= |(1,1/2)1/2,1/2\rangle = \langle 1,0,1/2,1/2|1/2,1/2\rangle|[2]1,0\rangle|[1]1/2,1/2\rangle + \\ &\quad \langle 1,1,1/2,-1/2|1/2,1/2\rangle|[2]1,1\rangle|[1]1/2,-1/2\rangle \\ &= -\frac{1}{\sqrt{6}}(|\uparrow\downarrow\uparrow\rangle + |\downarrow\uparrow\uparrow\rangle) + \sqrt{\frac{2}{3}}|\uparrow\uparrow\downarrow\rangle = \frac{1}{\sqrt{6}}(2|\uparrow\uparrow\downarrow\rangle - |\uparrow\downarrow\uparrow\rangle - |\downarrow\uparrow\uparrow\rangle) \quad (1.31)\end{aligned}$$

and

$$\begin{aligned}|[21],1/2,1/2\rangle_{E_\rho} &= |(0,1/2)1/2,1/2\rangle = \langle 0,0,1/2,1/2|1/2,1/2\rangle|[11]0,0\rangle|[1]1/2,1/2\rangle \\ &= \frac{1}{\sqrt{2}}(|\uparrow\downarrow\uparrow\rangle - |\downarrow\uparrow\uparrow\rangle). \quad (1.32)\end{aligned}$$

The three states above are in their maximum projection, so we can use S_- operator for three particles to get the missing states. In summary the next projections are obtained

$$\begin{aligned}\chi_{E_\lambda} \equiv |[21],1/2,1/2\rangle_{E_\lambda} &= \frac{1}{\sqrt{6}}(2|\uparrow\uparrow\downarrow\rangle - |\uparrow\downarrow\uparrow\rangle - |\downarrow\uparrow\uparrow\rangle) \\ \chi_{E_\rho} \equiv |[21],1/2,1/2\rangle_{E_\rho} &= \frac{1}{\sqrt{2}}(|\uparrow\downarrow\uparrow\rangle - |\downarrow\uparrow\uparrow\rangle \\ \chi^{-1/2}_{E_\lambda} \equiv |[21],1/2,-1/2\rangle_{E_\lambda} &= \frac{1}{\sqrt{6}}(|\downarrow\uparrow\downarrow\rangle + |\uparrow\downarrow\downarrow\rangle - 2|\downarrow\downarrow\uparrow\rangle) \\ \chi^{-1/2}_{E_\rho} \equiv |[21],1/2,-1/2\rangle_{E_\rho} &= \frac{1}{\sqrt{2}}(|\uparrow\downarrow\downarrow\rangle - |\downarrow\uparrow\downarrow\rangle). \quad (1.33)\end{aligned}$$

The spin projections of $M_S = 3/2$ are got through Eq. (1.30) as follows

$$\begin{aligned}\chi_{A_1} \equiv |[3],3/2,3/2\rangle_{A_1} &= |\uparrow\uparrow\uparrow\rangle \\ \chi^{1/2}_{A_1} \equiv |[3],3/2,1/2\rangle_{A_1} &= \frac{1}{\sqrt{3}}(|\uparrow\uparrow\downarrow\rangle + |\uparrow\downarrow\uparrow\rangle + |\downarrow\uparrow\uparrow\rangle) \\ \chi^{-1/2}_{A_1} \equiv |[3],3/2,-1/2\rangle_{A_1} &= \frac{1}{\sqrt{3}}(|\downarrow\downarrow\uparrow\rangle + |\downarrow\uparrow\downarrow\rangle + |\uparrow\downarrow\downarrow\rangle) \\ \chi^{-3/2}_{A_1} \equiv |[3],3/2,-3/2\rangle_{A_1} &= |\downarrow\downarrow\downarrow\rangle. \quad (1.34)\end{aligned}$$

1.2.4 Flavor wave function

Because of the symmetric nature of the isospin doublet u-d, the algebra that describes them is equivalent to the spin group $SU(2)$. The obtaining of baryon states with three constituent quarks is analogous to the derivation of spin states with three particles, where their degrees of freedom are projections $+1/2 \equiv \uparrow$ and $-1/2 \equiv \downarrow$. With this in mind, orthogonal states can be obtained directly by simply replacing in Eqs. (1.31) and (1.32), the projections $\uparrow$ and $\downarrow$, for the flavors u and d, respectively. Then, the following states are obtained:

$$\begin{aligned}|\phi_\lambda\rangle &= \frac{1}{\sqrt{6}}(2|uud\rangle - |udu\rangle - |duu\rangle) \\ |\phi_\rho\rangle &= \frac{1}{\sqrt{2}}(|udu\rangle - |duu\rangle). \quad (1.35)\end{aligned}$$

Because of the states $|\psi_1\rangle$ and $|\psi_2\rangle$ have the same symmetry as that of the permutations λ and ρ, their states are labeled as $|\psi_1\rangle = |\psi^\lambda\rangle$ for the symmetric and $|\psi_2\rangle = |\psi^\rho\rangle$ for the antisymmetric combination for the proton.

In order to obtain the rest of the antisymmetric (or symmetric) wave functions of the octet and decuplet, the flavor symmetry $SU(3)$ is exploited. In this approach, the initial flavor state of the proton is taken, and the other wave functions of the octet baryons are generated from the upper and lower operators $\hat{I}_{\pm}$, $\hat{V}_{\pm}$ and $\hat{U}_{\pm}$. The antisymmetric flavor wave function of the proton is associated with:

$$|\phi_p^\rho\rangle = \frac{1}{\sqrt{2}}(|udu\rangle - |duu\rangle). \tag{1.36}$$

The antisymmetric flavor wave function of the neutron can be obtained by applying the operator I_-, as follows

$$\begin{aligned} I_-|\phi_p^\rho\rangle &= d^\dagger u \frac{1}{\sqrt{2}}(|udu\rangle - |duu\rangle) = \frac{1}{\sqrt{2}}(|ddu\rangle + |udd\rangle - |ddu\rangle - |dud\rangle) \\ &= \frac{1}{\sqrt{2}}(|udd\rangle - |dud\rangle) \equiv |\phi_n^\rho\rangle. \end{aligned} \tag{1.37}$$

In the same way, applying U_- to the state of proton is obtained the antisymmetric Σ^+ flavor wave function associated with the next resulting state

$$U_-|\phi_p^\rho\rangle = s^\dagger d \frac{1}{\sqrt{2}}(|udu\rangle - |duu\rangle) = \frac{1}{\sqrt{2}}(|usu\rangle - |suu\rangle) \equiv |\phi_{\Sigma^+}^\rho\rangle. \tag{1.38}$$

Table 1.4: Flavor wave functions for octet baryons $J^P = \frac{1}{2}^+$.

Baryon	$\lvert(\lambda,\mu)I,I_3,Y\rangle$	$\lvert\phi^\lambda\rangle$	$\lvert\phi^\rho\rangle$
p	$\lvert(1,1)\frac{1}{2},\frac{1}{2},1\rangle$	$\frac{1}{\sqrt{6}}(2\lvert uud\rangle - \lvert udu\rangle - \lvert duu\rangle)$	$\frac{1}{\sqrt{2}}(\lvert udu\rangle - \lvert duu\rangle)$
Σ^+	$\lvert(1,1)1,1,0\rangle$	$-\frac{1}{\sqrt{6}}(\lvert usu\rangle + \lvert suu\rangle - 2\lvert uus\rangle)$	$-\frac{1}{\sqrt{2}}(\lvert suu\rangle - \lvert usu\rangle)$
Λ^0	$\lvert(1,1)0,0,0\rangle$	$\frac{1}{2}(\lvert sud\rangle - \lvert sdu\rangle$	$\frac{1}{\sqrt{12}}(2\lvert uds\rangle - 2\lvert dus\rangle + \lvert sdu\rangle$
		$-\lvert dsu\rangle + \lvert usd\rangle)$	$-\lvert sud\rangle + \lvert usd\rangle - \lvert dsu\rangle)$
Ξ^0	$\lvert(1,1)\frac{1}{2},\frac{1}{2},-1\rangle$	$-\frac{1}{\sqrt{6}}(2\lvert ssu\rangle - \lvert uss\rangle - \lvert sus\rangle)$	$-\frac{1}{\sqrt{2}}(\lvert sus\rangle - \lvert uss\rangle)$

If we follow the same idea of using the $SU(3)$ operators, it is possible to build the rest of the antisymmetric ρ wave functions of the baryon octet, as well as the symmetric one λ. As it was mentioned before, the states of this flavor multiplet are characterized by their labels (p,q); $(1,1)$ for the octet, $(3,0)$ for the decuplet and $(0,0)$ for the singlet. Additionally, we have the labels of isospin I, its projection I_3, and the hypercharge Y. The flavor wave functions are labeled as $|(p,q),I,I_3,Y\rangle$ and all of these states were obtained using the phase convention of Baird and Biedenharn [36, 37]. The results are shown in Table 1.4. Similarly, one can obtain the symmetric flavor wave function for decuplet just by simply replacing $\uparrow\rightarrow u$ and $\downarrow\rightarrow s$ in Eq. (1.35), so these results are shown on Table 1.5. The rest of the states either octet or decuplet can be derived from the lower and upper operators of $SU(3)$.

1.2.5 Spin-flavor wave functions

Up to this point, the wave functions of light baryons have already been obtained, for all their degrees of freedom separately. However, in order to have the total baryon wave function, it is still necessary

Table 1.5: Flavor wave functions for decuplet baryons $J^P = \frac{3}{2}^+$.

Barión	$\|(\lambda,\mu)I, I_3, Y\rangle$	$\|\phi^S\rangle$
Δ^{++}	$\|(3,0)\frac{3}{2}, \frac{3}{2}, 1\rangle$	$\|uuu\rangle$
Σ^{*+}	$\|(3,0)1, 1, 0\rangle$	$\frac{1}{\sqrt{3}}(\|uus\rangle + \|usu\rangle + \|suu\rangle)$
Ξ^{*0}	$\|(3,0)\frac{1}{2}, \frac{1}{2}, -1\rangle$	$\frac{1}{\sqrt{3}}(\|uss\rangle + \|sus\rangle + \|ssu\rangle)$
Ω^-	$\|(3,0)0, 0, -2\rangle$	$\|sss\rangle$

to discover the connection of these independent wave functions on the complete structure of the wave function. In order to comprehend the combinations of these states, it is necessary to develop the complete algebraic structure. This is accomplished by combining the orbital part $\mathcal{G}_{orb}$ with the internal spin-flavor-color part $\mathcal{G}_{sfc}$ of Eq. (1.1) as follows

$$\mathcal{G} \quad = \quad \mathcal{G}_{orb} \otimes \mathcal{G}_{sfc} = \mathcal{G}_{orb} \otimes SU_{sf}(6) \otimes SU_c(3), \tag{1.39}$$

this decomposition indicates how to combine the spin-flavor part with the color and the orbital part, in order to obtain the total baryon wave function.

Before continuing, it is necessary to check the symmetry properties of the three quarks as a system of indistinguishable or identical particles. All possible permutations of particle labels form the symmetric group of permutation S_3. The irreducible representation of S_3 is given by the following Young diagrams [3], [21] and [111]. For the orbital part, we use the notation ψ_S (symmetric), ψ_ρ, ψ_λ (with mixed symmetry) and ψ_A (antisymmetric), respectively.

The total wave function must be a color singlet, and the three quarks must satisfy the previously stated condition of the antisymmetry under any permutation of the three quarks

$$\psi_{A_2} \quad = \quad \left[\psi_A^{\rm c} \times \psi_S^{\rm osf}\right]_A \ , \tag{1.40}$$

which means that the permutation symmetry of the spatial wave function is the same as that of the spin-flavor part

$$\psi_S^{\rm osf} \quad = \quad \left[\psi_t^{\rm o} \times \psi_t^{\rm sf}\right]_S \ , \tag{1.41}$$

with $t = A_1, E, A_2$ and the square brackets denote the tensor coupling under the point group D_3.

The S_3 invariant space-spin-flavor baryon wave functions are given by [38]. For ground state $L^P = 0^+$ of the spin-flavor 56-plet

$$\begin{aligned} {}^2 8[56, 0^+] \quad &: \quad \psi_S(\chi_\rho\phi_\rho + \chi_\lambda\phi_\lambda)/\sqrt{2} \\ {}^4 10[56, 0^+] \quad &: \quad \psi_S\chi_S\phi_S \end{aligned} \tag{1.42}$$

For excited states with $L^P = 1^-$ corresponding with the spin-flavor 70-plet, the following configurations are considered

$$\begin{aligned} {}^2 8[70, 1^-] \quad &: \quad [\psi_\rho(\chi_\rho\phi_\lambda + \chi_\lambda\phi_\rho) + \psi_\lambda(\chi_\rho\phi_\rho - \chi_\lambda\phi_\lambda)]/2 \\ {}^4 8[70, 1^-] \quad &: \quad (\psi_\rho\phi_\rho + \psi_\lambda\phi_\lambda)\chi_S/\sqrt{2} \\ {}^2 10[70, 1^-] \quad &: \quad (\psi_\rho\chi_\rho + \psi_\lambda\chi_\lambda)\phi_S/\sqrt{2} \\ {}^2 1[70, 1^-] \quad &: \quad (\psi_\rho\chi_\lambda - \psi_\lambda\chi_\rho)\phi_A/\sqrt{2} \end{aligned} \tag{1.43}$$

Here the notation for these states is

$$|\psi\rangle \quad = \quad |^{2S+1}\mathsf{dim}\{SU_f(3)\}_J[\mathsf{dim}\{SU_{sf}(6)\}, L^P]\rangle \tag{1.44}$$

The orbital angular momentum L is coupled with the spin S to the total angular momentum J of the baryon, $\vec{J} = \vec{L} + \vec{S}$.

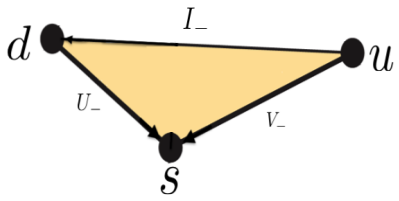

Fig. 1.3: Weight diagram for the three quark flavor representation and its relation with the lowering operators of $SU(3)$.

1.3 Four-flavor SU(4) quark model

In this second analysis, we introduced an extension of the quark model, going from the description of three to four flavors, that is, in addition to the three degrees of freedom (u, d and s) c is considered as an extra degree of freedom [39, 40, 41, 42]. Like in the previous case, the indistinguishability of particles in the coordinate space wave function is still preserved, because of the fact that in this model equal masses are taken. The new classification of states can now be carried out through the group $SU(4)$. There are 15 generators without trace for this group, and its representations are 15 traceless 4×4 matrices $F_i = \frac{\lambda_i}{2}$ [35]. These matrices correspond to a generalization of Pauli matrices for $SU(2)$, and the 3×3 Gell-Mann matrices for $SU(3)$. The λ_i are normalized in such way that $Tr(\lambda_i \lambda_j) = 2\delta_{ij}$. The 15 generators of $SU(4)$ can be divided into three weight operators

$$\begin{aligned} \hat{I}_3 &= \frac{1}{2}\lambda_3 = \frac{1}{2}(u^\dagger u - d^\dagger d) \\ \hat{Y} &= \frac{1}{\sqrt{3}}\lambda_8 = \frac{1}{3}(u^\dagger u + d^\dagger d - 2s^\dagger s) \\ \hat{Z} &= \frac{1}{2}\sqrt{\frac{3}{2}}\lambda_{15} = \frac{1}{4}(u^\dagger u + d^\dagger d + s^\dagger s - 3c^\dagger c), \end{aligned} \tag{1.45}$$

where the hat is placed over the generators in order to avoid confusion with the eigenvalues I_3, Y and Z. There are six operators with which it is possible to go over the triplet of quarks u, d and s from $SU(3)$ (see Fig. 1.3)

$$\begin{aligned} I_+ &= \frac{1}{2}(\lambda_1 + i\lambda_2) = u^\dagger d & I_- &= \frac{1}{2}(\lambda_1 - i\lambda_2) = d^\dagger u \\ U_+ &= \frac{1}{2}(\lambda_6 + i\lambda_7) = d^\dagger s & U_- &= \frac{1}{2}(\lambda_6 - i\lambda_7) = s^\dagger d \\ V_+ &= \frac{1}{2}(\lambda_4 + i\lambda_5) = u^\dagger s & V_- &= \frac{1}{2}(\lambda_4 - i\lambda_5) = s^\dagger u. \end{aligned} \tag{1.46}$$

Moreover, when we considering the remaining six operators of $SU(4)$, it is possible to move towards states with content of one heavy quark, for example a charm c quark (see Fig.1.4). For that reason, it can be noted that with this symmetry it is possible to go through the multiple-states with

$$\begin{aligned} K_+ &= \frac{1}{2}(\lambda_9 + i\lambda_{10}) = u^\dagger c & K_- &= \frac{1}{2}(\lambda_9 - i\lambda_{10}) = c^\dagger u \\ L_+ &= \frac{1}{2}(\lambda_{11} + i\lambda_{12}) = d^\dagger c & L_- &= \frac{1}{2}(\lambda_{11} - i\lambda_{12}) = c^\dagger d \\ M_+ &= \frac{1}{2}(\lambda_{13} + i\lambda_{14}) = s^\dagger c & M_- &= \frac{1}{2}(\lambda_{13} - i\lambda_{14}) = c^\dagger s. \end{aligned} \tag{1.47}$$

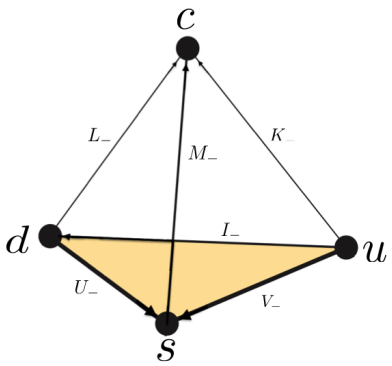

Fig. 1.4: Weight diagram for the four quark flavor representation and its relation with the lowering operators of $SU(4)$.

Its algebra relations are given as follows

$$\begin{array}{ll} [I_+, I_-] = 2\hat{I}_3 & [\hat{I}_3, I_\pm] = \pm I_\pm \\ [U_+, U_-] = 2U_3 & [U_3, U_\pm] = \pm U_\pm \\ [V_+, V_-] = 2V_3 & [V_3, V_\pm] = \pm V_\pm \\ [K_+, K_-] = 2\hat{K}_3 & [\hat{K}_3, K_\pm] = \pm K_\pm \\ [L_+, L_-] = 2L_3 & [L_3, L_\pm] = \pm L_\pm \\ [M_+, M_-] = 2M_3 & [M_3, M_\pm] = \pm M_\pm. \end{array} \tag{1.48}$$

The third components can be expressed in terms of $\hat{I}_3$, $\hat{Y}$ and $\hat{Z}$ as

$$\begin{aligned} U_3 &= -\frac{1}{2}\hat{I}_3 + \frac{3}{4}\hat{Y} \\ V_3 &= +\frac{1}{2}\hat{I}_3 + \frac{3}{4}\hat{Y} \\ K_3 &= +\frac{1}{2}\hat{I}_3 + \frac{1}{4}\hat{Y} + \frac{2}{3}\hat{Z} \\ L_3 &= -\frac{1}{2}\hat{I}_3 + \frac{1}{4}\hat{Y} + \frac{2}{3}\hat{Z} \\ M_3 &= -\frac{1}{2}\hat{Y} + \frac{2}{3}\hat{Z}. \end{aligned} \tag{1.49}$$

In view of this new treatment for the four flavors, these states can be classified by finding an irreducible representation of $SU(4)$ symmetry. This can be carried out by decoupling the spin-flavor basis, because we consider as independent the orbital and color parts of the rest of total wave function, so one has

$$\begin{array}{ccccc} SU_{\rm sf}(8) & \supset & SU_{\rm f}(4) & \otimes & SU_{\rm s}(2) \\ [f] & & [g] & & S \end{array} \tag{1.50}$$

Even when the mass difference restriction for heavy quarks can be implemented in the study of the orbital wave function, the flavor decomposition into subgroups can be useful for labeling ground state baryons with an additional quark content

$$\begin{array}{ccccccc} SU_{\rm f}(4) & \supset & SU_{\rm f}(3) & \otimes & U_{\rm Z}(1) & & \\ [g] & & [h] & & & & \\ & \supset & SU_{\rm I}(2) & \otimes & U_{\rm Y}(1) & \otimes & U_{\rm Z}(1) \\ & & I & & & & \\ & \supset & SO_{\rm I_3}(2) & \otimes & U_{\rm Y}(1) & \otimes & U_{\rm Z}(1). \\ & & I_3 & & Y & & Z \end{array} \tag{1.51}$$

The labels associated to these subgroups are related to the hypercharges Y and Z, and in turn these two are related to the baryon number $\mathcal{B}$, strangeness $\mathcal{S}$, charm C and bottom B. The relations can be rewritten as follows [43]

$$Y = \mathcal{B} + \mathcal{S} - \frac{C}{3} \tag{1.52}$$

$$Z = \frac{3}{4}\mathcal{B} - C \, . \tag{1.53}$$

The electric charge Q change in comparison with the previous one of Eq. (1.4), as a generalization of the Gell-Mann–Nishijima

$$Q = I_3 + \frac{\mathcal{B} + \mathcal{S} + C}{2} \, . \tag{1.54}$$

Again, as in the previous case of the three flavor scheme, here the Young tableau technique is also used to construct the allowed representation of multiquark systems. This justifies the fact that labels $[f]$, $[g]$ and $[h]$ are used for spin-flavor and flavor states of 4(3) types of flavors (according to the dimension of representation in $SU(n)$), respectively.

Considering the previous discussion, the flavor states can be identified with the following notation $|[g],[h],I,I_3,Y,Z\rangle$. The four quarks transform as the fundamental representation [1] of $SU(4)$ with

$$|\phi(u)\rangle = \left|[1],[1],\frac{1}{2},\frac{1}{2},\frac{1}{3},\frac{1}{4}\right\rangle \tag{1.55a}$$

$$|\phi(d)\rangle = \left|[1],[1],\frac{1}{2},-\frac{1}{2},\frac{1}{3},\frac{1}{4}\right\rangle \tag{1.55b}$$

$$|\phi(s)\rangle = \left|[1],[1],0,0,-\frac{2}{3},\frac{1}{4}\right\rangle \tag{1.55c}$$

$$|\phi(c)\rangle = \left|[1],[0],0,0,0,-\frac{3}{4}\right\rangle \, , \tag{1.55d}$$

and the four antiquarks according to the conjugate representation [111]

$$|\phi(\bar{u})\rangle = +\left|[111],[11],\frac{1}{2},-\frac{1}{2},-\frac{1}{3},-\frac{1}{4}\right\rangle, \tag{1.56a}$$

$$\left|\phi(\bar{d})\right\rangle = -\left|[111],[11],\frac{1}{2},\frac{1}{2},-\frac{1}{3},-\frac{1}{4}\right\rangle, \tag{1.56b}$$

$$|\phi(\bar{s})\rangle = +\left|[111],[11],0,0,\frac{2}{3},-\frac{1}{4}\right\rangle, \tag{1.56c}$$

$$|\phi(\bar{c})\rangle = -\left|[111],[111],0,0,0,\frac{3}{4}\right\rangle, \tag{1.56d}$$

where the phase convention of Baird and Biedenharn [36, 37] is used.

Even though the strong interaction does not distinguish between quarks of different flavor, the $SU_{\rm f}(4)$ flavor symmetry is broken dynamically by the quark masses. The spin, orbital and color parts are the same as before.

1.3.1 Classification of three-quark baryons with heavy quark content

For this study, it is convenient to use $SU(4)$ symmetry to find the configurations of qqq baryons with the possibility to have any of four types of flavors, among them u, d, s, and especially heavy baryons containing one or more heavy quarks Q (either a charm quark c, or a bottom quarks b).

Taking the product of representations in spin-flavor for the three quarks are obtained the possible configurations

$$[1]_8 \otimes [1]_8 \otimes [1]_8 = [3]_{120} \oplus 2\,[21]_{168} \oplus [111]_{56}, \tag{1.57}$$

Table 1.6: Spin-flavor classification of qqq states.

$SU_{\rm sf}(8)$	$\supset$	$SU_{\rm f}(4)$	$\otimes$	$SU_{\rm s}(2)$	
$[f]$	$\supset$	$[g]$	$\otimes$	$[g']$	$S=\frac{g'_1-g'_2}{2}$
$[3]_{120}$		$[3]_{20}$	$\otimes$	$[3]_4$	$\frac{3}{2}$
		$[21]_{20}$	$\otimes$	$[21]_2$	$\frac{1}{2}$

Table 1.7: $SU_{\rm f}(4)\supset SU_{\rm f}(3)\otimes U_{\rm Z}(1)$ flavor classification of three-quark states (here q refers to the light flavors: u, d, s).

$SU_{\rm f}(4)$	$\supset$	$SU_{\rm f}(3)$						
$[g]$	$\supset$	$[h]$						
$[3]_{20}$	$\supset$	$[3]_{10}$	$\oplus$	$[2]_6$	$\oplus$	$[1]_3$	$\oplus$	$[0]_1$
$[21]_{20}$	$\supset$	$[21]_8$	$\oplus$	$[2]_6\oplus[11]_3$	$\oplus$	$[1]_3$		
		$Z=\frac{3}{4}$		$Z=-\frac{1}{4}$		$Z=-\frac{5}{4}$		$Z=-\frac{9}{4}$
		qqq		qqc		qcc		ccc

[3] is a totally symmetric representation with dimension 120, [21] corresponds to a mixed-symmetric with dimension 168, and [111] is a totally antisymmetric representation with dimension 56.

The analysis of wave function is in the same way as that developed in Section 1.2 for q^3 baryons with just three flavors. Thus, the coupled spin-flavor wave function is symmetric as discussed before and the relevant part to be considered corresponds only to that symmetric representation [3] of Eq. (1.57). The flavor and spin decomposition of this spin-flavor configuration can be seen on Table 1.6. There are two flavor multiplets of $SU_{\rm f}(4)$, [3] associated with states $S^{\mathcal{P}}=3/2^+$ and [21] with $1/2^+$. With the aim of achieving an irreducible representation, a decomposition of four into three flavors can be made $SU_{\rm f}(4)\supset SU_{\rm f}(3)\otimes U_{\rm Z}(1)$, the result is shown in Table 1.7.

The symmetric 20-plet splits into a uds baryon decuplet, a sextet with one charm quark, a triplet with two charm quarks and a singlet consisting of three charm quarks. The 20-plet, with mixed symmetry, splits into a uds octet, a sextet and an anti-triplet with one charm quark and a triplet with two charm quarks (see Fig. 2.1).

Considering the previous analysis, it seems reasonable to assume that the baryon states of three quarks can be labeled by

$$\left|[f],(\alpha,\beta,\gamma),(\lambda,\mu),I,Y,Z,L^{\pi},S^{\mathcal{P}};J^{P}\right\rangle. \tag{1.58}$$

Where $[f]$ is the label for spin-flavor part (either symmetric [3], antisymmetric [111] or mixed symmetric [21]). Here the labels of the $SU(4)$ multiplet are used: $(\alpha,\beta,\gamma)=(g_1-g_2,g_2-g_3,g_3-g_4)$ to describe the flavor part with the isospin I, and for the case of the hypercharges Y and Z the labels of the $SU(3)$ multiplet are considered: $(\lambda,\mu)=(h_1-h_2,h_2-h_3)$ already introduced in Section 1.1.1. Furthermore, the orbital part is represented by the orbital angular momentum and parity L^{π}. The last labels are for the total angular momentum, which is given by the sum of orbital and spin parts $\vec{J}=\vec{L}+\vec{S}$. The total parity is given by the product of the orbital motion and the intrinsic parity of the quarks, $P=\pi\mathcal{P}$.

As an example, the nucleon wave function is given by

$$|N(939)\rangle=\left|[3],(1,1,0),(1,1),\frac{1}{2},1,\frac{3}{4},0^+,\frac{1}{2}^+;\frac{1}{2}^+\right\rangle. \tag{1.59}$$

Here $(\alpha,\beta,\gamma)=(1,1,0)$ denotes the $SU(4)$ mixed symmetry 20-plet, and $(\lambda,\mu)=(1,1)$ the $SU(3)$ flavor octet. In a similar way it is possible to represent the other baryons, even those with heavy quark content.

1.3.2 Heavy Baryons: qqQ

The total baryon wave function considered as a product of the color, spin, flavor and orbital parts has to be antisymmetric, Eq. (1.11). Furthermore, because the color part is antisymmetric, the orbital and spin-flavor parts necessarily have the same symmetry. This means that they can form any of the following combinations: symmetric, mixed symmetry or antisymmetric.

An additional reduction to construct the baryon wave functions with one heavy quark Q arises when the flavor of this quark is distinguished from the rest of constituents in the flavor wave function. By choosing Q in the third position and symmetrizing the remaining two flavors we can find either a completely symmetric, or a completely antisymmetric flavor wave function

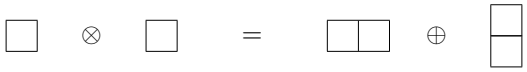

The symmetry sextet consists of the charge states of Σ_Q, two charge states of Ξ'_Q, and Ω_Q. The flavor wave functions with maximum charge are

$$\begin{aligned} \Sigma_Q &= uuQ \\ \Xi'_Q &= (us+su)Q/\sqrt{2} \\ \Omega_Q &= ssQ. \end{aligned} \tag{1.60}$$

The antisymmetric states form an antitriplet consisting of Λ_Q and two charge states of Ξ_Q

$$\begin{aligned} \Lambda_Q &= (ud-du)Q/\sqrt{2} \\ \Xi_Q &= (us-su)Q/\sqrt{2}. \end{aligned} \tag{1.61}$$

To form both the ground and excited states of the heavy baryons it is necessary to consider all the possible configurations of the wave functions. It is useful to take into account the more general derivation of the wave functions, the case of baryons with three invariant constituent quarks under permutation of themselves, see Section 1.3.1. From this point of view, the configuration of interest for this work will be a particular case of the Eqs.(1.42) and (1.43). In these expressions aside from the flavor part there are five wave functions; three for the spin part χ_ρ, χ_λ and χ_S, which for maximum spin projection are

$$\begin{aligned} \chi_{E_\rho} &= (\uparrow\downarrow - \downarrow\uparrow)\uparrow/\sqrt{2} \\ \chi_{E_\lambda} &= (2\uparrow\uparrow\downarrow - \uparrow\downarrow\uparrow - \downarrow\uparrow\uparrow)/\sqrt{6} \\ \chi_{A_1} &= \uparrow\uparrow\uparrow, \end{aligned} \tag{1.62}$$

and two for the radial part ψ_λ and ψ_ρ. The orbital wave function for the ground state is denoted by ψ_0. It was already mentioned that lambda and rho labels are associated with symmetry and antisymmetry under the interchange of the first two particles, respectively. The S label refers to the symmetric spin wave function with $S = 3/2$.

The color part factorizes in both the ground and excited states, and due to the orthogonality of the basis, the overlap of any two states in the color part will always be one. Moreover, because the processes in which we are interested are color independent, then it is enough to construct the baryon wave functions just considering the orbital-spin and flavor parts.

With this information, it is now straightforward to write the total wave functions of the baryons. In particular, for Σ_Q hyperons, since the flavor part is symmetric, then spin-orbital combinations must be symmetrically coupled. For the heavy baryons of the sextet one obtains the wave functions

$$\begin{aligned} {}^2\Sigma_Q &= uuQ[\psi_0 \times \chi_{E_\lambda}]_{J=1/2} \\ {}^4\Sigma_Q &= uuQ[\psi_0 \times \chi_{A_1}]_{J=3/2} \\ {}^2\rho(\Sigma_Q)_J &= uuQ[\psi_\rho \times \chi_{E_\rho}]_J \\ {}^2\lambda(\Sigma_Q)_J &= uuQ[\psi_\lambda \times \chi_{E_\lambda}]_J \\ {}^4\lambda(\Sigma_Q)_J &= uuQ[\psi_\lambda \times \chi_{A_1}]_J. \end{aligned} \tag{1.63}$$

for the Σ_Q hyperons,

$$\begin{aligned}
{}^2\Xi'_Q &= \frac{1}{\sqrt{2}}(us+su)Q[\psi_0\times\chi_{E_\lambda}]_{J=1/2}\\
{}^4\Xi'_Q &= \frac{1}{\sqrt{2}}(us+su)Q[\psi_0\times\chi_{A_1}]_{J=3/2}\\
{}^2\rho(\Xi'_Q)_J &= \frac{1}{\sqrt{2}}(us+su)Q[\psi_\rho\times\chi_{E_\rho}]_J\\
{}^2\lambda(\Xi'_Q)_J &= \frac{1}{\sqrt{2}}(us+su)Q[\psi_\lambda\times\chi_{E_\lambda}]_J\\
{}^4\lambda(\Xi'_Q)_J &= \frac{1}{\sqrt{2}}(us+su)Q[\psi_\lambda\times\chi_{A_1}]_J. \qquad (1.64)
\end{aligned}$$

for the Ξ'_Q hyperons, and

$$\begin{aligned}
{}^2\Omega_Q &= ssQ[\psi_0\times\chi_{E_\lambda}]_{J=1/2}\\
{}^4\Omega_Q &= ssQ[\psi_0\times\chi_{A_1}]_{J=3/2}\\
{}^2\rho(\Omega_Q)_J &= ssQ[\psi_\rho\times\chi_{E_\rho}]_J\\
{}^2\lambda(\Omega_Q)_J &= ssQ[\psi_\lambda\times\chi_{E_\lambda}]_J\\
{}^4\lambda(\Omega_Q)_J &= ssQ[\psi_\lambda\times\chi_{A_1}]_J. \qquad (1.65)
\end{aligned}$$

for the Ω_Q hyperons.

Similarly, for the heavy baryons of the anti-triplet one has

$$\begin{aligned}
{}^2\Lambda_Q &= \frac{1}{\sqrt{2}}(ud-du)Q[\psi_0\times\chi_{E_\rho}]_{J=1/2}\\
{}^2\rho(\Lambda_Q)_J &= \frac{1}{\sqrt{2}}(ud-du)Q[\psi_\rho\times\chi_{E_\lambda}]_J\\
{}^4\rho(\Lambda_Q)_J &= \frac{1}{\sqrt{2}}(ud-du)Q[\psi_\rho\times\chi_{A_1}]_J\\
{}^2\lambda(\Lambda_Q)_J &= \frac{1}{\sqrt{2}}(ud-du)Q[\psi_\lambda\times\chi_{E_\rho}]_J. \qquad (1.66)
\end{aligned}$$

for the Λ_Q hyperons, and

$$\begin{aligned}
{}^2\Xi_Q &= \frac{1}{\sqrt{2}}(us-su)Q[\psi_0\times\chi_{E_\rho}]_{J=1/2}\\
{}^2\rho(\Xi_Q)_J &= \frac{1}{\sqrt{2}}(us-su)Q[\psi_\rho\times\chi_{E_\lambda}]_J\\
{}^4\rho(\Xi_Q)_J &= \frac{1}{\sqrt{2}}(us-su)Q[\psi_\rho\times\chi_{A_1}]_J\\
{}^2\lambda(\Xi_Q)_J &= \frac{1}{\sqrt{2}}(us-su)Q[\psi_\lambda\times\chi_{E_\rho}]_J, \qquad (1.67)
\end{aligned}$$

for the Ξ_Q hyperons.

Chapter 2

Deformed quark model (qqQ or QQq)

2.1 Quark harmonic oscillator model: Hamiltonian for three particles $m_1 = m_2 \neq m_3$

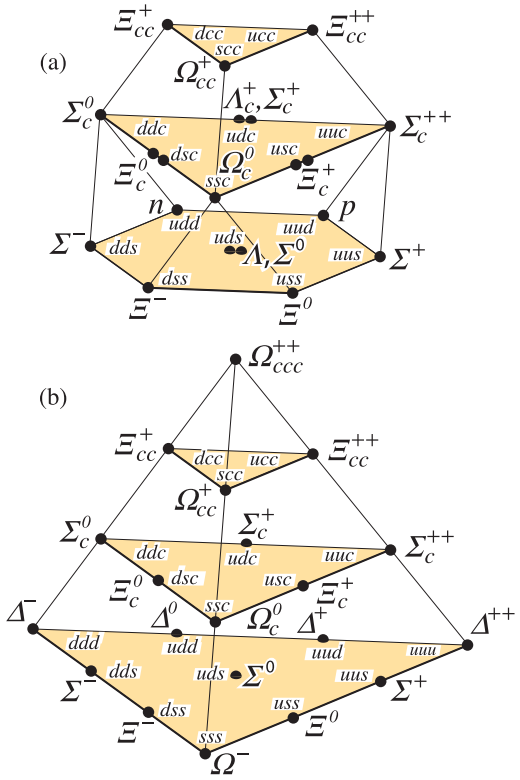

Fig. 2.1: $SU(4)$ multiplets of qqq baryons made of u, d, s, and c quarks: (a) the $[21]_{20}$ multiplet with $J^P = 1/2^+$ containing the baryon octet, and (b) the $[21]_{20}$ multiplet with $J^P = 3/2^+$ containing the baryon decuplet (taken from [43]).

The study of the orbital wave function of baryons with different quark masses now becomes relevant [44]. In a baryon configuration made of three constituent quarks, either Qqq or QQq, it is of special interest to make a distinction between the heavy quarks Q, and the light quarks q. We consider the harmonic oscillator potential, in order to describe the interaction between the three

effective quarks 1, 2 and 3. Thus, the Hamiltonian is of the form

$$H = \frac{{p_1}^2}{2m} + \frac{{p_2}^2}{2m} + \frac{{p_3}^2}{2m'} + \frac{1}{2}C\sum_{i<j}^{3}|\vec{r_i} - \vec{r_j}|^2, \tag{2.1}$$

where quarks 1 and 2 have equal masses m, while quark 3 has the mass m'.

If relative coordinates are used (similar to Jacobi coordinates, but modified for this system with different masses), Eq. (2.1) will be rewritten in a more convenient way. For this purpose the following coordinates and its corresponding transformation are defined

$$\begin{cases} \vec{\rho} = \frac{1}{\sqrt{2}}(\vec{r_1} - \vec{r_2}), \\ \vec{\lambda} = \frac{1}{\sqrt{6}}(\vec{r_1} + \vec{r_2} - 2\vec{r_3}), \\ \vec{R} = \frac{m(\vec{r_1}+\vec{r_2})+m'\vec{r_3}}{2m+m'} \end{cases} \Rightarrow \begin{cases} \vec{r_1} = \vec{R} + \frac{1}{\sqrt{2}}\vec{\rho} + \frac{\sqrt{\frac{3}{2}}m'}{2m+m'}\vec{\lambda} \\ \vec{r_2} = \vec{R} - \frac{1}{\sqrt{2}}\vec{\rho} + \frac{\sqrt{\frac{3}{2}}m'}{2m+m'}\vec{\lambda} \\ \vec{r_3} = \vec{R} - \frac{\sqrt{6}m}{2m+m'}\vec{\lambda}, \end{cases}$$

where the corresponding Jacobian to the change of Cartesian to Jacobi coordinates turns out to be

$$\prod_{i=1}^{3} d^3 r_i = 3\sqrt{3} d^3\rho d^3\lambda d^3 R. \tag{2.2}$$

With these new coordinates the harmonic oscillator Hamiltonian can be rewritten as a separable one for each coordinate. The problem now includes the center of mass motion plus two independent harmonic oscillators in the ρ- and λ-mode, with the same spring constant C, but different masses

$$H = \frac{{P_{CM}}^2}{2M} + \frac{{p_\rho}^2}{2m_\rho} + \frac{{p_\lambda}^2}{2m_\lambda} + \frac{3}{2}C\rho^2 + \frac{3}{2}C\lambda^2, \tag{2.3}$$

where the masses can be redefined as

$$M = 2m + m', \qquad m_\rho \equiv m, \qquad m_\lambda \equiv \frac{3mm'}{2m+m'}, \tag{2.4}$$

and

$$\vec{P}_{CM} = M\frac{d\vec{R}}{dt}, \qquad \vec{p_\rho} = m_\rho\frac{d\vec{\rho}}{dt}, \qquad \vec{p_\lambda} = m_\lambda\frac{d\vec{\lambda}}{dt}. \tag{2.5}$$

More explicitly

$$\begin{cases} \vec{p_\rho} = \frac{1}{\sqrt{2}}(\vec{p_1} - \vec{p_2}) \\ \vec{p_\lambda} = \frac{3}{\sqrt{6}}\frac{m'(\vec{p_1}+\vec{p_2})-2m\vec{p_3}}{2m+m'} \\ \vec{P} = \vec{p_1} + \vec{p_2} + \vec{p_3} \end{cases} \Rightarrow \begin{cases} \vec{p_1} = \frac{m}{M}\vec{P} + \frac{1}{\sqrt{2}}\vec{p}_\rho + \frac{1}{\sqrt{6}}\vec{p}_\lambda \\ \vec{p_2} = \frac{m}{M}\vec{P} - \frac{1}{\sqrt{2}}\vec{p}_\rho + \frac{1}{\sqrt{6}}\vec{p}_\lambda \\ \vec{p_3} = \frac{m'}{M}\vec{P} - \sqrt{\frac{2}{3}}\vec{p_\lambda}, \end{cases}$$

and equally

$$\prod_{i=1}^{3} d^3 p_i = \frac{1}{3\sqrt{3}} d^3 p_\rho d^3 p_\lambda d^3 P. \tag{2.6}$$

The eigenstates of the Hamiltonian from Eq. (2.3) are well known [45]. With the above change of coordinates, the baryon wave function $\psi_B^o(\vec{r}_1, \vec{r}_2, \vec{r}_3)$ is given by

$$\psi_B^o(\vec{r}_1, \vec{r}_2, \vec{r}_3) = \frac{1}{(2\pi)^{3/2}} e^{\vec{P}_{CM}\cdot\vec{R}} \psi_B^{rel}(\vec{\rho}, \vec{\lambda}), \tag{2.7}$$

where the relative wave functions are expressed in terms of the coupled harmonic oscillator wave functions

$$\psi_B^{rel}(\vec{\rho},\vec{\lambda}) = \frac{1}{\sqrt{3\sqrt{3}}} \sum_{m_\rho m_\lambda} \langle l_\rho m_\rho l_\lambda m_\lambda | LM\rangle \psi_{n_\rho l_\rho m_\rho}(\vec{\rho}) \psi_{n_\lambda l_\lambda m_\lambda}(\vec{\lambda}). \tag{2.8}$$

Then **the ground state** in this new coordinate space is

$$\psi_B^{rel}(\vec{\rho},\vec{\lambda}) = \frac{1}{\sqrt{3\sqrt{3}}} \frac{\alpha_\rho^{\frac{3}{2}}}{\pi^{\frac{3}{4}}} \frac{\alpha_\lambda^{\frac{3}{2}}}{\pi^{\frac{3}{4}}} e^{-\frac{\alpha_\rho^2}{2}\rho^2} e^{-\frac{\alpha_\lambda^2}{2}\lambda^2}. \tag{2.9}$$

Again, the relative wave functions for one radial λ-excitation and one radial ρ-excitation are

$$\psi_\lambda^{rel}(\vec{\rho},\vec{\lambda}) = \frac{1}{\sqrt{3\sqrt{3}}} \frac{\alpha_\rho^{3/2}}{\pi^{\frac{3}{4}}} e^{-\alpha_\rho^2\rho^2/2} \sqrt{\frac{8}{3\sqrt{\pi}}} \lambda \alpha_\lambda^{5/2} e^{-\alpha_\lambda^2\lambda^2/2} Y_{1,m_{l_\lambda}}(\hat{\lambda}), \tag{2.10}$$

and

$$\psi_\rho^{rel}(\vec{\rho},\vec{\lambda}) = \frac{1}{\sqrt{3\sqrt{3}}} \frac{\alpha_\lambda^{3/2}}{\pi^{\frac{3}{4}}} e^{-\alpha_\lambda^2\lambda^2/2} \sqrt{\frac{8}{3\sqrt{\pi}}} \rho \alpha_\rho^{5/2} e^{-\alpha_\rho^2\rho^2/2} Y_{1,m_{l_\rho}}(\hat{\rho}), \tag{2.11}$$

with the harmonic oscillator constants and frequencies given by

$$\alpha_i^2 = (3Cm_i)^{\frac{1}{2}} \qquad \text{and} \qquad \omega_i = \sqrt{\frac{3C}{m_i}}, \qquad i = \{\rho,\lambda\}. \tag{2.12}$$

By making a Fourier transform is easy to obtain the wave function for the ground state in momentum space

$$\psi_B^{rel}(\vec{p_\rho},\vec{p_\lambda}) = \sqrt{3\sqrt{3}} \frac{1}{\pi^{\frac{3}{4}}\alpha_\rho^{\frac{3}{2}}} \frac{1}{\pi^{\frac{3}{4}}\alpha_\lambda^{\frac{3}{2}}} e^{-\frac{1}{2\alpha_\rho^2}p_\rho^2} e^{-\frac{1}{2\alpha_\lambda^2}p_\lambda^2}, \tag{2.13}$$

and similar expressions can be obtained for radially excited states.

These results are also valid for qqq configurations in which all the quark masses are the same, so that the results discussed in Section 1.2.2 can be recovered.

So far, a simple analysis on frequencies can be done by considering the case where $m = m_1 = m_2 < m_3 = m'$; this condition is consistent with a system containing two light quarks and one heavy quark qqQ. As a consequence, $m_\lambda > m_\rho$, and then $\omega_\lambda < \omega_\rho$, *i.e.*, the λ state is less energetic than ρ state. The last condition obtained suggest that states with one quantum of excitation in λ will be more relevant for this configuration. A diagram corresponding to these energy modes is shown in Figure 2.2.

By contrast, for the other case where $m = m_1 = m_2 > m_3 = m'$ is associated with QQq, the conclusion is the opposite, and the largest contribution for baryons with two heavy quarks will be the ρ mode.

2.2 Mass spectra of heavy baryons

We characterize the mass spectra of baryons with a single heavy quark, where we consider a Hamiltonian given by

$$H = H_{ho} + A\, S^2 + B\, \vec{S}\cdot\vec{L} + E\, I^2 + G\, C_{2SU_f(3)}. \tag{2.14}$$

The first term is the conventional harmonic oscillator Hamiltonian, and the perturbation term is formed by the sum of the spin, spin-orbit, isospin and flavor dependent contributions. In this

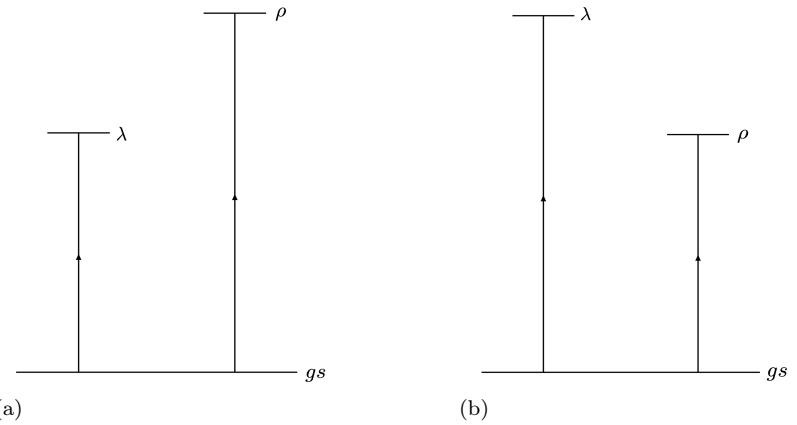

Fig. 2.2: Baryon energy levels for states with one quantum of excitation in λ and ρ, associated to qqQ configuration, with $m < m'$ (left), and for QQq configuration with $m > m'$ (right).

notation S, L, I and $C_{2SU_f(3)}$ are the spin, angular momentum, isospin and the quadratic Casimir operators. For this approach of the spectrum, we use the explicit form of H_{ho} in terms of Jacobi coordinates previously defined

$$\begin{aligned} H_{ho} &= \sum_{i=1}^{3}(m_i + \frac{p_i^2}{2m_i}) + \frac{1}{2}C\sum_{i<j}^{3}|\vec{r_i} - \vec{r_j}|^2 \\ &= 2m + m' + \frac{P_{CM}^2}{2(2m+m')} + \frac{{p_\rho}^2}{2m_\rho} + \frac{{p_\lambda}^2}{2m_\lambda} + \frac{1}{2}m_\rho\omega_\rho^2\rho^2 + \frac{1}{2}m_\lambda\omega_\lambda^2\lambda^2. \end{aligned} \tag{2.15}$$

Consequently, the mass spectrum of heavy baryons is analyzed with the mass formula

$$\begin{aligned} M &= 2m + m' + \omega_\rho n_\rho + \omega_\lambda n_\lambda + A\,S(S+1) \\ &\quad + B\,\frac{1}{2}\left[J(J+1) - L(L+1) - S(S+1)\right] \\ &\quad + E\,I(I+1) + G\,\frac{1}{3}\left[\lambda(\lambda+3) + \mu(\mu+3) + \lambda\mu\right]. \end{aligned} \tag{2.16}$$

Here n_ρ and n_λ denote the number of quanta in the ρ- and λ- oscillator, respectively. The labels (λ, μ) are the standard labels of $SU(3)$ already discussed. The parameters A, B, E and G in Eq. (2.14) were determined through the analysis of some known baryons from the experimental data.

Parameters

We obtain the quark masses by reproducing the ground state masses of $\Omega_c(2695)$, $\Omega_c^*(2765)$, $\Xi_{cc}(3621)$ and $\Sigma_b(5814)$. The two spring constants C, one for the charm and the other for the bottom sector, as the case may be, were fixed by reproducing the mass difference between $\Xi_c(2790)$ with $J^P = 1/2^-$ and the $\Xi_c(2469)$ ground state, and the difference between $\Lambda_b(5919)$ with $J^P = 1/2^-$ and the $\Lambda_b(5619)$ ground state, respectively. On the other hand, we obtain the rest of parameters by studying them term by term. For the spin-spin interaction, we estimate the mass difference between $\Sigma_c^*(2520)$ with $J^P = 3/2^+$ and $\Sigma_c(2469)$ with $J^P = 1/2^+$, and taking the isospin average. The spin-orbit part can be calculated by the mass difference of $\Lambda_c(2595)$ and $\Lambda_c(2625)$ with $S^P = 1/2^-$ and $S^P = 3/2^-$, respectively. The mass splitting due to the flavor dependent contribution can be obtained from the mass difference between Ξ_c^* and Ξ_c, with a mass of 2578.1 MeV and 2469.37 MeV, respectively, whereas for the bottom counterparts, we have Ξ_b^* and Ξ^b with masses 5935.02 MeV and 5793.2 MeV, respectively. We study the isospin-flavor contribution through the mass difference

Table 2.1: Parameters values for baryons with a single heavy quark $Q = c$, or $Q = b$.

	$Q = c$	$Q = b$	
$m_u = m_d$	295	295	MeV
m_s	450	450	MeV
m_Q	1605	4920	MeV
C	0.0328	0.0235	GeV^3
A	21.54 ± 0.37	6.73 ± 1.63	MeV
B	23.91 ± 0.31	5.15 ± 0.33	MeV
E	30.34 ± 0.23	26.00 ± 1.80	MeV
G	54.37 ± 0.58	70.91 ± 0.49	MeV

between the lightest charmed ground states Σ_c and Λ_c, and bottom ground states Σ_c and Λ_c. The list of these parameters are in Table 7.1.

Now, because we have explicitly classified and built all the baryon wave functions with a single heavy quark in previous sections, we know all their quantum numbers, so we can obtain their mass spectra. In Tables 2.2 and 2.3 we essentially present the list of states organized according to the notation $^{2S+1}L(B_Q)_{J^P}$, where the quantum numbers for each baryon B_Q are given. The pair (n_ρ, n_λ) represents the radial contributions of the states. Particularly, $(0, 0)$ is the configuration of the ground state ψ_0, whereas $(1, 0)$ and $(0, 1)$ represent one quantum of excitation in the ρ mode ψ_ρ and one quantum of excitation in the λ mode ψ_λ, respectively.

In addition, a comparison between the theoretical and the experimental masses can be done. A detailed discussion on the mass spectrum of Ω_Q can be found in [33], and a supplement in [46], while the spectra of baryons Ξ_Q and Ξ'_Q are established in [34]. It is important to emphasize that the only study that these publications have in common with the present work is the derivation of the mass spectrum for the heavy baryons already mentioned. However, the rest of their research is done with a different model.

Even though experimentally we have concise information about the heavy baryon spectrum with the knowledge of some resonances, theoretically, one still expects some missing resonances predicted by the quark model, and that is one of the reasons for the study in this work. Here, aside from comparing our results on singly charm and singly bottom baryon masses together with their assigned quantum numbers against the recently observed resonances and data in PDG [47], we also provide predictions of new states, which could be benchmarked with present and future LHCb measurements as well as with the lattice QCD (LQCD) computations [48, 49, 50, 50, 51, 52, 53, 54, 55, 56, 57, 58].

Mases of Σ_Q and Λ_Q baryons

From figures 2.3 to 2.6 we present our theoretical estimation (blue circles) of the mass spectra and quantum numbers for single charm baryons Σ_c and Λ_c, and single bottom baryons Σ_b and Λ_b. Besides, we contrast with the experimental information of resonances (red triangles). This comparison easily reveals the good agreement between the theoretical masses and the experimental data. Specially, if we focused on Σ_Q states of flavor sextet $\mathbf{6}$, all the assigned masses overlap with the experimental data and their uncertainties, where $\Sigma_c(2455)$ and $\Sigma_c(2520)$ are assigned to the ground states with $J^P = S^P = 1/2^+$ and $3/2^+$, respectively, while $\Sigma_c(2800)$ is to the $\lambda-$mode excitation with $J^P = 1/2^-$. Similarly, Σ_b and Σ_b^* resonances observed by LHCb [1] are assigned to the ground states with $J^P = S^P = 1/2^+$ and $3/2^+$, respectively, yet $\Sigma_b(6097)$ has a correspondence with one quantum of excitation in λ and $J^P = 1/2^-$.

For Λ_Q states of the flavor anti-triplet $\bar{\mathbf{3}}$ there is still a remarkable coincidence with the experimetal results in the bottom sector, where we associate Λ_b to the only ground state $S^P = 1/2^+$, whereas the λ-modes with $J^P = 1/2^-$ and $J^P = 3/2^-$ are assigned to $\Lambda_b(5912)$ and $\Lambda_b(5920)$ resonances [59]. In case of the charm sector a difference (less than 60 MeV) can be seen for $\Lambda_c(2592)$ and $\Lambda_c(2628)$. In our analysis it was assigned the $\lambda-$mode excitation with $J^P = 1/2^-$ and $3/2^-$ to these baryons, respectively.

Table 2.2: Single-charm baryons of ground state and with one quantum of radial excitation. Here we use the notation $^{2S+1}L(B_Q)_{J^P}$ to label the states by their quantum numbers, and (n_ρ, n_λ) are used to identify the radial contributions of the states.

State	M^{th}(MeV)	(n_ρ, n_λ)	I	L	S	J^P	M^{exp}(MeV)	Name
$^2(\Sigma_c)_{1/2^+}$	2453±2	(0,0)	1	0	$\frac{1}{2}$	$\frac{1}{2}^+$	2453.54 ± 0.31	$\Sigma_c(2455)$
$^4(\Sigma_c)_{3/2^+}$	2518±2	(0,0)	1	0	$\frac{3}{2}$	$\frac{3}{2}^+$	2518.13 ± 0.90	$\Sigma_c(2520)$
$^2\lambda(\Sigma_c)_{1/2^-}$	2819±2	(0,1)	1	1	$\frac{1}{2}$	$\frac{1}{2}^-$	2799.67 ± 9	$\Sigma_c(2800)$
$^4\lambda(\Sigma_c)_{1/2^-}$	2848±3	(0,1)	1	1	$\frac{3}{2}$	$\frac{1}{2}^-$		
$^2\lambda(\Sigma_c)_{3/2^-}$	2855±2	(0,1)	1	1	$\frac{1}{2}$	$\frac{3}{2}^-$		
$^4\lambda(\Sigma_c)_{3/2^-}$	2884±2	(0,1)	1	1	$\frac{3}{2}$	$\frac{3}{2}^-$		
$^4\lambda(\Sigma_c)_{5/2^-}$	2944±2	(0,1)	1	1	$\frac{3}{2}$	$\frac{5}{2}^-$		
$^2\rho(\Sigma_c)_{1/2^-}$	3007±2	(1,0)	1	1	$\frac{1}{2}$	$\frac{1}{2}^-$		
$^2\rho(\Sigma_c)_{3/2^-}$	3043±2	(1,0)	1	1	$\frac{1}{2}$	$\frac{3}{2}^-$		
$^2(\Xi'_c)_{1/2^+}$	2570±2	(0,0)	$\frac{1}{2}$	0	$\frac{1}{2}$	$\frac{1}{2}^+$	2578.90±0.5	$\Xi'_c(2578)$
$^4(\Xi'_c)_{3/2^+}$	2635±2	(0,0)	$\frac{1}{2}$	0	$\frac{3}{2}$	$\frac{3}{2}^+$	2645.97±0.27	$\Xi_c(2645)$
$^2\lambda(\Xi'_c)_{1/2^-}$	2905±2	(0,1)	$\frac{1}{2}$	1	$\frac{3}{2}$	$\frac{1}{2}^-$		
$^4\lambda(\Xi'_c)_{1/2^-}$	2934±3	(0,1)	$\frac{1}{2}$	1	$\frac{3}{2}$	$\frac{1}{2}^-$	2923.04±0.25	$\Xi_c(2923)$
$^2\lambda(\Xi'_c)_{3/2^-}$	2941±2	(0,1)	$\frac{1}{2}$	1	$\frac{1}{2}$	$\frac{3}{2}^-$	2938.55±0.21	$\Xi_c(2939)$
$^4\lambda(\Xi'_c)_{3/2^-}$	2970±2	(0,1)	$\frac{1}{2}$	1	$\frac{3}{2}$	$\frac{3}{2}^-$	2964.88±0.26	$\Xi_c(2965)$
$^4\lambda(\Xi'_c)_{5/2^-}$	3030±2	(0,1)	$\frac{1}{2}$	1	$\frac{3}{2}$	$\frac{5}{2}^-$		
$^2\rho(\Xi'_c)_{1/2^-}$	3060±2	(0,1)	$\frac{1}{2}$	1	$\frac{1}{2}$	$\frac{1}{2}^-$	3055.9±0.4	$\Xi_c(3055)$
$^2\rho(\Xi'_c)_{3/2^-}$	3096±2	(0,1)	$\frac{1}{2}$	1	$\frac{1}{2}$	$\frac{3}{2}^-$	3078.55±1.1	$\Xi_c(3080)$
$^2(\Omega_c)_{1/2^+}$	2702±2	(0,0)	0	0	$\frac{1}{2}$	$\frac{1}{2}^+$	2695.2±1.7	$\Omega_c(2695)$
$^4(\Omega_c)_{3/2^+}$	2767±2	(0,0)	0	0	$\frac{3}{2}$	$\frac{3}{2}^+$	2765.9±2.0	$\Omega_c(2770)$
$^2\lambda(\Omega_c)_{1/2^-}$	3016±2	(0,1)	0	1	$\frac{1}{2}$	$\frac{1}{2}^-$	3000.4±0.2	$\Omega_c(3000)$
$^4\lambda(\Omega_c)_{1/2^-}$	3045±3	(0,1)	0	1	$\frac{3}{2}$	$\frac{1}{2}^-$	3050.2±0.1	$\Omega_c(3050)$
$^2\lambda(\Omega_c)_{3/2^-}$	3052±2	(0,1)	0	1	$\frac{1}{2}$	$\frac{3}{2}^-$	3065.5±0.3	$\Omega_c(3066)$
$^4\lambda(\Omega_c)_{3/2^-}$	3080±2	(0,1)	0	1	$\frac{3}{2}$	$\frac{3}{2}^-$	3090.0±0.5	$\Omega_c(3090)$
$^4\lambda(\Omega_c)_{5/2^-}$	3140±2	(0,1)	0	1	$\frac{3}{2}$	$\frac{5}{2}^-$	3188±14	$\Omega_c(3188)$
$^2\rho(\Omega_c)_{1/2^-}$	3146±2	(1,0)	0	1	$\frac{1}{2}$	$\frac{1}{2}^-$		
$^2\rho(\Omega_c)_{3/2^-}$	3182±2	(1,0)	0	1	$\frac{1}{2}$	$\frac{3}{2}^-$		
$^2(\Lambda_c)_{1/2^+}$	2284±1	(0,0)	0	0	$\frac{1}{2}$	$\frac{1}{2}^+$	2286.46 ± 0.14	Λ_c
$^2\lambda(\Lambda_c)_{1/2^-}$	2650±1	(0,1)	0	1	$\frac{1}{2}$	$\frac{1}{2}^-$	2592.25 ± 0.28	$\Lambda_c(2595)$
$^2\lambda(\Lambda_c)_{3/2^-}$	2686±1	(0,1)	0	1	$\frac{1}{2}$	$\frac{3}{2}^-$	2628.11 ± 0.19	$\Lambda_c(2625)$
$^2\rho(\Lambda_c)_{1/2^-}$	2837±1	(1,0)	0	1	$\frac{1}{2}$	$\frac{1}{2}^-$		
$^4\rho(\Lambda_c)_{1/2^-}$	2866±2	(1,0)	0	1	$\frac{3}{2}$	$\frac{1}{2}^-$		
$^2\rho(\Lambda_c)_{3/2^-}$	2873±1	(1,0)	0	1	$\frac{1}{2}$	$\frac{3}{2}^-$		
$^4\rho(\Lambda_c)_{3/2^-}$	2902±2	(1,0)	0	1	$\frac{3}{2}$	$\frac{3}{2}^-$	2939.60 ± 1.5	$\Lambda_c(2940)$
$^4\rho(\Lambda_c)_{5/2^-}$	2962±2	(1,0)	0	1	$\frac{3}{2}$	$\frac{5}{2}^-$		
$^2(\Xi_c)_{1/2^+}$	2461±1	(0,0)	$\frac{1}{2}$	0	$\frac{1}{2}$	$\frac{1}{2}^+$	2469.43±0.26	$\Xi_c(2469)$
$^2\lambda(\Xi_c)_{1/2^-}$	2797±1	(0,1)	$\frac{1}{2}$	1	$\frac{1}{2}$	$\frac{1}{2}^-$	2793.25±0.5	$\Xi_c(2790)$
$^2\lambda(\Xi_c)_{3/2^-}$	2832±1	(0,1)	$\frac{1}{2}$	1	$\frac{1}{2}$	$\frac{3}{2}^-$	2818.5±0.28	$\Xi_c(2815)$
$^2\rho(\Xi_c)_{1/2^-}$	2951±1	(1,0)	$\frac{1}{2}$	1	$\frac{1}{2}$	$\frac{1}{2}^-$		
$^4\rho(\Xi_c)_{1/2^-}$	2980±2	(1,0)	$\frac{1}{2}$	1	$\frac{3}{2}$	$\frac{1}{2}^-$		
$^2\rho(\Xi_c)_{3/2^-}$	2987±1	(1,0)	$\frac{1}{2}$	1	$\frac{1}{2}$	$\frac{3}{2}^-$		
$^4\rho(\Xi_c)_{3/2^-}$	3016±2	(1,0)	$\frac{1}{2}$	1	$\frac{3}{2}$	$\frac{3}{2}^-$		
$^4\rho(\Xi_c)_{5/2^-}$	3076±2	(1,0)	$\frac{1}{2}$	1	$\frac{3}{2}$	$\frac{5}{2}^-$		

Table 2.3: Single-bottom baryons of ground state and with one quantum of radial excitation. Notation as in Table 2.2.

State	M^{th}(MeV)	(n_ρ, n_λ)	I	L	S	J^P	M^{exp}(MeV)	Name
$^2(\Sigma_b)_{1/2^+}$	5803±4	(0,0)	1	0	$\frac{1}{2}$	$\frac{1}{2}^+$	5812.78±0.13	Σ_b
$^4(\Sigma_b)_{3/2^+}$	5824±7	(0,0)	1	0	$\frac{3}{2}$	$\frac{3}{2}^+$	5832.50 ± 0.16	Σ_b^*
$^2\lambda(\Sigma_b)_{1/2^-}$	6097±4	(0,1)	1	1	$\frac{1}{2}$	$\frac{1}{2}^-$	6096.90 ± 1.7	$\Sigma_b(6097)$
$^4\lambda(\Sigma_b)_{1/2^-}$	6109±7	(0,1)	1	1	$\frac{3}{2}$	$\frac{1}{2}^-$		
$^2\lambda(\Sigma_b)_{3/2^-}$	6105±4	(0,1)	1	1	$\frac{1}{2}$	$\frac{3}{2}^-$		
$^4\lambda(\Sigma_b)_{3/2^-}$	6117±7	(0,1)	1	1	$\frac{3}{2}$	$\frac{3}{2}^-$		
$^4\lambda(\Sigma_b)_{5/2^-}$	6130±7	(0,1)	1	1	$\frac{3}{2}$	$\frac{5}{2}^-$		
$^2\rho(\Sigma_b)_{1/2^-}$	6287±4	(1,0)	1	1	$\frac{1}{2}$	$\frac{1}{2}^-$		
$^2\rho(\Sigma_b)_{3/2^-}$	6295±4	(1,0)	1	1	$\frac{1}{2}$	$\frac{3}{2}^-$		
$^2(\Xi'_b)_{1/2^+}$	5926±2	(0,0)	$\frac{1}{2}$	0	$\frac{1}{2}$	$\frac{1}{2}^+$	5935.02±0.05	$\Xi'_b(5935)$
$^4(\Xi'_b)_{3/2^+}$	5946±6	(0,0)	$\frac{1}{2}$	0	$\frac{3}{2}$	$\frac{3}{2}^+$	5955.33±0.13	$\Xi'^*_b(5954)$
$^2\lambda(\Xi'_b)_{1/2^-}$	6189±2	(0,1)	$\frac{1}{2}$	1	$\frac{3}{2}$	$\frac{1}{2}^-$		
$^4\lambda(\Xi'_b)_{1/2^-}$	6202±6	(0,1)	$\frac{1}{2}$	1	$\frac{3}{2}$	$\frac{1}{2}^-$		
$^2\lambda(\Xi'_b)_{3/2^-}$	6197±2	(0,1)	$\frac{1}{2}$	1	$\frac{1}{2}$	$\frac{3}{2}^-$		
$^4\lambda(\Xi'_b)_{3/2^-}$	6210±6	(0,1)	$\frac{1}{2}$	1	$\frac{3}{2}$	$\frac{3}{2}^-$		
$^4\lambda(\Xi'_b)_{5/2^-}$	6223±6	(0,1)	$\frac{1}{2}$	1	$\frac{3}{2}$	$\frac{5}{2}^-$	6226.90±2.0	$\Xi_b(6227)$
$^2\rho(\Xi'_b)_{1/2^-}$	6354±2	(0,1)	$\frac{1}{2}$	1	$\frac{1}{2}$	$\frac{1}{2}^-$		
$^2\rho(\Xi'_b)_{3/2^-}$	6362±2	(0,1)	$\frac{1}{2}$	1	$\frac{1}{2}$	$\frac{3}{2}^-$		
$^2(\Omega_b)_{1/2^+}$	6061±2	(0,0)	0	0	$\frac{1}{2}$	$\frac{1}{2}^+$	6046.1±1.7	Ω_b
$^4(\Omega_b)_{3/2^+}$	6082±6	(0,0)	0	0	$\frac{3}{2}$	$\frac{3}{2}^+$		
$^2\lambda(\Omega_b)_{1/2^-}$	6305±2	(0,1)	0	1	$\frac{1}{2}$	$\frac{1}{2}^-$	6315.6±0.6	$\Omega_b(6316)$
$^4\lambda(\Omega_b)_{1/2^-}$	6317±6	(0,1)	0	1	$\frac{3}{2}$	$\frac{1}{2}^-$	6339.7±0.6	$\Omega_b(6340)$
$^2\lambda(\Omega_b)_{3/2^-}$	6313±2	(0,1)	0	1	$\frac{1}{2}$	$\frac{3}{2}^-$	6330.3±0.6	$\Omega_b(6330)$
$^4\lambda(\Omega_b)_{3/2^-}$	6325±6	(0,1)	0	1	$\frac{3}{2}$	$\frac{3}{2}^-$	6349.9±0.6	$\Omega_b(6350)$
$^4\lambda(\Omega_b)_{5/2^-}$	6338±6	(0,1)	0	1	$\frac{3}{2}$	$\frac{5}{2}^-$		
$^2\rho(\Omega_b)_{1/2^-}$	6452±2	(1,0)	0	1	$\frac{1}{2}$	$\frac{1}{2}^-$		
$^2\rho(\Omega_b)_{3/2^-}$	6460±2	(1,0)	0	1	$\frac{1}{2}$	$\frac{3}{2}^-$		
$^2(\Lambda_b)_{1/2^+}$	5610±1	(0,0)	0	0	$\frac{1}{2}$	$\frac{1}{2}^+$	5619.62 ± 0.16	Λ_b
$^2\lambda(\Lambda_b)_{1/2^-}$	5903±1	(0,1)	0	1	$\frac{1}{2}$	$\frac{1}{2}^-$	5912.20 ± 0.13	$\Lambda_b(5912)$
$^2\lambda(\Lambda_b)_{3/2^-}$	5911±1	(0,1)	0	1	$\frac{1}{2}$	$\frac{3}{2}^-$	5920.00 ± 0.09	$\Lambda_b(5920)$
$^2\rho(\Lambda_b)_{1/2^-}$	6093±1	(1,0)	0	1	$\frac{1}{2}$	$\frac{1}{2}^-$		
$^4\rho(\Lambda_b)_{1/2^-}$	6105±6	(1,0)	0	1	$\frac{3}{2}$	$\frac{1}{2}^-$		
$^2\rho(\Lambda_b)_{3/2^-}$	6101±1	(1,0)	0	1	$\frac{1}{2}$	$\frac{3}{2}^-$		
$^4\rho(\Lambda_b)_{3/2^-}$	6113±6	(1,0)	0	1	$\frac{3}{2}$	$\frac{3}{2}^-$		
$^4\rho(\Lambda_b)_{5/2^-}$	6126±6	(1,0)	0	1	$\frac{3}{2}$	$\frac{5}{2}^-$		
$^2(\Xi_b)_{1/2^+}$	5784±2	(0,0)	$\frac{1}{2}$	0	$\frac{1}{2}$	$\frac{1}{2}^+$	5794.41±0.55	$\Xi_b(5794)$
$^2\lambda(\Xi_b)_{1/2^-}$	6048±2	(0,1)	$\frac{1}{2}$	1	$\frac{1}{2}$	$\frac{1}{2}^-$		
$^2\lambda(\Xi_b)_{3/2^-}$	6055±2	(0,1)	$\frac{1}{2}$	1	$\frac{1}{2}$	$\frac{3}{2}^-$		
$^2\rho(\Xi_b)_{1/2^-}$	6213±2	(1,0)	$\frac{1}{2}$	1	$\frac{1}{2}$	$\frac{1}{2}^-$		
$^4\rho(\Xi_b)_{1/2^-}$	6225±6	(1,0)	$\frac{1}{2}$	1	$\frac{3}{2}$	$\frac{1}{2}^-$		
$^2\rho(\Xi_b)_{3/2^-}$	6220±2	(1,0)	$\frac{1}{2}$	1	$\frac{1}{2}$	$\frac{3}{2}^-$		
$^4\rho(\Xi_b)_{3/2^-}$	6233±6	(1,0)	$\frac{1}{2}$	1	$\frac{3}{2}$	$\frac{3}{2}^-$		
$^4\rho(\Xi_b)_{5/2^-}$	6246±6	(1,0)	$\frac{1}{2}$	1	$\frac{3}{2}$	$\frac{5}{2}^-$		

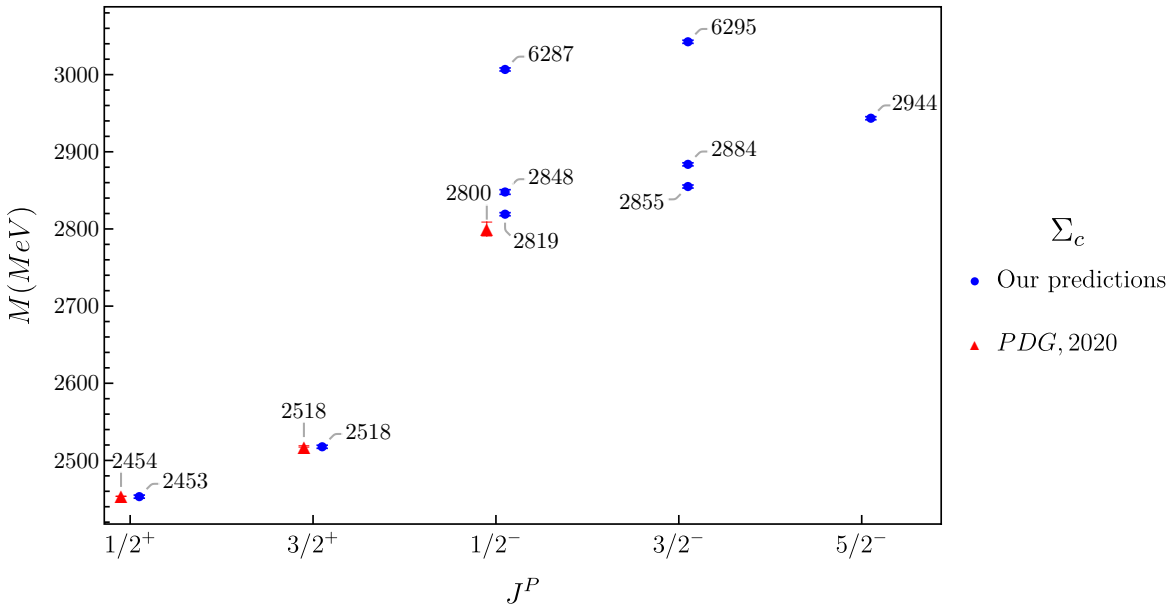

Fig. 2.3: Mass spectrum for the Σ_c baryons

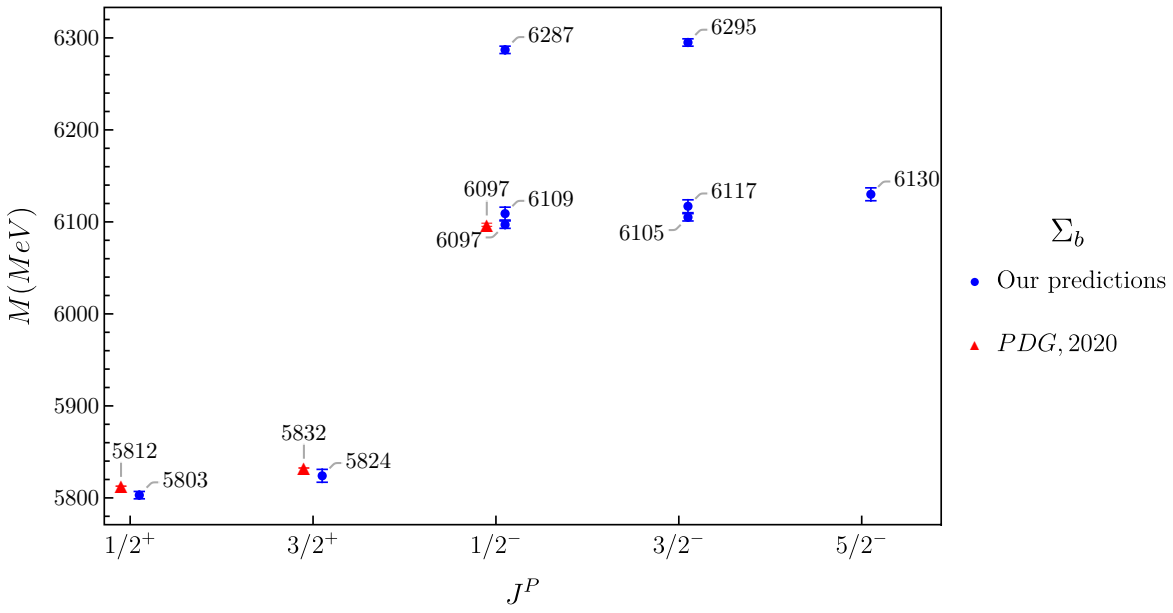

Fig. 2.4: Mass spectrum for the Σ_b baryons

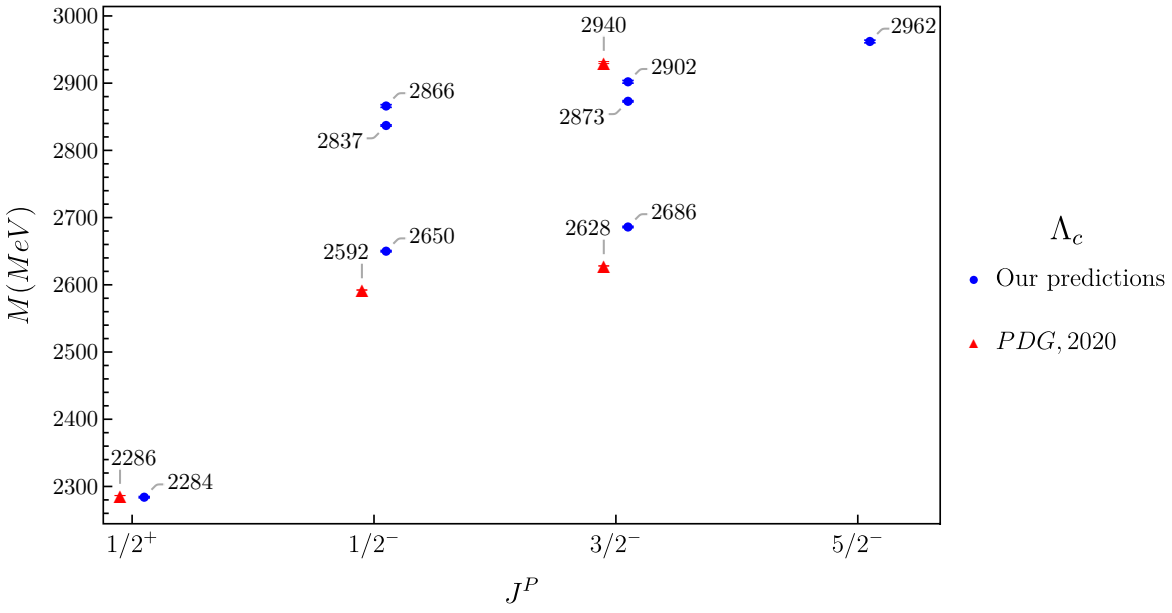

Fig. 2.5: Mass spectrum for the Λ_c baryons

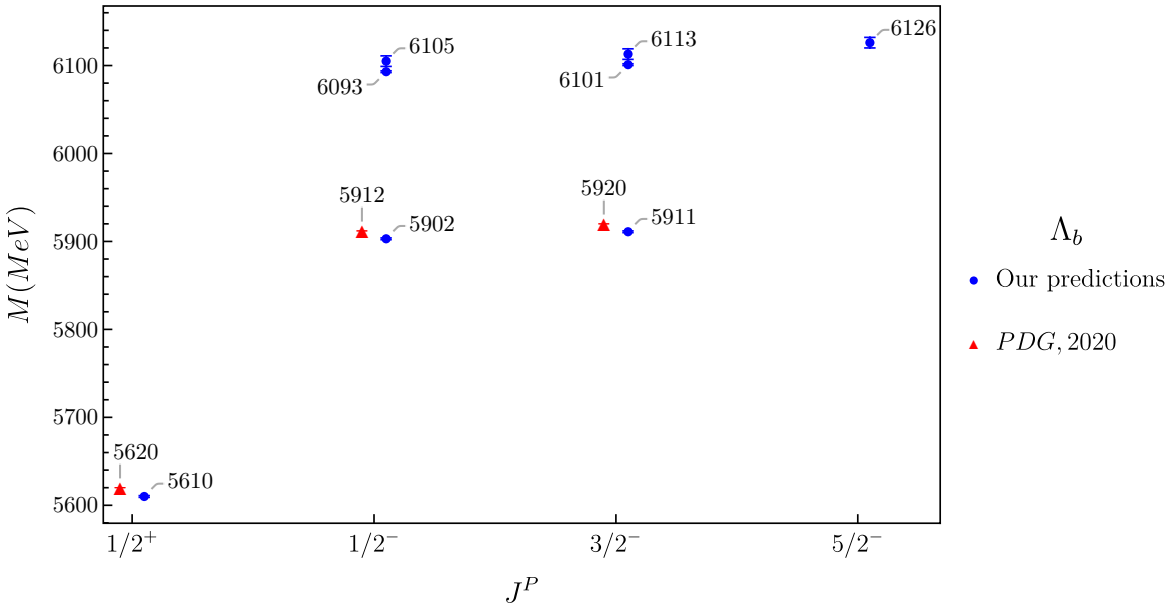

Fig. 2.6: Mass spectrum for the Λ_b baryons

Chapter 3

Strong Couplings of Heavy Baryons

The fundamental theory to study the hadrons and their dynamical process is QCD. However, there are many complications in the non-perturbative regime. Part of the problem is in explaining the transition from a completely relativistic theory to a non-relativistic approximate one, which strictly can only be done by discussing the strong interaction Hamiltonian (or Lagrangian) of the QCD. That is why in the quark model to deal with this problem it is assumed that this Hamiltonian is replaced by a "Hamiltonian model", where the gluons are integrated out from the action of the QCD [60]. Then, by using an effective Hamiltonian, an approximately satisfactory description of the hadrons in terms of only quarks is obtained, but which still has the essential characteristic of having a Dirac-like free part. These quarks are going to differ from the quark fields in the Lagrangian of QCD. Although these have the same quantum numbers as the fundamental quarks of QCD, they are different in their dynamical properties, like their mass. In principle, it is possible to transform the Hamiltonian with a Dirac-like part into a Hamiltonian that leads to the Schrödinger equation for the quarks under the non-relativistic approximation. In relation to the above, there are two hypotheses in which the quark model is based: 1. This Hamiltonian in the non-relativistic case has as its main characteristic eigenstates with a defined number of quarks and antiquarks (the so-called approximation of valence quarks) and 2. The constituent quarks in the non-relativistic limit obey the Schrödinger equation to a reasonably good approximation.

3.1 The interaction Hamiltonian

Given the energetic nature of the heavy baryons announced in recent years by the LHCb collaboration, it is of primary interest to obtain a description for the strong couplings between the singly heavy baryons and the pseudoscalar mesons. To this end, we choose to study the strong decays in the framework of the Elementary-meson emission model [60], which propose an effective interaction Hamiltonian . This Hamiltonian can be derived by introducing a vector-axial coupling through a Lagrangian density that considers the interaction between the axial current of quarks and the derivative of the pseudoscalar meson field

$$\mathcal{L}_I(x) = -\frac{g_{qq'M}}{2m}\bar{q}(x)\gamma^\mu\gamma_5\tau^a q(x)\partial_\mu\varphi^a(x). \tag{3.1}$$

This is motivated by a simplified description of the emission and absorption of mesons, described in terms of an elementary quantum. In this model, a hadron composed of quarks emits a meson through one of its constituent quarks in such a way that the total number of quarks is conserved. In order to obtain the Hamiltonian of interaction, is necessary to write the total lagrangian

$$\mathcal{L} = i\sum_q \bar{q}(x)(\partial_\mu\gamma^\mu - m_q)q(x) + \frac{1}{2}\left(\partial_\mu\varphi^a(x)\partial^\mu\varphi^a(x) - m^2(\varphi^a(x))^2\right) + \mathcal{L}_I(x), \tag{3.2}$$

where for simplicity such an expression has its indices suppressed. The momentum π^0 is given by

$$\pi^0 = \partial^0\varphi^a - \frac{g_{qq'M}}{2m}\bar{q}\gamma^0\tau^a\gamma_5 q. \tag{3.3}$$

Here the isospin part is in τ^a flavor matrices . Then the Hamiltonian density is

$$\begin{aligned}\mathcal{H}(\vec{x}) &= \sum_q \bar{q}(-i\gamma\cdot\nabla + m_q)q + \frac{1}{2}(\pi^0)^2 + \frac{1}{2}(\nabla\varphi^a)^2 + \frac{1}{2}m^2(\varphi^a)^2 \\ &+ \frac{g_{qq'M}}{2m}\left(\bar{q}\gamma^\mu\tau^a\gamma_5 q\pi^0 - \bar{q}\gamma\tau^a\gamma_5 q\cdot\nabla\varphi^a\right) + \frac{1}{2}\left(\frac{g_{qq'M}}{2m}\bar{q}\gamma^0\tau^a\gamma_5 q\right)^2 \end{aligned} \tag{3.4}$$

If we work in the interaction representation, then the free-meson Hamiltonian density are the sum of the quadratic terms with π^0 and φ

$$\mathcal{H}_0(\vec{x}) = \frac{1}{2}\left((\pi^0)^2 + (\nabla\varphi^a)^2 + m^2(\varphi^a)^2\right), \tag{3.5}$$

where

$$\frac{\partial\varphi(\vec{x})}{\partial t} = \frac{\delta\mathcal{H}_0}{\delta\pi^0} = \pi^0(x), \tag{3.6}$$

and then the Hamiltonian interaction density will be

$$\mathcal{H}_I(\vec{x}) = \frac{g_{qq'M}}{2m}\left(\bar{q}\gamma^\mu\tau^a\gamma_5 q\partial^0\varphi^a - \bar{q}\gamma\tau^a\gamma_5 q\cdot\nabla\varphi^a\right) + \frac{1}{2}\left(\frac{g_{qq'M}}{2m}\bar{q}\gamma^0\gamma_5 q\right)^2. \tag{3.7}$$

One can notice that the difference between $H_I(x)$ and $L_I(x)$ is only in the four-fermionic term of Eq. (3.7). However, because we want to consider only meson-emission and we are working in first order in he coupling constant, this four-fermion term is irrelevant. At the end, we have $H_I(x) = -L_I(x)$.

Therefore, the effective interaction Hamiltonian is

$$H_s = \int d^3x \frac{g_{qq'M}}{2m}\bar{q}(\vec{x})\gamma^\mu\gamma_5\tau^a q(\vec{x})\partial_\mu\varphi^a(\vec{x}). \tag{3.8}$$

This interaction, like the fundamental interactions of QCD between fermions and gauge bosons, is a three-line interaction. In this case, between the quarks and the elementary meson as in the Fig. 4.1 at the quark level. This resolution in quarks naturally restricts our study to a non-relativistic approach. The interaction Hamiltonian in the non-relativistic approximation is given by [38, 60, 61]

$$H_s = \frac{1}{(2\pi)^{3/2}(2k_0)^{1/2}}\sum_{j=1}^{3} X_j^M\left[2g(\vec{s_j}\cdot\vec{k})e^{-i\vec{k}\cdot\vec{r_j}} + h\vec{s_j}\cdot\left(\vec{p_j}e^{-i\vec{k}\cdot\vec{r_j}} + e^{-i\vec{k}\cdot\vec{r_j}}\vec{p_j}\right)\right]. \tag{3.9}$$

In a non-relativistic approximation at the level of hadrons composed of constituent quarks, the decay mechanism of a baryon in two hadrons corresponds directly to the creation of a pair $q\bar{q}$. Here X_j^M is the flavor operator, whose effect on the initial baryon states B_Q is the emission of one meson M through the jth constituent quark, so that the total number of quarks is conserved in the strong decay $B_Q \to B'_Q + M$. The diagram associated to this process is shown in Figure 4.1. The Hamiltonian also depends on the spin, coordinate and momentum of the jth constituent quark, $\vec{s_j}$, $\vec{r_j}$ and $\vec{p_j}$, respectively. The meson energy is denoted by $k_0 = E_M = E_{B_Q} - E_{B'_Q}$, and $\vec{k} = \vec{P}_M = \vec{P} - \vec{P}' = k\hat{z}$ corresponds to the momentum carried by the meson. Of course, $\vec{P} = P_z\hat{z}$ and $\vec{P}' = P'_z\hat{z}$ are the momentum of the initial and final baryon. Furthermore, we have two coupling constants g and h for each term in the transition operator. The fixed values of these constants will be discussed later.

For convenience, the above operator Eq.(3.9) can be simplified by using Jacobi coordinates and also by taking the rest frame of the initial baryon. Once we implement these tools, the operator is reduced to a new and more operational expression:

$$H_s = \frac{1}{(2\pi)^{3/2}(2k_0)^{1/2}}\sum_{j=1}^{3}\left\{X_j^M\left[(2gk - \frac{m_j}{M}hk)s_{j,z}\hat{U}_j + 2hs_{j,z}\hat{T}_{j,z} + h\left(s_{j,+}\hat{T}_{j,-} + s_{j,-}\hat{T}_{j,+}\right)\right]\right\}, \tag{3.10}$$

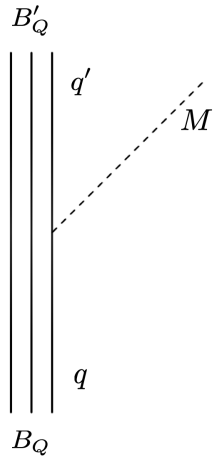

Fig. 3.1: Elementary-meson emission in a strong decay $B_Q \to B'_Q + M$.

where the momentum conservation $P_z - P'_z = k$ was used such that $P_z + P'_z = 2P_z - k$, and the rest frame of B_Q ($P_z = 0$) was adopted in order to eliminate the center of mass momentum. The explicit operators related with each jth constituent are given by

$$\hat{U}_1 = e^{-i\frac{1}{\sqrt{2}}k\rho_z - i\frac{\sqrt{3/2}m'}{2m+m'}k\lambda_z}, \qquad \hat{U}_2 = e^{i\frac{1}{\sqrt{2}}k\rho_z - i\frac{\sqrt{3/2}m'}{2m+m'}k\lambda_z}, \qquad \hat{U}_3 = e^{i\frac{\sqrt{6}m}{2m+m'}k\lambda_z} \tag{3.11}$$

$$\hat{T}_{1,m} = \frac{1}{2}\left[\left(\frac{1}{\sqrt{2}}P_{\rho,m} + \frac{1}{\sqrt{6}}P_{\lambda,m}\right)\hat{U}_1 + \hat{U}_1\left(\frac{1}{\sqrt{2}}P_{\rho,m} + \frac{1}{\sqrt{6}}P_{\lambda,m}\right)\right] \tag{3.12}$$

$$\hat{T}_{2,m} = \frac{1}{2}\left[\left(-\frac{1}{\sqrt{2}}P_{\rho,m} + \frac{1}{\sqrt{6}}P_{\lambda,m}\right)\hat{U}_2 + \hat{U}_2\left(-\frac{1}{\sqrt{2}}P_{\rho,m} + \frac{1}{\sqrt{6}}P_{\lambda,m}\right)\right] \tag{3.13}$$

$$\hat{T}_{3,m} = -\frac{1}{2}\left(\sqrt{\frac{2}{3}}P_{\lambda,m}\hat{U}_3 + \hat{U}_3\sqrt{\frac{2}{3}}P_{\lambda,m}\right). \tag{3.14}$$

The label m is used to denote either the z component (also called zero component 0) of the momentum operator, or the projections $\pm$ from the momentum ladder operators. In the strong decays of present interest the initial baryon state has the total angular momentum $\vec{J} = \vec{L} + \vec{S}$, where $\vec{L}$ can be either $\vec{L} = 0$ or $\vec{L} = 1$. The final baryon B'_Q considered here is from ground state and then always has $\vec{L}' = 0$, i.e. $\vec{J}' = \vec{S}'$. The helicity amplitude for the strong the decays is given by

$$\begin{aligned}
\mathcal{A}_\nu(k) &= \langle\psi_{B'_Q}; 1/2, \nu|H_s|\psi_{B_Q}; J, \nu\rangle, \qquad \nu = 1/2,\ 3/2. \\
&= \sum_{m=\{0,1,-1\}} \langle 10S\nu - m|J\nu\rangle\langle\psi_{B'_Q}00; S'\nu|H_s|\psi_{B_Q}L, m; S, \nu - m\rangle \\
&= \frac{1}{(2\pi)^{3/2}(2k_0)^{1/2}}\left\{\langle L0S\nu|J\nu\rangle\sum_{j=1}^{3}\zeta_{j,0}Z_{j,0}(k) + \frac{1}{2}\langle L1S\nu - 1|J\nu\rangle\sum_{j=1}^{3}\zeta_{j,+}Z_{j,-}(k)\right. \\
&\quad \left. + \frac{1}{2}\langle L - 1S\nu + 1|J\nu\rangle\sum_{j=1}^{3}\zeta_{j,-}Z_{j,+}(k)\right\}
\end{aligned} \tag{3.15}$$

with the radial matrix elements defined from the next functions

$$Z^\alpha_{j,0}(k) \equiv \left(2gk - \frac{m_j}{M}hk\right)U^\alpha_j(k) + 2hT^\alpha_{j,0}(k) \tag{3.16}$$

and

$$Z^{\alpha}_{j,\pm}(k) \equiv 2hT^{\alpha}_{j,\pm}(k). \tag{3.17}$$

The explicit definition of this matrix elements are

$$U^{\alpha}_{j} \equiv \langle\psi_{gs}|e^{-i\vec{k}\cdot\vec{r}_j}|\psi_{\alpha}\rangle, \tag{3.18}$$

$$T^{\alpha}_{j,0} \equiv \langle\psi_{gs}|\hat{T}^{\alpha}_{j,0}|\psi_{\alpha}\rangle \tag{3.19}$$

and

$$T^{\alpha}_{j,\pm} \equiv \langle\psi_{gs}|\hat{T}^{\alpha}_{j,\pm}|\psi_{\alpha}\rangle. \tag{3.20}$$

The analytical results for each of these radial matrix elements are classified according to the initial and final orbital baryon wave function:

Ground state to ground state

$$\begin{aligned}
U_3(k) &= e^{-\frac{3m^2k^2}{2\alpha_\lambda^2(2m+m')^2}} \\
U_1(k) = U_2(k) &= e^{-\frac{k^2}{8\alpha_\rho^2}} e^{-\frac{3m'^2k^2}{8\alpha_\lambda^2(2m+m')^2}}
\end{aligned}$$

$$\begin{aligned}
T_{3,0}(k) &= m'k_0\left[-\frac{3m^2k}{\alpha_\lambda^2(2m+m')^2}\right] e^{-\frac{3m^2k^2}{2\alpha_\lambda^2(2m+m')^2}} \\
T_{1,0}(k) = T_{2,0}(k) &= mk_0\left[-\frac{k}{4\alpha_\rho^2} - \frac{3m'^2k^2}{4\alpha_\lambda^2(2m+m')^2}\right] e^{-\frac{k^2}{8\alpha_\rho^2}} e^{-\frac{3m'^2k^2}{8\alpha_\lambda^2(2m+m')^2}}
\end{aligned}$$

One quantum of excitation in ρ to ground state

$$\begin{aligned}
U^{\rho}_3 &= 0 \\
U^{\rho}_1 = -U^{\rho}_2 &= -i\frac{k}{2\alpha_\rho} e^{-\frac{k^2}{8\alpha_\rho^2}} e^{-\frac{3m'^2k^2}{8\alpha_\lambda^2(2m+m')^2}} \\
T^{\rho}_{3,0} &= 0 \\
T^{\rho}_{1,0} = -T^{\rho}_{2,0} &= -i\frac{mk_0}{2\alpha_\rho} e^{-\frac{k^2}{8\alpha_\rho^2}} e^{-\frac{3m'^2k^2}{8\alpha_\lambda^2(2m+m')^2}} \left[1 - \frac{k^2}{4\alpha_\rho^2} - \frac{3m'^2k^2}{4\alpha_\lambda^2(2m+m')^2}\right] \\
T^{\rho}_{3,\pm} &= 0 \\
T^{\rho}_{1,\pm} = -T^{\rho}_{2,\pm} &= \mp i\frac{mk_0}{\sqrt{2}\alpha_\rho} e^{-\frac{k^2}{8\alpha_\rho^2}} e^{-\frac{3m'^2k^2}{8\alpha_\lambda^2(2m+m')^2}}
\end{aligned} \tag{3.21}$$

One quantum of excitation in λ to ground state

$$\begin{aligned}
U_3^\lambda &= i\frac{\sqrt{3}m}{2m+m'}\frac{k}{\alpha_\lambda}e^{-\frac{3m^2k^2}{2\alpha_\lambda^2(2m+m')^2}} \\
U_1^\lambda = U_2^\lambda &= -i\frac{k}{2\sqrt{3}\alpha_\lambda}\frac{3m'}{2m+m'}e^{-\frac{k^2}{8\alpha_\rho^2}}e^{-\frac{3m'^2k^2}{8\alpha_\lambda^2(2m+m')^2}} \\
T_{3,0}^\lambda &= i\frac{k_0}{\alpha_\lambda}\frac{\sqrt{3}mm'}{2m+m'}\left[1-\frac{3m^2k^2}{\alpha_\lambda^2(2m+m')^2}\right]e^{-\frac{3m^2k^2}{2\alpha_\lambda^2(2m+m')^2}} \\
T_{1,0}^\lambda = T_{2,0}^\lambda &= -i\frac{k_0}{2\sqrt{3}\alpha_\lambda}\frac{3mm'}{2m+m'}e^{-\frac{k^2}{8\alpha_\rho^2}}e^{-\frac{3m'^2k^2}{8\alpha_\lambda^2(2m+m')^2}}\left[1-\frac{k^2}{4\alpha_\rho^2}-\frac{3m'^2k^2}{4\alpha_\lambda^2(2m+m')^2}\right] \\
T_{3,\pm}^\lambda &= \pm im'k_0\frac{\sqrt{6}m}{(2m+m')\alpha_\lambda}e^{-\frac{3m^2k^2}{2\alpha_\lambda^2(2m+m')^2}} \\
T_{1,\pm}^\lambda &= T_{2,\pm}^\lambda = \mp i\frac{\sqrt{6}mk_0}{2\alpha_\lambda}\frac{m'}{2m+m'}e^{-\frac{k^2}{8\alpha_\rho^2}}e^{-\frac{3m'^2k^2}{8\alpha_\lambda^2(2m+m')^2}}.
\end{aligned} \tag{3.22}$$

On the other hand, the spin-flavor matrix elements are

$$\zeta_{j,0} \equiv \langle\psi_{B'_Q}|X_j^M S_{j,0}|\psi_{B_Q}\rangle \tag{3.23}$$

and

$$\zeta_{j,\pm} \equiv \langle\psi_{B'_Q}|X_j^M S_{j,\pm}|\psi_{B_Q}\rangle. \tag{3.24}$$

In turn, these matrix elements are split into the spin contribution of the $S_{j,m}$ operator, with the initial and final spin wave functions from Eqs. (1.62), and the flavor matrix elements of X_j^M for the flavor wave functions ϕ and ϕ'.

Because of the flavor symmetry properties of the total wave function for every single charm (or bottom) baryon, it is just necessary to calculate the spin expectation values for only two baryons, and the rest of baryon decays are similar to these first two, see Eqs (1.63) - (1.65). We take Σ_Q and Λ_Q, such that one is symmetric and the other is antisymmetric in flavor, respectively. This fact restricts the spin-orbit combinations, in such a way that we obtain all the independent spin configurations.

Table 3.1: Spin matrix elements $s_{i,m}$ for strong decays of heavy baryons $B_Q \to B'_Q + M$. The final states are from the $[21]_{20}$ multiplet with $J^P = 1/2^+$.

Initial State B	ν	$s_{1,-}$	$s_{2,-}$	$s_{3,-}$	$s_{1,z}$	$s_{2,z}$	$s_{3,z}$	$s_{1,+}$	$s_{2,+}$	$s_{3,+}$
${}^2\rho(\Sigma_Q)_J$	$\frac{1}{2}$	0	0	0	$-\frac{1}{2\sqrt{3}}$	$\frac{1}{2\sqrt{3}}$	0	$-\frac{1}{\sqrt{3}}$	$\frac{1}{\sqrt{3}}$	0
${}^2\lambda(\Sigma_Q)_J$	$\frac{1}{2}$	0	0	0	$\frac{1}{3}$	$\frac{1}{3}$	$-\frac{1}{6}$	$\frac{2}{3}$	$\frac{2}{3}$	$-\frac{1}{3}$
${}^4\lambda(\Sigma_Q)_J$	$\frac{1}{2}$	$-\frac{1}{\sqrt{6}}$	$-\frac{1}{\sqrt{6}}$	$\frac{2}{\sqrt{6}}$	$\frac{1}{3\sqrt{2}}$	$\frac{1}{3\sqrt{2}}$	$-\frac{2}{3\sqrt{2}}$	$\frac{1}{3\sqrt{2}}$	$\frac{1}{3\sqrt{2}}$	$-\frac{2}{3\sqrt{2}}$
${}^2\rho(\Lambda_Q)_J$	$\frac{1}{2}$	0	0	0	$-\frac{1}{2\sqrt{3}}$	$\frac{1}{2\sqrt{3}}$	0	$-\frac{1}{\sqrt{3}}$	$\frac{1}{\sqrt{3}}$	0
${}^2\lambda(\Lambda_Q)_J$	$\frac{1}{2}$	0	0	0	0	0	$\frac{1}{2}$	0	0	1
${}^4\rho(\Sigma_Q)_J$	$\frac{1}{2}$	$-\frac{1}{\sqrt{2}}$	$\frac{1}{\sqrt{2}}$	0	$\frac{1}{\sqrt{6}}$	$-\frac{1}{\sqrt{6}}$	0	$\frac{1}{\sqrt{6}}$	$-\frac{1}{\sqrt{6}}$	0

Table 3.2: Spin matrix elements $s_{i,m}$ with helicities $\nu = 1/2$ and $\nu = 3/2$ for strong decays of heavy baryons $B_Q \to B'_Q + M$. The final states are from the $[21]_{20}$ multiplet with $J^P = 3/2^+$.

Initial State B	ν	$s_{1,-}$	$s_{2,-}$	$s_{3,-}$	$s_{1,z}$	$s_{2,z}$	$s_{3,z}$	$s_{1,+}$	$s_{2,+}$	$s_{3,+}$
$^2\rho(\Sigma_Q)_J$	$\frac{1}{2}$	0	0	0	$\frac{1}{\sqrt{6}}$	$-\frac{1}{\sqrt{6}}$	0	$-\frac{1}{\sqrt{6}}$	$\frac{1}{\sqrt{6}}$	0
	$\frac{3}{2}$	0	0	0	0	0	0	$-\frac{1}{\sqrt{2}}$	$\frac{1}{\sqrt{2}}$	0
$^2\lambda(\Sigma_Q)_J$	$\frac{1}{2}$	0	0	0	$\frac{1}{3\sqrt{2}}$	$\frac{1}{3\sqrt{2}}$	$-\frac{2}{3\sqrt{2}}$	$-\frac{1}{3\sqrt{2}}$	$-\frac{1}{3\sqrt{2}}$	$\frac{2}{3\sqrt{2}}$
	$\frac{3}{2}$	0	0	0	0	0	0	$-\frac{1}{\sqrt{6}}$	$-\frac{1}{\sqrt{6}}$	$\frac{2}{\sqrt{6}}$
$^4\lambda(\Sigma_Q)_J$	$\frac{1}{2}$	$\frac{1}{\sqrt{3}}$	$\frac{1}{\sqrt{3}}$	$\frac{1}{\sqrt{3}}$	$\frac{1}{6}$	$\frac{1}{6}$	$\frac{1}{6}$	$\frac{2}{3}$	$\frac{2}{3}$	$\frac{2}{3}$
	$\frac{3}{2}$	0	0	0	$\frac{1}{2}$	$\frac{1}{2}$	$\frac{1}{2}$	$\frac{1}{\sqrt{3}}$	$\frac{1}{\sqrt{3}}$	$\frac{1}{\sqrt{3}}$
$^2\rho(\Lambda_Q)_J$	$\frac{1}{2}$	0	0	0	$\frac{1}{3\sqrt{2}}$	$\frac{1}{3\sqrt{2}}$	$-\frac{2}{3\sqrt{2}}$	$-\frac{1}{3\sqrt{2}}$	$-\frac{1}{3\sqrt{2}}$	$\frac{2}{3\sqrt{2}}$
	$\frac{3}{2}$	0	0	0	0	0	0	$-\frac{1}{\sqrt{6}}$	$-\frac{1}{\sqrt{6}}$	$\frac{2}{\sqrt{6}}$
$^2\lambda(\Lambda_Q)_J$	$\frac{1}{2}$	0	0	0	$\frac{1}{\sqrt{6}}$	$-\frac{1}{\sqrt{6}}$	0	$-\frac{1}{\sqrt{6}}$	$\frac{1}{\sqrt{6}}$	0
	$\frac{3}{2}$	0	0	0	0	0	0	$-\frac{1}{\sqrt{2}}$	$\frac{1}{\sqrt{2}}$	0
$^4\rho(\Sigma_Q)_J$	$\frac{1}{2}$	$\frac{1}{\sqrt{3}}$	$\frac{1}{\sqrt{3}}$	$\frac{1}{\sqrt{3}}$	$\frac{1}{6}$	$\frac{1}{6}$	$\frac{1}{6}$	$\frac{2}{3}$	$\frac{2}{3}$	$\frac{2}{3}$
	$\frac{3}{2}$	0	0	0	$\frac{1}{2}$	$\frac{1}{2}$	$\frac{1}{2}$	$\frac{1}{\sqrt{3}}$	$\frac{1}{\sqrt{3}}$	$\frac{1}{\sqrt{3}}$

Evaluation of the spin matrix elements are straightforward (results are presented in Tables 3.1 and 3.2), whereas the flavor matrix elements require a little more effort in order to be evaluated channel by channel. Fortunately, they can be calculated directly through the Wigner-Eckart theorem

$$\begin{aligned}\langle\phi'|X_j^M|\phi\rangle &= \langle(p_2,q_2),I_2,M_{I_2},Y_2|T^{(p,q),I,M_I,Y}|(p_1,q_1),I_1,M_{I_1},Y_1\rangle \\ &= \langle I_1,M_{I_1},I,M_I|I_2,M_{I_2}\rangle\sum_\gamma\left\langle\begin{matrix}(p_1,q_1) & (p,q)\\ I_1,Y_1 & I,Y\end{matrix}\middle|\begin{matrix}(p_2,q_2)_\gamma\\ I_2,Y_2\end{matrix}\right\rangle\langle(p_2,q_2)||T^{(p,q)}||(p_1,q_1)\rangle_\gamma.\end{aligned} \tag{3.25}$$

Here (p_i,q_i) refers to the $SU(3)$ labels from the flavor baryon multiplets, so they can be $(2,0)$ for the sextets, one with $J^P = 1/2^+$ or the other with $J^P = 3/2^+$, and $(0,1)$ for the anti-triplet with $J^P = 1/2^+$. The labels (p,q) are for the flavor meson multiplets $(1,1)$ or $(0,0)$. The subindex γ is associated to the different multiplicities, where the notation here involves the quantum numbers $(p,q),I,M_I,Y$ corresponding with the reduction of flavor algebra, Eq.(1.2).

A simplification on the flavor matrix elements in Eq. (3.25) is directly proportional (through the isospin Clebsh-Gordan coefficients) to the isoscalar factors times the reduced matrix elements. This separation allow us, on the one hand, to calculate the dependence on isospin I, M_I and hypercharge Y, and on the other hand to evaluate separately the couplings of the flavor multiplets (p,q). The results of this last couplings are in Table 3.3. The nonzero isoscalar factors in their matrix

representation for each decay channel are given by

$$(20) \longrightarrow (20) \oplus (11)$$
$$\begin{pmatrix} \Sigma_Q \\ \Xi'_Q \\ \Omega_Q \end{pmatrix} \longrightarrow \begin{pmatrix} \Sigma_Q\pi & \Sigma_Q\eta_8 & \Xi'_Q K \\ \Sigma_Q\bar{K} & \Xi'_Q\pi & \Xi'_Q\eta_8 \quad \Omega_Q K \\ & \Xi'_Q\bar{K} & \Omega_Q\eta_8 \end{pmatrix} = \frac{1}{\sqrt{40}} \begin{pmatrix} 24 & -4 & 12 \\ 18 & 9 & 1 \quad 12 \\ & 24 & 16 \end{pmatrix}^{1/2}$$

$$(20) \longrightarrow (01) \oplus (11)$$
$$\begin{pmatrix} \Sigma_Q \\ \Xi'_Q \\ \Omega_Q \end{pmatrix} \longrightarrow \begin{pmatrix} \Xi_Q K & \Lambda_Q\pi \\ \Xi_Q\eta_8 & \Xi_Q\pi \quad \Lambda_Q\bar{K} \\ & \Xi_Q\bar{K} \end{pmatrix} = \frac{1}{\sqrt{8}} \begin{pmatrix} -4 & 4 \\ -3 & 3 \quad 2 \\ & 8 \end{pmatrix}^{1/2}$$

$$(20) \longrightarrow (20) \oplus (00)$$
$$\begin{pmatrix} \Sigma_Q \\ \Xi'_Q \\ \Omega_Q \end{pmatrix} \longrightarrow \begin{pmatrix} \Sigma_Q\eta_1 \\ \Xi'_Q\eta_1 \\ \Omega_Q\eta_1 \end{pmatrix} = \begin{pmatrix} 1 \\ 1 \\ 1 \end{pmatrix}$$

$$(01) \longrightarrow (01) \oplus (11)$$
$$\begin{pmatrix} \Lambda_Q \\ \Xi_Q \end{pmatrix} \longrightarrow \begin{pmatrix} \Xi_Q K & \Lambda_Q\eta_8 \\ \Xi_Q\pi & \Xi_Q\eta_8 \quad \Lambda_Q\bar{K} \end{pmatrix} = \frac{1}{\sqrt{16}} \begin{pmatrix} -12 & 4 \\ -9 & -1 \quad 6 \end{pmatrix}^{1/2}$$

$$(01) \longrightarrow (20) \oplus (11)$$
$$\begin{pmatrix} \Lambda_Q \\ \Xi_Q \end{pmatrix} \longrightarrow \begin{pmatrix} \Xi'_Q K & \Sigma_Q\pi \\ \Omega_Q K & \Xi'_Q\eta_8 \quad \Xi'_Q\pi \quad \Sigma_Q\bar{K} \end{pmatrix} = \frac{1}{\sqrt{16}} \begin{pmatrix} -4 & -12 \\ 4 & -3 \quad 3 \quad -6 \end{pmatrix}^{1/2}$$

$$(01) \longrightarrow (01) \oplus (00)$$
$$\begin{pmatrix} \Lambda_Q \\ \Xi_Q \end{pmatrix} \longrightarrow \begin{pmatrix} \Xi_Q\eta_1 \\ \Lambda_Q\eta_1 \end{pmatrix} = \begin{pmatrix} 1 \\ 1 \end{pmatrix} \tag{3.26}$$

The spin-flavor matrix elements for an specific channel are calculated by multiplying their corresponding spin part, isospin Clebsh-Gordan coefficient, isoscalar factor and reduced matrix element together. Consequently, by also incorporating the orbital matrix elements, the helicity amplitudes $\mathcal{A}_\nu(k)$ of Eq. (3.15) are obtained.

Finally, the strong decay width of baryons by the emission of a pseudoscalar meson is

$$\Gamma(B_Q \to B'_Q + M) = 2\pi\rho \frac{2}{2J+1} \sum_{\nu>0} |\mathcal{A}_\nu(k)|^2, \tag{3.27}$$

where we take the rest frame of the final baryon B'_Q, in which the momentum of the emitted meson is given by

$$k^2 = -m_M^2 + \frac{(m_{B_Q}^2 - m_{B'_Q}^2 + m_M^2)^2}{4m_{B_Q}^2} \tag{3.28}$$

and the phase space factor is

$$\rho = 4\pi \frac{E_{B'_Q} E_M k}{m_{B_Q}}. \tag{3.29}$$

Table 3.3: $SU_f(3)$ Reduced Matrix Elements

$\langle(p_2,q_2)\|\|T^{(p,q)}\|\|(p_1,q_1)\rangle$				
(p_2,q_2)	(p_1,q_1)	$\langle T_1\rangle$	$\langle T_2\rangle$	$\langle T_3\rangle$
(2,0)	(2,0)	$\sqrt{\frac{10}{3}}$	$\sqrt{\frac{10}{3}}$	0
(2,0)	(0,1)	$\sqrt{2}$	- $\sqrt{2}$	0
(0,1)	(0,1)	- $\frac{2}{\sqrt{3}}$	- $\frac{2}{\sqrt{3}}$	0
(0,1)	(2,0)	2	-2	0

Of course, the energies of the resulting baryon and meson in these process are given by $E_{B'_Q} = \sqrt{m^2_{B'_Q} + k^2}$ and $E_M = \sqrt{m^2_M + k^2}$, respectively.

The theoretical strong decay widths were calculated as the sum of several significant contributions coming from the possible isospin channels. Each one of these combinations was established from selection rules of their quantum numbers. The numerical contribution to the total decay width from every initial ground or excited baryon state B_Q was evaluated, and the possible decay channels are configurations of ground state baryons B' and pseudoscalar mesons M. In any case, every one of these baryon states comes from either the flavor sextet $\mathbf{6}$ (with $S^P = 1/2^+$ or $3/2^+$) or the flavor anti-triplet $\bar{\mathbf{3}}$ (with $S^P = 1/2^+$). The results can be found from Table 3.4 to 3.9.

The results of the total strong decay widths calculated in the elementary-meson emission model are shown in Tables 3.10 and 3.11, and they are of the order of a few MeV. In these strong couplings there are two parameters g and h, which where fitted from the experimental widhts of two omega strong decays, they are $\Omega_c(3050)$ and $\Omega_c(3066)$, and are fixed for all the single charm and single bottom baryon decays calculated in this work. Specially, these resonances were marked with a star in Table 3.10. The values of these parameters are $g = 1.821$ GeV^{-1} and $h = -0.356$ GeV^{-1}.

3.1.1 Strong decay widths of Σ_Q and Λ_Q baryons

The total decay widths for Σ_Q states $\Gamma(^{2S+1}L(\Sigma_Q)_{J^P})$, are at most composed from the sum of four individual contributions. They correspond to different isospin channels as

$$\begin{aligned}\Gamma(^{2S+1}L(\Sigma_Q)_{J^P}) &= \Gamma(\Sigma_Q^* \to \Sigma_Q + \pi) + \Gamma(\Sigma_Q^* \to \Lambda_Q + \pi) \\ &\quad + \Gamma(\Sigma_Q^* \to {}^4\Sigma_Q + \pi) + \Gamma(\Sigma_Q^* \to \Sigma_Q + \eta),\end{aligned} \tag{3.30}$$

where we simplify the notation by choosing $^{2S+1}L(\Sigma_Q)_{J^P} \equiv \Sigma_Q^*$, and hereafter we generalize to all singly heavy quark baryons with $^{2S+1}L(B_Q)_{J^P} \equiv B_Q^*$. For Σ_c the first three terms are the most relevant, since those give the greatest contribution to the total width, as can be seen in Table 3.4. However, the fourth term of the η channel is different from zero (but much smaller than 1 MeV). In fact, a similar situation occurs for Σ_b, and this term is absent.

As far as currently information is available, the ground state resonances $\Sigma_c(2455)$ and $\Sigma_c(2520)$ are entirely dominated by the $\Lambda_c\pi$ channel in approximately 100% of the branching fraction [47, 62], and that is what naturally our study reflects. The $\Sigma_c(2800)$ resonance is assigned in our formalism to the state $^2\lambda(\Xi'_c)_{1/2^-}$. The decay width in this case was reported by the Belle Colaboration [63] and later confirmed by BaBar [64], where experimentally is reported $\Gamma = 69.67 \pm 41$ MeV with a large statistical uncertainty. In our prediction based in three channels $\Sigma_c\pi$, $\Lambda_c\pi$ and $\Sigma_c\pi$ we report a width consistently below this data.

In 2019 the LHCb Collaboration announced the observation of ground states $\Sigma_b^\pm$ with spin-parity $J^P = 1/2^+$ and $\Sigma_b^{*\pm}$ with $3/2^+$, where their masses and widths were measured with high precision [1]. Of course in comparison with the charm sector, now these widths are governed by the final states $\Lambda_b^0\pi^\pm$, as can be well understood in our description, see Table 3.5. In the same experimental

Table 3.4: Decay modes for charmed baryons Σ_c and Λ_c. Decay widhts are in MeV units.

State	$\Gamma(\Sigma_c\pi)$	$\Gamma(\Sigma_c\eta)$	$\Gamma(\Lambda_c\pi)$	$\Gamma(\Lambda_c\eta)$	$\Gamma(\Sigma_c^*\pi)$
$^2(\Sigma_c)_{1/2^+}$	–	–	0.572	–	–
$^4(\Sigma_c)_{3/2^+}$	–	–	3.458	–	–
$^2\lambda(\Sigma_c)_{1/2^-}$	0.827	–	1.963	–	0.763
$^4\lambda(\Sigma_c)_{1/2^-}$	1.038	–	4.884	–	0.877
$^2\lambda(\Sigma_c)_{3/2^-}$	6.193	–	4.679	–	0.947
$^4\lambda(\Sigma_c)_{3/2^-}$	0.400	–	0.964	–	5.396
$^4\lambda(\Sigma_c)_{5/2^-}$	3.209	–	5.643	–	8.226
$^2\rho(\Sigma_c)_{1/2^-}$	4.403	0.153	–	–	14.84
$^2\rho(\Sigma_c)_{3/2^-}$	8.997	0.099	–	–	12.242
$^2(\Lambda_c)_{1/2^+}$	–	–	–	–	–
$^2\lambda(\Lambda_c)_{1/2^-}$	0.035	–	–	–	–
$^2\lambda(\Lambda_c)_{3/2^-}$	0.043	–	–	–	–
$^2\rho(\Lambda_c)_{1/2^-}$	2.235	–	–	0.114	1.921
$^4\rho(\Lambda_c)_{1/2^-}$	1.648	–	–	0.274	1.382
$^2\rho(\Lambda_c)_{3/2^-}$	10.320	–	–	0.081	1.839
$^4\rho(\Lambda_c)_{3/2^-}$	0.728	–	–	0.123	13.054
$^4\rho(\Lambda_c)_{5/2^-}$	4.7165	–	–	1.004	12.683

data analysis, it was observed the resonance $\Sigma_b(6097)$, and reported with the assumption of relative angular momentum between the Λ_b^0 and $\pi^\pm$ taken to be 1. In our study we expect a total of five P-wave states described as λ-excitations and two P-wave states as ρ-excitations. From these excited states, we do the assignment $^2\lambda(\Sigma_b)_{1/2^-} \to \Sigma_b(6097)$.

We obtain the total decay widths for Λ_Q states, essentially, as the sum of three different partial widths

$$\Gamma(^{2S+1}L(\Lambda_Q)_{J^P}) = \Gamma(\Lambda_Q^* \to \Sigma_Q + \pi) + \Gamma(\Lambda_Q^* \to \Lambda_Q + \eta) + \Gamma(\Lambda_Q^* \to {}^4\Sigma_Q + \pi). \tag{3.31}$$

Unlike the Σ_Q states, for Λ_Q we expect the opposite description, such that we predict negative parity P-wave states as follows; five in ρ-mode and two in λ-mode. For these excited states we do the assignment $^2\lambda(\Lambda_c)_{1/2^-} \to \Lambda_c(2595)$, $^2\lambda(\Lambda_c)_{3/2^-} \to \Lambda_c(2625)$ and $^4\lambda(\Lambda_c)_{3/2^-} \to \Lambda_c(2940)$ while for states with bottom we link them as $^2\lambda(\Lambda_b)_{3/2^-} \to \Lambda_b(5912)$ and $^2\lambda(\Lambda_b)_{3/2^-} \to \Lambda_b(5920)$. Particularly, the strong decay widths for these last two resonances, together with the ground state Λ_b (Λ_c), are zero within our study with the elementary-meson emission model, where the LHCb Collaboration gives small upper limits [59] of less than 0.67 MeV, see Table 3.11. This fact shows a good agreement of our calculations with the data. One can observe that the smaller numbers are calculated for the widths of Λ_b, in comparison with Λ_c.

Experimentally, one has the total decay widths to compare with. In our study we report the decay widths they are within all these benchmarks for Σ_Q and Λ_Q, as is shown in Tables 3.10 and 3.11. This comparison gives support to our analysis and reveals a reasonable agreement from our calculations to the experimental data.

Although the structure of states for both single charm and single bottom baryons is similar from the quark model point of view, the large gap between their masses, in general, leads to smaller widths for charm sector in comparison with bottom sector.

3.1.2 Strong decay widths of Ξ_Q and Ξ_Q' baryons

In our classification we distinguish between baryons with a prime Ξ_Q' belonging to a flavor sextet **6**, and those without prime Ξ_Q belonging to a flavor antitriplet $\bar{\mathbf{3}}$. Nevertheless, all states coming from both Ξ_Q and Ξ_Q' are always isospin doublets, so they are related between themselves through $SU_f(2)$ flavor symmetry in their light quark structure.

Table 3.5: Decay modes for charmed baryons Σ_b and Λ_b. Decay widhts are in MeV units.

State	$\Gamma(\Sigma_b\pi)$	$\Gamma(\Lambda_b\pi)$	$\Gamma(\Sigma_b^*\pi)$
$^2(\Sigma_b)_{1/2^+}$	–	1.693	–
$^4(\Sigma_b)_{3/2^+}$	–	2.691	–
$^2\lambda(\Sigma_b)_{1/2^-}$	0.227	2.170	0.824
$^4\lambda(\Sigma_b)_{1/2^-}$	0.188	4.605	0.528
$^2\lambda(\Sigma_b)_{3/2^-}$	2.744	4.760	0.512
$^4\lambda(\Sigma_b)_{3/2^-}$	0.167	0.974	2.232
$^4\lambda(\Sigma_b)_{5/2^-}$	1.200	5.940	3.155
$^2\rho(\Sigma_b)_{1/2^-}$	2.941	–	12.017
$^2\rho(\Sigma_b)_{3/2^-}$	6.496	–	8.914
$^2(\Lambda_b)_{1/2^+}$	–	–	–
$^2\lambda(\Lambda_b)_{1/2^-}$	–	–	–
$^2\lambda(\Lambda_b)_{3/2^-}$	–	–	–
$^2\rho(\Lambda_b)_{1/2^-}$	0.196	–	0.783
$^4\rho(\Lambda_b)_{1/2^-}$	0.168	–	0.505
$^2\rho(\Lambda_b)_{3/2^-}$	2.650	–	0.485
$^4\rho(\Lambda_b)_{3/2^-}$	0.162	–	2.119
$^4\rho(\Lambda_b)_{5/2^-}$	1.172	–	3.055

From all studied baryons, the $\Xi_{c/b}^{(')}$ have the widest nonzero contribution of isospin channels, for in general they can be written maximum with 7 terms

$$\begin{aligned}\Gamma(^{2S+1}L(\Xi_Q^{(')})_{J^P}) &= \Gamma(\Xi_Q^{(')*}\to\Sigma_Q+\bar{K})+\Gamma(\Xi_Q^{(')*}\to\Lambda_Q+\bar{K})+\Gamma(\Xi_Q^{(')*}\to\Xi_Q+\pi)\\ &+\Gamma(\Xi_Q^{(')*}\to\Xi_Q+\eta)+\Gamma(\Xi_Q^{(')*}\to\Xi_Q'+\pi)+\Gamma(\Xi_Q^{(')*}\to{}^4\Sigma_Q+\bar{K})\\ &+\Gamma(\Xi_Q^{(')*}\to{}^4\Xi_Q'+\pi).\end{aligned}\tag{3.32}$$

There has been a lot of progress in the understanding of the $\Xi_Q^{(')}$ spectra. From a few years ago to date, the LHCb, Belle, BaBar together with other Collaborations have accumulated more and more data such that new resonances appear, among them, the following resonances have been reported $\Xi_c(2645)$, $\Xi_c(2790)$, $\Xi_c(2815)$, $\Xi_c(2930)$, $\Xi_c(2970)$, $\Xi_c(3055)$, $\Xi_c(3080)$ and $\Xi_c(3123)$. In our study we analyze some of these resonances in order to access and comprehend the spectra and the strong decays of all $\Xi_Q^{(')}$ baryons.

First of all we make the next states assignment: for positive parity S-wave states we have $^2(\Xi_c')_{1/2^+}\to\Xi_c(2578)$, $^4(\Xi_c')_{3/2^+}\to\Xi_c^*(2645)$, while for negative parity P-wave states $^2\rho(\Xi_c')_{1/2^-}\to\Xi_c(3055)$, $^2\rho(\Xi_c')_{3/2^-}\to\Xi_c(3080)$.

For baryons from the antitriplet $\bar{\mathbf{3}}$ we keep the analogue correspondence $^2(\Xi_c)_{1/2^+}\to\Xi_c(2469)$ for ground state, while $^2\lambda(\Xi_c)_{1/2^-}\to\Xi_c(2790)$ and $^2\lambda(\Xi_c)_{3/2^-}\to\Xi_c(2815)$ are λ-excitations.

Very recently, the results of the LHCb showed new single charm resonances $\Xi_c^0(2923)$ and $\Xi_c^0(2939)$ in the channel $\Lambda_c^+K^-$ [2]. Additionally the Collaboration reported the $\Xi_c^0(2965)$ state very close to the already known $\Xi_c^0(2970)$. They were observed with not only their masses and widths, but also with a possible relation between them. In our analysis, we establish the following assignment to these states $^4\lambda(\Xi_c')_{1/2^-}\to\Xi_c(2923)$, $^2\lambda(\Xi_c')_{3/2^-}\to\Xi_c(2939)$ and $^4\lambda(\Xi_c')_{3/2^-}\to\Xi_c(2965)$.

As has been previously discussed there exist a $SU_f(3)$ flavor symmetry relation between any baryon B_Q of the same multiplet, because the wave function of every single charm or single bottom baryon fundamentally differ each other only in the flavor part. Now, since the symmetry properties of wave functions for baryons $\Xi_Q^{(')}$ are not independent from Σ_Q and Λ_Q, by construction we have the same number of states for $\Xi_Q^{'}$ than for Σ_Q, that is to say, 9 states, and equality, the same 8 states for Ξ_Q than for Λ_Q (including in both cases the ground states).

Table 3.6: Decay modes for charmed baryons Ξ_c, Ξ_c' and Ω_c. Decay widhts are in MeV units.

State	$\Gamma(\Sigma_c\bar{K})$	$\Gamma(\Lambda_c\bar{K})$	$\Gamma(\Xi_c\pi)$	$\Gamma(\Xi_c\eta)$	$\Gamma(\Xi_c'\pi)$	$\Gamma(\Sigma_c^*\bar{K})$	$\Gamma(\Xi_c^{*'}\pi)$
$^2(\Xi_c')_{1/2^+}$	–	–	–	–	–	–	–
$^4(\Xi_c')_{3/2^+}$	–	–	0.698	–	–	–	–
$^2\lambda(\Xi_c')_{1/2^-}$	–	0.023	0.663	–	0.091	–	0.178
$^4\lambda(\Xi_c')_{1/2^-}$	–	0.178	1.622	–	0.083	–	0.130
$^2\lambda(\Xi_c')_{3/2^-}$	–	1.731	2.920	–	1.726	–	0.177
$^4\lambda(\Xi_c')_{3/2^-}$	0.003	0.426	0.656	–	0.113	–	0.924
$^4\lambda(\Xi_c')_{5/2^-}$	0.668	3.400	4.724	0.018	1.077	0.061	2.326
$^2\rho(\Xi_c')_{1/2^-}$	0.002	–	–	–	1.056	0.849	4.224
$^2\rho(\Xi_c')_{3/2^-}$	4.091	–	–	–	3.453	1.446	3.154
$^2(\Xi_c)_{1/2^+}$	–	–	–	–	–	–	–
$^2\lambda(\Xi_c)_{1/2^-}$	–	–	–	–	0.026	–	0.001
$^2\lambda(\Xi_c)_{3/2^-}$	–	–	–	–	0.164	–	0.053
$^2\rho(\Xi_c)_{1/2^-}$	0.756	0.262	1.077	–	0.337	–	0.435
$^4\rho(\Xi_c)_{1/2^-}$	0.689	0.980	2.670	–	0.287	–	0.328
$^2\rho(\Xi_c)_{3/2^-}$	0.436	2.479	3.625	–	2.756	–	0.398
$^4\rho(\Xi_c)_{3/2^-}$	0.077	0.557	0.783	–	0.169	1.043	1.993
$^4\rho(\Xi_c)_{5/2^-}$	1.583	3.705	5.092	0.071	1.368	1.407	3.413

For baryons with one bottom quark, since 2015 LHCb observed $\Xi_b^-(5935)$ and $\Xi_b^-(5955)$ resonances close to the threshold $\Xi_b\pi$ [3], where in the quark model we associate them with spin-parity $J^P = 1/2^+$ and $3/2^+$ prime ground states, respectively. For unprimed resonances Ξ_b and Ξ_b^* [4, 5] we assign the same quantum numbers. Of course, the main difference between our previous assignation are the multiplets to which those baryons belongs.

On the other hand, there had been other resonances: $\Xi_b^0(5945)$ was reported decaying to $\Xi_b\pi$ [6], and $\Xi_b^-(6227)$ was observed in 2018 in both Λ_bK and $\Xi_b\pi$ channels [7], with a width of $\simeq 18$ MeV. Because of the mass and width of the last resonance, in our analysis we assigned our state $^4\lambda(\Xi_b')_{5/2^-}$ to $\Xi_b^-(6227)$. Now, with more statistics that resonance is confirmed by the LHCb Collaboration [65].

We calculate not only the decay widths for every assigned state, but also the widths for the rest of the spectra $\Xi_{c/b}^{(')}$. Our results are listed in Table 3.10 for charm $\Xi_c^{(')}$ and in Table 3.11 for bottom $\Xi_b^{(')}$, in order that they can be compared with the experimental widths, and also with other works. All of the strong decays are in good agreement with the experimental data, with the only exception of $\Xi_c(3080)$, where our result is slightly above of the effective value. Therefore, it can be said that the resonances can be satisfactorily understood within the elementary-meson emission model.

3.1.3 Strong decay widths of Ω_Q baryons

According to the study of the isoscalar factors for the Ω_Q strong decays there are a total of three non zero contributions for the total decay widths, and they are $\Xi_Q'\bar{K}$, $\Xi_Q\bar{K}$ and $^4\Xi_Q'\bar{K}$. Then we have

$$\Gamma(^{2S+1}L(\Omega_Q)_{J^P}) \quad = \quad \Gamma(\Omega_Q^* \to \Xi_Q' + \bar{K}) + \Gamma(\Omega_Q^* \to \Xi_Q + \bar{K}) + \Gamma(\Omega_Q^* \to {}^4\Xi_Q' + \bar{K}). \quad (3.33)$$

In 2017, the LHCb Collaboration announced the observation of five resonances $\Omega_c(3000)$, $\Omega_c(3050)$, $\Omega_c(3065)$, $\Omega_c(3090)$ and $\Omega_c(3119)$ [8, 9]. At the same time, a further resonance was reported $\Omega_c(3188)$, but because the absence of enough statistic, they did not claim it as an authentic resonance. All these signals were discovered in the $\Xi_c^+K^-$ decay channel. One year later, the Belle Collaboration confirmed the observation of the first four resonances together with $\Omega_c(3188)$, however, they do not observe the $\Omega_c(3119)$.

Table 3.7: Decay modes for bottom baryons Ξ_b and Ξ_b'. Decay widhts are in MeV units.

State	$\Gamma(\Sigma_b\bar{K})$	$\Gamma(\Lambda_b\bar{K})$	$\Gamma(\Xi_b\pi)$	$\Gamma(\Xi_b'\pi)$	$\Gamma(\Sigma_b^*\bar{K})$	$\Gamma(\Xi_b^{*'}\pi)$
$^2(\Xi_b')_{1/2^+}$	–	–	–	–	–	–
$^4(\Xi_b')_{3/2^+}$	–	–	0.288	–	–	–
$^2\lambda(\Xi_b')_{1/2^-}$	–	0.033	0.642	0.001	–	0.158
$^4\lambda(\Xi_b')_{1/2^-}$	–	0.001	1.542	0.001	–	0.111
$^2\lambda(\Xi_b')_{3/2^-}$	–	1.068	2.754	0.610	–	0.100
$^4\lambda(\Xi_b')_{3/2^-}$	–	0.277	0.599	0.040	–	0.430
$^4\lambda(\Xi_b')_{5/2^-}$	–	2.161	3.950	0.324	–	0.807
$^2\rho(\Xi_b')_{1/2^-}$	–	–	–	0.645	0.401	3.908
$^2\rho(\Xi_b')_{3/2^-}$	1.005	–	–	2.301	1.267	2.627
$^2(\Xi_b)_{1/2^+}$	–	–	–	–	–	–
$^2\lambda(\Xi_b)_{1/2^-}$	–	–	–	–	–	–
$^2\lambda(\Xi_b)_{3/2^-}$	–	–	–	–	–	–
$^2\rho(\Xi_b)_{1/2^-}$	–	0.009	0.631	0.009	–	0.205
$^4\rho(\Xi_b)_{1/2^-}$	–	0.089	1.442	0.013	–	0.131
$^2\rho(\Xi_b)_{3/2^-}$	–	1.164	2.264	0.684	–	0.119
$^4\rho(\Xi_b)_{3/2^-}$	–	0.278	0.483	0.043	–	0.506
$^4\rho(\Xi_b)_{5/2^-}$	–	1.925	3.076	0.312	–	0.814

Table 3.8: Decay modes for charmed baryons Ω_c. Decay widhts are in MeV units.

State	$\Gamma(\Xi_c'\bar{K})$	$\Gamma(\Xi_c\bar{K})$	$\Gamma(^4\Xi_c'\bar{K})$
$^2(\Omega_c)_{1/2^+}$	–	–	–
$^4(\Omega_c)_{3/2^+}$	–	–	–
$^2\lambda(\Omega_c)_{1/2^-}$	–	1.924	–
$^4\lambda(\Omega_c)_{1/2^-}$	–	0.800	–
$^2\lambda(\Omega_c)_{3/2^-}$	–	3.500	–
$^4\lambda(\Omega_c)_{3/2^-}$	0.004	1.047	–
$^4\lambda(\Omega_c)_{5/2^-}$	1.799	14.046	0.988
$^2\rho(\Omega_c)_{1/2^-}$	0.838	–	0.005
$^2\rho(\Omega_c)_{3/2^-}$	4.580	–	2.586

The experimental knowledge on Ω_b has been expanded this year with the inclusion of more resonances to the spectra, since the LHCb collaboration reported 4 signals in $\Omega_b(6316)$, $\Omega_b(6330)$, $\Omega_b(6340)$ and $\Omega_b(6350)$ in the $\Xi_b^0K^-$ mass spectrum [10].

In this work we assign the quantum numbers of ground and excited states Ω_Q through the quark model. In tables 2.2 and 2.3 we presented our predictions for the mass spectra and we compare our results with the experimental data. Right there can bee seen all the assignments between our different states with the resonances.

Finally, looking at the total decay widths on Tables 3.10 and 3.11, for both sectors charm and bottom it can be seen a good agreement between our results and the experimental widths.

Some of the strong decay channels are forbidden by phase space.

Table 3.9: Decay modes for charmed baryons Ω_b. Decay widhts are in MeV units.

State	$\Gamma(\Xi_b' K)$	$\Gamma(\Xi_b K)$	$\Gamma(^4\Xi_b' K)$
$^2(\Omega_b)_{1/2^+}$	–	–	–
$^4(\Omega_b)_{3/2^+}$	–	–	–
$^2\lambda(\Omega_b)_{1/2^-}$	–	3.263	–
$^4\lambda(\Omega_b)_{1/2^-}$	–	3.663	–
$^2\lambda(\Omega_b)_{3/2^-}$	–	2.460	–
$^4\lambda(\Omega_b)_{3/2^-}$	–	0.149	–
$^4\lambda(\Omega_b)_{5/2^-}$	–	1.831	–
$^2\rho(\Omega_b)_{1/2^-}$	2.507	–	0.002
$^2\rho(\Omega_b)_{3/2^-}$	0.401	–	2.474

Table 3.10: Decay widths for charmed baryons in MeV.

State	Present work	Ref. [33, 34]	Ref. [66]	Exp	$\Gamma_{\rm tot}^{\rm exp}$
$^2(\Sigma_c)_{1/2^+}$	0.57	$\cdots$	$\cdots$	$\Sigma_c(2455)$	1.86 ± 0.19
$^4(\Sigma_c)_{3/2^+}$	3.36	$\cdots$	$\cdots$	$\Sigma_c(2520)$	15.04 ± 0.45
$^2\lambda(\Sigma_c)_{1/2^-}$	3.55	$\cdots$	22.65	$\Sigma_c(2800)$	69.67 ± 41
$^4\lambda(\Sigma_c)_{1/2^-}$	6.80	$\cdots$	17.63		
$^2\lambda(\Sigma_c)_{3/2^-}$	11.82	$\cdots$	36.5		
$^4\lambda(\Sigma_c)_{3/2^-}$	6.76	$\cdots$	24.69		
$^4\lambda(\Sigma_c)_{5/2^-}$	17.08	$\cdots$	33.22		
$^2\rho(\Sigma_c)_{1/2^-}$	19.40	$\cdots$	$\cdots$		
$^2\rho(\Sigma_c)_{3/2^-}$	21.34	$\cdots$	$\cdots$		
$^2(\Lambda_c)_{1/2^+}$	–	$\cdots$	$\cdots$	Λ_c	
$^2\lambda(\Lambda_c)_{1/2^-}$	0.05	$\cdots$	$\cdots$	$\Lambda_c(2595)$	2.6 ± 0.6
$^2\lambda(\Lambda_c)_{3/2^-}$	0.06	$\cdots$	$\cdots$	$\Lambda_c(2625)$	< 0.97
$^2\rho(\Lambda_c)_{1/2^-}$	4.27	$\cdots$	$\cdots$		
$^4\rho(\Lambda_c)_{1/2^-}$	3.31	$\cdots$	$\cdots$		
$^2\rho(\Lambda_c)_{3/2^-}$	12.24	$\cdots$	$\cdots$		
$^4\rho(\Lambda_c)_{3/2^-}$	13.90	$\cdots$	$\cdots$	$\Lambda_c(2940)$	20 ± 6
$^4\rho(\Lambda_c)_{5/2^-}$	18.40	$\cdots$	$\cdots$		
$^2(\Xi_c')_{1/2^+}$	–	–	$\cdots$	$\Xi_c'(2578)$	
$^4(\Xi_c')_{3/2^+}$	0.70	0.07	$\cdots$	$\Xi_c(2645)$	2.25 ± 0.41
$^2\lambda(\Xi_c')_{1/2^-}$	0.96	0.96	21.67		
$^4\lambda(\Xi_c')_{1/2^-}$	2.01	0.70	37.05	$\Xi_c(2923)$	7.1 ± 2.0
$^2\lambda(\Xi_c')_{3/2^-}$	6.55	3.56	20.89	$\Xi_c(2939)$	10.2 ± 0.14
$^4\lambda(\Xi_c')_{3/2^-}$	2.12	2.39	12.33	$\Xi_c(2965)$	14.1 ± 1.6
$^4\lambda(\Xi_c')_{5/2^-}$	12.28	7.66	20.2		
$^2\rho(\Xi_c')_{1/2^-}$	6.13	16.98	$\cdots$	$\Xi_c(3055)$	7.8 ± 1.9
$^2\rho(\Xi_c')_{3/2^-}$	12.14	8.70	$\cdots$	$\Xi_c(3080)$	4.6 ± 3.3
$^2(\Xi_c)_{1/2^+}$	–	–	$\cdots$	$\Xi_c(2469)$	
$^2\lambda(\Xi_c)_{1/2^-}$	0.02	0.49	3.61	$\Xi_c(2790)$	9.5 ± 2.0
$^2\lambda(\Xi_c)_{3/2^-}$	0.22	0.63	2.11	$\Xi_c(2815)$	2.48 ± 0.5
$^2\rho(\Xi_c)_{1/2^-}$	2.87	2.42	$\cdots$		
$^4\rho(\Xi_c)_{1/2^-}$	4.95	2.28	$\cdots$		
$^2\rho(\Xi_c)_{3/2^-}$	9.69	9.25	$\cdots$		
$^4\rho(\Xi_c)_{3/2^-}$	4.62	6.82	$\cdots$		
$^4\rho(\Xi_c)_{5/2^-}$	16.64	8.75	$\cdots$		
$^2(\Omega_c)_{1/2^+}$	–	–	$\cdots$	$\Omega_c(2695)$	$< 10^{-7}$
$^4(\Omega_c)_{3/2^+}$	–	–	$\cdots$	$\Omega_c(2770)$	
$^2\lambda(\Omega_c)_{1/2^-}$	1.92	0.48	4.38/4.28	$\Omega_c(3000)$	4.6 ± 0.6
$^4\lambda(\Omega_c)_{1/2^-}$	0.8*	1.0	–	$\Omega_c(3050)$	0.8 ± 0.2
$^2\lambda(\Omega_c)_{3/2^-}$	3.5*	3.5	4.96	$\Omega_c(3066)$	3.5 ± 0.4
$^4\lambda(\Omega_c)_{3/2^-}$	1.05	1.09	0.94	$\Omega_c(3090)$	8.7 ± 1.0
$^4\lambda(\Omega_c)_{5/2^-}$	16.83	9.87	9.53	$\Omega_c(3188)$	60 ± 26
$^2\rho(\Omega_c)_{1/2^-}$	6.28	4.92	$\cdots$		
$^2\rho(\Omega_c)_{3/2^-}$	7.04	3.82	$\cdots$		

Table 3.11: Decay widths for bottom baryons in MeV.

State	Present work	Ref. [33, 34]	Ref. [66]	Exp	$\Gamma_{\rm tot}^{\rm exp}$(MeV)
$^2(\Sigma_b)_{1/2^+}$	1.69	···	···	Σ_b	5.08 ± 0.365
$^4(\Sigma_b)_{3/2^+}$	2.69	···	···	Σ_b^*	10.01 ± 0.5
$^2\lambda(\Sigma_b)_{1/2^-}$	3.22	···	22.66	$\Sigma_b(6097)$	29.95 ± 4.6097
$^4\lambda(\Sigma_b)_{1/2^-}$	5.32	···	14.21		
$^2\lambda(\Sigma_b)_{3/2^-}$	8.02	···	39.29		
$^4\lambda(\Sigma_b)_{3/2^-}$	3.37	···	26.29		
$^4\lambda(\Sigma_b)_{5/2^-}$	10.29	···	38.34		
$^2\rho(\Sigma_b)_{1/2^-}$	14.96	···	···		
$^2\rho(\Sigma_b)_{3/2^-}$	15.41	···	···		
$^2(\Lambda_b)_{1/2^+}$	–	···	···	Λ_b	
$^2\lambda(\Lambda_b)_{1/2^-}$	–	···	···	$\Lambda_b(5912)$	< 0.66
$^2\lambda(\Lambda_b)_{3/2^-}$	–	···	···	$\Lambda_b(5920)$	< 0.63
$^2\rho(\Lambda_b)_{1/2^-}$	0.98	···	···		
$^4\rho(\Lambda_b)_{1/2^-}$	0.67	···	···		
$^2\rho(\Lambda_b)_{3/2^-}$	3.14	···	···		
$^4\rho(\Lambda_b)_{3/2^-}$	2.28	···	···		
$^4\rho(\Lambda_b)_{5/2^-}$	4.23	···	···		
$^2(\Xi_b')_{1/2^+}$	–	–	0.078	$\Xi_b'(5935)$	< 0.08
$^4(\Xi_b')_{3/2^+}$	0.29	0.03	0.98	$\Xi_b(5955)$	1.25 ± 0.6
$^2\lambda(\Xi_b')_{1/2^-}$	0.83	1.10	27.05		
$^4\lambda(\Xi_b')_{1/2^-}$	1.65	0.92	32.24		
$^2\lambda(\Xi_b')_{3/2^-}$	4.53	3.25	24.15		
$^4\lambda(\Xi_b')_{3/2^-}$	1.35	1.72	15.83		
$^4\lambda(\Xi_b')_{5/2^-}$	7.24	3.97	24.39	$\Xi_b(6227)$	18 ± 6
$^2\rho(\Xi_b')_{1/2^-}$	4.95	14.01	···		
$^2\rho(\Xi_b')_{3/2^-}$	7.20	6.19	···		
$^2(\Xi_b)_{1/2^+}$	–	–	···	$\Xi_b(5794)$	
$^2\lambda(\Xi_b)_{1/2^-}$	–	–	2.88		
$^2\lambda(\Xi_b)_{3/2^-}$	–	–	2.95		
$^2\rho(\Xi_b)_{1/2^-}$	0.85	1.63	···		
$^4\rho(\Xi_b)_{1/2^-}$	1.68	1.60	···		
$^2\rho(\Xi_b)_{3/2^-}$	4.23	4.18	···		
$^4\rho(\Xi_b)_{3/2^-}$	1.31	2.8	···		
$^4\rho(\Xi_b)_{5/2^-}$	6.13	4.69	···		
$^2(\Omega_b)_{1/2^+}$	–	–	···	Ω_b	$< 10^{-7}$
$^4(\Omega_b)_{3/2^+}$	–	–	···		
$^2\lambda(\Omega_b)_{1/2^-}$	3.26	0.50	49.38	$\Omega_b(6316)$	$< 2.8 \pm 4.2$
$^4\lambda(\Omega_b)_{1/2^-}$	3.66	2.79	94.98	$\Omega_b(6340)$	$< 1.5 \pm 1.8$
$^2\lambda(\Omega_b)_{3/2^-}$	2.46	1.14	1.82	$\Omega_b(6330)$	$< 3.1 \pm 4.7$
$^4\lambda(\Omega_b)_{3/2^-}$	0.15	0.62	0.22	$\Omega_b(6350)$	$< 2.8 \pm 3.2$
$^4\lambda(\Omega_b)_{5/2^-}$	1.83	4.28	1.60		
$^2\rho(\Omega_b)_{1/2^-}$	2.51	4.92	···		
$^2\rho(\Omega_b)_{3/2^-}$	2.88	3.82	···		

Chapter 4

Electromagnetic Couplings of Heavy Baryons

In the present Chapter is proposed an effective interaction Hamiltonian between the quark current and the electromagnetic field, with the proposal of considering process with the interaction of three lines between the quarks and the photon. Here is considered the emission (or absorption) of a photon by a quark. A general and detailed discussion of this process as well as the reduction of to a non-relativistic approximation is presented later in Chapter 6. Here we focus in the non-relativistic approximation of the electromagnetic interaction Hamiltonian.

4.1 The interaction Hamiltonian

A process of electromagnetic decay between a heavy baryon B_Q and a baryon of the ground state B'_Q is produced by the emission of a left-handed photon as a result of the electromagnetic coupling with the constituent quarks of the resonance.

$$B_Q \to B'_Q + \gamma \tag{4.1}$$

The non-relativistic Hamiltonian of interaction for the electromagnetic couplings is given by [38]

$$\mathcal{H}_{em} = 2\sqrt{\frac{\pi}{k_0}} \sum_{j=1}^{3} \mu_j \left[k s_{j,-} e^{-i\vec{k}\cdot\vec{r}_j} - \frac{1}{2g} \left(p_{j,-} e^{-i\vec{k}\cdot\vec{r}_j} + e^{-i\vec{k}\cdot\vec{r}_j} p_{j,-} \right) \right], \tag{4.2}$$

where $\vec{r}_j$, $\vec{p}_j$, $\vec{S}_j$ and μ_i are the coordinate, momentum, spin and magnetic moment of the $j$ht constituent, respectively. k_0 is the photon energy and $\vec{k} = k\hat{z}$ the momentum carried by the emitted photon along the quantization axis, z. The parameter g is related to the quark scale magnetic moment, which is taken to be $g = 1$, in order to have the magnetic moment of the proton. A simplification can be obtained by taking the photon momentum k with left-handed polarization $\epsilon^{*\mu} = \frac{1}{\sqrt{2}}(0, 1, -i, 0)$. The Feynman diagram related to this process is shown in Figure 4.1

The electromagnetic decays of a given baryon can be completely specified by defining matrix elements of Hamiltonian operator Eq. (4.2). In general, the expression for the helicity amplitudes of electromagnetic decays are denoted as

$$\mathcal{A}_\nu = \langle \psi_{B'_Q}; J', \nu - 1 | \mathcal{H}_{em} | \psi_{B_Q}; J, \nu \rangle, \qquad \nu = 1/2,\ 3/2. \tag{4.3}$$

Since the final states in which we are interested on are the ground states corresponding to baryons with total angular momentum and parity $\frac{1}{2}^+$ from Fig. 2.1, the possible values of the helicity can only be $\nu = \frac{1}{2}, -\frac{1}{2}$. One of them is between the initial baryon state with helicity $\nu = \frac{1}{2}$ and the final state with $\nu = -\frac{1}{2}$. The second possible matrix element is where the initial baryon has $\nu = \frac{3}{2}$ and

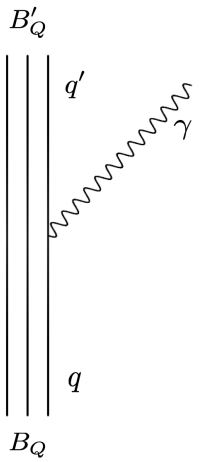

Fig. 4.1: Photon emission in a radiative decay $B_Q \to B'_Q + \gamma$.

the final state $\nu = \frac{1}{2}$. As was discussed in the previous section we are interested in radially excited states with at most one orbital excitation. Therefore, the selection rules for the quantum numbers of the initial baryons states B_Q turn out to be

$$\begin{aligned} J &= 1/2; \qquad \nu = 1/2 \\ J &= 3/2; \qquad \nu = 1/2, 3/2; \\ J &= 5/2; \qquad \nu = 1/2, 3/2. \end{aligned} \tag{4.4}$$

In order to calculate the helicity amplitudes of the baryons, it is necessary to expand the basis of total angular momentum $|(n_\rho l_\rho)(n_\lambda l_\lambda)L, S; JM\rangle$ to the uncoupled basis of angular momentum.

The final state is a ground state baryon with $L' = 0$ and $J' = S'$

$$|L = 1, S; JM\rangle = \sum_{m_l m_s} \langle L m_l S m_s | JM\rangle |L m_l, S m_s\rangle. \tag{4.5}$$

As a consequence the helicity amplitude can be reexpressed as

$$\begin{aligned} \mathcal{A}_\nu(k) &= \sum_{m_l, m_s} \langle L m_l S m_s | J\nu\rangle \langle \psi_{B'_Q} 0, 0; S' \nu - 1 | \mathcal{H}_{em} | \psi_{B_Q} L, m_l; S, m_s\rangle \\ &= 2\sqrt{\frac{\pi}{k_0}} \left\{ \langle L, 0; S\nu | J, \nu\rangle \langle \psi_{B'_Q} 0, 0; S', \nu - 1 | \sum_{j=1}^{3} \mu_j k s_{j,-} \hat{U}_j | \psi_{B_Q} L, 0; S, \nu\rangle \right. \\ &\quad \left. - \langle L, 1; S\nu - 1 | J, \nu\rangle \langle \psi_{B'_Q} 0, 0; S', \nu - 1 | \sum_{j=1}^{3} \mu_j \frac{1}{2g} \hat{T}_{j,-} | \psi_{B_Q} L, 1; S, \nu - 1\rangle \right\}, \end{aligned} \tag{4.6}$$

with the operators $\hat{U}_j$ and $\hat{T}_{j,-}$ previously defined.

Evidently, the relevant term with the information of the spin-flip part from the electromagnetic interaction Hamiltonian is the first one of Eq. (4.6). Indeed, the operator $\mu_j s_{j,-}$ only acts on the spin-flavor part of the total baryon wave function. The second term has the contribution of the orbit-flip due to the form of the operator $\hat{T}_{j,-}$ which gives a nonzero contribution for a decay where initial state corresponds to a radially excited state and final state corresponds to a ground state.

Table 4.1: Non vanishing spin-flip amplitudes for helicities $\nu = 1/2$ and $\nu = 3/2$ in the electromagnetic decays $\Sigma_Q^*(uuQ) \to {}^2\Sigma_Q(uuQ) + \gamma$ (top), $\Sigma_Q^*(uuQ) \to {}^4\Sigma_Q(uuQ) + \gamma$ (middle) and $\Sigma_Q^*(udQ) \to {}^2\Lambda_Q(udQ) + \gamma$ (bottom).

Σ_Q^*	ν	$\langle\mu_1 s_{1,-}\rangle$	$\langle\mu_2 s_{2,-}\rangle$	$\langle\mu_3 s_{3,-}\rangle$	CG
${}^4\Sigma_Q$	$\frac{1}{2}$	$-\frac{1}{3\sqrt{2}}\mu_u$	$-\frac{1}{3\sqrt{2}}\mu_u$	$\frac{2}{3\sqrt{2}}\mu_Q$	$\langle 00\frac{3}{2}\frac{1}{2}\vert J\frac{1}{2}\rangle$
	$\frac{3}{2}$	$-\frac{1}{\sqrt{6}}\mu_u$	$-\frac{1}{\sqrt{6}}\mu_u$	$\frac{2}{\sqrt{6}}\mu_Q$	$\langle 00\frac{3}{2}\frac{3}{2}\vert J\frac{3}{2}\rangle$
${}^2\rho(\Sigma_Q)_J$	$\frac{1}{2}$	$-\frac{1}{\sqrt{3}}\mu_u$	$\frac{1}{\sqrt{3}}\mu_u$	0	$\langle 10\frac{1}{2}\frac{1}{2}\vert J\frac{1}{2}\rangle$
${}^2\lambda(\Sigma_Q)_J$	$\frac{1}{2}$	$\frac{2}{3}\mu_u$	$\frac{2}{3}\mu_u$	$-\frac{1}{3}\mu_Q$	$\langle 10\frac{1}{2}\frac{1}{2}\vert J\frac{1}{2}\rangle$
${}^4\lambda(\Sigma_Q)_J$	$\frac{1}{2}$	$-\frac{1}{3\sqrt{2}}\mu_u$	$-\frac{1}{3\sqrt{2}}\mu_u$	$\frac{\sqrt{2}}{3}\mu_Q$	$\langle 10\frac{3}{2}\frac{1}{2}\vert J\frac{1}{2}\rangle$
	$\frac{3}{2}$	$-\frac{1}{\sqrt{6}}\mu_u$	$-\frac{1}{\sqrt{6}}\mu_u$	$\frac{2}{\sqrt{6}}\mu_Q$	$\langle 10\frac{3}{2}\frac{3}{2}\vert J\frac{3}{2}\rangle$
${}^2\rho(\Sigma_Q)_J$	$\frac{1}{2}$	$\frac{1}{\sqrt{6}}\mu_u$	$-\frac{1}{\sqrt{6}}\mu_u$	0	$\langle 10\frac{1}{2}\frac{1}{2}\vert J\frac{1}{2}\rangle$
${}^2\lambda(\Sigma_Q)_J$	$\frac{1}{2}$	$\frac{1}{3\sqrt{2}}\mu_u$	$\frac{1}{3\sqrt{2}}\mu_u$	$-\frac{2}{3\sqrt{2}}\mu_Q$	$\langle 10\frac{1}{2}\frac{1}{2}\vert J\frac{1}{2}\rangle$
${}^4\lambda(\Sigma_Q)_J$	$\frac{1}{2}$	$\frac{2}{3}\mu_u$	$\frac{2}{3}\mu_u$	$\frac{2}{3}\mu_Q$	$\langle 10\frac{3}{2}\frac{1}{2}\vert J\frac{1}{2}\rangle$
	$\frac{3}{2}$	$\frac{1}{\sqrt{3}}\mu_u$	$\frac{1}{\sqrt{3}}\mu_u$	$\frac{1}{\sqrt{3}}\mu_Q$	$\langle 10\frac{3}{2}\frac{3}{2}\vert J\frac{3}{2}\rangle$
${}^2\Sigma_Q$	$\frac{1}{2}$	$-\frac{1}{2\sqrt{3}}(\mu_u-\mu_d)$	$-\frac{1}{2\sqrt{3}}(\mu_u-\mu_d)$	0	$\langle 00\frac{1}{2}\frac{1}{2}\vert J\frac{1}{2}\rangle$
${}^4\Sigma_Q$	$\frac{1}{2}$	$-\frac{1}{2\sqrt{6}}(\mu_u-\mu_d)$	$-\frac{1}{2\sqrt{6}}(\mu_u-\mu_d)$	0	$\langle 00\frac{3}{2}\frac{1}{2}\vert J\frac{1}{2}\rangle$
	$\frac{3}{2}$	$-\frac{1}{2\sqrt{2}}(\mu_u-\mu_d)$	$-\frac{1}{2\sqrt{2}}(\mu_u-\mu_d)$	0	$\langle 00\frac{3}{2}\frac{3}{2}\vert J\frac{3}{2}\rangle$
${}^2\lambda(\Sigma_Q)_J$	$\frac{1}{2}$	$-\frac{1}{2\sqrt{3}}(\mu_u-\mu_d)$	$-\frac{1}{2\sqrt{3}}(\mu_u-\mu_d)$	0	$\langle 10\frac{1}{2}\frac{1}{2}\vert J\frac{1}{2}\rangle$
${}^4\lambda(\Sigma_Q)_J$	$\frac{1}{2}$	$-\frac{1}{2\sqrt{6}}(\mu_u-\mu_d)$	$-\frac{1}{2\sqrt{6}}(\mu_u-\mu_d)$	0	$\langle 10\frac{3}{2}\frac{1}{2}\vert J\frac{1}{2}\rangle$
	$\frac{3}{2}$	$-\frac{1}{2\sqrt{2}}(\mu_u-\mu_d)$	$-\frac{1}{2\sqrt{2}}(\mu_u-\mu_d)$	0	$\langle 10\frac{3}{2}\frac{3}{2}\vert J\frac{3}{2}\rangle$

Table 4.2: Non vanishing spin-flip amplitudes for helicities $\nu = 1/2$ and $\nu = 3/2$ in the electromagnetic decays $\Lambda_Q^*(udQ) \to {}^2\Lambda_Q(udQ) + \gamma$ (top), $\Lambda_Q^*(udQ) \to {}^2\Sigma_Q(udQ) + \gamma$ (middle) and $\Lambda_Q^*(udQ) \to {}^4\Sigma_Q(udQ) + \gamma$ (bottom).

Λ_Q^*	ν	$\langle\mu_1 s_{1,-}\rangle$	$\langle\mu_2 s_{2,-}\rangle$	$\langle\mu_3 s_{3,-}\rangle$	CG
${}^2\lambda(\Lambda_Q)_J$	$\frac{1}{2}$	0	0	μ_Q	$\langle 10\frac{1}{2}\frac{1}{2}\vert J\frac{1}{2}\rangle$
${}^2\rho(\Lambda_Q)_J$	$\frac{1}{2}$	$-\frac{1}{\sqrt{12}}(\mu_u+\mu_d)$	$\frac{1}{\sqrt{12}}(\mu_u+\mu_d)$	0	$\langle 10\frac{1}{2}\frac{1}{2}\vert J\frac{1}{2}\rangle$
${}^4\rho(\Lambda_Q)_J$	$\frac{1}{2}$	$-\frac{1}{2\sqrt{6}}(\mu_u+\mu_d)$	$\frac{1}{2\sqrt{6}}(\mu_u+\mu_d)$	0	$\langle 10\frac{3}{2}\frac{1}{2}\vert J\frac{1}{2}\rangle$
	$\frac{3}{2}$	$-\frac{1}{2\sqrt{2}}(\mu_u+\mu_d)$	$\frac{1}{2\sqrt{2}}(\mu_u+\mu_d)$	0	$\langle 10\frac{3}{2}\frac{3}{2}\vert J\frac{3}{2}\rangle$
${}^2\lambda(\Lambda_Q)_J$	$\frac{1}{2}$	$-\frac{1}{2\sqrt{3}}(\mu_u-\mu_d)$	$-\frac{1}{2\sqrt{3}}(\mu_u-\mu_d)$	0	$\langle 10\frac{1}{2}\frac{1}{2}\vert J\frac{1}{2}\rangle$
${}^2\rho(\Lambda_Q)_J$	$\frac{1}{2}$	$\frac{1}{3}(\mu_u-\mu_d)$	$-\frac{1}{3}(\mu_u-\mu_d)$	0	$\langle 10\frac{1}{2}\frac{1}{2}\vert J\frac{1}{2}\rangle$
${}^4\rho(\Lambda_Q)_J$	$\frac{1}{2}$	$-\frac{1}{6\sqrt{2}}(\mu_u-\mu_d)$	$\frac{1}{6\sqrt{2}}(\mu_u-\mu_d)$	0	$\langle 10\frac{3}{2}\frac{1}{2}\vert J\frac{1}{2}\rangle$
	$\frac{3}{2}$	$-\frac{1}{2\sqrt{6}}(\mu_u-\mu_d)$	$\frac{1}{2\sqrt{6}}(\mu_u-\mu_d)$	0	$\langle 10\frac{3}{2}\frac{3}{2}\vert J\frac{3}{2}\rangle$
${}^2\lambda(\Lambda_Q)_J$	$\frac{1}{2}$	$\frac{1}{2\sqrt{6}}(\mu_u-\mu_d)$	$\frac{1}{2\sqrt{6}}(\mu_u-\mu_d)$	0	$\langle 10\frac{1}{2}\frac{1}{2}\vert J\frac{1}{2}\rangle$
${}^2\rho(\Lambda_Q)_J$	$\frac{1}{2}$	$\frac{1}{6\sqrt{2}}(\mu_u-\mu_d)$	$-\frac{1}{6\sqrt{2}}(\mu_u-\mu_d)$	0	$\langle 10\frac{1}{2}\frac{1}{2}\vert J\frac{1}{2}\rangle$
${}^4\rho(\Lambda_Q)_J$	$\frac{1}{2}$	$\frac{1}{3}(\mu_u-\mu_d)$	$-\frac{1}{3}(\mu_u-\mu_d)$	0	$\langle 10\frac{3}{2}\frac{1}{2}\vert J\frac{1}{2}\rangle$
	$\frac{3}{2}$	$\frac{1}{2\sqrt{3}}(\mu_u-\mu_d)$	$-\frac{1}{2\sqrt{3}}(\mu_u-\mu_d)$	0	$\langle 10\frac{3}{2}\frac{3}{2}\vert J\frac{3}{2}\rangle$

Similarly to the strong couplings, in the electromagnetic decays there is a contribution from both the matrix elements corresponding to the radial part, and a contribution from the spin-flavor part of the total baryon wave function. In the Appendix B, I present an illustrative example to obtain both types of contributions for an electromagnetic decay process, whose initial state has one quantum of radial excitation in λ, and the decaying baryon is from ground state. Here the transition matrix element is evaluated for an operator $\hat{U}_{\lambda,3}$ defined implicitly from $\vec{r}_3$ in the baryon coordinate system.

The results of the radial contribution of the orbital matrix elements for both the spin-flip and

the orbit-flip operator are given by

$$\begin{aligned} U_1^\rho = -U_2^\rho &= -i\frac{k}{2\alpha_\rho}e^{-\frac{k^2}{8\alpha_\rho^2}}e^{-\frac{3}{8}\left(\frac{m'k}{\alpha_\lambda(2m+m')}\right)^2} \\ U_3^\rho &= 0 \\ U_1^\lambda = U_2^\lambda &= -i\frac{1}{2\alpha_\lambda}\frac{\sqrt{3}m'k}{2m+m'}e^{-\frac{k^2}{8\alpha_\rho^2}}e^{-\frac{3m'^2k^2}{8\alpha_\lambda^2(2m+m')^2}} \\ U_3^\lambda &= i\frac{\sqrt{3}m}{2m+m'}\frac{k}{\alpha_\lambda}e^{-\frac{3m^2k^2}{2\alpha_\lambda^2(2m+m')^2}} \end{aligned} \tag{4.7}$$

and

$$\begin{aligned} T_1^\rho = -T_2^\rho &= imk_0\frac{1}{\sqrt{2}\alpha_\rho}e^{-\frac{k^2}{8\alpha_\rho^2}}e^{-\frac{3}{8}\left(\frac{m'k}{\alpha_\lambda(2m+m')}\right)^2} \\ T_3^\rho &= 0 \\ T_1^\lambda = T_2^\lambda &= imk_0\frac{\sqrt{6}}{2}\frac{1}{\alpha_\lambda}\frac{m'}{2m+m'}e^{-\frac{k^2}{8\alpha_\rho^2}}e^{-\frac{3}{8}\left(\frac{m'k}{\alpha_\lambda(2m+m')}\right)^2} \\ T_3^\lambda &= -im'k_0\frac{\sqrt{6}m}{2m+m'}\frac{1}{\alpha_\lambda}e^{-\frac{3}{2}\left(\frac{mk}{\alpha_\lambda(2m+m')}\right)^2}, \end{aligned} \tag{4.8}$$

respectively, where definitions of $U_{\alpha,i}$ and $T_{\alpha,i}$ with $\alpha = \rho, \lambda$ and $i = 1, 2, 3$ are the usual ones as those presented in the strong couplings. For the ground states one obtains

$$U_{3,0} = e^{-\frac{3m^2k^2}{2\alpha_\lambda^2(2m+m')^2}} \tag{4.9}$$

$$U_{1,0} = U_{2,0} = e^{-\frac{k^2}{8\alpha_\rho^2}}e^{-\frac{3m'^2k^2}{8\alpha_\lambda^2(2m+m')^2}} \tag{4.10}$$

As it was already discussed, for the single charm and single bottom baryons, we have symmetry relations in their wave function Eqs. (1.63) - (1.65), particularly, in their spin-orbit part we obtained only two independent combinations. We choose take Σ_Q and Λ_Q, such that the rest of heavy baryons in the sextet **6** and/or in the antitriplet $\bar{\mathbf{3}}$ representations can be obtained by means of the flavor symmetry of $SU_f(3)$.

In this work, we are interested in studying the radiative decay widths of the singly heavy baryons not only for spin-parity $J^P = 1/2^+$ -sextet and -antitriplet, but also for the spin-parity $J^P = 3/2^+$ -sextet. For this proposal we focused on all the independent transitions going from states ${}^{2S+1}L(\Sigma_Q)_{J^P} \equiv \Sigma_Q^*$ and ${}^{2S+1}L(\Lambda_Q)_{J^P} \equiv \Lambda_Q^*$ towards the allowed ground states. Thus, we have on the one hand $\Sigma_Q^* \to {}^2\Sigma_Q + \gamma$, $\Sigma_Q^* \to {}^4\Sigma_Q + \gamma$ and $\Sigma_Q^* \to {}^2\Lambda_Q + \gamma$, and on the other hand $\Lambda_Q^* \to {}^2\Lambda_Q + \gamma$, $\Lambda_Q^* \to {}^2\Sigma_Q + \gamma$ and $\Lambda_Q^* \to {}^4\Sigma_Q + \gamma$. We calculate the contribution of the spin-flavor matrix elements from the electromagnetic Hamiltonian 4.2, for both the spin- and the orbit-flip terms. Our results are listed in Tables 4.1 - 4.4.

Taking all the matrix elements and factors into account, it is straightforward to write the analytical expressions of the helicity amplitudes. We present our results in Tables 4.5 and 4.6.

Table 4.4: Non vanishing orbit-flip amplitudes for helicities $\nu = 1/2$ and $\nu = 3/2$ in the electromagnetic decays $\Lambda_Q^*(udQ) \to {}^2\Lambda_Q(udQ) + \gamma$ (top), $\Lambda_Q^*(udQ) \to {}^2\Sigma_Q(udQ) + \gamma$ (middle) and $\Lambda_Q^*(udQ) \to {}^4\Sigma_Q(udQ) + \gamma$ (bottom).

Λ_Q^*	ν	$\langle\mu_1\rangle$	$\langle\mu_2\rangle$	$\langle\mu_3\rangle$	CG
${}^2\lambda(\Lambda_Q)_J$	$\frac{1}{2}$	$\frac{1}{2}(\mu_u+\mu_d)$	$\frac{1}{2}(\mu_u+\mu_d)$	μ_Q	$\langle 11\frac{1}{2}\text{-}\frac{1}{2}\vert J\frac{1}{2}\rangle$
${}^2\lambda(\Lambda_Q)_J$	$\frac{3}{2}$	$\frac{1}{2}(\mu_u+\mu_d)$	$\frac{1}{2}(\mu_u+\mu_d)$	μ_Q	$\langle 11\frac{1}{2}\frac{1}{2}\vert J\frac{3}{2}\rangle$
${}^2\rho(\Lambda_Q)_J$	$\frac{1}{2}$	$\frac{1}{2}(\mu_u-\mu_d)$	$\text{-}\frac{1}{2}(\mu_u-\mu_d)$	0	$\langle 11\frac{1}{2}\text{-}\frac{1}{2}\vert J\frac{1}{2}\rangle$
${}^2\rho(\Lambda_Q)_J$	$\frac{3}{2}$	$\frac{1}{2}(\mu_u-\mu_d)$	$\text{-}\frac{1}{2}(\mu_u-\mu_d)$	0	$\langle 11\frac{1}{2}\frac{1}{2}\vert J\frac{3}{2}\rangle$
${}^4\rho(\Lambda_Q)_J$	$\frac{1}{2}$	$\frac{1}{2}(\mu_u-\mu_d)$	$\text{-}\frac{1}{2}(\mu_u-\mu_d)$	0	$\langle 11\frac{3}{2}\text{-}\frac{1}{2}\vert J\frac{1}{2}\rangle$
${}^4\rho(\Lambda_Q)_J$	$\frac{3}{2}$	$\frac{1}{2}(\mu_u-\mu_d)$	$\text{-}\frac{1}{2}(\mu_u-\mu_d)$	0	$\langle 11\frac{3}{2}\frac{1}{2}\vert J\frac{3}{2}\rangle$

Table 4.3: Non vanishing orbit-flip amplitudes for helicities $\nu = 1/2$ and $\nu = 3/2$ in the electromagnetic decays $\Sigma_Q^*(uuQ) \to {}^2\Sigma_Q(uuQ) + \gamma$ (top), $\Sigma_Q^*(uuQ) \to {}^4\Sigma_Q(uuQ) + \gamma$ (middle) and $\Sigma_Q^*(udQ) \to {}^2\Lambda_Q((udQ)) + \gamma$ (bottom).

Σ_Q^*	ν	$\langle\mu_1\rangle$	$\langle\mu_2\rangle$	$\langle\mu_3\rangle$	CG
${}^2\lambda(\Sigma_Q)_J$	$\frac{1}{2}$	μ_u	μ_u	μ_Q	$\langle 11\frac{1}{2}\text{-}\frac{1}{2}\vert J\frac{1}{2}\rangle$
	$\frac{3}{2}$	μ_u	μ_u	μ_Q	$\langle 11\frac{1}{2}\frac{1}{2}\vert J\frac{3}{2}\rangle$
${}^4\lambda(\Sigma_Q)_J$	$\frac{1}{2}$	μ_u	μ_u	μ_Q	$\langle 11\frac{3}{2}\text{-}\frac{1}{2}\vert J\frac{1}{2}\rangle$
	$\frac{3}{2}$	μ_u	μ_u	μ_Q	$\langle 11\frac{3}{2}\frac{1}{2}\vert J\frac{3}{2}\rangle$
${}^2\rho(\Sigma_Q)_J$	$\frac{1}{2}$	$\frac{1}{2}(\mu_u - \mu_d)$	$-\frac{1}{2}(\mu_u - \mu_d)$	0	$\langle 11\frac{1}{2}\text{-}\frac{1}{2}\vert J\frac{1}{2}\rangle$
	$\frac{3}{2}$	$\frac{1}{2}(\mu_u - \mu_d)$	$-\frac{1}{2}(\mu_u - \mu_d)$	0	$\langle 11\frac{1}{2}\frac{1}{2}\vert J\frac{3}{2}\rangle$

The helicity amplitude is related to the radiative decay width through

$$\Gamma(B_Q \to B'_Q + \gamma) = 2\pi\rho\frac{1}{(2\pi)^3}\frac{2}{2J+1}\sum_{\nu>0}|\mathcal{A}_\nu(k)|^2. \tag{4.11}$$

Here the widths are calculated in the rest frame of the final baryon B'_Q, where the momentum of the emitted photon is

$$k = \frac{m_{B_Q}^2 - m_{B'_Q}^2}{2m_{B_Q}}, \tag{4.12}$$

and the phase space factor has the following form

$$\rho = 4\pi\frac{E_{B'_Q}k^2}{m_{B_Q}}. \tag{4.13}$$

The energy of the decaying baryon in this process is $E_{B'_Q} = \sqrt{m_{B'_Q}^2 + k^2}$. The value of factor $g = 1$ is taken for all electromagnetic decays.

We estimate the radiative decay widths, and compared our results with other approaches. In Table 4.7 we present our result between ground states. From Tables 4.8 to 4.14 we have the electromagnetic decay widths for radially excited states. Unlike the case of strong couplings where we obtained widths of a few MeV, in electromagnetic couplings we obtain smaller widths of the order of KeV.

A few months ago, for the first time The Belle Collaboration reported the electromagnetic decay of the excited charm baryons $\Xi_c(2790)$ and $\Xi_c(2815)$. They determined the partial widths of the electromagnetic decays for neutral baryons as $\Gamma(\Xi_c^0(2815) \to \Xi_c^0 + \gamma) = 320 \pm 45$ KeV and $\Gamma(\Xi_c^0(2790) \to \Xi_c^0 + \gamma) = 800 \pm 320$ KeV, while for charged baryons they gave the following upper limits to their widths $\Gamma(\Xi_c^+(2815) \to \Xi_c^+ + \gamma) < 80$ KeV and $\Gamma(\Xi_c^+(2790) \to \Xi_c^+ + \gamma) < 350$ KeV.

We already identify these resonances with λ-exited states and we calculated the radiative decay widths as $\Gamma(\Xi_c^0(2815) \to \Xi_c^0 + \gamma) = 711.45$ KeV, $\Gamma(\Xi_c^0(2790) \to \Xi_c^0 + \gamma) = 547.16$ KeV, $\Gamma(\Xi_c^+(2815) \to \Xi_c^+ + \gamma) = 2.80$ KeV and $\Gamma(\Xi_c^+(2790) \to \Xi_c^+ + \gamma) = 0.92$ KeV.

Table 4.5: Helicity amplitudes for photocouplings of heavy baryons, $\Sigma_Q^*(uuQ) \to {}^2\Sigma_Q(uuQ) + \gamma$ (top), $\Sigma_Q^*(uuQ) \to {}^4\Sigma_Q(uuQ) + \gamma$ (middle) and $\Sigma_Q^*(udQ) \to {}^2\Lambda_Q(udQ) + \gamma$ (bottom).

Σ_Q^*	J	$A_{\frac{1}{2}}/2\sqrt{\frac{\pi}{k_0}}$	$A_{\frac{3}{2}}/2\sqrt{\frac{\pi}{k_0}}$
${}^4\Sigma_Q$	$\frac{3}{2}$	$k\frac{2}{3\sqrt{2}}\left(-\mu_u U_{0,1} + \mu_Q U_{0,3}\right)$	$k\frac{2}{\sqrt{6}}\left(-\mu_u U_{0,1} + \mu_Q U_{0,3}\right)$
${}^2\lambda(\Sigma_Q)_J$	$\frac{1}{2}$	$k\frac{1}{3\sqrt{3}}\left(-4\mu_u U_{\lambda,1} + \mu_Q U_{\lambda,3}\right) - \frac{1}{g}\sqrt{\frac{2}{3}}\left(2\mu_u T_{\lambda,1} + \mu_Q T_{\lambda,3}\right)$	0
	$\frac{3}{2}$	$k\frac{1}{3}\sqrt{\frac{2}{3}}\left(4\mu_u U_{\lambda,1} - \mu_Q U_{\lambda,3}\right) - \frac{1}{g}\frac{1}{\sqrt{3}}\left(2\mu_u T_{\lambda,1} + \mu_Q T_{\lambda,3}\right)$	$-\frac{1}{g}\left(2\mu_u T_{\lambda,1} + \mu_Q T_{\lambda,3}\right)$
${}^2\rho(\Sigma_Q)_J$	$\frac{1}{2}$	$\frac{2}{3}k\mu_u U_{\rho,1}$	0
	$\frac{3}{2}$	$-\frac{2\sqrt{2}}{3}k\mu_u U_{\rho,1}$	0
${}^4\lambda(\Sigma_Q)_J$	$\frac{1}{2}$	$k\frac{1}{3}\sqrt{\frac{2}{3}}\left(\mu_u U_{\lambda,1} - \mu_Q U_{\lambda,3}\right)$	0
	$\frac{3}{2}$	$k\frac{1}{3}\sqrt{\frac{2}{15}}\left(\mu_u U_{\lambda,1} - \mu_Q U_{\lambda,3}\right)$	$k\frac{2}{\sqrt{10}}\left(\mu_u U_{\lambda,1} - \mu_Q U_{\lambda,3}\right)$
	$\frac{5}{2}$	$k\sqrt{\frac{2}{15}}\left(-\mu_u U_{\lambda,1} + \mu_Q U_{\lambda,3}\right)$	$k\frac{2}{\sqrt{15}}\left(-\mu_u U_{\lambda,1} + \mu_Q U_{\lambda,3}\right)$
${}^2\lambda(\Sigma_Q)_J$	$\frac{1}{2}$	$-k\frac{2}{3\sqrt{6}}\left(\mu_u U_{\lambda,1} - \mu_Q U_{\lambda,3}\right)$	0
	$\frac{3}{2}$	$k\frac{2}{3\sqrt{3}}\left(\mu_u U_{\lambda,1} - \mu_Q U_{\lambda,3}\right)$	0
${}^2\rho(\Sigma_Q)_J$	$\frac{1}{2}$	$-\frac{2}{3\sqrt{2}}k\mu_u U_{\rho,1}$	0
	$\frac{3}{2}$	$\frac{2}{3}k\mu_u U_{\rho,1}$	0
${}^4\lambda(\Sigma_Q)_J$	$\frac{1}{2}$	$-k\frac{2}{3\sqrt{3}}\left(2\mu_u U_{\lambda,1} + \mu_Q U_{\lambda,3}\right) - \frac{1}{g}\frac{1}{\sqrt{6}}\left(2\mu_u T_{\lambda,1} + \mu_Q T_{\lambda,3}\right)$	0
	$\frac{3}{2}$	$-k\frac{2}{3\sqrt{15}}\left(2\mu_u U_{\lambda,1} + \mu_Q U_{\lambda,3}\right) - \frac{1}{g}\sqrt{\frac{8}{15}}\left(2\mu_u T_{\lambda,1} + \mu_Q T_{\lambda,3}\right)$	$-k\frac{1}{\sqrt{5}}\left(2\mu_u U_{\lambda,1} + \mu_Q U_{\lambda,3}\right) - \frac{1}{g}\sqrt{\frac{2}{5}}\left(2\mu_u T_{\lambda,1} + \mu_Q T_{\lambda,3}\right)$
	$\frac{5}{2}$	$k\frac{2}{\sqrt{15}}\left(2\mu_u U_{\lambda,1} + \mu_Q U_{\lambda,3}\right) - \frac{1}{g}\sqrt{\frac{3}{10}}\left(2\mu_u T_{\lambda,1} + \mu_Q T_{\lambda,3}\right)$	$k\sqrt{\frac{2}{15}}\left(2\mu_u U_{\lambda,1} + \mu_Q U_{\lambda,3}\right) - \frac{1}{g}\sqrt{\frac{3}{5}}\left(2\mu_u T_{\lambda,1} + \mu_Q T_{\lambda,3}\right)$
${}^2\Sigma_Q$	$\frac{1}{2}$	$-k\frac{1}{\sqrt{3}}\left(\mu_u - \mu_d\right)U_{0,1}$	0
${}^4\Sigma_Q$	$\frac{3}{2}$	$-k\frac{1}{\sqrt{6}}\left(\mu_u - \mu_d\right)U_{0,1}$	$-k\frac{1}{\sqrt{2}}\left(\mu_u - \mu_d\right)U_{0,1}$
${}^2\lambda(\Sigma_Q)_J$	$\frac{1}{2}$	$k\frac{1}{3}\left(\mu_u - \mu_d\right)U_{\lambda,1}$	0
	$\frac{3}{2}$	$-k\frac{\sqrt{2}}{3}\left(\mu_u - \mu_d\right)U_{\lambda,1}$	0
${}^2\rho(\Sigma_Q)_J$	$\frac{1}{2}$	$-\frac{1}{g}\sqrt{\frac{2}{3}}\left(\mu_u - \mu_d\right)T_{\rho,1}$	0
	$\frac{3}{2}$	$-\frac{1}{g}\frac{1}{\sqrt{3}}\left(\mu_u - \mu_d\right)T_{\rho,1}$	$-\frac{1}{g}\left(\mu_u - \mu_d\right)T_{\rho,1}$
${}^4\lambda(\Sigma_Q)_J$	$\frac{1}{2}$	$k\frac{1}{3\sqrt{2}}\left(\mu_u - \mu_d\right)U_{\lambda,1}$	0
	$\frac{3}{2}$	$k\frac{1}{3\sqrt{10}}\left(\mu_u - \mu_d\right)U_{\lambda,1}$	$k\sqrt{\frac{3}{10}}\left(\mu_u - \mu_d\right)U_{\lambda,1}$
	$\frac{5}{2}$	$-k\frac{1}{\sqrt{10}}\left(\mu_u - \mu_d\right)U_{\lambda,1}$	$-k\frac{1}{\sqrt{5}}\left(\mu_u - \mu_d\right)U_{\lambda,1}$

Table 4.6: Helicity amplitudes for photocouplings of heavy baryons, $\Lambda_Q^*(udQ) \to {}^2\Lambda_Q(udQ) + \gamma$ (top), $\Lambda_Q^*(udQ) \to {}^2\Sigma_Q(udQ) + \gamma$ (middle) and $\Lambda_Q^*(udQ) \to {}^4\Sigma_Q(udQ) + \gamma$ (bottom).

Λ_Q^*	J	$\mathcal{A}_{\frac{1}{2}}/2\mu\sqrt{\frac{\pi}{k_0}}$	$\mathcal{A}_{\frac{3}{2}}/2\mu\sqrt{\frac{\pi}{k_0}}$
${}^2\lambda(\Lambda_Q)_J$	$\frac{1}{2}$	$-k\frac{1}{\sqrt{3}}\mu_Q U_{\lambda,3} - \frac{1}{g}\sqrt{\frac{2}{3}}\left((\mu_u+\mu_d)T_{\lambda,1} + \mu_Q T_{\lambda,3}\right)$	0
	$\frac{3}{2}$	$k\sqrt{\frac{2}{3}}\mu_Q U_{\lambda,3} - \frac{1}{g}\frac{1}{\sqrt{3}}\left((\mu_u+\mu_d)T_{\lambda,1} + \mu_Q T_{\lambda,3}\right)$	$-\frac{1}{g}\left((\mu_u+\mu_d)T_{\lambda,1} + \mu_Q T_{\lambda,3}\right)$
${}^2\rho(\Lambda_Q)_J$	$\frac{1}{2}$	$k\frac{1}{3}(\mu_u+\mu_d)U_{\rho,1}$	0
	$\frac{3}{2}$	$-k\frac{\sqrt{2}}{3}(\mu_u+\mu_d)U_{\rho,1}$	0
${}^4\rho(\Lambda_Q)_J$	$\frac{1}{2}$	$k\frac{1}{\sqrt{3}}\frac{1}{\sqrt{6}}(\mu_u+\mu_d)U_{\rho,1}$	0
	$\frac{3}{2}$	$k\frac{1}{3\sqrt{10}}(\mu_u+\mu_d)U_{\rho,1}$	$\sqrt{\frac{3}{10}}k(\mu_u+\mu_d)U_{\rho,1}$
	$\frac{5}{2}$	$-k\frac{1}{\sqrt{10}}(\mu_u+\mu_d)U_{\rho,1}$	$-\frac{1}{\sqrt{5}}k(\mu_u+\mu_d)U_{\rho,1}$
${}^2\lambda(\Lambda_Q)_J$	$\frac{1}{2}$	$k\frac{1}{3}(\mu_u-\mu_d)U_{\lambda,1}$	0
	$\frac{3}{2}$	$-k\frac{\sqrt{2}}{3}(\mu_u-\mu_d)U_{\lambda,1}$	0
${}^2\rho(\Lambda_Q)_J$	$\frac{1}{2}$	$-k\frac{2}{3\sqrt{3}}(\mu_u-\mu_d)U_{\rho,1} - \frac{1}{g}\sqrt{\frac{2}{3}}(\mu_u-\mu_d)T_{\rho,1}$	0
	$\frac{3}{2}$	$k\frac{4}{3\sqrt{6}}(\mu_u-\mu_d)U_{\rho,1} - \frac{1}{g}\frac{1}{\sqrt{3}}(\mu_u-\mu_d)T_{\rho,1}$	$-\frac{1}{g}(\mu_u-\mu_d)T_{\rho,1}$
${}^4\rho(\Lambda_Q)_J$	$\frac{1}{2}$	$k\frac{1}{3\sqrt{6}}(\mu_u-\mu_d)U_{\rho,1}$	0
	$\frac{3}{2}$	$k\frac{1}{3\sqrt{30}}(\mu_u-\mu_d)U_{\rho,1}$	$k\sqrt{\frac{3}{30}}(\mu_u-\mu_d)U_{\rho,1}$
	$\frac{5}{2}$	$-k\frac{1}{\sqrt{30}}(\mu_u-\mu_d)U_{\rho,1}$	$-k\sqrt{\frac{2}{30}}(\mu_u-\mu_d)U_{\rho,1}$
${}^2\lambda(\Lambda_Q)_J$	$\frac{1}{2}$	$-k\frac{1}{3\sqrt{2}}(\mu_u-\mu_d)U_{\lambda,1}$	0
	$\frac{3}{2}$	$k\frac{1}{3}(\mu_u-\mu_d)U_{\lambda,1}$	0
${}^2\rho(\Lambda_Q)_J$	$\frac{1}{2}$	$-k\frac{1}{3\sqrt{6}}(\mu_u-\mu_d)U_{\rho,1}$	0
	$\frac{3}{2}$	$k\frac{1}{3\sqrt{3}}(\mu_u-\mu_d)U_{\rho,1}$	0
${}^4\rho(\Lambda_Q)_J$	$\frac{1}{2}$	$-k\frac{2}{3\sqrt{3}}(\mu_u-\mu_d)U_{\rho,1} - \frac{1}{g}\frac{1}{\sqrt{6}}(\mu_u-\mu_d)T_{\rho,1}$	0
	$\frac{3}{2}$	$-k\frac{2}{3\sqrt{15}}(\mu_u-\mu_d)U_{\rho,1} - \frac{1}{g}2\sqrt{\frac{2}{15}}(\mu_u-\mu_d)T_{\rho,1}$	$-k\frac{1}{\sqrt{5}}(\mu_u-\mu_d)U_{\rho,1} - \frac{1}{g}\sqrt{\frac{2}{5}}(\mu_u-\mu_d)T_{\rho,1}$
	$\frac{5}{2}$	$k\frac{2}{\sqrt{15}}(\mu_u-\mu_d)U_{\rho,1} - \frac{1}{g}\sqrt{\frac{3}{10}}(\mu_u-\mu_d)T_{\rho,1}$	$k\frac{2}{\sqrt{30}}(\mu_u-\mu_d)U_{\rho,1} - \frac{1}{g}\sqrt{\frac{3}{5}}(\mu_u-\mu_d)T_{\rho,1}$

Table 4.7: Radiative decay widths of ground states baryons in KeV units.

$B_Q \to B'_Q\gamma$	Present	LCQSR[67, 68, 69]	BM[70]	VDM [71]	*ChQM* [66]	NRQM [72]	HBChPT [73]	RQM [74]	hCQM
$^4\Sigma_c^{++} \to {}^2\Sigma_c^{++}\gamma$	1.79	2.65 ± 1.60	0.826	3.567	3.94	1.15	1.20		1.32[75], 0.85 [76]
$^4\Sigma_c^{+} \to {}^2\Sigma_c^{+}\gamma$	0.00	0.40 ± 0.22	0.004	0.187	0.004	$< 10^{-4}$	0.04	0.14 ± 0.004	1×10^{-4} [75], 9×10^{-5} [76]
$^4\Sigma_c^{0} \to {}^2\Sigma_c^{0}\gamma$	1.79	0.08 ± 0.042	1.08	1.049	3.43	1.12	0.49		1.072 [75], 1.20 [76], 1.55 [77]
$^4\Xi_c^{\prime +} \to {}^2\Xi_c^{\prime +}\gamma$	0.03	0.274	0.011	0.485	0.004		0.07		
$^4\Xi_c^{\prime 0} \to {}^2\Xi_c^{\prime 0}\gamma$	1.53	2.142	1.03	1.317	3.03		0.42		
$^4\Omega_c^{0} \to {}^2\Omega_c^{0}\gamma$	1.30	0.932	1.07	1.439	0.89	2.02	0.32		0.34 [76], 1.44 [77]
$^2\Sigma_c^{+} \to {}^2\Lambda_c^{+}\gamma$	67.92	50.0 ± 17.0	46.1		80.60	60.55	65.6	60.7 ± 1.5	71.20 [75], 58.13 [76]
$^4\Sigma_c^{+} \to {}^2\Lambda_c^{+}\gamma$	137.85	130 ± 35	126	409.3	373	154.48	161.8	151 ± 4	171.9 [75], 143.97 [76], 213.3 [77]
$^2\Xi_c^{\prime +} \to {}^2\Xi_c^{+}\gamma$	17.84	8.5 ± 2.5	10.2		42.3		5.43	12.7 ± 1.5	
$^4\Xi_c^{\prime +} \to {}^2\Xi_c^{+}\gamma$	60.36	52 ± 32	44.3	152.4	139	63.32	21.6	54 ± 3	17.48[76]
$^2\Xi_c^{\prime 0} \to {}^2\Xi_c^{0}\gamma$	0.38	0.27 ± 0.06	0.0015		0.00		0.46	0.17 ± 0.002	
$^4\Xi_c^{\prime 0} \to {}^2\Xi_c^{0}\gamma$	1.28	0.66 ± 0.41	0.908	1.318	0.00	0.30	1.84	0.68 ± 0.04	0.45 [76], 0.91 [77]
$^4\Sigma_b^{+} \to {}^2\Sigma_b^{+}\gamma$	0.10	0.46 ± 0.28	0.054	0.137	0.25	0.08	0.05		
$^4\Sigma_b^{0} \to {}^2\Sigma_b^{0}\gamma$	0.01	0.028 ± 0.02	0.005	0.006	0.02	$< 10^{-3}$	3×10^{-3}		
$^4\Sigma_b^{-} \to {}^2\Sigma_b^{-}\gamma$	0.02	0.11 ± 0.076	0.01	0.040	0.06	0.01	0.013		
$^4\Xi_b^{\prime 0} \to {}^2\Xi_b^{\prime 0}\gamma$	0.01	0.131	0.004	0.281	5.19		1.5×10^{-3}		
$^4\Xi_b^{\prime -} \to {}^4\Xi_b^{\prime -}\gamma$	0.01	0.303	0.005	0.702	15.0		8.2×10^{-3}		
$^4\Omega_b^{-} \to {}^2\Omega_b^{-}\gamma$	0.052	0.092	0.006	2.873	0.1	0.03	0.031		
$^2\Sigma_b^{0} \to {}^2\Lambda_b^{0}\gamma$	98.30	152.0 ± 60.0	58.9		130	94.79	108.0		
$^4\Sigma_b^{0} \to {}^2\Lambda_b^{0}\gamma$	120.07	114 ± 62	81.1	221.5	335	128.62	142.1		
$^2\Xi_b^{\prime 0} \to {}^2\Xi_b^{0}\gamma$	35.05	47.0 ± 21.0	14.7		84.6		13.0		
$^4\Xi_b^{\prime 0} \to {}^2\Xi_b^{0}\gamma$	47.96	135 ± 85	24.7	270.8	104	18.79	17.2		
$^2\Xi_b^{\prime -} \to {}^2\Xi_b^{-}\gamma$	0.74	3.3 ± 1.3	0.118		0.00		1.0		
$^4\Xi_b^{\prime -} \to {}^2\Xi_b^{-}\gamma$	1.02	1.50 ± 0.095	0.278	2.246	0.00	0.09	1.4		

Table 4.8: Decay Widths for Photocouplings of Σ_c Baryons in KeV units.

$B_Q \to B'_Q\gamma$	M(MeV)	Present work	$ChQM$ [66, 78]	Ref. [79]	LCQSR[80]
$^2\lambda(\Sigma_c^{++})_{1/2} \to {}^2\Sigma_c^{++}\gamma$	2799.67 ± 9	46.36	283	51.0 ± 9.1	$440(1 \pm 0.25)$
$^4\lambda(\Sigma_c^{++})_{1/2} \to {}^2\Sigma_c^{++}\gamma$	2818.34	23.47	8.54		$36(1 \pm 0.4)$
$^2\lambda(\Sigma_c^{++})_{3/2} \to {}^2\Sigma_c^{++}\gamma$	2843.57	609.54	210		$9(1 \pm 0.1)$
$^4\lambda(\Sigma_c^{++})_{3/2} \to {}^2\Sigma_c^{++}\gamma$	2861.43	77.17	17.5		
$^4\lambda(\Sigma_c^{++})_{5/2} \to {}^2\Sigma_c^{++}\gamma$	2933.26	63.32	13.6		
$^2\rho(\Sigma_c^{++})_{1/2} \to {}^2\Sigma_c^{++}\gamma$	2980.23	144.18	–		
$^2\rho(\Sigma_c^{++})_{3/2} \to {}^2\Sigma_c^{++}\gamma$	3023.33	143.09	–		
$^2\lambda(\Sigma_c^{+})_{1/2} \to {}^2\Sigma_c^{+}\gamma$	2799.67 ± 9	38.17	1.60	28.4 ± 3.3	
$^4\lambda(\Sigma_c^{+})_{1/2} \to {}^2\Sigma_c^{+}\gamma$	2818.34	2.72	0.92		
$^2\lambda(\Sigma_c^{+})_{3/2} \to {}^2\Sigma_c^{+}\gamma$	2843.57	19.48	4.64		
$^4\lambda(\Sigma_c^{+})_{3/2} \to {}^2\Sigma_c^{+}\gamma$	2861.43	9.37	1.86		
$^4\lambda(\Sigma_c^{+})_{5/2} \to {}^2\Sigma_c^{+}\gamma$	2933.26	8.54	1.46		
$^2\rho(\Sigma_c^{+})_{1/2} \to {}^2\Sigma_c^{+}\gamma$	2980.23	8.14	–		
$^2\rho(\Sigma_c^{+})_{3/2} \to {}^2\Sigma_c^{+}\gamma$	3023.33	8.08	–		
$^2\lambda(\Sigma_c^{0})_{1/2} \to {}^2\Sigma_c^{0}\gamma$	2799.67 ± 9	367.29	205	9.1 ± 1.5	
$^4\lambda(\Sigma_c^{0})_{1/2} \to {}^2\Sigma_c^{0}\gamma$	2818.34	2.38	1.02		
$^2\lambda(\Sigma_c^{0})_{3/2} \to {}^2\Sigma_c^{0}\gamma$	2843.57	878.16	245		
$^4\lambda(\Sigma_c^{0})_{3/2} \to {}^2\Sigma_c^{0}\gamma$	2861.43	7.10	2.12		
$^4\lambda(\Sigma_c^{0})_{5/2} \to {}^2\Sigma_c^{0}\gamma$	2933.26	4.46	1.64		
$^2\rho(\Sigma_c^{0})_{1/2} \to {}^2\Sigma_c^{0}\gamma$	2980.23	39.72	–		
$^2\rho(\Sigma_c^{0})_{3/2} \to {}^2\Sigma_c^{0}\gamma$	3023.33	39.42	–		
$^2\lambda(\Lambda_c^{+})_{1/2} \to {}^2\Lambda_c^{+}\gamma$	2592.25 ± 0.28	2.72	0.26	274.3 ± 52	$189(1 \pm 0.3)$
$^2\lambda(\Lambda_c^{+})_{3/2} \to {}^2\Lambda_c^{+}\gamma$	2628.11 ± 0.19	15.08	0.30		
$^2\rho(\Lambda_c^{+})_{1/2} \to {}^2\Lambda_c^{+}\gamma$	2786.41	8.03	1.59		
$^4\rho(\Lambda_c^{+})_{1/2} \to {}^2\Lambda_c^{+}\gamma$	2804.28	4.02	0.80		
$^2\rho(\Lambda_c^{+})_{3/2} \to {}^2\Lambda_c^{+}\gamma$	2829.51	8.01	2.35		
$^4\rho(\Lambda_c^{+})_{3/2} \to {}^2\Lambda_c^{+}\gamma$	2939.60 ± 1.5	10.31	3.29		
$^4\rho(\Lambda_c^{+})_{5/2} \to {}^2\Lambda_c^{+}\gamma$	2919.20	6.31	–		
$^2\lambda(\Xi_c^{+})_{1/2} \to {}^2\Xi_c^{+}\gamma$	2793.25	0.92	4.65	249.6 ± 41.9	$265(1 \pm 0.4)$
$^2\lambda(\Xi_c^{+})_{3/2} \to {}^2\Xi_c^{+}\gamma$	2818.50	2.80	2.80		
$^2\rho(\Xi_c^{+})_{1/2} \to {}^2\Xi_c^{+}\gamma$	2951	16.16	1.39		
$^4\rho(\Xi_c^{+})_{1/2} \to {}^2\Xi_c^{+}\gamma$	2980	8.63	0.75	56.4 ± 19.2	
$^2\rho(\Xi_c^{+})_{3/2} \to {}^2\Xi_c^{+}\gamma$	2987	17.47	1.88		
$^4\rho(\Xi_c^{+})_{3/2} \to {}^2\Xi_c^{+}\gamma$	3016	25.33	2.81		
$^4\rho(\Xi_c^{+})_{5/2} \to {}^2\Xi_c^{+}\gamma$	3076	16.35	–		
$^2\lambda(\Xi_c^{0})_{1/2} \to {}^2\Xi_c^{0}\gamma$	2793.25	547.16	263	119.3 ± 21.7	$2.7(1 \pm 0.3)$
$^2\lambda(\Xi_c^{0})_{3/2} \to {}^2\Xi_c^{0}\gamma$	2818.50	711.45	292		
$^2\rho(\Xi_c^{0})_{1/2} \to {}^2\Xi_c^{0}\gamma$	2951	26.45	5.57		
$^4\rho(\Xi_c^{0})_{1/2} \to {}^2\Xi_c^{0}\gamma$	2980	14.12	3.00	2.5 ± 1.7	
$^2\rho(\Xi_c^{0})_{3/2} \to {}^2\Xi_c^{0}\gamma$	2987	28.59	7.50		
$^4\rho(\Xi_c^{0})_{3/2} \to {}^2\Xi_c^{0}\gamma$	3016	41.46	11.2		
$^4\rho(\Xi_c^{0})_{5/2} \to {}^2\Xi_c^{0}\gamma$	3076	26.75	–		
$^2\lambda(\Xi_c^{'+})_{1/2} \to {}^2\Xi_c^{'+}\gamma$	2905	11.92	0.03		$21(1 \pm 0.2)$
$^4\lambda(\Xi_c^{'+})_{1/2} \to {}^2\Xi_c^{'+}\gamma$	2923.04	2.86	0.33		
$^2\lambda(\Xi_c^{'+})_{3/2} \to {}^2\Xi_c^{'+}\gamma$	2938.55	11.90	12.1		
$^4\lambda(\Xi_c^{'+})_{3/2} \to {}^2\Xi_c^{'+}\gamma$	2964.88	11.64	2.06		
$^4\lambda(\Xi_c^{'+})_{5/2} \to {}^2\Xi_c^{'+}\gamma$	3030	11.74	1.63		
$^2\rho(\Xi_c^{'+})_{1/2} \to {}^2\Xi_c^{'+}\gamma$	3055.90	16.14	–		
$^2\rho(\Xi_c^{'+})_{3/2} \to {}^2\Xi_c^{'+}\gamma$	3078.55	17.06	–		
$^2\lambda(\Xi_c^{'0})_{1/2} \to {}^2\Xi_c^{'0}\gamma$	2905	451.00	472		$132(1 \pm 0.2)$
$^4\lambda(\Xi_c^{'0})_{1/2} \to {}^2\Xi_c^{'0}\gamma$	2923.04	0.81	0.20		
$^2\lambda(\Xi_c^{'0})_{3/2} \to {}^2\Xi_c^{'0}\gamma$	2938.55	840.62	302		
$^4\lambda(\Xi_c^{'+})_{3/2} \to {}^2\Xi_c^{'0}\gamma$	2964.88	2.68	1.21		
$^4\lambda(\Xi_c^{'+})_{5/2} \to {}^2\Xi_c^{'0}\gamma$	3030	1.76	0.93		
$^2\rho(\Xi_c^{'0})_{1/2} \to {}^2\Xi_c^{'+}\gamma$	3055.90	26.41	–		
$^2\rho(\Xi_c^{'0})_{3/2} \to {}^2\Xi_c^{'0}\gamma$	3078.55	27.92	–		
$^2\lambda(\Omega_c^{0})_{1/2} \to {}^2\Omega_c^{0}\gamma$	3000.4	449.87	0.36/0.20 mixed		
$^4\lambda(\Omega_c^{0})_{1/2} \to {}^2\Omega_c^{0}\gamma$	3050.2	0.22	0.36/0.20 mixed		
$^2\lambda(\Omega_c^{0})_{3/2} \to {}^2\Omega_c^{0}\gamma$	3065.6	872.73	0.35		
$^4\lambda(\Omega_c^{0})_{3/2} \to {}^2\Omega_c^{0}\gamma$	3090.2	0.62	1.12×10^{-3}		
$^4\lambda(\Omega_c^{0})_{5/2} \to {}^2\Omega_c^{0}\gamma$	3188	0.14	1.00×10^{-4}		
$^2\rho(\Omega_c^{0})_{1/2} \to {}^2\Omega_c^{0}\gamma$	3146	15.72	–		
$^2\rho(\Omega_c^{0})_{3/2} \to {}^2\Omega_c^{0}\gamma$	3182	17.75	–		

Table 4.9: Decay Widths for Photocouplings of Σ_c Baryons in KeV units.

$B_Q \to B'_Q\gamma$	M(MeV)	Present work	$ChQM$ [66, 78]
${}^2\lambda(\Sigma_c^{++})_{1/2} \to {}^4\Sigma_c^{++}\gamma$	2799.67 ± 9	8.06	3.04
${}^4\lambda(\Sigma_c^{++})_{1/2} \to {}^4\Sigma_c^{++}\gamma$	2818.34	0.15	387
${}^2\lambda(\Sigma_c^{++})_{3/2} \to {}^4\Sigma_c^{++}\gamma$	2843.57	13.67	14.7
${}^4\lambda(\Sigma_c^{++})_{3/2} \to {}^4\Sigma_c^{++}\gamma$	2861.43	58.16	181
${}^4\lambda(\Sigma_c^{++})_{5/2} \to {}^4\Sigma_c^{++}\gamma$	2933.26	438.40	168
${}^2\rho(\Sigma_c^{++})_{1/2} \to {}^4\Sigma_c^{++}\gamma$	2980.23	67.28	–
${}^2\rho(\Sigma_c^{++})_{3/2} \to {}^4\Sigma_c^{++}\gamma$	3023.33	71.15	–
${}^2\lambda(\Sigma_c^{+})_{1/2} \to {}^4\Sigma_c^{+}\gamma$	2799.67 ± 9	0.81	0.31
${}^4\lambda(\Sigma_c^{+})_{1/2} \to {}^4\Sigma_c^{+}\gamma$	2818.34	10.65	1.75
${}^2\lambda(\Sigma_c^{+})_{3/2} \to {}^4\Sigma_c^{+}\gamma$	2843.57	1.45	1.55
${}^4\lambda(\Sigma_c^{+})_{3/2} \to {}^4\Sigma_c^{+}\gamma$	2861.43	23.82	0.68
${}^4\lambda(\Sigma_c^{+})_{5/2} \to {}^4\Sigma_c^{+}\gamma$	2933.26	6.29	0.89
${}^2\rho(\Sigma_c^{+})_{1/2} \to {}^4\Sigma_c^{+}\gamma$	2980.23	3.80	–
${}^2\rho(\Sigma_c^{+})_{3/2} \to {}^4\Sigma_c^{+}\gamma$	3023.33	4.02	–
${}^2\lambda(\Sigma_c^{0})_{1/2} \to {}^4\Sigma_c^{0}\gamma$	2799.67 ± 9	1.08	0.39
${}^4\lambda(\Sigma_c^{0})_{1/2} \to {}^4\Sigma_c^{0}\gamma$	2818.34	37.73	289
${}^2\lambda(\Sigma_c^{0})_{3/2} \to {}^4\Sigma_c^{0}\gamma$	2843.57	1.67	1.82
${}^4\lambda(\Sigma_c^{0})_{3/2} \to {}^4\Sigma_c^{0}\gamma$	2861.43	265.45	159
${}^4\lambda(\Sigma_c^{0})_{5/2} \to {}^4\Sigma_c^{0}\gamma$	2933.26	655.27	160
${}^2\rho(\Sigma_c^{0})_{1/2} \to {}^4\Sigma_c^{0}\gamma$	2980.23	18.53	–
${}^2\rho(\Sigma_c^{0})_{3/2} \to {}^4\Sigma_c^{0}\gamma$	3023.33	19.60	–
${}^2\lambda(\Xi_c^{'+})_{1/2} \to {}^4\Xi_c^{'+}\gamma$	2905	1.01	1.61
${}^4\lambda(\Xi_c^{'+})_{1/2} \to {}^4\Xi_c^{'+}\gamma$	2923.04	1.94	0.16
${}^2\lambda(\Xi_c^{'+})_{3/2} \to {}^4\Xi_c^{'+}\gamma$	2938.55	1.62	1.59
${}^4\lambda(\Xi_c^{'+})_{3/2} \to {}^4\Xi_c^{'+}\gamma$	2964.88	3.72	1.64
${}^4\lambda(\Xi_c^{'+})_{5/2} \to {}^4\Xi_c^{'+}\gamma$	3030	2.16	2.35
${}^2\rho(\Xi_c^{'+})_{1/2} \to {}^4\Xi_c^{'+}\gamma$	3055.90	6.21	–
${}^2\rho(\Xi_c^{'+})_{3/2} \to {}^4\Xi_c^{'+}\gamma$	3078.55	6.95	–
${}^2\lambda(\Xi_c^{'0})_{1/2} \to {}^4\Xi_c^{'0}\gamma$	2905	0.38	1.00
${}^4\lambda(\Xi_c^{'0})_{1/2} \to {}^4\Xi_c^{'0}\gamma$	2923.04	51.61	125
${}^2\lambda(\Xi_c^{'0})_{3/2} \to {}^4\Xi_c^{'0}\gamma$	2938.55	0.55	1.05
${}^4\lambda(\Xi_c^{'0})_{3/2} \to {}^4\Xi_c^{'0}\gamma$	2964.88	289.26	187
${}^4\lambda(\Xi_c^{'0})_{5/2} \to {}^4\Xi_c^{'0}\gamma$	3030	586.26	192
${}^2\rho(\Xi_c^{'0})_{1/2} \to {}^4\Xi_c^{'0}\gamma$	3055.90	10.16	–
${}^2\rho(\Xi_c^{'0})_{3/2} \to {}^4\Xi_c^{'0}\gamma$	3078.55	11.33	–
${}^2\lambda(\Omega_c^{0})_{1/2} \to {}^4\Omega_c^{0}\gamma$	3000.4	0.09	$0.02/0.08_{\text{mixed}}$
${}^4\lambda(\Omega_c^{0})_{1/2} \to {}^4\Omega_c^{0}\gamma$	3050.2	64.84	$0.02/0.08_{\text{mixed}}$
${}^2\lambda(\Omega_c^{0})_{3/2} \to {}^4\Omega_c^{0}\gamma$	3065.6	0.17	5.17×10^{-4}
${}^4\lambda(\Omega_c^{0})_{3/2} \to {}^4\Omega_c^{0}\gamma$	3090.2	326.91	0.33
${}^4\lambda(\Omega_c^{0})_{5/2} \to {}^4\Omega_c^{0}\gamma$	3188	661.96	0.18
${}^2\rho(\Omega_c^{0})_{1/2} \to {}^4\Omega_c^{0}\gamma$	3146	5.42	–
${}^2\rho(\Omega_c^{0})_{3/2} \to {}^4\Omega_c^{0}\gamma$	3182	6.74	–

Table 4.10: Decay Widths for Photocouplings of Σ_b Baryons in KeV units.

$B_Q \to B'_Q\gamma$	M(MeV)	Present work	$ChQM$ [66]
$^2\lambda(\Sigma_b^+)_{1/2} \to {}^2\Sigma_b^+\gamma$	6096.90 ± 1.7	411.59	1016
$^4\lambda(\Sigma_b^+)_{1/2} \to {}^2\Sigma_b^+\gamma$	6109.42	10.44	5.31
$^2\lambda(\Sigma_b^+)_{3/2} \to {}^2\Sigma_b^+\gamma$	6104.68	1206.75	483
$^4\lambda(\Sigma_b^+)_{3/2} \to {}^2\Sigma_b^+\gamma$	6117.14	31.57	13.1
$^4\lambda(\Sigma_b^+)_{5/2} \to {}^2\Sigma_b^+\gamma$	6130.02	22.85	8.07
$^2\rho(\Sigma_b^+)_{1/2} \to {}^2\Sigma_b^+\gamma$	6287.12	105.26	–
$^2\rho(\Sigma_b^+)_{3/2} \to {}^2\Sigma_b^+\gamma$	6294.85	105.74	–
$^2\lambda(\Sigma_b^0)_{1/2} \to {}^2\Sigma_b^0\gamma$	6096.90 ± 1.7	35.15	74.9
$^4\lambda(\Sigma_b^0)_{1/2} \to {}^2\Sigma_b^0\gamma$	6109.42	0.56	0.32
$^2\lambda(\Sigma_b^0)_{3/2} \to {}^2\Sigma_b^0\gamma$	6104.68	87.66	37.9
$^4\lambda(\Sigma_b^0)_{3/2} \to {}^2\Sigma_b^0\gamma$	6117.14	1.71	0.80
$^4\lambda(\Sigma_b^0)_{5/2} \to {}^2\Sigma_b^0\gamma$	6130.02	1.23	0.49
$^2\rho(\Sigma_b^0)_{1/2} \to {}^2\Sigma_b^0\gamma$	6287.12	5.94	–
$^2\rho(\Sigma_b^0)_{3/2} \to {}^2\Sigma_b^0\gamma$	6294.85	5.97	–
$^2\lambda(\Sigma_b^-)_{1/2} \to {}^2\Sigma_b^-\gamma$	6096.90 ± 1.7	71.06	212
$^4\lambda(\Sigma_b^-)_{1/2} \to {}^2\Sigma_b^-\gamma$	6109.42	2.99	1.37
$^2\lambda(\Sigma_b^-)_{3/2} \to {}^2\Sigma_b^-\gamma$	6104.68	256.94	94.0
$^4\lambda(\Sigma_b^-)_{3/2} \to {}^2\Sigma_b^-\gamma$	6117.14	9.04	3.39
$^4\lambda(\Sigma_b^-)_{5/2} \to {}^2\Sigma_b^-\gamma$	6130.02	6.55	2.08
$^2\rho(\Sigma_b^-)_{1/2} \to {}^2\Sigma_b^-\gamma$	6287.12	28.99	–
$^2\rho(\Sigma_b^-)_{3/2} \to {}^2\Sigma_b^-\gamma$	6294.85	29.13	–
$^2\lambda(\Lambda_b^0)_{1/2} \to {}^2\Lambda_b^0\gamma$	5912.20 ± 0.13	65.30	50.2
$^2\lambda(\Lambda_b^0)_{3/2} \to {}^2\Lambda_b^0\gamma$	5920.00 ± 0.09	68.91	52.8
$^2\rho(\Lambda_b^0)_{1/2} \to {}^2\Lambda_b^0\gamma$	6093.30	5.92	1.62
$^4\rho(\Lambda_b^0)_{1/2} \to {}^2\Lambda_b^0\gamma$	6105.77	2.98	0.81
$^2\rho(\Lambda_b^0)_{3/2} \to {}^2\Lambda_b^0\gamma$	6101.03	5.95	1.81
$^4\rho(\Lambda_b^0)_{3/2} \to {}^2\Lambda_b^0\gamma$	6113.49	8.35	2.54
$^4\rho(\Lambda_b^0)_{5/2} \to {}^2\Lambda_b^0\gamma$	6126.37	5.35	–
$^2\lambda(\Xi_b^0)_{1/2} \to {}^2\Xi_b^0\gamma$	6048	143.67	63.6
$^2\lambda(\Xi_b^0)_{3/2} \to {}^2\Xi_b^0\gamma$	6055	152.14	68.3
$^2\rho(\Xi_b^0)_{1/2} \to {}^2\Xi_b^0\gamma$	6213	11.03	1.86
$^4\rho(\Xi_b^0)_{1/2} \to {}^2\Xi_b^0\gamma$	6225	5.72	0.93
$^2\rho(\Xi_b^0)_{3/2} \to {}^2\Xi_b^0\gamma$	6220	11.28	2.10
$^4\rho(\Xi_b^0)_{3/2} \to {}^2\Xi_b^0\gamma$	6233	16.36	2.94
$^4\rho(\Xi_b^0)_{5/2} \to {}^2\Xi_b^0\gamma$	6246	10.82	–
$^2\lambda(\Xi_b^-)_{1/2} \to {}^2\Xi_b^-\gamma$	6048	143.96	135
$^2\lambda(\Xi_b^-)_{3/2} \to {}^2\Xi_b^-\gamma$	6055	148.21	147
$^2\rho(\Xi_b^-)_{1/2} \to {}^2\Xi_b^-\gamma$	6213	18.05	7.19
$^4\rho(\Xi_b^-)_{1/2} \to {}^2\Xi_b^-\gamma$	6225	9.36	3.59
$^2\rho(\Xi_b^-)_{3/2} \to {}^2\Xi_b^-\gamma$	6220	18.46	8.13
$^4\rho(\Xi_b^-)_{3/2} \to {}^2\Xi_b^-\gamma$	6233	26.78	11.4
$^4\rho(\Xi_b^-)_{5/2} \to {}^2\Xi_b^-\gamma$	6246	17.71	–
$^2\lambda(\Xi_b^{\prime 0})_{1/2} \to {}^2\Xi_b^{\prime 0}\gamma$	6189	95.15	76.3
$^4\lambda(\Xi_b^{\prime 0})_{1/2} \to {}^2\Xi_b^{\prime 0}\gamma$	6202	0.79	0.25
$^2\lambda(\Xi_b^{\prime 0})_{3/2} \to {}^2\Xi_b^{\prime 0}\gamma$	6197	191.27	43.9
$^4\lambda(\Xi_b^{\prime 0})_{3/2} \to {}^2\Xi_b^{\prime 0}\gamma$	6210	2.44	0.67
$^4\lambda(\Xi_b^{\prime 0})_{5/2} \to {}^2\Xi_b^{\prime 0}\gamma$	6226.90	1.90	0.44
$^2\rho(\Xi_b^{\prime 0})_{1/2} \to {}^2\Xi_b^{\prime 0}\gamma$	6354	11.11	
$^2\rho(\Xi_b^{\prime 0})_{3/2} \to {}^2\Xi_b^{\prime 0}\gamma$	6362	11.39	
$^2\lambda(\Xi_b^{\prime -})_{1/2} \to {}^2\Xi_b^{\prime -}\gamma$	6189	80.91	190
$^4\lambda(\Xi_b^{\prime -})_{1/2} \to {}^2\Xi_b^{\prime -}\gamma$	6202	1.40	1.48
$^2\lambda(\Xi_b^{\prime -})_{3/2} \to {}^2\Xi_b^{\prime -}\gamma$	6197	200.34	92.3
$^4\lambda(\Xi_b^{\prime -})_{3/2} \to {}^2\Xi_b^{\prime -}\gamma$	6210	4.33	2.94
$^4\lambda(\Xi_b^{\prime -})_{5/2} \to {}^2\Xi_b^{\prime -}\gamma$	6226.90	3.38	1.88
$^2\rho(\Xi_b^{\prime -})_{1/2} \to {}^2\Xi_b^{\prime -}\gamma$	6354	18.18	–
$^2\rho(\Xi_b^{\prime -})_{3/2} \to {}^2\Xi_b^{\prime -}\gamma$	6362	18.64	–
$^2\lambda(\Omega_b^-)_{1/2} \to {}^2\Omega_b^-\gamma$	6305	71.62	154
$^4\lambda(\Omega_b^-)_{1/2} \to {}^2\Omega_b^-\gamma$	6317	0.89	0.64
$^2\lambda(\Omega_b^-)_{3/2} \to {}^2\Omega_b^-\gamma$	6313	157.90	83.4
$^4\lambda(\Omega_b^-)_{3/2} \to {}^2\Omega_b^-\gamma$	6325	2.75	1.81
$^4\lambda(\Omega_b^-)_{5/2} \to {}^2\Omega_b^-\gamma$	6338	2.05	1.21
$^2\rho(\Omega_b^-)_{1/2} \to {}^2\Omega_b^-\gamma$	6452	10.85	–
$^2\rho(\Omega_b^-)_{3/2} \to {}^2\Omega_b^-\gamma$	6460	11.19	–

Table 4.11: Decay Widths for Photocouplings of Σ_b Baryons in KeV units.

$B_Q \to B'_Q\gamma$	M(MeV)	Present work	$ChQM$ [66]
${}^2\lambda(\Sigma_b^+)_{1/2} \to {}^4\Sigma_b^+\gamma$	6096.90 ± 1.7	7.21	16.9
${}^4\lambda(\Sigma_b)_{1/2} \to {}^4\Sigma_b^+\gamma$	6109.42	34.94	867
${}^2\lambda(\Sigma_b^+)_{3/2} \to {}^4\Sigma_b^+\gamma$	6104.68	7.95	15.6
${}^4\lambda(\Sigma_b)_{3/2} \to {}^4\Sigma_b^+\gamma$	6117.14	317.94	527
${}^4\lambda(\Sigma_b^+)_{5/2} \to {}^4\Sigma_b^+\gamma$	6130.02	805.74	426
${}^2\rho(\Sigma_b^+)_{1/2} \to {}^4\Sigma_b^+\gamma$	6287.12	51.49	–
${}^2\rho(\Sigma_b^+)_{3/2} \to {}^4\Sigma_b^+\gamma$	6294.85	52.04	–
${}^2\lambda(\Sigma_b^0)_{1/2} \to {}^4\Sigma_b^0\gamma$	6096.90 ± 1.7	0.39	1.03
${}^4\lambda(\Sigma_b^0)_{1/2} \to {}^4\Sigma_b^0\gamma$	6109.42	3.66	63.6
${}^2\lambda(\Sigma_b^0)_{3/2} \to {}^4\Sigma_b^0\gamma$	6104.68	0.43	0.95
${}^4\lambda(\Sigma_b^0)_{3/2} \to {}^4\Sigma_b^0\gamma$	6117.14	26.30	39.8
${}^4\lambda(\Sigma_b^0)_{5/2} \to {}^4\Sigma_b^0\gamma$	6130.02	56.99	32.6
${}^2\rho(\Sigma_b^0)_{1/2} \to {}^4\Sigma_b^0\gamma$	6287.12	2.91	–
${}^2\rho(\Sigma_b^0)_{3/2} \to {}^4\Sigma_b^0\gamma$	6294.85	2.94	–
${}^2\lambda(\Sigma_b^-)_{1/2} \to {}^4\Sigma_b^-\gamma$	6096.90 ± 1.7	2.05	4.36
${}^4\lambda(\Sigma_b^-)_{1/2} \to {}^4\Sigma_b^-\gamma$	6109.42	4.33	182
${}^2\lambda(\Sigma_b^-)_{3/2} \to {}^4\Sigma_b^-\gamma$	6104.68	2.27	4.02
${}^4\lambda(\Sigma_b^-)_{3/2} \to {}^4\Sigma_b^-\gamma$	6117.14	57.59	107
${}^4\lambda(\Sigma_b^-)_{5/2} \to {}^4\Sigma_b^-\gamma$	6130.02	176.61	85.3
${}^2\rho(\Sigma_b^-)_{1/2} \to {}^4\Sigma_b^-\gamma$	6287.12	14.18	–
${}^2\rho(\Sigma_b^-)_{3/2} \to {}^4\Sigma_b^-\gamma$	6294.85	14.33	–
${}^2\lambda(\Xi_b^{'0})_{1/2} \to {}^4\Xi_b^{'0}\gamma$	6189	0.50	0.89
${}^4\lambda(\Xi_b^{'0})_{1/2} \to {}^4\Xi_b^{'0}\gamma$	6202	13.26	69.5
${}^2\lambda(\Xi_b^{'0})_{3/2} \to {}^4\Xi_b^{'0}\gamma$	6197	0.57	0.90
${}^4\lambda(\Xi_b^{'0})_{3/2} \to {}^4\Xi_b^{'0}\gamma$	6210	70.24	47.5
${}^4\lambda(\Xi_b^{'0})_{5/2} \to {}^4\Xi_b^{'0}\gamma$	6226.90	122.68	41.5
${}^2\rho(\Xi_b^{'0})_{1/2} \to {}^4\Xi_b^{'0}\gamma$	6354	5.18	–
${}^2\rho(\Xi_b^{'0})_{3/2} \to {}^4\Xi_b^{'0}\gamma$	6362	5.35	–
${}^2\lambda(\Xi_b^{'-})_{1/2} \to {}^4\Xi_b^{'-}\gamma$	6189	0.89	3.54
${}^4\lambda(\Xi_b^{'-})_{1/2} \to {}^4\Xi_b^{'-}\gamma$	6202	9.26	164
${}^2\lambda(\Xi_b^{'-})_{3/2} \to {}^4\Xi_b^{'-}\gamma$	6197	1.00	3.60
${}^4\lambda(\Xi_b^{'-})_{3/2} \to {}^4\Xi_b^{'-}\gamma$	6210	61.86	104
${}^4\lambda(\Xi_b^{'-})_{5/2} \to {}^4\Xi_b^{'-}\gamma$	6226.90	133.21	88.2
${}^2\rho(\Xi_b^{'-})_{1/2} \to {}^4\Xi_b^{'-}\gamma$	6354	8.48	–
${}^2\rho(\Xi_b^{'-})_{3/2} \to {}^4\Xi_b^{'-}\gamma$	6362	8.75	–
${}^2\lambda(\Omega_b^-)_{1/2} \to {}^4\Omega_b^-\gamma$	6305	0.43	1.49
${}^4\lambda(\Omega_b^-)_{1/2} \to {}^4\Omega_b^-\gamma$	6317	9.44	99.23
${}^2\lambda(\Omega_b^-)_{3/2} \to {}^4\Omega_b^-\gamma$	6313	0.49	1.51
${}^4\lambda(\Omega_b^-)_{3/2} \to {}^4\Omega_b^-\gamma$	6325	50.39	70.68
${}^4\lambda(\Omega_b^-)_{5/2} \to {}^4\Omega_b^-\gamma$	6338	87.05	63.26
${}^2\rho(\Omega_b^-)_{1/2} \to {}^4\Omega_b^-\gamma$	6452	4.53	–
${}^2\rho(\Omega_b^-)_{3/2} \to {}^4\Omega_b^-\gamma$	6460	4.74	–

Table 4.12: Decay Widths in KeV units.

$B_Q \to B'_Q\gamma$	M(MeV)	Present work	$ChQM$ [66]	Ref. [79]	LCQSR [80]
$^2\lambda(\Sigma_c^+)_{1/2} \to {}^2\Lambda_c^+\gamma$	2799.67 ± 9	86.51	48.3	33.5 ± 8.8	
$^4\lambda(\Sigma_c^+)_{1/2} \to {}^2\Lambda_c^+\gamma$	2818.34	44.91	52.1		$701(1\pm0.4)$
$^2\lambda(\Sigma_c^+)_{3/2} \to {}^2\Lambda_c^+\gamma$	2843.57	89.79	87.3		
$^4\lambda(\Sigma_c^+)_{3/2} \to {}^2\Lambda_c^+\gamma$	2861.43	124.24	105		
$^4\lambda(\Sigma_c^+)_{5/2} \to {}^2\Lambda_c^+\gamma$	2933.26	73.28	59.4		
$^2\rho(\Sigma_c^+)_{1/2} \to {}^2\Lambda_c^+\gamma$	2980.23	164.57	–		
$^2\rho(\Sigma_c^+)_{3/2} \to {}^2\Lambda_c^+\gamma$	3023.33	132.325	–		
$^2\lambda(\Lambda_c^+)_{1/2} \to {}^2\Sigma_c^+\gamma$	2592.25 ± 0.28	1.27	0.45	2.1 ± 0.4	$29(1 \pm 0.3)$
$^2\lambda(\Lambda_c^+)_{3/2} \to {}^2\Sigma_c^+\gamma$	2628.11 ± 0.19	3.48	1.17		
$^2\rho(\Lambda_c^+)_{1/2} \to {}^2\Sigma_c^+\gamma$	2786.41	147.98	41.6		
$^4\rho(\Lambda_c^+)_{1/2} \to {}^2\Sigma_c^+\gamma$	2804.28	9.96	48.0		
$^2\rho(\Lambda_c^+)_{3/2} \to {}^2\Sigma_c^+\gamma$	2829.51	696.78	0.08		
$^4\rho(\Lambda_c^+)_{3/2} \to {}^2\Sigma_c^+\gamma$	2939.60 ± 1.5	36.06	0.55		
$^4\rho(\Lambda_c^+)_{5/2} \to {}^2\Sigma_c^+\gamma$	2919.20	24.17	–		
$^2\lambda(\Xi_c^+)_{1/2} \to {}^2\Xi_c^{'+}\gamma$	2793.25	5.78	1.43		$54(1 \pm 0.4)$
$^2\lambda(\Xi_c^+)_{3/2} \to {}^2\Xi_c^{'+}\gamma$	2818.50	8.96	2.32		
$^2\rho(\Xi_c^+)_{1/2} \to {}^2\Xi_c^{'+}\gamma$	2951	251.52	128		
$^4\rho(\Xi_c^+)_{1/2} \to {}^2\Xi_c^{'+}\gamma$	2980	7.76	0.41	40.1 ± 6.9	
$^2\rho(\Xi_c^+)_{3/2} \to {}^2\Xi_c^{'+}\gamma$	2987	810.98	110		
$^4\rho(\Xi_c^+)_{3/2} \to {}^2\Xi_c^{'+}\gamma$	3016	25.92	1.85		
$^4\rho(\Xi_c^+)_{5/2} \to {}^2\Xi_c^{'+}\gamma$	3076	20.15	–		
$^2\lambda(\Xi_c^0)_{1/2} \to {}^2\Xi_c^{'0}\gamma$	2793.25	0.12	0.00	1.3 ± 1.4	$0.54(1 \pm 0.4)$
$^2\lambda(\Xi_c^0)_{3/2} \to {}^2\Xi_c^{'0}\gamma$	2818.50	0.19	0.00		
$^2\rho(\Xi_c^0)_{1/2} \to {}^2\Xi_c^{'0}\gamma$	2951	5.33	0.00		
$^4\rho(\Xi_c^0)_{1/2} \to {}^2\Xi_c^{'0}\gamma$	2980	0.16	0.00	9.2 ± 1.0	
$^2\rho(\Xi_c^0)_{3/2} \to {}^2\Xi_c^{'0}\gamma$	2987	17.20	0.00		
$^4\rho(\Xi_c^0)_{3/2} \to {}^2\Xi_c^{'0}\gamma$	3016	0.55	0.00		
$^4\rho(\Xi_c^0)_{5/2} \to {}^2\Xi_c^{'0}\gamma$	3076	0.43	–		
$^2\lambda(\Xi_c^{'+})_{1/2} \to {}^2\Xi_c^+\gamma$	2905	53.30	46.4		$214(1 \pm 0.3)$
$^4\lambda(\Xi_c^{'+})_{1/2} \to {}^2\Xi_c^+\gamma$	2923.04	28.62	14.5		
$^2\lambda(\Xi_c^{'+})_{3/2} \to {}^2\Xi_c^+\gamma$	2938.55	60.32	46.1		
$^4\lambda(\Xi_c^{'+})_{3/2} \to {}^2\Xi_c^+\gamma$	2964.88	90.65	54.6		
$^4\lambda(\Xi_c^{'+})_{5/2} \to {}^2\Xi_c^+\gamma$	3030	63.58	32.0		
$^2\rho(\Xi_c^{'+})_{1/2} \to {}^2\Xi_c^+\gamma$	3055.90	429.50	–		
$^2\rho(\Xi_c^{'+})_{3/2} \to {}^2\Xi_c^+\gamma$	3078.55	396.70	–		
$^2\lambda(\Xi_c^{'0})_{1/2} \to {}^2\Xi_c^0\gamma$	2905	1.13	0.00		$4.8(1 \pm 0.3)$
$^4\lambda(\Xi_c^{'0})_{1/2} \to {}^2\Xi_c^0\gamma$	2923.04	0.61	0.00		
$^2\lambda(\Xi_c^{'0})_{3/2} \to {}^2\Xi_c^0\gamma$	2938.55	1.28	0.00		
$^4\lambda(\Xi_c^{'0})_{3/2} \to {}^2\Xi_c^0\gamma$	2964.88	1.92	0.00		
$^4\lambda(\Xi_c^{'0})_{5/2} \to {}^2\Xi_c^0\gamma$	3030	1.35	0.00		
$^2\rho(\Xi_c^{'0})_{1/2} \to {}^2\Xi_c^0\gamma$	3055.90	9.10	–		
$^2\rho(\Xi_c^{'0})_{3/2} \to {}^2\Xi_c^0\gamma$	3078.55	8.41	–		

Table 4.13: Decay Widths in KeV units.

$B_Q \to B'_Q\gamma$	M(MeV)	Present work	$ChQM$ [66]
${}^2\lambda(\Sigma_b^0)_{1/2} \to {}^2\Lambda_b^0\gamma$	6096.90 ± 1.7	89.34	133
${}^4\lambda(\Sigma_b^0)_{1/2} \to {}^2\Lambda_b^0\gamma$	6109.42	44.89	63.6
${}^2\lambda(\Sigma_b^0)_{3/2} \to {}^2\Lambda_b^0\gamma$	6104.68	89.68	129
${}^4\lambda(\Sigma_b^0)_{3/2} \to {}^2\Lambda_b^0\gamma$	6117.14	125.69	170
${}^4\lambda(\Sigma_b^0)_{5/2} \to {}^2\Lambda_b^0\gamma$	6130.02	80.41	83.3
${}^2\rho(\Sigma_b^0)_{1/2} \to {}^2\Lambda_b^0\gamma$	6287.12	97.10	–
${}^2\rho(\Sigma_b^0)_{3/2} \to {}^2\Lambda_b^0\gamma$	6294.85	90.98	–
${}^2\lambda(\Lambda_b^0)_{1/2} \to {}^2\Sigma_b^0\gamma$	5912.20 ± 0.13	0.39	0.14
${}^2\lambda(\Lambda_b^0)_{3/2} \to {}^2\Sigma_b^0\gamma$	5920.00 ± 0.09	0.56	0.21
${}^2\rho(\Lambda_b^0)_{1/2} \to {}^2\Sigma_b^0\gamma$	6093.30	140.41	16.2
${}^4\rho(\Lambda_b^0)_{1/2} \to {}^2\Sigma_b^0\gamma$	6105.77	4.05	0.02
${}^2\rho(\Lambda_b^0)_{3/2} \to {}^2\Sigma_b^0\gamma$	6101.03	432.40	15.1
${}^4\rho(\Lambda_b^0)_{3/2} \to {}^2\Sigma_b^0\gamma$	6113.49	12.28	0.07
${}^4\rho(\Lambda_b^0)_{5/2} \to {}^2\Sigma_b^0\gamma$	6126.37	8.92	–
${}^2\lambda(\Xi_b^0)_{1/2} \to {}^2\Xi_b^{'0}\gamma$	6048	0.53	1.32
${}^2\lambda(\Xi_b^0)_{3/2} \to {}^2\Xi_b^{'0}\gamma$	6055	0.70	1.68
${}^2\rho(\Xi_b^0)_{1/2} \to {}^2\Xi_b^{'0}\gamma$	6213	206.94	94.3
${}^4\rho(\Xi_b^0)_{1/2} \to {}^2\Xi_b^{'0}\gamma$	6225	3.06	0.16
${}^2\rho(\Xi_b^0)_{3/2} \to {}^2\Xi_b^{'0}\gamma$	6220	489.41	69.4
${}^4\rho(\Xi_b^0)_{3/2} \to {}^2\Xi_b^{'0}\gamma$	6233	9.33	0.80
${}^4\rho(\Xi_b^0)_{5/2} \to {}^2\Xi_b^{'0}\gamma$	6246	6.82	–
${}^2\lambda(\Xi_b^-)_{1/2} \to {}^2\Xi_b^{'-}\gamma$	6048	0.01	0.00
${}^2\lambda(\Xi_b^-)_{3/2} \to {}^2\Xi_b^{'-}\gamma$	6055	0.01	0.00
${}^2\rho(\Xi_b^-)_{1/2} \to {}^2\Xi_b^{'-}\gamma$	6213	4.39	0.00
${}^4\rho(\Xi_b^-)_{1/2} \to {}^2\Xi_b^{'-}\gamma$	6225	0.06	0.00
${}^2\rho(\Xi_b^-)_{3/2} \to {}^2\Xi_b^{'-}\gamma$	6220	10.38	0.00
${}^4\rho(\Xi_b^-)_{3/2} \to {}^2\Xi_b^{'-}\gamma$	6233	0.20	0.00
${}^4\rho(\Xi_b^-)_{5/2} \to {}^2\Xi_b^{'-}\gamma$	6246	0.14	–
${}^2\lambda(\Xi_b^{'0})_{1/2} \to {}^2\Xi_b^0\gamma$	6189	55.68	72.2
${}^4\lambda(\Xi_b^{'0})_{1/2} \to {}^2\Xi_b^0\gamma$	6202	29.40	34.0
${}^2\lambda(\Xi_b^{'0})_{3/2} \to {}^2\Xi_b^0\gamma$	6197	57.63	72.8
${}^4\lambda(\Xi_b^{'0})_{3/2} \to {}^2\Xi_b^0\gamma$	6210	84.78	94.0
${}^4\lambda(\Xi_b^{'0})_{5/2} \to {}^2\Xi_b^0\gamma$	6226.90	57.45	47.7
${}^2\rho(\Xi_b^{'0})_{1/2} \to {}^2\Xi_b^0\gamma$	6354	273.84	–
${}^2\rho(\Xi_b^{'0})_{3/2} \to {}^2\Xi_b^0\gamma$	6362	261.91	–
${}^2\lambda(\Xi_b^{'-})_{1/2} \to {}^2\Xi_b^-\gamma$	6189	1.18	0.00
${}^4\lambda(\Xi_b^{'-})_{1/2} \to {}^2\Xi_b^-\gamma$	6202	0.62	0.00
${}^2\lambda(\Xi_b^{'-})_{3/2} \to {}^2\Xi_b^-\gamma$	6197	1.22	0.00
${}^4\lambda(\Xi_b^{'-})_{3/2} \to {}^2\Xi_b^-\gamma$	6210	1.80	0.00
${}^4\lambda(\Xi_b^{'-})_{5/2} \to {}^2\Xi_b^-\gamma$	6226.90	1.21	0.00
${}^2\rho(\Xi_b^{'-})_{1/2} \to {}^2\Xi_b^-\gamma$	6354	5.81	–
${}^2\rho(\Xi_b^{'-})_{3/2} \to {}^2\Xi_b^-\gamma$	6362	5.56	–

Table 4.14: Decay Widths in KeV units.

$B_Q \to B'_Q\gamma$	M(MeV)	Present work	$ChQM$ [66]
${}^2\lambda(\Lambda_c^+)_{1/2} \to {}^4\Sigma_c^+\gamma$	2592.25 ± 0.28	0.03	0.05
${}^2\lambda(\Lambda_c^+)_{3/2} \to {}^4\Sigma_c^+\gamma$	2628.11 ± 0.19	0.22	0.26
${}^2\rho(\Lambda_c^+)_{1/2} \to {}^4\Sigma_c^+\gamma$	2786.41	5.19	0.02
${}^4\rho(\Lambda_c^+)_{1/2} \to {}^4\Sigma_c^+\gamma$	2804.28	6.70	0.09
${}^2\rho(\Lambda_c^+)_{3/2} \to {}^4\Sigma_c^+\gamma$	2829.51	7.05	6.81
${}^4\rho(\Lambda_c^+)_{3/2} \to {}^4\Sigma_c^+\gamma$	2939.60 ± 1.5	118.56	17.40
${}^4\rho(\Lambda_c^+)_{5/2} \to {}^4\Sigma_c^+\gamma$	2919.20	511.46	–
${}^2\lambda(\Xi_c^+)_{1/2} \to {}^4\Xi_c^{'+}\gamma$	2793.25	0.59	0.44
${}^2\lambda(\Xi_c^+)_{3/2} \to {}^4\Xi_c^{'+}\gamma$	2818.50	1.17	0.99
${}^2\rho(\Xi_c^+)_{1/2} \to {}^4\Xi_c^{'+}\gamma$	2951	3.63	0.25
${}^4\rho(\Xi_c^+)_{1/2} \to {}^4\Xi_c^{'+}\gamma$	2980	22.99	43.4
${}^2\rho(\Xi_c^+)_{3/2} \to {}^4\Xi_c^{'+}\gamma$	2987	5.12	0.52
${}^4\rho(\Xi_c^+)_{3/2} \to {}^4\Xi_c^{'+}\gamma$	3016	197.06	58.1
${}^4\rho(\Xi_c^+)_{5/2} \to {}^4\Xi_c^{'+}\gamma$	3076	561.27	–
${}^2\lambda(\Xi_c^0)_{1/2} \to {}^4\Xi_c^{'0}\gamma$	2793.25	0.01	0.00
${}^2\lambda(\Xi_c^0)_{3/2} \to {}^4\Xi_c^{'0}\gamma$	2818.50	0.03	0.00
${}^2\rho(\Xi_c^0)_{1/2} \to {}^4\Xi_c^{'0}\gamma$	2951	0.08	0.00
${}^4\rho(\Xi_c^0)_{1/2} \to {}^4\Xi_c^{'0}\gamma$	2980	0.49	0.00
${}^2\rho(\Xi_c^0)_{3/2} \to {}^4\Xi_c^{'0}\gamma$	2987	0.11	0.00
${}^4\rho(\Xi_c^0)_{3/2} \to {}^4\Xi_c^{'0}\gamma$	3016	4.18	0.00
${}^4\rho(\Xi_c^0)_{5/2} \to {}^4\Xi_c^{'0}\gamma$	3076	11.90	–
${}^2\lambda(\Lambda_b^0)_{1/2} \to {}^4\Sigma_b^0\gamma$	5912.20 ± 0.13	0.07	0.09
${}^2\lambda(\Lambda_b^0)_{3/2} \to {}^4\Sigma_b^0\gamma$	5920.00 ± 0.09	0.11	0.15
${}^2\rho(\Lambda_b^0)_{1/2} \to {}^4\Sigma_b^0\gamma$	6093.30	2.77	0.02
${}^4\rho(\Lambda_b^0)_{1/2} \to {}^4\Sigma_b^0\gamma$	6105.77	11.18	8.25
${}^2\rho(\Lambda_b^0)_{3/2} \to {}^4\Sigma_b^0\gamma$	6101.03	3.06	0.03
${}^4\rho(\Lambda_b^0)_{3/2} \to {}^4\Sigma_b^0\gamma$	6113.49	109.74	9.90
${}^4\rho(\Lambda_b^0)_{5/2} \to {}^4\Sigma_b^0\gamma$	6126.37	291.42	–
${}^2\lambda(\Xi_b^0)_{1/2} \to {}^4\Xi_b^{'0}\gamma$	6048	0.11	2.04
${}^2\lambda(\Xi_b^0)_{3/2} \to {}^4\Xi_b^{'0}\gamma$	6055	0.16	2.64
${}^2\rho(\Xi_b^0)_{1/2} \to {}^4\Xi_b^{'0}\gamma$	6213	2.11	0.62
${}^4\rho(\Xi_b^0)_{1/2} \to {}^4\Xi_b^{'0}\gamma$	6225	24.08	80.0
${}^2\rho(\Xi_b^0)_{3/2} \to {}^4\Xi_b^{'0}\gamma$	6220	2.31	0.80
${}^4\rho(\Xi_b^0)_{3/2} \to {}^4\Xi_b^{'0}\gamma$	6233	155.84	78.0
${}^4\rho(\Xi_b^0)_{5/2} \to {}^4\Xi_b^{'0}\gamma$	6246	313.78	–
${}^2\lambda(\Xi_b^-)_{1/2} \to {}^4\Xi_b^{'-}\gamma$	6048	0.002	0.00
${}^2\lambda(\Xi_b^-)_{3/2} \to {}^4\Xi_b^{'-}\gamma$	6055	0.003	0.00
${}^2\rho(\Xi_b^-)_{1/2} \to {}^4\Xi_b^{'-}\gamma$	6213	0.04	0.00
${}^4\rho(\Xi_b^-)_{1/2} \to {}^4\Xi_b^{'-}\gamma$	6225	0.51	0.00
${}^2\rho(\Xi_b^-)_{3/2} \to {}^4\Xi_b^{'-}\gamma$	6220	0.05	0.00
${}^4\rho(\Xi_b^-)_{3/2} \to {}^4\Xi_b^{'-}\gamma$	6233	3.31	0.00
${}^4\rho(\Xi_b^-)_{5/2} \to {}^4\Xi_b^{'-}\gamma$	6246	6.66	–

Chapter 5

$qqqq\bar{q}$ Pentaquarks

In 2015 the LHCb collaboration announced the observation of two resonances in the $J/\psi\, p$ channel consistent with pentaquark states, one with mass of $4380\pm8 \pm 29$ MeV and the other with $4449.8\pm1.7 \pm 2.5$ MeV, both candidates were analyzed from the $\Lambda_b^0 \to J/\psi\, p\, K^-$ decay. Although they did not determine the angular momentum and parity of $P_c(4380)^+$ and $P_c(4450)^+$, their fit solution suggested two states with opposite parity and possible spin 3/2 and 5/2 [11]. Later, in 2019 with more data and statistics the LHCb collaboration discovered a new narrow pentaquark state $P_c(4312)^+$ [13], and confirmed not only the pentaquark signal $P_c(4450)^+$, but also this was observed to consist of two narrow peaks $P_c(4440)^+$ and $P_c(4457)^+$. One of the ways to confirm the nature of the pentaquark signal is to photoproduce the states P_c using an electromagnetic probe: $p(uud) + \gamma \to P_c(uudc\bar{c})$. This process is relevant the for current experimental efforts at JLab [81]. However, since in none of those announcements the quantum numbers of these resonances were determined, their understanding and interpretation remains as an open problem. For this reason we are interested in studying not only ground but also exited pentaquark states, and how to photoproduce them.

In our previous work on pentaquarks [82] through the constituent quark model we made a complete classification of the ground state pentaquarks, where we essentially distinguished the four constituent quarks from the antiquark. Nevertheless, we did not introduce any distinction between the heavy from the light quarks, nor did we evaluate the orbital contribution to the photoproduction of pentaquark. In the present work we address and solve not only these problems, but also obtain the decay widths for the photoproduction of ground and radially excited pentaquarks configurations, $qqqQ\bar{Q}$, where q denotes the light quarks (u, d, s) and Q the heavy quarks (c, b).

5.1 Pentaquark wave functions

In order to construct the pentaquark wave functions for both ground and excited states, we implement two conditions: *(i) the pentaquark wave function should be antisymmetric under any permutation of the three light quarks*, and *(ii) as all physical states, it should be a color singlet.* As a matter of fact, in this work we use the first condition different from our previous work [82], since here we focus on distinguishing the heavy from the light quarks. Of course, the number of pentaquark states is the same in both classification schemes. The spin part is standard and is obtained in a straightforward way.

In the following, the wave function of each of the degrees of freedom for the pentaquark is derived, starting with the orbital part by introducing an harmonic oscillator quark model, followed by the spin, whose obtaining is direct and standard. Subsequently, the flavor part is constructed by fixing the charm and the anti-charm $c\bar{c}$ quarks in the fourth and fifth position of the states, and antisymmetrizing with respect to the three remaining light quarks. Finally, the color wave function is constructed for states with 4 quarks and by coupling at the end the fifth quark.

5.1.1 Orbital wave function

The Hamiltonian proposed in the harmonic oscillator quark model for the five quarks is

$$H = \frac{{p_1}^2}{2m} + \frac{{p_2}^2}{2m} + \frac{{p_3}^2}{2m} + \frac{{p_4}^2}{2m'} + \frac{{p_5}^2}{2m'} + \frac{1}{2}C\sum_{i<j}^{5}|\vec{r_i} - \vec{r_j}|^2, \tag{5.1}$$

where oscillators 1, 2 and 3 have equal masses m, while 4 and 5 have m'.

If relative coordinates are used (similar to Jacobi coordinates, but modified for this system with different quark masses), Eq. 5.1 can be rewritten in a more convenient way. For this purpose the following coordinates are defined

$$\begin{cases} \vec{\rho} \equiv \frac{1}{\sqrt{2}}(\vec{r_1} - \vec{r_2}) \\ \vec{\lambda} \equiv \frac{1}{\sqrt{6}}(\vec{r_1} + \vec{r_2} - 2\vec{r_3}) \\ \vec{\eta} \equiv \frac{1}{\sqrt{2}}(\vec{r_4} - \vec{r_5}) \\ \vec{\zeta} \equiv \sqrt{\frac{6}{5}}\left[\frac{1}{3}(\vec{r_1} + \vec{r_2} + \vec{r_3}) - \frac{1}{2}(\vec{r_4} + \vec{r_5})\right] \\ \vec{R} \equiv \frac{m(\vec{r_1}+\vec{r_2}+\vec{r_3})+m'(\vec{r_4}+\vec{r_5})}{3m+2m'} \end{cases} \Rightarrow \begin{cases} \vec{r_1} = \frac{1}{\sqrt{2}}\vec{\rho} + \frac{1}{\sqrt{6}}\vec{\lambda} + \frac{\sqrt{\frac{10}{3}}m'}{3m+2m'}\vec{\zeta} + \vec{R} \\ \vec{r_2} = -\frac{1}{\sqrt{2}}\vec{\rho} + \frac{1}{\sqrt{6}}\vec{\lambda} + \frac{\sqrt{\frac{10}{3}}m'}{3m+2m'}\vec{\zeta} + \vec{R} \\ \vec{r_3} = -\sqrt{\frac{2}{3}}\vec{\lambda} + \frac{\sqrt{\frac{10}{3}}m'}{3m+2m'}\vec{\zeta} + \vec{R} \\ \vec{r_4} = \frac{1}{\sqrt{2}}\vec{\eta} - \frac{\sqrt{\frac{15}{2}}m}{3m+2m'}\vec{\zeta} + \vec{R} \\ \vec{r_5} = -\frac{1}{\sqrt{2}}\vec{\eta} - \frac{\sqrt{\frac{15}{2}}m}{3m+2m'}\vec{\zeta} + \vec{R} \end{cases}$$

its Jacobian corresponding to the change from Cartesian coordinates turns out to be

$$\prod_{i=1}^{5} d^3r_i = 5\sqrt{5}d^3\rho d^3\lambda d^3\eta d^3\zeta d^3R. \tag{5.2}$$

Moreover, their conjugate momentum associated to the above coordinates are

$$\begin{cases} \vec{p_\rho} = \frac{1}{\sqrt{2}}(\vec{p_1} - \vec{p_2}) \\ \vec{p_\lambda} = \frac{1}{\sqrt{6}}(\vec{p_1} + \vec{p_2} - 2\vec{p_3}) \\ \vec{p_\eta} = \frac{1}{\sqrt{2}}(\vec{p_4} - \vec{p_5}) \\ \vec{p_\zeta} = \sqrt{\frac{10}{3}}\frac{m'}{M}(\vec{p_1} + \vec{p_2} + \vec{p_3}) - \sqrt{\frac{15}{2}}\frac{m}{M}(\vec{p_4} + \vec{p_5}) \\ \vec{P} = \vec{p_1} + \vec{p_2} + \vec{p_3} + \vec{p_4} + \vec{p_5} \end{cases} \Rightarrow \begin{cases} \vec{p_1} = \frac{1}{\sqrt{2}}\vec{p_\rho} + \frac{1}{\sqrt{6}}\vec{p_\lambda} + \sqrt{\frac{2}{15}}\vec{p_\zeta} + \frac{m}{M}\vec{P} \\ \vec{p_2} = -\frac{1}{\sqrt{2}}\vec{p_\rho} + \frac{1}{\sqrt{6}}\vec{p_\lambda} + \sqrt{\frac{2}{15}}\vec{p_\zeta} + \frac{m}{M}\vec{P} \\ \vec{p_3} = -\sqrt{\frac{2}{3}}\vec{p_\lambda} + \sqrt{\frac{2}{15}}\vec{p_\zeta} + \frac{m}{M}\vec{P} \\ \vec{p_4} = \frac{1}{\sqrt{2}}\vec{p_\eta} - \sqrt{\frac{3}{10}}\vec{p_\zeta} + \frac{m'}{M}\vec{P} \\ \vec{P_5} = -\frac{1}{\sqrt{2}}\vec{p_\eta} - \sqrt{\frac{3}{10}}\vec{p_\zeta} + \frac{m'}{M}\vec{P}, \end{cases}$$

and equally,

$$\prod_{i=1}^{5} d^3p_i = \frac{1}{5\sqrt{5}}d^3p_\rho d^3p_\lambda d^3p_\eta d^3p_\zeta d^3P. \tag{5.3}$$

In the new coordinates the Hamiltonian separates into center-of-mass motion, plus four independent harmonic oscillators ρ, λ, η and ζ

$$H = \frac{P^2}{2M} + \frac{{p_\rho}^2}{2m_\rho} + \frac{{p_\lambda}^2}{2m_\lambda} + \frac{{p_\eta}^2}{2m_\eta} + \frac{{p_\zeta}^2}{2m_\zeta} + \frac{5}{2}C\rho^2 + \frac{5}{2}C\lambda^2 + \frac{5}{2}C\eta^2 + \frac{5}{2}C\zeta^2, \tag{5.4}$$

with the same spring constant C, but in general with different masses (and therefore different frequencies) defined as follows

$$M = 3m + 2m', \qquad m_\rho = m_\lambda \equiv m, \qquad m_\eta \equiv m', \qquad m_\zeta \equiv \frac{5mm'}{3m+2m'}, \tag{5.5}$$

where the corresponding harmonic oscillator constants and frequencies are given by

$$\alpha_i^2 = (5Cm_i)^{\frac{1}{2}}, \qquad \omega_i = \sqrt{\frac{5C}{m_i}}, \qquad i = \{\rho, \lambda, \eta, \zeta\}. \tag{5.6}$$

or more explicitly

$$\alpha_\rho^2 = (5Cm)^{\frac{1}{2}} = \alpha_\lambda^2, \qquad \alpha_\eta^2 = (5Cm')^{\frac{1}{2}}, \qquad \alpha_\zeta^2 = (5C\frac{5mm'}{3m+2m'})^{\frac{1}{2}}. \tag{5.7}$$

In order to see the effect of the light and heavy quark masses, we rewrite the harmonic oscillator constants α_ζ and α_η in terms of just α_ρ^2, through a as follows

$$\alpha_\eta^2 = \alpha_\rho^2\sqrt{a}, \qquad \alpha_\zeta^2 = \alpha_\rho^2\sqrt{\frac{5a}{3+2a}}, \qquad a \equiv \frac{m'}{m}. \tag{5.8}$$

Of course, coordinates and momenta are also related by

$$\vec{P} = M\frac{d\vec{R}}{dt}, \qquad \vec{p_\rho} = m_\rho\frac{d\vec{\rho}}{dt}, \qquad \vec{p_\lambda} = m_\lambda\frac{d\vec{\lambda}}{dt}, \qquad \vec{p_\eta} = m_\eta\frac{d\vec{\eta}}{dt}, \qquad \vec{p_\zeta} = m_\zeta\frac{d\vec{\zeta}}{dt}. \tag{5.9}$$

In the following we study not only the orbital wave function, but also the color, spin and flavor wave functions by means of their symmetry properties under interchange of any of the three light quarks, condition (i). This can be investigated though the irreducible representation of the permutation group S_3: one has the symmetric $f = [3]$, antisymmetric $f = [111]$ or mixed symmetric $[21]$ representations, or equivalently by those of the point group D_3 which is isomorphic to S_3 as A_1, A_2 and E, respectively. Here I use the later notation, where A_1 and A_2 are one-dimensional, and E two-dimensional whose components are written as E_ρ and E_λ. As a result, we can label our wave function based on their symmetry properties.

The eigenstates of Hamiltonian 5.4 are well known. **The ground state pentaquark** in momentum space is given by

$$\psi^o_{A_1}(gs) = \delta^3(\vec{P} - \vec{K_{Pc}})\sqrt{5\sqrt{5}}\psi^o_0(\vec{p}_\rho)\psi^o_0(\vec{p}_\lambda)\psi^o_0(\vec{p}_\eta)\psi^o_0(\vec{p}_\zeta), \tag{5.10}$$

where

$$\psi^o_0(\vec{p}_i) = \frac{1}{\pi^{3/4}\alpha_i^{3/2}}e^{-\frac{1}{2\alpha_i^2}p_i^2} \tag{5.11}$$

is the solution for a three-dimensional harmonic oscillator in the ground state and oscillating in the i-mode. The wave functions for excited states with one orbital excitation in some of the i-modes are given by

$$\psi^o_{E_\rho}(\rho) = \delta^3(\vec{P} - \vec{K_{Pc}})\sqrt{5\sqrt{5}}\psi^o_1(\vec{p}_\rho)\psi^o_0(\vec{p}_\lambda)\psi^o_0(\vec{p}_\eta)\psi^o_0(\vec{p}_\zeta) \tag{5.12}$$

$$\psi^o_{E_\lambda}(\lambda) = \delta^3(\vec{P} - \vec{K_{Pc}})\sqrt{5\sqrt{5}}\psi^o_1(\vec{p}_\rho)\psi^o_1(\vec{p}_\lambda)\psi^o_0(\vec{p}_\eta)\psi^o_0(\vec{p}_\zeta) \tag{5.13}$$

$$\psi^o_{A_1}(\eta) = \delta^3(\vec{P} - \vec{K_{Pc}})\sqrt{5\sqrt{5}}\psi^o_0(\vec{p}_\rho)\psi^o_0(\vec{p}_\lambda)\psi^o_1(\vec{p}_\eta)\psi^o_0(\vec{p}_\zeta) \tag{5.14}$$

$$\psi^o_{A_1}(\zeta) = \delta^3(\vec{P} - \vec{K_{Pc}})\sqrt{5\sqrt{5}}\psi^o_0(\vec{p}_\rho)\psi^o_0(\vec{p}_\lambda)\psi^o_0(\vec{p}_\eta)\psi^o_1(\vec{p}_\zeta), \tag{5.15}$$

so that

$$\psi^o_1(\vec{p}_i) = i\sqrt{\frac{8}{3}}\frac{p_i}{\pi^{1/4}\alpha_i^{5/2}}Y_{1,\mu}(\hat{p}_i)e^{-\frac{1}{2\alpha_i^2}p_i^2} \tag{5.16}$$

is the first excited state for one oscillator in momentum space. By making a Fourier transform one can also obtain the corresponding wave functions in coordinate space.

$$\psi^o_{A_1}(gs) = \frac{1}{(2\pi)^{3/2}}e^{\vec{P}\cdot\vec{R}}\frac{1}{\sqrt{5\sqrt{5}}}\psi^o_0(\vec{\rho})\psi^o_0(\vec{\lambda})\psi^o_0(\vec{\eta})\psi^o_0(\vec{\zeta}), \tag{5.17}$$

with

$$\psi_0^o(\vec{r}_i) = \frac{\alpha_i^{3/2}}{\pi^{3/4}} e^{-\frac{\alpha_i^2}{2} r_i^2} \tag{5.18}$$

is the solution for a three-dimensional harmonic oscillator in the ground state and oscillating in the i-mode. The wave functions for excited states with one orbital excitation in some of the i-modes are given by

$$\psi^o_{E_\rho}(\rho) = \frac{1}{(2\pi)^{3/2}} e^{\vec{P}\cdot\vec{R}} \frac{1}{\sqrt{5\sqrt{5}}} \psi_1^o(\vec{\rho})\psi_0^o(\vec{\lambda})\psi_0^o(\vec{\eta})\psi_0^o(\vec{\zeta}) \tag{5.19}$$

$$\psi^o_{E_\lambda}(\lambda) = \frac{1}{(2\pi)^{3/2}} e^{\vec{P}\cdot\vec{R}} \frac{1}{\sqrt{5\sqrt{5}}} \psi_1^o(\vec{\rho})\psi_1^o(\vec{\lambda})\psi_0^o(\vec{\eta})\psi_0^o(\vec{\zeta}) \tag{5.20}$$

$$\psi^o_{A_1}(\eta) = \frac{1}{(2\pi)^{3/2}} e^{\vec{P}\cdot\vec{R}} \frac{1}{\sqrt{5\sqrt{5}}} \psi_0^o(\vec{\rho})\psi_0^o(\vec{\lambda})\psi_1^o(\vec{\eta})\psi_0^o(\vec{\zeta}) \tag{5.21}$$

$$\psi^o_{A_1}(\zeta) = \frac{1}{(2\pi)^{3/2}} e^{\vec{P}\cdot\vec{R}} \frac{1}{\sqrt{5\sqrt{5}}} \psi_0^o(\vec{\rho})\psi_0^o(\vec{\lambda})\psi_0^o(\vec{\eta})\psi_1^o(\vec{\zeta}), \tag{5.22}$$

where

$$\psi_1^o(\vec{r}_i) = i\sqrt{\frac{8}{3}} \frac{\alpha_i^{5/2} r_i}{\pi^{1/4}} Y_{1,\mu}(\hat{r}_i) e^{-\frac{\alpha_i^2}{2} r_i^2} \tag{5.23}$$

The same analysis on frequencies as in heavy baryons can be done, if we consider the above masses and specially $m' > m$ this implies $m_\eta > m_\zeta > m = m_\rho = m_\lambda$, which is equivalent to have a system with two heavy and three light quarks $qqqQ\bar{Q}$. From the above and taking into account the inverse relation on frequencies with masses follows that $\omega_\eta < \omega_\zeta < \omega_\rho = \omega_\lambda$. This is the order of relevance for each modes, where the less nonzero energetic orbital state is the best candidate to contribute to the photocouplings [82].

5.1.2 Color wave function

In [82], we obtained the q^4 color wave functions specified by the Young tableaux [211] under the permutation group S_4 with F_1 symmetry under the tetrahedral group. In that study, once the antiquark $\bar{q}$ with Young tableaux [11] was coupled to the q^4 color wave function, the complete pentaquark color wave functions were obtained, and the color singlet [222] condition under $SU(3)$ group was satisfy. The color wave functions for the pentaquark are explicitly given by

$$\begin{aligned}\left|\psi^c_{E_\rho}\right\rangle = \frac{1}{12}\big[&|((2gbr - 2bgr - rgb + grb + rbg - brg)r + 3(rgr - grr)b - 3(rbr - brr)g)\bar{r}\rangle \\ &+|((2brg - 2rbg - gbr + bgr + grb - rgb)g + 3(gbg - bgg)r - 3(grg - rgg)b)\bar{g}\rangle \\ &+|((2rgb - 2grb - brg + rbg + bgr - gbr)b + 3(brb - rbb)g - 3(bgb - gbb)r)\bar{b}\rangle\big],\end{aligned} \tag{5.24}$$

$$\begin{aligned}\left|\psi^c_{E_\lambda}\right\rangle = \frac{1}{4\sqrt{3}}\big[&|((2rrg - rgr - grr)b - (2rrb - rbr - brr)g + (rgb + grb - rbg - brg)r)\bar{r}\rangle \\ &+|((2ggb - gbg - bgg)r - (2ggr - grg - rgg)b + (gbr + bgr - grb - rgb)g)\bar{g}\rangle \\ &+|((2bbr - brb - rbb)g - (2bbg - bgb - gbb)r + (brg + rbg - bgr - gbr)b)\bar{b}\rangle\big]\end{aligned} \tag{5.25}$$

and

$$\begin{aligned}\left|\psi^c_{A_2}\right\rangle = \frac{1}{3\sqrt{2}}\big[&|((rgb - grb + brg - rbg + gbr - bgr)r)\bar{r}\rangle \\ &+|((rgb - grb + brg - rbg + gbr - bgr)g)\bar{g}\rangle \\ &+|((rgb - grb + brg - rbg + gbr - bgr)b)\bar{b}\rangle\big]\end{aligned} \tag{5.26}$$

The labels E_ρ, E_λ and A_2 refer to the symmetry properties of the color wave function under the permutation of the first (three) light quarks.

5.1.3 Spin wave function

The construction of spin wave functions for pentaquark configurations is developed in an analogous way than the analysis followed by a system with three particles, where in Eqs. (1.33) and (1.34) we obtained the following spin states with maximum projection

$$\begin{aligned} |[3],3/2,3/2\rangle_{A_1} &= |\uparrow\uparrow\uparrow\rangle \\ |[21],1/2,1/2\rangle_{E_\rho} &= \frac{1}{\sqrt{2}}(|\uparrow\downarrow\uparrow\rangle - |\downarrow\uparrow\uparrow\rangle \\ |[21],1/2,1/2\rangle_{E_\lambda} &= \frac{1}{\sqrt{6}}(2|\uparrow\uparrow\downarrow\rangle - |\uparrow\downarrow\uparrow\rangle - |\downarrow\uparrow\uparrow\rangle). \end{aligned} \tag{5.27}$$

In the case of **four quarks**, the wave functions are given by the Young tableaux [4] for $S = 2$, [31] for $S = 1$ and [22] for $S = 0$. The fourth quark can be coupled with the states of three quarks through the following relation with the Clebsh-Gordan coefficients

$$|(S_{123},S_4)SM_S\rangle = \sum_{M_{123},M_4} \langle S_{123}M_{123},S_4M_4|S,M_S\rangle |S_{123}M_{123}\rangle |S_4M_4\rangle. \tag{5.28}$$

Therefore one obtains the following states with $S = M_S$ and labeled by $|[f]S,M_S\rangle$

$$\begin{aligned} |[4],2,2\rangle_{A_1} &= |(3/2,1/2)2,2\rangle = |[3]3/2,3/2\rangle_{A_1}|\uparrow\rangle \\ |[31],1,1\rangle_{E_\rho} &= |(1/2,1/2)1,1\rangle = |[21]1/2,1/2\rangle_{E_\rho}|\uparrow\rangle \\ |[31],1,1\rangle_{E_\lambda} &= |(1/2,1/2)1,1\rangle = |[21]1/2,1/2\rangle_{E_\lambda}|\uparrow\rangle \\ |[31],1,1\rangle_{A_1} &= |(3/2,1/2)1,1\rangle = \frac{\sqrt{3}}{2}|[3]3/2,3/2\rangle_{A_1}|\downarrow\rangle - \frac{1}{2}|[3]3/2,1/2\rangle_{A_1}|\uparrow\rangle \\ |[22],0,0\rangle_{E_\rho} &= |(1/2,1/2)0,0\rangle = \frac{1}{\sqrt{2}}|[21]1/2,1/2\rangle_{E_\rho}|\downarrow\rangle - \frac{1}{\sqrt{2}}|[21]1/2,-1/2\rangle_{E_\rho}|\uparrow\rangle \\ |[22],0,0\rangle_{E_\lambda} &= |(1/2,1/2)0,0\rangle = \frac{1}{\sqrt{2}}|[21]1/2,1/2\rangle_{E_\lambda}|\downarrow\rangle - \frac{1}{\sqrt{2}}|[21]1/2,-1/2\rangle_{E_\lambda}|\uparrow\rangle, \end{aligned} \tag{5.29}$$

where the labels of these states comes from the symmetric permutation group S_3. The rest of the spin projections can be calculated by applying the lowering operator in spin space.

Finally, the construction of the wave functions for the **five quarks** can be done by coupling one quark state to the four spin states obtained before, as follows

$$|(S_{1234},S_5)SM_S\rangle = \sum_{M_{1234},M_5} \langle S_{1234}M_{1234},S_5M_5|S,M_S\rangle |S_{1234}M_{1234}\rangle |S_5M_5\rangle. \tag{5.30}$$

The explicit spin wave functions of the pentaquarks, with $S = M_S$ are given by

$$
\begin{aligned}
|\chi_{A_1}, 5/2, 5/2\rangle &= |(2,1/2)5/2, 5/2\rangle = |[4],2,2\rangle_{A_1}|\uparrow\rangle \\
|\chi_{A_1}, 3/2, 3/2\rangle &= |(2,1/2)3/2, 3/2\rangle = \frac{2}{\sqrt{5}}|[4],2,2\rangle_{A_1}|\downarrow\rangle - \frac{1}{\sqrt{5}}|[4],2,1\rangle_{A_1}|\uparrow\rangle \\
|\chi_{E_\rho}, 3/2, 3/2\rangle &= |(1,1/2)3/2, 3/2\rangle = |[31],1,1\rangle_{E_\rho}|\uparrow\rangle \\
|\chi_{E_\lambda}, 3/2, 3/2\rangle &= |(1,1/2)3/2, 3/2\rangle = |[31],1,1\rangle_{E_\lambda}|\uparrow\rangle \\
|\chi_{A_1}, 3/2, 3/2\rangle &= |(1,1/2),3/2, 3/2\rangle = |[31],1,1\rangle_{A_1}|\uparrow\rangle \\
|\chi_{E_\rho}, 1/2, 1/2\rangle &= |(1,1/2)1/2, 1/2\rangle = \sqrt{\frac{2}{3}}|[31],1,1\rangle_{E_\rho}|\downarrow\rangle - \frac{1}{\sqrt{3}}|[31],1,0\rangle_{E_\rho}|\uparrow\rangle \\
|\chi_{E_\lambda}, 1/2, 1/2\rangle &= |(1,1/2)1/2, 1/2\rangle = \sqrt{\frac{2}{3}}|[31],1,1\rangle_{E_\lambda}|\downarrow\rangle - \frac{1}{\sqrt{3}}|[31],1,0\rangle_{E_\lambda}|\uparrow\rangle \\
|\chi_{A_1}, 1/2, 1/2\rangle &= |(1,1/2)1/2, 1/2\rangle = \sqrt{\frac{2}{3}}|[31],1,1\rangle_{A_1}|\downarrow\rangle - \frac{1}{\sqrt{3}}|[31],1,0\rangle_{A_1}|\uparrow\rangle \\
|\chi_{E_\rho}, 1/2, 1/2\rangle &= |(0,1/2)1/2, 1/2\rangle = \frac{1}{2\sqrt{3}}|[22],0,0\rangle_{E_\rho}|\uparrow\rangle \\
|\chi_{E_\lambda}, 1/2, 1/2\rangle &= |(0,1/2)1/2, 1/2\rangle = \frac{1}{2\sqrt{3}}|[22],0,0\rangle_{E_\lambda}|\uparrow\rangle
\end{aligned}
\tag{5.31}
$$

Here the notation $|\chi_t, S, M_S\rangle$ is used, where labels χ_t keep the symmetry information under interchange of any of the three light quarks associated to the permutation group S_3. Again, the other spin projections can be obtained by using the lowering operator.

5.1.4 Flavor wave function

Since we are interested in obtaining the pentaquark flavor wave functions with the explicit distinction of the heavy quarks, we fixed the charm quark c in the four position and the anti-charm $\bar{c}$ in the fifth position of the states, so that we antisymmetrize with respect to the three remaining flavors. Therefore the three possible configurations are

$$|\phi_{A_1}\rangle = \left|\frac{1}{\sqrt{3}}(uud + udu + duu)c\bar{c}\right\rangle, \tag{5.32}$$

$$|\phi_{E_\rho}\rangle = \left|\frac{1}{\sqrt{2}}(ud - du)uc\bar{c}\right\rangle, \tag{5.33}$$

$$|\phi_{E_\lambda}\rangle = \left|\frac{1}{\sqrt{6}}(2uud - udu - duu)c\bar{c}\right\rangle, \tag{5.34}$$

for the antisymmetric A_1, and mixed symetric E_ρ and E_λ wave functions under S_3, respectively.

5.1.5 Ground-state pentaquarks

In this work the interest is in constructing the pentaquark configurations with $J^P = 3/2^-$ for ground state and $J^P = 3/2^+$ for the excited states. Since the total ground state pentaquark wave function (with orbital angular momentum and parity $L^P = 0^+$) has to be antisymmetric (A_2), it can be written as

$$\psi = \left[\psi^{\rm o}_{A_1} \times \psi^{\rm csf}_{A_2}\right]_{A_2}, \tag{5.35}$$

where the symmetric (A_1) orbital wave function is coupled with the antisymmetric color-spin-flavor part, and due to the symmetry properties of the color part one can have

$$
\begin{aligned}
\psi^{\rm csf}_{A_2} &= \left[\psi^{\rm c}_{A_2} \times \psi^{\rm sf}_{A_1}\right]_{A_2}, \\
\psi^{\rm csf}_{A_2} &= \left[\psi^{\rm c}_{E} \times \psi^{\rm sf}_{E}\right]_{A_2},
\end{aligned}
\tag{5.36}
$$

In turn we obtain the following combinations for the spin-flavor part

$$\begin{aligned}
\psi^{\rm sf}_{A_1} &= [\phi_{A_1}\times\chi_{A_1}]_{A_1}=\phi_{A_1}\chi_{A_1},\\
\psi^{\rm sf}_{A_1} &= [\phi_{E}\times\chi_{E}]_{A_1}=\frac{1}{\sqrt{2}}(\phi_{E_\rho}\chi_{E_\rho}+\phi_{E_\lambda}\chi_{E_\lambda}),\\
\psi^{\rm sf}_{E} &= [\phi_{A_1}\times\chi_{E}]_{E}=\phi_{A_1}\chi_{E},\\
\psi^{\rm sf}_{E} &= [\phi_{E}\times\chi_{A_1}]_{E}=\phi_{E}\chi_{A_1},\\
\psi^{\rm sf}_{E} &= [\phi_{E}\times\chi_{E}]_{E}=\left\{\begin{array}{l}\frac{1}{\sqrt{2}}(\phi_{E_\rho}\chi_{E_\lambda}+\phi_{E_\lambda}\chi_{E_\rho}),\\ \frac{1}{\sqrt{2}}(\phi_{E_\rho}\chi_{E_\rho}-\phi_{E_\lambda}\chi_{E_\lambda}),\end{array}\right.\\
\psi^{\rm sf}_{A_2} &= [\phi_{E}\times\chi_{E}]_{A_2}=\frac{1}{\sqrt{2}}(\phi_{E_\lambda}\chi_{E_\rho}-\phi_{E_\rho}\chi_{E_\lambda}).
\end{aligned}\tag{5.37}$$

Considering all the above, in order to satisfy conditions for the totally antisymmetric wave function and the color singlet states, there are five configurations for the ground states pentaquark

$$\psi_1 = \psi^o_{A_1}\psi^c_{A_2}\phi_{A_1}\chi_{A_1},\tag{5.38}$$

$$\psi_2 = \frac{1}{\sqrt{2}}\psi^o_{A_1}\psi^c_{A_2}(\phi_{E_\rho}\chi_{E_\rho}+\phi_{E_\lambda}\chi_{E_\lambda}),\tag{5.39}$$

$$\psi_3 = \frac{1}{\sqrt{2}}\psi^o_{A_1}(\psi^c_{E_\lambda}\phi_{E_\rho}-\psi^c_{E_\rho}\phi_{E_\lambda})\chi_{A_1},\tag{5.40}$$

$$\psi_4 = \frac{1}{\sqrt{2}}\psi^o_{A_1}\phi_{A_1}(\psi^c_{E_\lambda}\chi_{E_\rho}-\psi^c_{E_\rho}\chi_{E_\lambda}),\tag{5.41}$$

$$\psi_5 = \frac{1}{2}\psi^o_{A_1}\left[\phi^c_\lambda(\phi_{E_\rho}\chi_{E_\lambda}+\phi_{E_\lambda}\chi_{E_\rho})-\phi^c_{E_\rho}(\phi_{E_\rho}\chi_{E_\rho}-\phi_{E_\lambda}\chi_{E_\lambda})\right].\tag{5.42}$$

5.1.6 Orbital-excited pentaquarks

The wave functions of the excited pentaquarks can be obtained if we guide ourselves by similar restrictions on the symmetry of total wave function and color confinement. States with one quantum of radial excitation, $L^P=1^-$, have different symmetry properties in their wave functions. The orbital wave function for one quantum of excitation is either mixed symmetric E for an excitation in ρ or λ, $\psi^o_{E_\rho}(\rho)$ and $\psi^o_{E_\lambda}(\lambda)$ or symmetric A_1 for an excitation in η or ζ, $\psi^o_{A_1}(\eta)$ and $\psi^o_{A_1}(\zeta)$.

The orbital part of the pentaquark wave function can have aside from $\psi^o=\psi^o_E$ for the excitation in the ρ and λ coordinates, the wave functions $\psi^o=\psi^o_{A_1}(\eta)$, $\psi^o_{A_1}(\zeta)$ for one quantum of excitation in the η or ζ coordinate, respectively. Then for this case the total wave functions can be

$$\begin{aligned}
\psi &= \left[\psi^{\rm o}_{A_1}\times\psi^{\rm csf}_{A_2}\right]_{A_2}\\
\psi &= \left[\psi^{\rm o}_{E}\times\psi^{\rm csf}_{E}\right]_{A_2},
\end{aligned}\tag{5.43}$$

and besides the orbital part, we have the color symmetry properties, so that we can have either the same sort of combinations as for the ground state pentaquarks

$$\begin{aligned}
\psi^{\rm csf}_{A_2} &= \left[\psi^{\rm c}_{A_2}\times\psi^{\rm sf}_{A_1}\right]_{A_2}\\
\psi^{\rm csf}_{A_2} &= \left[\psi^{\rm c}_{E}\times\psi^{\rm sf}_{E}\right]_{A_2},
\end{aligned}\tag{5.44}$$

or new configurations

$$\begin{aligned}
\psi^{\rm csf}_{E} &= \left[\psi^{\rm c}_{A_2}\times\psi^{\rm sf}_{E}\right]_{E},\\
\psi^{\rm csf}_{E} &= \left[\psi^{\rm c}_{E}\times\psi^{\rm sf}_{A_2}\right]_{E},\\
\psi^{\rm csf}_{E} &= \left[\psi^{\rm c}_{E}\times\psi^{\rm sf}_{A_1}\right]_{E},\\
\psi^{\rm csf}_{E} &= \left[\psi^{\rm c}_{E}\times\psi^{\rm sf}_{E}\right]_{E}.
\end{aligned}\tag{5.45}$$

The explicit form of all these possible configurations are

$$\psi_1 = \psi^o_\eta \psi^c_{A_2} \phi_{A_1} \chi_{A_1} \tag{5.46}$$

$$\psi_2 = \frac{1}{\sqrt{2}} \psi^o_\eta \psi^c_{A_2} (\phi_{E_\rho} \chi_{E_\rho} + \phi_{E_\lambda} \chi_{E_\lambda}) \tag{5.47}$$

$$\psi_3 = \frac{1}{\sqrt{2}} \psi^o_\eta (\psi^c_{E_\lambda} \phi_{E_\rho} - \psi^c_{E_\rho} \phi_{E_\lambda}) \chi_{A_1} \tag{5.48}$$

$$\psi_4 = \frac{1}{\sqrt{2}} \psi^o_\eta \phi_{A_1} (\psi^c_{E_\lambda} \chi_{E_\rho} - \psi^c_{E_\rho} \chi_{E_\lambda}) \tag{5.49}$$

$$\psi_5 = \frac{1}{2} \psi^o_\eta \left[\psi^c_{E_\lambda} (\phi_{E_\rho} \chi_{E_\lambda} + \phi_{E_\lambda} \chi_{E_\rho}) - \psi^c_\rho (\phi_{E_\rho} \chi_{E_\rho} - \phi_{E_\lambda} \chi_{E_\lambda}) \right], \tag{5.50}$$

for one quantum of excitation in the η mode, and

$$\psi_6 = \psi^o_\zeta \psi^c_{A_2} \phi_{A_1} \chi_{A_1} \tag{5.51}$$

$$\psi_7 = \frac{1}{\sqrt{2}} \psi^o_\zeta \psi^c_{A_2} (\phi_{E_\rho} \chi_{E_\rho} + \phi_{E_\lambda} \chi_{E_\lambda}) \tag{5.52}$$

$$\psi_8 = \frac{1}{\sqrt{2}} \psi^o_\zeta (\psi^c_{E_\lambda} \phi_{E_\rho} - \psi^c_{E_\rho} \phi_{E_\lambda}) \chi_{A_1} \tag{5.53}$$

$$\psi_9 = \frac{1}{\sqrt{2}} \psi^o_\zeta \phi_{A_1} (\psi^c_{E_\lambda} \chi_{E_\rho} - \psi^c_{E_\rho} \chi_{E_\lambda}) \tag{5.54}$$

$$\psi_{10} = \frac{1}{2} \psi^o_\zeta \left[\psi^c_{E_\lambda} (\phi_{E_\rho} \chi_{E_\lambda} + \phi_{E_\lambda} \chi_{E_\rho}) - \psi^c_\rho (\phi_{E_\rho} \chi_{E_\rho} - \phi_{E_\lambda} \chi_{E_\lambda}) \right], \tag{5.55}$$

for the excitation in ζ.

On the other hand, the explicit nine possible pentaquark configurations with excitation in the ρ and λ coordinates in the orbital part are

$$\psi_{11} = \frac{1}{\sqrt{2}} (\psi^o_{E_\rho} \psi^c_{E_\lambda} - \psi^o_{E_\lambda} \psi^c_{E_\rho}) \phi_{A_1} \chi_{A_1} \tag{5.56}$$

$$\psi_{12} = \frac{1}{2} (\psi^o_{E_\rho} \psi^c_{E_\lambda} - \psi^o_{E_\lambda} \psi^c_{E_\rho}) (\phi_{E_\rho} \chi_{E_\rho} + \phi_{E_\lambda} \chi_{E_\lambda}) \tag{5.57}$$

$$\psi_{13} = \frac{1}{2} \left[\psi^o_{E_\rho} (\psi^c_{E_\rho} \chi_{E_\rho} - \psi^c_{E_\lambda} \chi_{E_\lambda}) - \psi^o_{E_\lambda} (\psi^c_{E_\rho} \chi_{E_\lambda} + \psi^c_{E_\lambda} \chi_{E_\rho}) \right] \phi_{A_1} \tag{5.58}$$

$$\psi_{14} = \frac{1}{2} \left[\psi^o_{E_\rho} (\psi^c_{E_\rho} \phi_{E_\rho} - \psi^c_{E_\lambda} \phi_{E_\lambda}) - \psi^o_{E_\lambda} (\psi^c_{E_\rho} \phi_{E_\lambda} + \psi^c_{E_\lambda} \phi_{E_\rho}) \right] \chi_{A_1} \tag{5.59}$$

$$\begin{aligned} \psi_{15} = \frac{1}{2\sqrt{2}} \Big\{ & \psi^o_{E_\rho} \left[\psi^c_{E_\rho} (\phi_{E_\rho} \chi_{E_\lambda} + \phi_{E_\lambda} \chi_{E_\rho}) - \psi^c_{E_\lambda} (\phi_{E_\rho} \chi_{E_\rho} - \phi_{E_\lambda} \chi_{E_\lambda}) \right] \\ & - \psi^o_{E_\lambda} \left[\psi^c_{E_\rho} (\phi_{E_\rho} \chi_{E_\rho} - \phi_{E_\lambda} \chi_{E_\lambda}) + \psi^c_{E_\lambda} (\phi_{E_\rho} \chi_{E_\lambda} + \phi_{E_\lambda} \chi_{E_\rho}) \right] \Big\} \end{aligned} \tag{5.60}$$

$$\psi_{16} = \frac{1}{\sqrt{2}} (\psi^o_{E_\rho} \chi_{E_\rho} + \psi^o_{E_\lambda} \chi_{E_\lambda}) \psi^c_{A_2} \phi_{A_1} \tag{5.61}$$

$$\psi_{17} = \frac{1}{\sqrt{2}} (\psi^o_{E_\rho} \phi_{E_\rho} + \psi^o_{E_\lambda} \phi_{E_\lambda}) \psi^c_{A_2} \chi_{A_1} \tag{5.62}$$

$$\psi_{18} = \frac{1}{2} \left[(\psi^o_{E_\rho} (\phi_{E_\rho} \chi_{E_\lambda} + \phi_{E_\lambda} \chi_{E_\rho}) + \psi^o_{E_\lambda} (\phi_{E_\rho} \chi_{E_\rho} - \phi_{E_\lambda} \chi_{E_\lambda}) \right] \psi^c_{A_2} \tag{5.63}$$

$$\psi_{19} = \frac{1}{2} (\psi^o_{E_\lambda} \psi^c_{E_\lambda} + \psi^o_{E_\rho} \psi^c_{E_\rho}) (\phi_{E_\lambda} \chi_{E_\rho} - \phi_{E_\rho} \chi_{E_\lambda}). \tag{5.64}$$

$$\tag{5.65}$$

Chapter 6

Photocouplings of hidden-charm pentaquarks

In this chapter we study the photocouplings for pentaquarks in both ground and excited states. The Hamiltonian of interaction for electromagnetic couplings is given by [60]

$$H = e \int d^3x \hat{J}^\mu(\vec{x}) A_\mu(\vec{x}) \tag{6.1}$$

where A_μ is the electromagnetic field and J^μ is the quark current given by

$$\hat{J}^\mu(\vec{x}) = \sum_q \bar{q}(\vec{x}) e_q \gamma^\mu q(\vec{x}). \tag{6.2}$$

Here, the sum runs over all flavors. For each flavor q, there is a quark field $q(\vec{x})$ (Dirac spinor field) and e_q is the quark charge in the flavor space, in e units. For simplicity, we chose this implicit notation to avoid to add other flavor index. These field are expressed in terms of the creation an annihilation operators of second quantization

$$A_\mu(\vec{x}) = \int \frac{d^3k}{(2\pi)^{\frac{3}{2}}} \frac{1}{\sqrt{2k^0}} \left[a_\mu(\vec{k}) e^{i\vec{k}\cdot\vec{x}} + a_\mu^\dagger(\vec{k}) e^{-i\vec{k}\cdot\vec{x}} \right] \tag{6.3}$$

$$q(\vec{x}) = \int \frac{d^3p}{(2\pi)^{\frac{3}{2}}} \left(\frac{m}{p^0} \right)^{\frac{1}{2}} \sum_s \left[u_s(\vec{p}) b_s(\vec{p}) e^{i\vec{p}\cdot\vec{x}} + v_s(\vec{p}) d_s^\dagger(\vec{p}) e^{-i\vec{p}\cdot\vec{x}} \right] \tag{6.4}$$

with the commutation and anticommutation relations given by

$$\left[a_\mu(\vec{k}), a_\nu^\dagger(\vec{k}') \right] = -g_{\mu\nu} \delta^3(\vec{k} - \vec{k}'), \tag{6.5}$$

$$\left\{ b_s(\vec{p}), b_{s'}^\dagger(\vec{p'}) \right\} = \left\{ d_s(\vec{p}), d_{s'}^\dagger(\vec{p'}) \right\} = \delta_{ss'} \delta^3(\vec{p} - \vec{p'}), \tag{6.6}$$

and the normalization of plane waves

$$\langle \vec{k}, \mu | \vec{k}', \nu \rangle = -g_{\mu\nu} \delta^3(\vec{k} - \vec{k}') \tag{6.7}$$

$$\langle \vec{p}, s | \vec{p}', s' \rangle = \delta_{ss'} \delta^3(\vec{p} - \vec{p'}). \tag{6.8}$$

The spinors have the normalization

$$u_s^\dagger(\vec{p}) u_{s'}(\vec{p'}) = v_s^\dagger(\vec{p}) v_{s'}(\vec{p'}) = \frac{p^0}{m} \delta_{ss'}. \tag{6.9}$$

Considering all these conventions for the interaction Hamiltonian and the electromagnetic field, the electric charge e is expressed in Heaviside-Lorentz units. The quark current is

$$\begin{aligned}\hat{J}^{\mu}(\vec{x}) &= \sum_{q}\int\frac{d^3p'}{(2\pi)^{\frac{3}{2}}}\left(\frac{m}{p'^0}\right)^{\frac{1}{2}}\sum_{s'}\left[\bar{u}_{s'}(\vec{p'})b^{\dagger}_{s'}(\vec{p'})e^{-i\vec{p'}\cdot\vec{x}}+\bar{v}_{s'}(\vec{p'})d_{s'}(\vec{p'})e^{i\vec{p'}\cdot\vec{x}}\right]e_q\gamma^{\mu}\\ &\int\frac{d^3p}{(2\pi)^{\frac{3}{2}}}\left(\frac{m}{p^0}\right)^{\frac{1}{2}}\sum_{s}\left[u_s(\vec{p})b_s(\vec{p})e^{i\vec{p}\cdot\vec{x}}+v_s(\vec{p})d^{\dagger}_s(\vec{p})e^{-i\vec{p}\cdot\vec{x}}\right] \qquad (6.10)\end{aligned}$$

in turn this current can be expanded into four currents which can be taken into account depending on the type of process to be analyzed

$$J^{\mu}_1(\vec{x}) = \int\frac{d^3p}{(2\pi)^{\frac{3}{2}}}\left(\frac{m}{p^0}\right)^{\frac{1}{2}}\int\frac{d^3p'}{(2\pi)^{\frac{3}{2}}}\left(\frac{m}{p'^0}\right)^{\frac{1}{2}}\sum_{q}\sum_{ss'}\bar{u}_{s'}(\vec{p'})e_q\gamma^{\mu}u_s(\vec{p})b^{\dagger}_{s'}(\vec{p'})b_s(\vec{p})e^{i(\vec{p}-\vec{p'})\cdot\vec{x}} \qquad (6.11)$$

$$J^{\mu}_2(\vec{x}) = \int\frac{d^3p}{(2\pi)^{\frac{3}{2}}}\left(\frac{m}{p^0}\right)^{\frac{1}{2}}\int\frac{d^3p'}{(2\pi)^{\frac{3}{2}}}\left(\frac{m}{p'^0}\right)^{\frac{1}{2}}\sum_{q}\sum_{ss'}\bar{u}_{s'}(\vec{p'})e_q\gamma^{\mu}v_s(\vec{p})d^{\dagger}_{s'}(\vec{p'})b^{\dagger}_s(\vec{p})e^{i(-\vec{p}-\vec{p'})\cdot\vec{x}} \qquad (6.12)$$

$$J^{\mu}_3(\vec{x}) = \int\frac{d^3p}{(2\pi)^{\frac{3}{2}}}\left(\frac{m}{p^0}\right)^{\frac{1}{2}}\int\frac{d^3p'}{(2\pi)^{\frac{3}{2}}}\left(\frac{m}{p'^0}\right)^{\frac{1}{2}}\sum_{q}\sum_{ss'}\bar{v}_{s'}(\vec{p'})e_q\gamma^{\mu}u_s(\vec{p})d_{s'}(\vec{p'})b_s(\vec{p})e^{i(\vec{p}+\vec{p'})\cdot\vec{x}} \qquad (6.13)$$

$$J^{\mu}_4(\vec{x}) = \int\frac{d^3p}{(2\pi)^{\frac{3}{2}}}\left(\frac{m}{p^0}\right)^{\frac{1}{2}}\int\frac{d^3p'}{(2\pi)^{\frac{3}{2}}}\left(\frac{m}{p'^0}\right)^{\frac{1}{2}}\sum_{q}\sum_{ss'}\bar{v}_{s'}(\vec{p'})e_q\gamma^{\mu}v_s(\vec{p})d_{s'}(\vec{p'})d^{\dagger}_s(\vec{p})e^{i(\vec{p'}-\vec{p})\cdot\vec{x}}. \qquad (6.14)$$

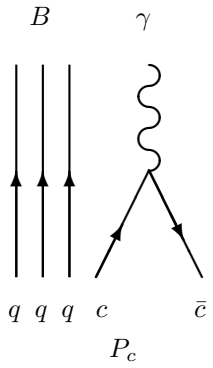

Fig. 6.1: Electromagnetic decay of pentaquark P_c into a baryon B and a photon, $P_c \to B + \gamma$.

The operator $J^{\mu}_1(\vec{x})$ by its structure is related to an elastic process between quarks, the operator $J^{\mu}_2(\vec{x})$ is related to a process of creating a quark-antiquark pair while operator $J^{\mu}_3(\vec{x})$ represents a process involving **the annihilation of a quark-antiquark pair** and finally $J^{\mu}_4(\vec{x})$ represents an

elastic process between antiquarks. In this way the effective Hamiltonian can be separates in four terms denoted by

$$H_i = e\int d^3x J_i^{\mu}(\vec{x})A_{\mu}(\vec{x}) \tag{6.15}$$

The prime interest of this work is calculate the photocouplings for pentaquarks, in particular an electromagnetic decay process between the pentaquark (configuration $qqqc\bar{c}$) and the proton (qqq), hence the relevant term for this decay process $P_c \to p + \gamma$ is the annihilation of a $c\bar{c}$ pair

$$\begin{aligned} H_3 &= e\int d^3x \int \frac{d^3p}{(2\pi)^{\frac{3}{2}}}\left(\frac{m}{p^0}\right)^{\frac{1}{2}} \int \frac{d^3p'}{(2\pi)^{\frac{3}{2}}}\left(\frac{m}{p'^0}\right)^{\frac{1}{2}} \int \frac{d^3k}{(2\pi)^{\frac{3}{2}}}\frac{1}{\sqrt{2k^0}}\sum_q\sum_{ss'}\bar{v}_{s'}(\vec{p'})e_q\gamma^{\mu}u_s(\vec{p}) \\ &\quad d_{s'}(\vec{p'})b_s(\vec{p})e^{i(\vec{p}+\vec{p'})\cdot\vec{x}}\left[a_{\mu}(\vec{k})e^{i\vec{k}\cdot\vec{x}} + a_{\mu}^{\dagger}(\vec{k})e^{-i\vec{k}\cdot\vec{x}}\right] \end{aligned} \tag{6.16}$$

$$\begin{aligned} H_3 &= e\int \frac{d^3p}{(2\pi)^{\frac{3}{2}}}\left(\frac{m}{p^0}\right)^{\frac{1}{2}} \int \frac{d^3p'}{(2\pi)^{\frac{3}{2}}}\left(\frac{m}{p'^0}\right)^{\frac{1}{2}} \int \frac{d^3k}{(2\pi)^{\frac{3}{2}}}\frac{1}{\sqrt{2k^0}}\sum_q\sum_{ss'}\bar{v}_{s'}(\vec{p'})e_q\gamma^{\mu}u_s(\vec{p})d_{s'}(\vec{p'})b_s(\vec{p}) \\ &\quad \left[a_{\mu}(\vec{k})\delta^3(\vec{p}+\vec{p'}+\vec{k}) + a_{\mu}^{\dagger}(\vec{k})\delta^3(\vec{p}+\vec{p'}-\vec{k})\right]. \end{aligned} \tag{6.17}$$

In particular, the *emission* and *absorption* processes of a photon with momentum $\vec{k}$ depend completely in the creation and annihilation operator terms of the electromagnetic field, respectively.

In the non-relativistic limit the quark currents for H_3 can be reduce as follows (see Appendix A)

$$\begin{aligned} \bar{v}_{s'}(\vec{p'})\gamma^0 u_s(\vec{p}) &\to \chi_{s'}^{\dagger}\frac{\vec{\sigma}\cdot(\vec{p}+\vec{p'})}{2m}\chi_s \\ \bar{v}_{s'}(\vec{p'})\gamma^k u_s(\vec{p}) &\to \chi_{s'}^{\dagger}\sigma^k\chi_s \end{aligned} \tag{6.18}$$

6.1 Electromagnetic decays by pair-annihilation

Since the current interest is in the photoproduction of pentaquark $P_c(uudc\bar{c}) \to p(uud) + \gamma$, we need the ground states for both the proton and the pentaquark. The wave function for the proton hereafter will be denoted as $|B\rangle$ and is given in the momentum space in terms of the creation operators of quarks acting on the vacuum state and the normalization factor $1/\sqrt{3!}$ corresponding with three identical particles.

$$|B\rangle = \frac{1}{\sqrt{6}}\int\prod_{i=6}^{8} d^3p_i\Psi_p(\vec{p_6},\vec{p_7},\vec{p_8})b_6^{\dagger}(\vec{p_6})b_7^{\dagger}(\vec{p_7})b_8^{\dagger}(\vec{p_8})|0\rangle. \tag{6.19}$$

The pentaquark wave function is

$$|P_c\rangle = \frac{1}{\sqrt{6}}\int\prod_{i=1}^{5} d^3p_i\Psi_{P_c}(\vec{p_1},\vec{p_2},\vec{p_3},\vec{p_4},\vec{p_5})b_1^{\dagger}(\vec{p_1})b_2^{\dagger}(\vec{p_2})b_3^{\dagger}(\vec{p_3})b_4^{\dagger}(\vec{p_4})d_5^{\dagger}(\vec{p_5})|0\rangle. \tag{6.20}$$

Because we are fixing the charm and the anticharm quarks, while we antisymmetrized the rest three light quarks, the normalization factor in this case is also $1/\sqrt{3!}$.

6.1.1 Decay width for the photoproduction of pentaquarks

The radiative decay widths for pentaquark states (similar to the heavy baryons) can be calculated from the helicity amplitudes as [38, 83, 84]

$$\Gamma(P_c \to B + \gamma) = 2\pi\rho\frac{2}{2J+1}\sum_{\nu>0}|A_{\nu}(k)|^2\ , \tag{6.21}$$

where ρ is the phase space factor calculated in the rest frame of the pentaquark

$$\rho = 4\pi \frac{E_B k^2}{m_{P_c}}, \tag{6.22}$$

and $E_B = \sqrt{m_B^2 + k^2}$ is the energy of the baryon (in this case proton). The square of the four-momentum $(k_0, \vec{k})$ of photon is given by

$$Q^2 = Q^\mu Q_\mu = k_0^2 - k^2, \tag{6.23}$$

such that if one study the energy and momentum conservation for this dynamical process (see Appendix C), then the following relation is obtained

$$k^2 = \left(\frac{Q^2 - m_{P_c}^2 - m_B^2}{2m_{P_c}} \right)^2 - m_B^2. \tag{6.24}$$

Of course $k = |\vec{k}|$ is the magnitude of the three-momentum of the photon at which the photoproduction of the pentaquark occurs.

Since the squared mass of the photon is $Q^2 = 0$, the previous equation is reduced to

$$k = \frac{m_{P_c}^2 - m_B^2}{2m_{P_c}}. \tag{6.25}$$

By using the effective values of proton, $m_B = 0.938\ GeV$, and pentaquark, $m_{P_c} = 4.450\ GeV$, in Eq. (6.25), one obtains the momentum of the photon for the photoproduction channel as $k = 2.12\ GeV$.

The helicity amplitude for this process is defined as the transition matrix element between the pentaquark and proton through

$$A_\nu(k) = \langle B, 1/2, \nu - 1; \gamma \left| H_3 \right| P_c, 3/2, \nu \rangle, \tag{6.26}$$

where ν is the helicity label. For each configuration of pentaquark states there is a matrix element to be evaluated, as follows

$$\begin{aligned} A_\nu(k) = \langle \gamma B | H_3 | P_c \rangle = & \; e \int \frac{d^3x}{(2\pi)^3} \int d^3p_9 \int d^3p_{10} \int \frac{d^3k}{(2\pi)^{\frac{3}{2}}} \frac{1}{\sqrt{2k^0}} \\ & \sum_q \sum_{s,s'} \langle \gamma B | \bar{v}_{s'}(\vec{p_{10}}) \gamma^\mu e_q u_s(\vec{p_9}) d_{s'}(\vec{p_{10}}) b_s(\vec{p_9}) a_\mu^\dagger(\vec{k}) e^{-i\vec{k}\cdot\vec{x}} | P_c \rangle e^{i(\vec{p_9} + \vec{p_{10}})\cdot\vec{x}}. \end{aligned} \tag{6.27}$$

Considering just the *emission* process of a photon with momentum $\vec{k}$ and polarization ϵ_μ^*, we have

$$\langle \vec{k}, \epsilon | A_\mu(\vec{x}) | 0 \rangle = \frac{1}{(2\pi)^{\frac{3}{2}}} \frac{1}{\sqrt{2k^0}} \epsilon_\mu^* e^{-i\vec{k}\cdot\vec{x}}, \tag{6.28}$$

so, after considering the matrix element of $A_\mu(\vec{x})$ and integrating into coordinate space, the Eq. (6.27) is reduced to

$$\begin{aligned} \langle \gamma B | H_3 | P_c \rangle = & \; \frac{e}{6} \int \prod_{i=1}^{10} d^3p_i \frac{1}{(2\pi)^{\frac{3}{2}} \sqrt{2k_0}} \sum_q \sum_{s,s'} \Psi_B^*(\vec{p_6}, \vec{p_7}, \vec{p_8}) \bar{v}_{s'} \gamma^\mu e_q u_s \epsilon_\mu^* \Psi_{P_c}(\vec{p_1}, \vec{p_2}, \vec{p_3}, \vec{p_4}, \vec{p_5}) \\ & \delta^3(\vec{p_9} + \vec{p_{10}} - \vec{k})(-1) \langle 0 | b_8 b_7 b_6 b_s d_{s'} b_1^\dagger b_2^\dagger b_3^\dagger b_4^\dagger d_5^\dagger | 0 \rangle. \end{aligned} \tag{6.29}$$

The resulting matrix element can be evaluated by doing all the contractions between fermion operators through the anti commutation relations of Eq. (6.6) in such a way that terms of annihilation

acting on vacuum vanishes, for example $d_{s'}d_5^\dagger|0\rangle = (\delta_{s',5}\delta^3(\vec{p_{10}}-\vec{p_5}) - d_5^\dagger d_{s'})|0\rangle = \delta_{s',5}\delta^3(\vec{p_{10}}-\vec{p_5})|0\rangle$. Besides is used the antisymmetric property of the wave function for fermions under interchange of any two particles to rename the subscripts and simplified the expressions, as follows

$$\begin{aligned}\langle 0|b_8 b_7 b_6 b_s b_1^\dagger b_2^\dagger b_3^\dagger b_4^\dagger d_{s'} d_5^\dagger|0\rangle &= -3\delta_{s',5}\delta^3(\vec{p_{10}}-\vec{p_5})\delta_{s,4}\delta^3(\vec{p_9}-\vec{p_4})\langle 0|b_8 b_7 b_6 b_1^\dagger b_2^\dagger b_3^\dagger|0\rangle \\ &= -3!\delta_{s',5}\delta^3(\vec{p_{10}}-\vec{p_5})\delta_{s,4}\delta^3(\vec{p_9}-\vec{p_4})\delta_{1,6}\delta^3(\vec{p_1}-\vec{p_6}) \\ &\quad \delta_{7,2}\delta^3(\vec{p_7}-\vec{p_2})\delta_{8,3}\delta^3(\vec{p_8}-\vec{p_3}). \end{aligned} \tag{6.30}$$

Choosing the left-handed polarization for photon, we have $\epsilon_\mu* = \frac{1}{\sqrt{2}}(0,-1,i,0)$

$$\begin{aligned}\langle \gamma B|H_3|P_c\rangle &= \frac{e}{(2\pi)^{\frac{3}{2}}\sqrt{2k_0}}\int\prod_{i=1}^{10} d^3p_i \Psi_B^*(\vec{p_6},\vec{p_7},\vec{p_8})\sum_q\sum_{s,s'}\bar{v}_{s'}\gamma^\mu e_q u_s \epsilon_\mu^* \Psi_{P_c}(\vec{p_1},\vec{p_2},\vec{p_3},\vec{p_4},\vec{p_5}) \\ &\quad \delta^3(\vec{p_9}+\vec{p_{10}}-\vec{k_1})\delta_{s',5}\delta^3(\vec{p_{10}}-\vec{p_5})\delta_{s,4}\delta^3(\vec{p_9}-\vec{p_4})\delta_{1,6}\delta^3(\vec{p_1}-\vec{p_6}) \\ &\quad \delta_{7,2}\delta^3(\vec{p_7}-\vec{p_2})\delta_{8,3}\delta^3(\vec{p_8}-\vec{p_3}) \\ &= \frac{e}{(2\pi)^{\frac{3}{2}}\sqrt{2k_0}}\int\prod_{i=1}^{5} d^3p_i \Psi_B^*(\vec{p_1},\vec{p_2},\vec{p_3})\sum_q\sum_{4,5}\bar{v}_5\gamma^\mu e_q u_4 \epsilon_\mu^* \Psi_{P_c}(\vec{p_1},\vec{p_2},\vec{p_3},\vec{p_4},\vec{p_5}) \\ &\quad \delta^3(\vec{p_4}+\vec{p_5}-\vec{k}). \end{aligned} \tag{6.31}$$

From the non-relativistic limit of Eq. (6.18), the left-handed polarization vector and the orthogonality properties of Pauli spinors, one has

$$\begin{aligned}\langle \gamma B|H_3|P_c\rangle &= \frac{e}{(2\pi)^{\frac{3}{2}}\sqrt{2k_0}}\int\prod_{i=1}^{5} d^3p_i \Psi_B^*(\vec{p_1},\vec{p_2},\vec{p_3})\sum_q\sum_{4,5}(-(\vec{\sigma}\cdot\vec{\epsilon})\delta_{4,5})e_q \Psi_{P_c}(\vec{p_1},\vec{p_2},\vec{p_3},\vec{p_4},\vec{p_5}) \\ &\quad \delta^3(\vec{p_4}+\vec{p_5}-\vec{k}), \end{aligned} \tag{6.32}$$

where $\vec{\sigma}\cdot\vec{\epsilon} = -\frac{\sigma_-}{\sqrt{2}}$, and because q index is asociated implicitly to the spinor index s by definition (in this case $s = 4 = 5$), then the implicit sum on q reduces to label 4, which corresponds to fixed the flavor label of charm quark. Therefore, at the end we obtained the following reduced expression

$$\langle \gamma B|H_3|P_c\rangle = \frac{e}{(2\pi)^{\frac{3}{2}}\sqrt{2k_0}}\int\prod_{i=1}^{5} d^3p_i \Psi_B^*(\vec{p_1},\vec{p_2},\vec{p_3})\frac{\sigma_-}{\sqrt{2}}e_c \Psi_{P_c}(\vec{p_1},\vec{p_2},\vec{p_3},\vec{p_4},\vec{p_5})\delta^3(\vec{p_4}+\vec{p_5}-\vec{k}). \tag{6.33}$$

This result corresponds to an electromagnetic decay processes of pentaquark P_c into a baryon B, Fig. 6.2, where three particles are observers and the photo-coupling is between the fourth quark c and the fifth antiquark $\bar{c}$. The position of $c\bar{c}$ are taken fixed without loss of generality in order to evaluate the spin flavor matrix elements. It can be shown that the results are invariant regardless of the contraction of quark c in any position with antiquark $\bar{c}$ fixed as a convention in the fifth position (taken as distinguishable from the rest).

$$\begin{aligned}A_\nu(k) = \langle \gamma B|H_3|P_c\rangle &= \frac{e}{(2\pi)^{\frac{3}{2}}2\sqrt{k_0}}\langle \psi_B^{csf}\frac{1}{2},\nu-1|e_c\sigma_-|\psi_{P_c}^{csf}\frac{3}{2},\nu\rangle \\ &\quad \int\prod_{i=1}^{5} d^3p_i \psi_B^*(\vec{p_1},\vec{p_2},\vec{p_3})\psi_{P_c}(\vec{p_1},\vec{p_2},\vec{p_3},\vec{p_4},\vec{p_5})\delta^3(\vec{p_4}+\vec{p_5}-\vec{k}) \\ &= \frac{e}{(2\pi)^{\frac{3}{2}}2\sqrt{k_0}}\langle \psi_B^{csf}\frac{1}{2},\nu-1|e_c\sigma_-|\psi_{P_c}^{csf}\frac{3}{2},\nu\rangle F(k). \end{aligned} \tag{6.34}$$

The total wave function is split in $\Psi \equiv \psi^{csf}\psi$, where ψ itself is denoted as the orbital wave function. In this way it is enough to calculate the matrix elements for these degrees of freedom separated from the orbital overlap, so that in the integral expression of Eq. (6.34), the **form factor** $F(k)$, *gives the orbital contribution to the photoproduction of pentaquark from the orbital part of the pentaquark wave function.*

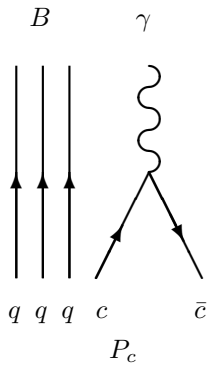

Fig. 6.2: Electromagnetic decay of pentaquark P_c into a baryon B and a photon, $P_c \to B + \gamma$.

6.2 Color-Spin-Flavor Matrix Elements

A first analysis of these matrix elements has already been done for a case of the ground states pentaquarks with identical quarks and an antiquark $q^4\bar{q}$. These results were published and are found in Table 11 of our first work on pentaquarks. [82].

An important result obtained in that analysis of these expectation values is the relation between the helicity amplitudes 1/2 and 3/2. It is direct to demonstrate that they are proportional by studying the commutation properties of their operators, as follows.

Writing the operator that contracts particle 4 with 5 as

$$\theta = \sum_{i=1}^{4} a_\uparrow(4) a_\uparrow(5) \tag{6.35}$$

and the operator whose propose is lower the spin projection of the i-th quark can be defined as

$$S_- = \sum_{i=1}^{5} a_\downarrow^\dagger(i) a_\uparrow(i) \tag{6.36}$$

then without loss of generality we can calculate the helicity amplitude matrix element of the pentaquark with $S = 3/2$, which is the only possibility different from zero for all the matrix elements

$$\begin{aligned} \langle \chi_B; 1/2, -1/2 | \theta | \chi_{P_c}; 3/2, 1/2 \rangle &= \frac{1}{\sqrt{3}} \langle \chi_B; 1/2, -1/2 | \theta S_- | \chi_{P_c}; 3/2, 3/2 \rangle \\ &= \frac{1}{\sqrt{3}} \langle \chi_B; 1/2, -1/2 | S_- \theta + [\theta, S_-] | \chi_{P_c}; 3/2, 3/2 \rangle \\ &= \frac{1}{\sqrt{3}} \langle \chi_B; 1/2, 1/2 | \theta | \chi_{P_c}; 3/2, 3/2 \rangle. \end{aligned} \tag{6.37}$$

As a conclusion the proportionality factor for the transition matrix elements with initial pentaquark spin states with spin 1/2 and 3/2 is $1/\sqrt{3}$. In the following, I will derive the explicit value of this transition matrix elements for the cases of interest.

6.2.1 Ground state pentaquarks

The operator of the electromagnetic couplings affects the total pentaquark wave functions and specially the color part. For each configuration of color $\psi^c_{E_\rho}$, $\psi^c_{E_\lambda}$ and $\psi^c_{A_2}$ derived in Eqs. (5.24)-(5.26) we can compute the overlap with the nucleon wave function separately. The color singlet for the nucleon B and its product with the meson J/ψ is

$$\psi^c_{BJ/\psi} = \frac{1}{\sqrt{6}}(rgb - grb + gbr - bgr + brg - rbg)\frac{1}{\sqrt{3}}(r\bar{r} + g\bar{g} + b\bar{b}) \tag{6.38}$$

There are three pentaquark configurations that do not contribute to the photocouplings due their color part, since we have the following overlaps

$$\begin{aligned} \langle\psi^c_{BJ/\psi}|\psi^c_{E_\rho}\rangle &= 0 \\ \langle\psi^c_{BJ/\psi}|\psi^c_{E_\lambda}\rangle &= 0 \\ \langle\psi^c_{BJ/\psi}|\psi^c_{A_2}\rangle &= 1. \end{aligned} \tag{6.39}$$

Additionally, because the final state of the process is the proton of the octet, the only configuration relevant for the photocoupling is ψ_2 of Eq. (5.39). Taking the example with helicity $\nu = 3/2$ is straightforward to get

$$\langle\psi^{csf}_B\frac{1}{2},\nu-1 = \frac{1}{2}|e_c\sigma_-|\psi^{csf}_{Pc}\frac{3}{2},\nu=\frac{3}{2}\rangle = \frac{1}{2}\langle\psi_S\psi^c_A(\phi_\rho\chi_\rho+\phi_\lambda\chi_\lambda)|\psi_S\psi^c_A(\phi_\rho\chi_\rho+\phi_\lambda\chi_\lambda)\rangle = e_c. \tag{6.40}$$

The matrix element for helicity amplitude $\nu = 1/2$ is then given by

$$\langle\psi^{csf}_B\frac{1}{2},\nu-1 = -\frac{1}{2}|e_c\sigma_-|\psi^{csf}_{Pc}\frac{3}{2},\nu=\frac{1}{2}\rangle = \frac{e_c}{\sqrt{3}}. \tag{6.41}$$

The photocouplings to the other pentaquark configurations ψ_1, ψ_3, ψ_4 and ψ_5 vanish.

6.2.2 Pentaquarks with one quantum of orbital excitation in ρ and λ

For this modes, we need to study the nine configurations of Eqs. (5.56)-(5.64). Considering the overlaps of color part, we can discard five configurations, from Eq. (5.56) to (5.60) and since the calculation of the matrix elements for the other three involves the following overlaps $\langle\phi_S|\phi_\rho\rangle = \langle\phi_S|\phi_\lambda\rangle = \langle\chi_\rho|\chi_S\rangle = \langle\chi_\lambda|\chi_S\rangle = 0$. Thus, the complete photocouplings are zero for these modes.

6.2.3 Pentaquarks with one quantum of orbital excitation in η and ζ

In this case due to the correspondence of the excited radial part with the symmetric wave function $\psi_S \to \psi_{\eta,\zeta}$ whose color-spin-flavor matrix elements were calculated in Eq. (6.40) and (6.41), we obtain the same results.

$$\langle\psi^{csf}_B\frac{1}{2},\nu-1 = \frac{1}{2}|e_c\sigma_-|\psi^{csf}_{Pc\ \eta,\zeta}\frac{3}{2},\nu=\frac{3}{2}\rangle = e_c \tag{6.42}$$

and

$$\langle\psi^{csf}_B\frac{1}{2},\nu-1 = -\frac{1}{2}|e_c\sigma_-|\psi^{csf}_{Pc\ \eta,\zeta}\frac{3}{2},\nu=\frac{1}{2}\rangle = \frac{e_c}{\sqrt{3}} \tag{6.43}$$

Chapter 7

Harmonic Oscillator Quark Model

In this Chapter, the aim is to evaluate the remaining part of the photocoupling of the pentaquarks, Eq. (6.34), this basically corresponds to the overlap $F(\vec{p_1},\vec{p_2},\vec{p_3},\vec{p_4},\vec{p_5})$ of both the wave functions of the pentaquark and the proton. To build these wave functions we will implement two different descriptions. On the one hand we will consider in this section a harmonic oscillator approximation, HO, and on the other hand in the next section we will use an approximation with a Coulomb-type potential in the Hypercentral Quark Model. With these two techniques we obtain the widths for the pentaquark photoproduction process in two different and comparable ways.

7.1 Proton Charge Radius

In Chapter 1, we study the orbital proton wave function, where from Eqs. (1.19) and (1.21) it can be written explicitly in coordinates space

$$\psi_p^{gs} = \frac{1}{(2\pi)^{3/2}} e^{\vec{P}_{CM}\cdot\vec{R}} \frac{1}{\sqrt{3\sqrt{3}}} \frac{\beta^3}{\pi^{\frac{3}{2}}} e^{-\beta^2(\rho^2+\lambda^2)/2}. \tag{7.1}$$

The observable corresponding to the proton charge radius is calculated (within the harmonic oscillator model) as the following expectation value

$$\begin{aligned} r_p^2 = \langle r_{ch}^2\rangle_p &= \langle\psi_p^{gs}|\sum_{i=1}^{3} e_i(\vec{r_i}-\vec{R})^2|\psi_p^{gs}\rangle \\ &= \frac{1}{3}(2e_u+e_d)\langle\psi_p^{gs}|\rho^2+\lambda^2|\psi_p^{gs}\rangle \\ &= \frac{1}{\beta^2}, \end{aligned} \tag{7.2}$$

where $\vec{R}$ is the center-of-mass vector for the proton. For convenience, here we use β (instead of α from Section 1.2.2) to denote the harmonic oscillator constant, and it can be determined by fitting the proton radius.

7.2 Pentaquark Charge Radius

The explicit ground state pentaquark wave function in coordinate space is given by

$$\psi_{Pc}^{gs} = \frac{1}{(2\pi)^{3/2}} e^{\vec{P}\cdot\vec{R}} \frac{1}{\sqrt{5\sqrt{5}}} \frac{\alpha_\rho^{\frac{3}{2}}}{\pi^{\frac{3}{4}}} \frac{\alpha_\lambda^{\frac{3}{2}}}{\pi^{\frac{3}{4}}} \frac{\alpha_\eta^{\frac{3}{2}}}{\pi^{\frac{3}{4}}} \frac{\alpha_\zeta^{\frac{3}{2}}}{\pi^{\frac{3}{4}}} e^{-\frac{\alpha_\rho^2}{2}\rho^2} e^{-\frac{\alpha_\lambda^2}{2}\lambda^2} e^{-\frac{\alpha_\eta^2}{2}\eta^2} e^{-\frac{\alpha_\zeta^2}{2}\zeta^2}, \tag{7.3}$$

where again from Eq. (5.8) one has the following relations

$$\alpha_\rho^2 = \alpha_\lambda^2, \qquad \alpha_\eta^2 = \alpha_\rho^2\sqrt{a}, \qquad \alpha_\zeta^2 = \alpha_\rho^2\sqrt{\frac{5a}{3+2a}}, \qquad a \equiv \frac{m'}{m}. \tag{7.4}$$

One of the important observables that we can now calculate with this wave function is the charge radius of the pentaquark

$$\begin{aligned} r^2 \equiv \langle R_{ch}^2\rangle_{P_c} &= \langle\psi_{P_c}^{gs}|\sum_{i=1}^{5} e_i(\vec{r_i}-\vec{R})^2|\psi_{P_c}^{gs}\rangle \\ &= \frac{1}{3}(2e_u+e_d)\langle\psi_{P_c}^{gs}|\vec{\rho}^2+\vec{\lambda}^2+\frac{10m'^2}{(3m+2m')^2}\vec{\zeta}^2|\psi_{P_c}^{gs}\rangle \\ &= \frac{1}{\alpha_\rho^2}\left(1+\frac{1}{5}\left(\frac{5a}{3+2a}\right)^{\frac{3}{2}}\right), \end{aligned} \tag{7.5}$$

with $\vec{R}$, in this case is the center-of-mass vector of the pentaquark. It is important to mention that R_{ch}^2 is not fixed, because we do not know the experimental value of the charge radius for the pentaquark. However, this is a useful relation to watch what happen at the limits $a \to 0$ and $a \to \infty$, where $a = m'/m$ was defined in Eq. (5.8). In the first case we have $m' << m$, that is to say, considering just the three valence light quarks with masses m, we see that Eq. (7.5) reproduce the correct limit of proton charge radius $R_{ch}^2 = \frac{1}{\alpha_\rho^2}$ from Eq.(7.2), as it should. On the other hand, taken the case $m' >> m$, we obtain a finite value of $\frac{1}{\alpha_\rho^2}\left(1+\frac{1}{2}\left(\frac{5}{2}\right)^{\frac{1}{2}}\right)$.

7.3 Orbital matrix element

To obtain the overlap between pentaquark and proton states it is necessary to compute, from Eq. (6.34), the next integral on five momentums

$$F(k) = \int\prod_{i=1}^{5} d^3p_i\,\psi_B^*(\vec{p_1},\vec{p_2},\vec{p_3})\psi_{P_c}(\vec{p_1},\vec{p_2},\vec{p_3},\vec{p_4},\vec{p_5})\delta^3(\vec{p_4}+\vec{p_5}-\vec{k}). \tag{7.6}$$

7.3.1 Ground state pentaquark

The total baryon (and proton in particular) wave function in momentum space can be expressed in terms of its relative wave function from (1.21), so one has

$$\begin{aligned} \psi_B(\vec{p_1},\vec{p_2},\vec{p_3}) &= \delta^3(\vec{p_1}+\vec{p_2}+\vec{p_3}-\vec{K_B})\psi_B^{rel}(\vec{p_\rho},\vec{p_\lambda}). \\ &= \delta^3(\frac{3m}{M}\vec{P}+\sqrt{\frac{6}{5}}\vec{p_\zeta}-\vec{K_B})\sqrt{3\sqrt{3}}\left(\frac{1}{\pi^{\frac{3}{4}}\beta^{\frac{3}{2}}}\right)^2 e^{-\frac{1}{2\beta^2}(p_\rho^2+p_\lambda^2)}, \end{aligned} \tag{7.7}$$

with β the harmonic oscillator constant of proton.

Similarly, in Eq. (5.10), it was obtained the wave function of pentaquark in momentum space, and explicitly is given by

$$\begin{aligned} \psi_{Pc}(\vec{p_1},\vec{p_2},\vec{p_3},\vec{p_4},\vec{p_5}) &= \delta^3(\vec{P}-\vec{K_{Pc}})\psi_{Pc}^{rel}(\vec{p_\rho},\vec{p_\lambda},\vec{p_\eta},\vec{p_\zeta}) \\ &= \delta^3(\vec{P}-\vec{K_{Pc}})\sqrt{5\sqrt{5}}\frac{1}{\pi^{\frac{3}{4}}\alpha_\rho^{\frac{3}{2}}}\frac{1}{\pi^{\frac{3}{4}}\alpha_\lambda^{\frac{3}{2}}}\frac{1}{\pi^{\frac{3}{4}}\alpha_\eta^{\frac{3}{2}}}\frac{1}{\pi^{\frac{3}{4}}\alpha_\zeta^{\frac{3}{2}}} \\ &\quad e^{-\frac{1}{2\alpha_\rho^2}p_\rho^2}e^{-\frac{1}{2\alpha_\lambda^2}p_\lambda^2}e^{-\frac{1}{2\alpha_\eta^2}p_\eta^2}e^{-\frac{1}{2\alpha_\zeta^2}p_\zeta^2}. \end{aligned} \tag{7.8}$$

Now, with the above ground state wave functions, the orbital part contribution can be evaluated. For this propose, Eq. (7.6) is written in terms of Jacobi coordinates

$$\begin{aligned} F_{gs}(k) &= \frac{3^{\frac{3}{4}}5^{\frac{3}{4}}}{5\sqrt{5}}\left(\frac{1}{\pi^{3/4}\beta^{3/2}}\right)^2\left(\frac{1}{\pi^2\alpha_\rho^2\alpha_\eta\alpha_\zeta}\right)^{3/2}\int d^3p_\rho d^3p_\lambda d^3p_\eta d^3p_\zeta d^3P \\ &\quad \delta^3(\frac{3m}{M}\vec{P}+\sqrt{\frac{6}{5}}\vec{p_\zeta}-\vec{K_B})\delta^3(\vec{P}-\vec{K_{Pc}})\delta^3\left(\frac{2m'}{M}\vec{P}-\sqrt{\frac{6}{5}}\vec{p_\zeta}-\vec{k}\right) \\ &\quad e^{-\frac{1}{2\beta^2}(p_\rho^2+p_\lambda^2)}e^{-\frac{1}{2\alpha_\rho^2}p_\rho^2}e^{-\frac{1}{2\alpha_\lambda^2}p_\lambda^2}e^{-\frac{1}{2\alpha_\eta^2}p_\eta^2}e^{-\frac{1}{2\alpha_\zeta^2}p_\zeta^2}. \end{aligned} \tag{7.9}$$

Here

$$\delta^3\left(\vec{p_4}+\vec{p_5}-\vec{k_1}\right) = \delta^3\left(\frac{2m'}{M}\vec{P}-\sqrt{\frac{6}{5}}\vec{p_\zeta}-\vec{K_B}\right) \tag{7.10}$$

and

$$\delta^3\left(\frac{3m}{M}\vec{P}+\sqrt{\frac{6}{5}}\vec{p_\zeta}-\vec{K_B}\right) = \frac{1}{\left|\sqrt{\frac{6}{5}}\right|^3}\delta^3\left(\vec{p_\zeta}-\sqrt{\frac{5}{6}}(\vec{K_B}-\frac{3m}{M}\vec{P})\right). \tag{7.11}$$

Doing the integrals of P and p_ζ one obtains

$$\begin{aligned} F_{gs}(k) &= \frac{3^{\frac{3}{4}}5^{\frac{3}{4}}}{5\sqrt{5}}\left(\frac{1}{\pi^{3/4}\beta^{3/2}}\right)^2\left(\frac{1}{\pi^2\alpha_\rho^2\alpha_\eta\alpha_\zeta}\right)^{3/2}\left(\sqrt{\frac{5}{6}}\right)^3\int_{-\infty}^{\infty}\int_{-\infty}^{\infty}\int_{-\infty}^{\infty}d^3p_\rho d^3p_\lambda d^3p_\eta \\ &\quad \delta^3\left(\vec{K}_{P_c}-\vec{K_B}-\vec{k}\right)e^{-\frac{1}{2\beta^2}(p_\rho^2+p_\lambda^2)}e^{-\frac{1}{2\alpha_\rho^2}(p_\rho^2+p_\lambda^2)}e^{-\frac{1}{2\alpha_\eta^2}p_\eta^2}e^{-\frac{1}{2\alpha_\zeta^2}\frac{5}{6}\left(\vec{K_B}-\frac{3m}{M}\vec{K_{P_c}}\right)^2}. \end{aligned} \tag{7.12}$$

The integrals on $\vec{p_\rho}$, $\vec{p_\lambda}$ and $\vec{p_\eta}$ are direct, since these functions are just gaussians. Working in the rest frame of pentaquark, $\vec{K_{P_c}}=0$, then the momentum of baryon B (proton) becomes the momentum of the outgoing photon $\vec{K_B}=\vec{k}$. Therefore, the orbital part for the **ground state pentaquark** is

$$\begin{aligned} F_{gs}(k) &= \sqrt{\frac{5\sqrt{5}}{3\sqrt{3}}}\left(\frac{2\alpha_\rho\beta}{\alpha_\rho^2+\beta^2}\right)^3\left(\frac{\alpha_\eta}{\alpha_\zeta}\right)^{3/2}e^{-\frac{5}{12\alpha_\zeta^2}k^2} \\ &= \left(\frac{\sqrt{5(2a+3)}}{3}\right)^{\frac{3}{4}}\left(\frac{2\alpha_\rho\beta}{\alpha_\rho^2+\beta^2}\right)^3e^{-\frac{5}{12\alpha_\rho^2}\sqrt{\frac{2a+3}{5a}}k^2}, \end{aligned} \tag{7.13}$$

where β is inversely proportional to the proton charge radius, Eq. (7.2), α_ρ can be parametrized in terms of the pentaquark charge radius r, Eq. (7.5), and $a=m'/m$ was defined in Eq. (5.8). The graph for this result, Eq. (7.13), can be seen in Fig. 7.1 in terms of the charge radius, once we fix the value of the outgoing photon as $k=2.1\ GeV$ obtained by studying the dynamical analysis of photoproduction of the pentaquark in Eq. (6.25).

In Fig. 7.1 can also be seen the behavior of the orbital matrix element in terms of k, when we take the charge radius of pentaquark equal to $1fm$ (experimental charge radius of proton is $\approx 0.84fm$). Just as a matter of analysis, in all these plots we include aside from the curves with the mass of the heavy quark m' as the mass of the constituent charm quark m_c, also the plots as if we were considering either the mass of the bottom quark $m'=m_b$ or the mass of up and down quarks $m'=m_u=m_d$. *Equally important, we can analyze the behaviour of the form factor from Eq. (7.13) as a function of the charge radius of the pentaquark $F_{gs}(r)$. This can be done, since the coefficient α_ρ is related to the charge radius of pentaquark r by Eq. (7.5).*

7.3.2 Parameters for pentaquarks

Table 7.1: Parameters values for pentaquarks $uudQ\bar{Q}$ with heavy quarks $Q = u = d$, $Q = c$, $Q = b$. Although $k = 2.12\ GeV$ is the photon momentum calculated for the hidden charm pentaquak, here we use the same value of k to estimate the orbital contribution of every hypothetical pentaquark with different heavy quark mass m_Q.

	$Q = u = d$	$Q = c$	$Q = b$	
$m = m_u = m_d$	320	320	320	MeV
$m' = m_Q$	320	1500	4920	MeV
k	2.12	2.12	2.12	GeV
$\beta = 1/r_p$	1.19	1.19	1.19	fm

In our previous work [82], through a mass formula, we estimate values of the constituent quark masses $u = d$ and c. In the same manner is calculated the mass for quark b. Also, the momentum of the photon k was obtained by means of the dynamical analysis of the photoproduction process, and parameter β was determined from the proton charge radius r_p in Eq. (7.2). The values for this parameters are given in Table 7.1.

7.3.3 Pentaquark with one quantum of excitation in ζ

From the pentaquark signals discovered by LHCb it is not clear to which quantum numbers they are assigned. For this reason we consider to study not only the ground-state pantaquarks, but also the orbital-excited pentaquark states. From our analysis of the previous section on the color-spin-flavor matrix elements Eqs. 6.42 and 6.43, we notice that the only excited pentaquark states that contributed to the photoproduction process, are those with only one orbital excitation in η or ζ. Moreover, it can be shown that the only non-vanishing contribution in the orbital matrix element of Eq.(7.6), is for ζ and the result is

$$F_\zeta(k) = -i\sqrt{\frac{5}{3}}\sqrt{\frac{5\sqrt{5}}{3\sqrt{3}}}\frac{\alpha_\eta^{3/2}}{\alpha_\zeta^{5/2}}\left(\frac{2\alpha_\rho\beta}{\alpha_\rho^2+\beta^2}\right)^3\left|\left(1-\frac{3m}{M}\right)\vec{K}_{P_c^*}-\vec{K}_1\right|e^{-\frac{5}{6}\left|\left(1-\frac{3m}{M}\right)\vec{K}_{P_c^*}-\vec{K}_1\right|^2/2\alpha_\zeta^2}. \tag{7.14}$$

Taking the pentaquark at the rest frame one obtains

$$F_\zeta(k) = -i\sqrt{\frac{5}{3}}\sqrt{\frac{5\sqrt{5}}{3\sqrt{3}}}\frac{\alpha_\eta^{3/2}}{\alpha_\zeta^{5/2}}\left(\frac{2\alpha_\rho\beta}{\alpha_\rho^2+\beta^2}\right)^3 k\, e^{-\frac{5}{6}k^2/2\alpha_\zeta^2}, \tag{7.15}$$

or in terms of the mass ratio $a = m'/m$, one has

$$F_\zeta(k) = -i\sqrt{\frac{5}{3}}\left(\frac{\sqrt{5(2a+3)}}{3}\right)^{\frac{3}{4}}\left(\frac{2\alpha_\rho\beta}{\alpha_\rho^2+\beta^2}\right)^3\frac{k}{\alpha_\rho\left(\frac{5a}{2a+3}\right)^{\frac{1}{4}}}e^{-5k^2/12\alpha_\rho^2\sqrt{\frac{5a}{2a+3}}}. \tag{7.16}$$

The effect of this result on the photoproduction of the ζ-excited pentaquark is shown in Fig. 7.2. Again, α_ρ can be written in terms of the pentaquark charge radius Eq. (7.5), while β is fixed by the charge radius of proton. The last equation in terms of quotient a can also be studied as ground state, when we take different values for the mass of quark Q.

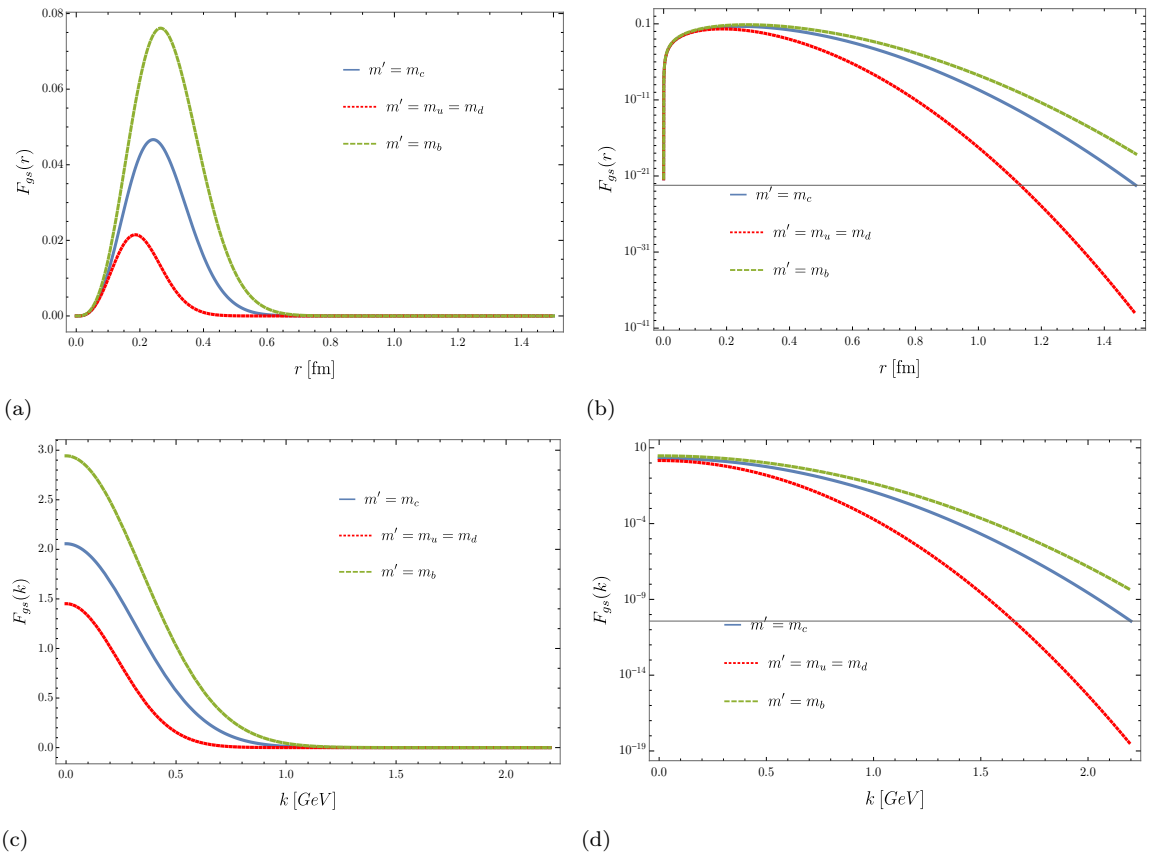

Fig. 7.1: Orbital contribution to the photoproduction of the ground state pentaquark $P_c(uudQ\bar{Q})$ in the Harmonic Oscillator Model. The solid blue line represents the case with the hidden charm pentaquarks $m_Q = m' = m_c$, while the red dotted line and the green dashed line contemplate an hypothetical pentaquark made of only light quarks $m_Q = m' = m_u = m_d$, and with bottom quark $m_Q = m' = m_b$, respectively. Graphs (a) and (b) are given in terms of the pentaquark charge radius r, where the momentum of photon was taken as $2.1GeV$. By contrast, (c) and (d) are given in terms of the photon momentum k, so that the pentaquark charge radius was fixed in $1fm$. Graphs (b) and (d) are in logarithm scale.

7.4 Discussion of results

One can study the orbital contribution F as a function of not only the momentum of the photon $F(k)$, but also as a function of the pentaquark charge radius $F(r)$, from Eq. (7.5). One of the facts one can see in $F(r)$ for both ground $F_{gs}(r)$ and excited states $F_\zeta(r)$ is that, there is only a small contribution of the orbital function to the radiative decay width for a short range of the pentaquark charge radius r (approximately between 0.1 and 0.5 fm). After the function reaches its maximum, as r grows, the orbital part starts to decrease exponentially.

Moreover, close to the neighborhood of $k = 2.1GeV$ where the photoproduction occurs, we observe a very small factor for the orbital matrix element, of the order of $\sim 10^{-9}$. This factor will even become smaller once we take its square modulus, in order to calculate the radiative decay widths of pentaquarks $\Gamma(P_c \to B + \gamma)$, Eqs. (6.21) and (6.26). Thus, since the phase space factor is a constant whose value do not change significantly our previous result, we found that the photoproduction channel of pentaquark is highly suppressed.

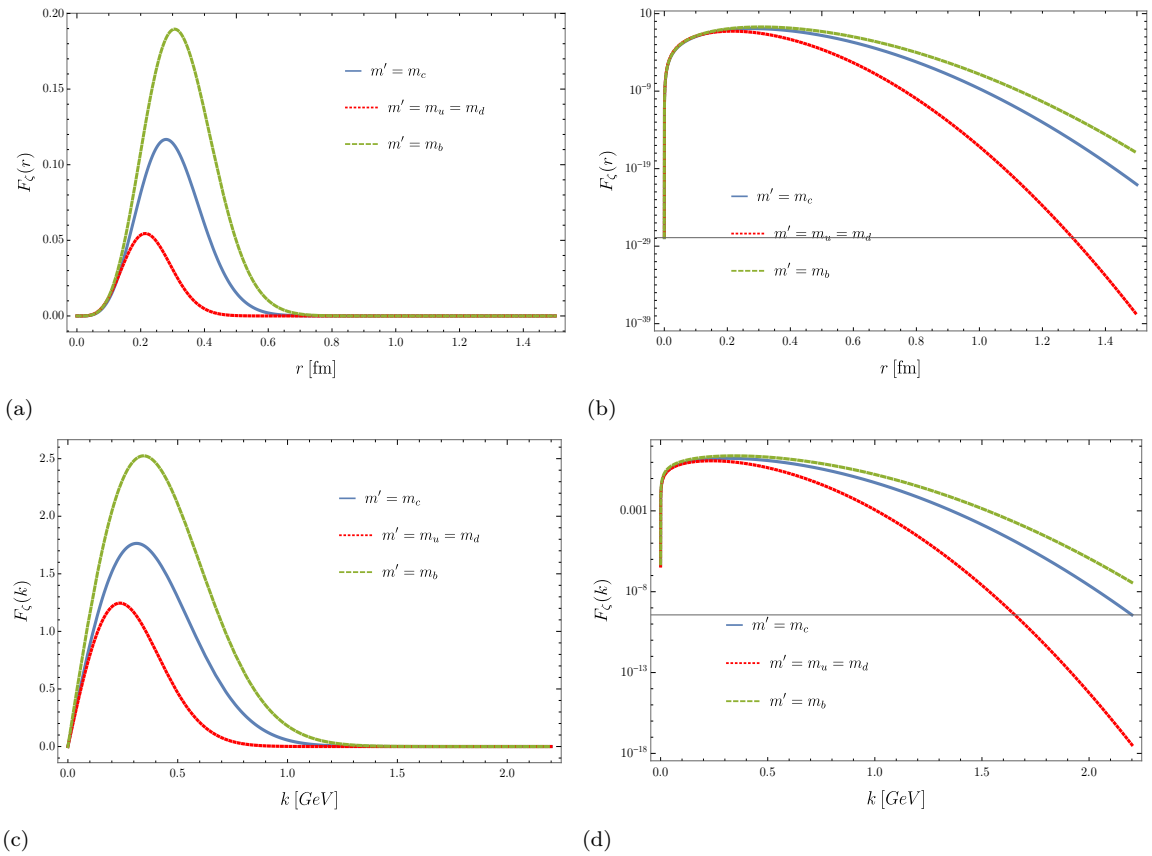

Fig. 7.2: Similar to Fig. 7.1, here are shown the orbital contribution to the photoproduction of one orbital excited pentaquark in the ζ mode. In (a) and (b) the overlap is expressed as a function of the pentaquark charge radius r with momentum of the photon $k = 2.1GeV$, while in (c) and (d) F is function of k, where $r = 1fm$. The right graphs are in logarithmic scale respect to the left ones.

A similar behaviour occurs for functions depending on k: $F_{gs}(k)$ and $F_\zeta(k)$. A notorious difference is in $k = 0$, since $F_{gs}(k = 0) = 0$, while $F_\zeta(k = 0)$ starts in a fixed value, according to the analytical expressions of Eqs. (7.13) and (7.15). Another comparison incorporating both of our perspectives of the orbital contribution to the fotoproduction of the ground and excited hidden charm pentaquarks is shown in Figure 7.3.

Finally, because we have the form factors, from Eq. (6.21) we can calculate the radiative decay widths in terms of either the pentaquark charge radius r, or the photon momentum k. The results are presented in Fig. 7.4.

In general, it can be concluded that no matter how big the mass of the heavy quark $m_Q = m'$ is, after certain range one can ensure that the bigger of the photon momentum k (or pentaquark charge radius r) is, the much smaller the orbital factor F becomes. Of course, this behaviour is dominated by the decreasing exponential trend as we found analitically from Eq. (7.13) to (7.16).

Because of the nature of our results, which are model dependent, it is of special interest to know whether the results of the Harmonic Oscillator still holds true in a different model. For that reason we investigated a new approach with a different treatment and formalism, the Hypercentral Model. The last model consider fundamentally an hypercoulomb potential, and it will be presented in the next section.

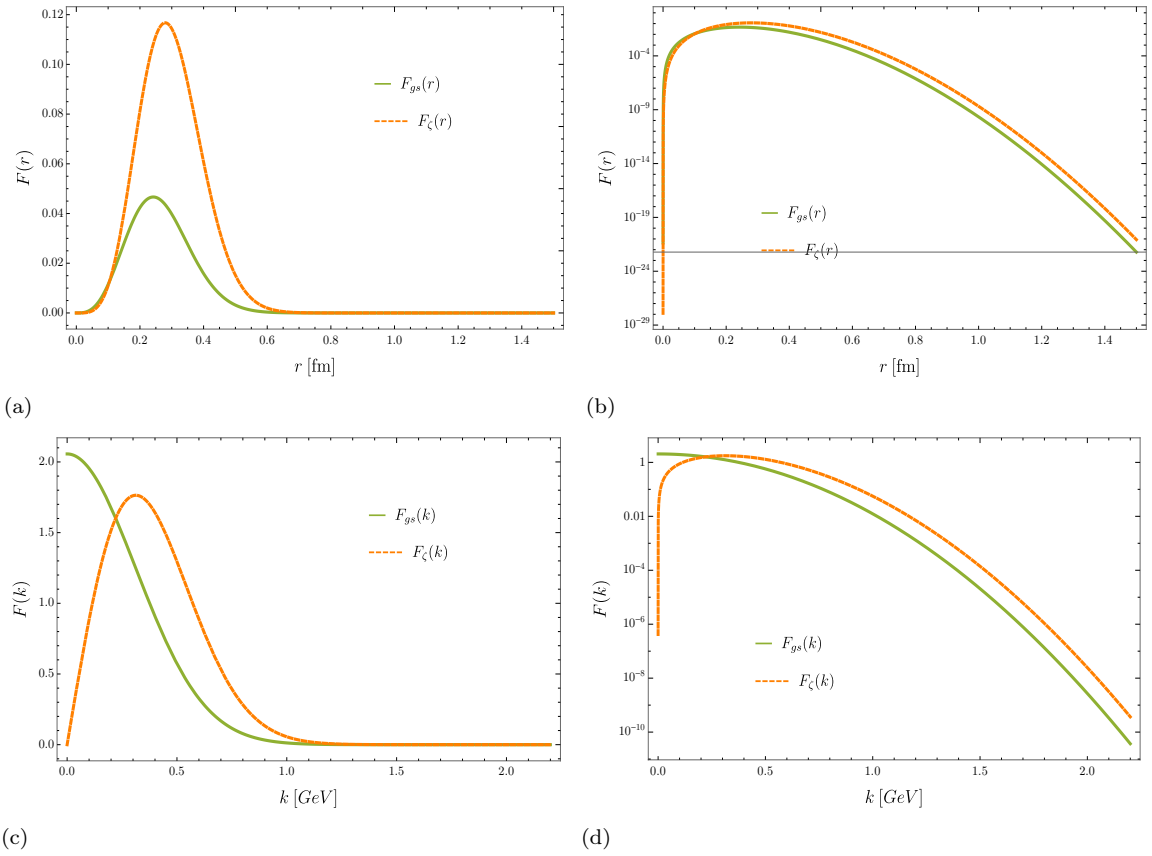

Fig. 7.3: Comparison between the ground and the only orbital excited pentaquark state $P_c(uudc\bar{c})$ for functions $F_{gs}(k)$, $F_{gs}(r)$, $F_\zeta(k)$ and $F_\zeta(r)$ in the Harmonic Oscillator Model.

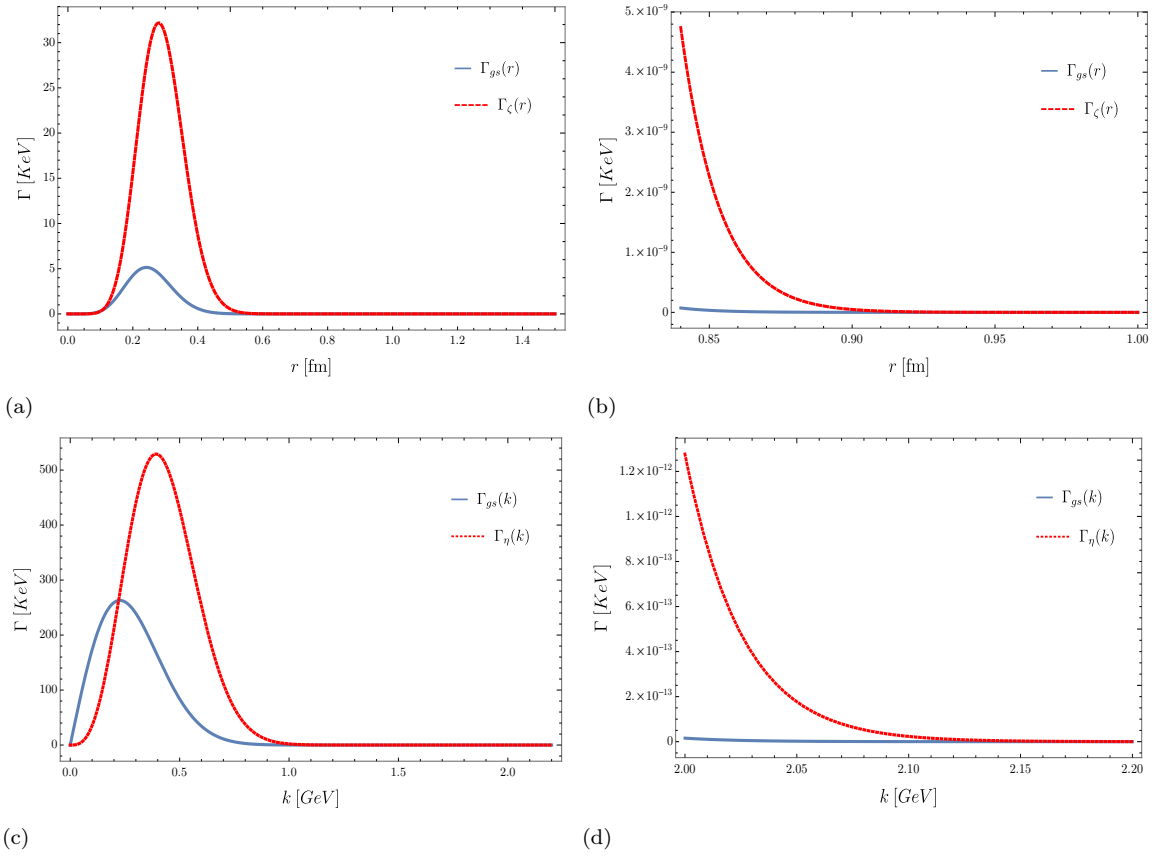

Fig. 7.4: Electromagnetic decay widths for the photoproduction of ground and orbital excited pentaquarks in the harmonic oscillator model: $P_c^*(uudc\bar{c}) \to p + \gamma$. The widths are given in KeV units and as a function of both the pentaquark charge radius and the momentum of the photon. In (b) and (d) are shown the zoom from (a) and (c) around the region of interest, 1 fm and 2.1 GeV, respectively.

Chapter 8

Hypercentral Quark Model

In this section, I present an independent solution of the orbital contribution to the photoproduction of pentaquark through the hypercentral approximation, HC. This model is based fundamentally in a Coulomb-like interaction, which with the introduction of the hyperspherical coordinates can be written as a hyper-Coulomb potential with dependence only in a new coordinate, called the hyperradius [85, 86, 87]. This formalism can be applied for systems with three particles and has been successful into describe many aspects of the light baryons [88, 89], including to the low-lying states of the spectra. This treatment can also be extended to N-body quantum systems in three dimensions [85, 90] and in particular to configuration with five particles, as compact pentaquarks.

8.1 Proton

Considering a system with three particles with different masses m_i, $i = 1, 2, 3.$, in a potential depending only on x, then

$$H = \sum_{i=1}^{3} \frac{{p_i}^2}{2m_i} + V(x). \tag{8.1}$$

The Jacobi coordinates for this Hamiltonian, can be defined as

$$\begin{cases} \vec{\rho} = \vec{r_2} - \vec{r_1}, \\ \vec{\lambda} = \left(\vec{r_3} - \frac{m_1\vec{r_1}+m_2\vec{r_2}}{M_2}\right)\left(\frac{m_3(M_2)^2}{m_1m_2(M_3)}\right)^{\frac{1}{2}}, \\ \vec{R} = \frac{m_1\vec{r_1}+m_2\vec{r_2}+m_3\vec{r_3}}{M_3} \end{cases} \Rightarrow \begin{cases} \vec{r}_1 = -\frac{m_2}{M_2}\vec{\rho} - \frac{m_1m_2}{(M_2)^2}\left(\frac{m_3(M_2)^2}{m_1m_2(M_3)}\right)^{\frac{1}{2}}\vec{\lambda} + \vec{R} \\ \vec{r}_2 = \frac{m_1}{M_2}\vec{\rho} - \frac{m_1m_2}{(M_2)^2}\left(\frac{m_3(M_2)^2}{m_1m_2(M_3)}\right)^{\frac{1}{2}}\vec{\lambda} + \vec{R} \\ \vec{r}_3 = \frac{M_2}{M_3}\left(\frac{m_1m_2(M_3)}{m_3(M_2)^2}\right)^{\frac{1}{2}}\vec{\lambda} + \vec{R} \end{cases} \tag{8.2}$$

where the Jacobian associated with this transformation is

$$\prod_{i=1}^{3} d^3r_i = \left(\frac{m_1m_2M_3}{M_2^2m_3}\right)^{\frac{3}{2}} d^3\rho d^3\lambda d^3R. \tag{8.3}$$

The relation of these coordinates with x, can be obtained through the hyperspherical coordinates. Here x is called the hyperradius and five angles are introduced: ξ is the hyperangle and the pair of angles associated with $\vec{\rho}$ and $\vec{\lambda}$ are $\Omega_\rho = (\theta_\rho, \phi_\rho)$, and $\Omega_\lambda = (\theta_\lambda, \phi_\lambda)$, respectively. The correspondence between both coordinate system is

$$x = \sqrt{\vec{\rho}^2 + \vec{\lambda}^2} \qquad \text{and} \qquad \xi = arctg\left(\frac{\rho}{\lambda}\right). \tag{8.4}$$

Working on a description of the system with Jacobi coordinates, one can separate the center of mass kinetic energy from the relative motion

$$H = \frac{{P_{CM}}^2}{2M_3} + \frac{{p_\rho}^2}{\mu} + \frac{{p_\lambda}^2}{\mu} + V(\vec{\rho}, \vec{\lambda}). \tag{8.5}$$

Considering the six-dimensional Coulumb potential

$$V(x) = -\frac{\tau}{\sqrt{\vec{\rho}^2 + \vec{\lambda}^2}}, \tag{8.6}$$

and the previous relations of Eq. (8.4), is possible to rewrite the Hamiltonian as

$$H = \frac{{P_{CM}}^2}{2M_3} - \frac{1}{2m}\left[\frac{\partial^2}{\partial x^2} + \frac{5}{x}\frac{\partial}{\partial x} - \frac{\Lambda^2(\Omega_\rho, \Omega_\lambda, \xi)}{x^2}\right] - \frac{\tau}{x}. \tag{8.7}$$

The solution for the CM motion are plane waves, and the complete ground state eigenfunction (without any radial excitation) for this Hamiltonian is

$$\psi_p(\vec{x_1}, \vec{x_2}, \vec{x_3}) = \frac{1}{(2\pi)^{\frac{3}{2}}} e^{-i\vec{K_p}\cdot\vec{R_p}} \phi_p(\vec{\rho}, \vec{\lambda}) = \left[\frac{(2g_3)^6}{5!}\right]^{\frac{1}{2}} \frac{1}{\pi^{\frac{3}{2}}} e^{-g_3 x} \left(\frac{M_2^2 m_3}{m_1 m_2 M_3}\right)^{\frac{3}{4}} \frac{1}{(2\pi)^{\frac{3}{2}}} e^{-i\vec{K_p}\cdot\vec{R_p}}, \tag{8.8}$$

with

$$g_3 = \frac{\tau\mu}{\sqrt{2}\frac{5}{2}}, \qquad \text{and} \qquad \mu = \frac{2m_1 m_2}{m_1 + m_2}. \tag{8.9}$$

We associate the masses m_i, with those masses of the constituent u and d quarks, and therefore this wave function to the proton.

8.2 Proton Charge Radius

In this Hypercentral model is calculated the charge radius for proton. By taking equal masses $m_1 = m_2 = m_3$ one has

$$\begin{aligned} \langle r_{ch}^2 \rangle_p &= \int \prod_{i=1}^{3} d^3 r_i \psi_p^* \sum_{j=1}^{3} \left(\vec{r_j} - \vec{R}\right)^2 e_j \psi_p \\ &= \frac{7}{4}\left(\frac{\frac{5}{2}\sqrt{2}}{\tau\mu}\right)^2 e. \end{aligned} \tag{8.10}$$

If one takes the above approach along with the constituent quark masses of $m_u = m_d = 320MeV$, and uses the experimental value: $\langle r_{ch} \rangle_p = 0.84fm$, then one obtains $\tau = 3.43$.

8.3 Pentaquark

We consider a Hamiltonian of five particles with different masses m_i

$$H = \sum_{i=1}^{5} \frac{{p_i}^2}{2m_i} + V(x) \tag{8.11}$$

where the potential is assumed to depend on x only, such that each individual particle is subject to the same potential $V(x)$. Then we introduce the Jacobi coordinates with a convenient normalization:

$$\left\{\begin{array}{l}\vec{\rho}=\vec{r_2}-\vec{r_1}\\ \vec{\lambda}=\frac{1}{\sqrt{N_\lambda}}\left(\vec{r_3}-\frac{m_1\vec{r_1}+m_2\vec{r_2}}{M_2}\right)\\ \vec{\eta}=\frac{1}{\sqrt{N_\eta}}\left(\vec{r_4}-\frac{m_1\vec{r_1}+m_2\vec{r_2}+m_3\vec{r_3}}{M_3}\right)\\ \vec{\zeta}=\frac{1}{\sqrt{N_\zeta}}\left(\vec{r_5}-\frac{m_1\vec{r_1}+m_2\vec{r_2}+m_3\vec{r_3}+m_4\vec{r_4}}{M_4}\right)\\ \vec{R}=\frac{m_1\vec{r_1}+m_2\vec{r_2}+m_3\vec{r_3}+m_4\vec{r_4}+m_5\vec{r_5}}{M_5}\end{array}\right. \Rightarrow \left\{\begin{array}{l}\vec{r_1}=-\frac{m_2}{M_2}\vec{\rho}-\frac{\sqrt{N_\lambda}m_3}{M_3}\vec{\lambda}-\frac{\sqrt{N_\eta}m_4}{M_4}\vec{\eta}-\frac{\sqrt{N_\zeta}m_5}{M_5}\zeta+\vec{R}\\ \vec{r_2}=\frac{m_1}{M_2}\vec{\rho}-\frac{\sqrt{N_\lambda}m_3}{M_3}\vec{\lambda}-\frac{\sqrt{N_\eta}m_4}{M_4}\vec{\eta}-\frac{\sqrt{N_\zeta}m_5}{M_5}\zeta+\vec{R}\\ \vec{r_3}=\frac{\sqrt{N_\lambda}M_2}{M_3}\vec{\lambda}-\frac{\sqrt{N_\eta}m_4}{M_4}\vec{\eta}-\frac{\sqrt{N_\zeta}m_5}{M_5}\zeta+\vec{R}\\ \vec{r_4}=\frac{\sqrt{N_\eta}M_3}{M_4}\vec{\eta}-\frac{\sqrt{N_\zeta}m_5}{M_5}\zeta+\vec{R}\\ \vec{r_5}=\frac{\sqrt{N_\zeta}M_4}{M_5}\zeta+\vec{R}\end{array}\right.$$

The four vectors $\vec{\rho}$, $\vec{\lambda}$, $\vec{\eta}$ and $\vec{\zeta}$ have a total of twelve components, and the normalization factors are

$$N_\lambda=\frac{m_1m_2M_3}{M_2^2m_3},\qquad N_\eta=\frac{m_1m_2M_4}{M_2M_3m_4},\qquad N_\zeta=\frac{m_1m_2M_5}{M_2M_4m_5}, \tag{8.12}$$

with the notation in masses is simplified by

$$M_n=\sum_{i=1}^{n}m_i,\qquad n=2,3,4,5. \tag{8.13}$$

The Jacobian from Cartesian to Jacobi coordinates is

$$\prod_{i=1}^{5}d^3r_i=\left(\frac{m_1^3m_2^3M_5}{M_2^4m_3m_4m_5}\right)^{\frac{3}{2}}d^3\rho d^3\lambda d^3\eta d^3\zeta d^3R. \tag{8.14}$$

This transformation separates the kinetic energy into the center of mass, and furthermore, into four independent Jacobi terms, with the same reduced mass $\mu=\frac{2m_1m_2}{m_1+m_2}$

$$H=\frac{P^2}{2M_5}+\frac{{p_\rho}^2}{\mu}+\frac{{p_\lambda}^2}{\mu}+\frac{{p_\eta}^2}{\mu}+\frac{{p_\zeta}^2}{\mu}+V(x). \tag{8.15}$$

Jacobi coordinates separate the system into a Schrödinger equation for the relative motion of the five particles in a potential field $V(x)$ and a Schrödinger equation for the motion of the center of mass. In this case, the five particle wave function is also separable into a product of the center-of-mass times the relative parts. Naturally the center-of-mass solution is trivial and shows that the system moves as a free particle of total mass M_5.
For the purpose of find the eigenfunctions for the relative movement of this Hamiltonian it is introduce a new change of coordinates to the twelve-dimentional hyperspherical polar coordinates, where aside from the hyperradius

$$x=\sqrt{\rho^2+\lambda^2+\eta^2+\zeta^2}, \tag{8.16}$$

we consider the three hyperangles given by

$$\begin{aligned}\xi_1 &= \arctan\left(\frac{\rho}{\lambda}\right)\\ \xi_2 &= \arctan\left(\frac{\eta}{\zeta}\right)\\ \xi &= \arctan\left(\sqrt{\frac{\rho^2+\lambda^2}{\eta^2+\zeta^2}}\right),\end{aligned} \tag{8.17}$$

and the four pairs of angles associated with $\vec{\rho}$, $\vec{\lambda}$, $\vec{\eta}$ and $\vec{\zeta}$ defined by $\Omega_\rho=(\theta_\rho,\phi_\rho)$, $\Omega_\lambda=(\theta_\lambda,\phi_\lambda)$, $\Omega_\eta=(\theta_\eta,\phi_\eta)$ and $\Omega_\zeta=(\theta_\zeta,\phi_\zeta)$, respectively. The Jacobian for this change of coordinates is

$$\prod_{i=1}^{5}d^3r_i=\left(\frac{m_1^3m_2^3M_5}{M_2^4m_3m_4m_5}\right)^{\frac{3}{2}}d^3Rx^{11}dxd\Omega, \tag{8.18}$$

with

$$d\Omega = (\cos\xi_1)^2(\sin\xi_1)^2 d\xi_1 (\cos\xi_2)^2(\sin\xi_2)^2 d\xi_2 (\cos\xi)^5(\sin\xi)^5 d\xi d\Omega_\rho d\Omega_\lambda d\Omega_\eta \Omega_\zeta. \tag{8.19}$$

For these new coordinates we express the kinetic energy as

$$T = \frac{P^2}{2M_5} - \frac{1}{2\mu}\left(\frac{\partial^2}{\partial x^2} + \frac{11}{x}\frac{\partial}{\partial x} - \frac{\Lambda^2(\Omega)}{x^2}\right), \tag{8.20}$$

so that $\Lambda^2(\Omega)$ is the generalized angular momentum operator in twelve dimensions and Ω contains the information of all the angular coordinates. Since the operator $\Lambda^2(\Omega)$ is given in hyperspherical coordinates, it satisfies the following eigenvalue equation

$$\Lambda^2(\Omega) Y_{[\gamma]}(\Omega) = \gamma(\gamma+10) Y_{[\gamma]}(\Omega), \tag{8.21}$$

where $\gamma(\gamma+10)$ are the eigenvalues, and $Y_{[\gamma]}(\Omega)$ the hyperspherical harmonics. Here $[\gamma]$ is a shorthand notation for the quantum numbers $\gamma, \gamma_1, \gamma_2, l_\rho, m_\rho, l_\lambda, m_\lambda, l_\eta, m_\eta, l_\zeta, m_\zeta$.

For potentials that only depends on the hyperradius x the Schrödinger equation of the relative motion can be separated into a hyperangular and a hyperradial equation.

8.3.1 Hyperradial equation

The hyperradial Schrödinger equation is given by

$$\left[-\frac{1}{2\mu}\left(\frac{\partial^2}{\partial x^2} + \frac{11}{x}\frac{\partial}{\partial x} - \frac{\gamma(\gamma+10)}{x^2}\right) - \frac{\tau}{x}\right] R_{\omega\gamma}(x) = E R_{\omega\gamma}(x) \tag{8.22}$$

which can be solved analytically to obtain

$$E = -\frac{\mu\tau^2}{2(\omega+\frac{11}{2})^2} \tag{8.23}$$

$$R_{\omega\gamma}(x) = \sqrt{\frac{(\omega-\gamma)!(2g)^{12}}{(\omega+\gamma+10)!(2\omega+11)}}(2gx)^\gamma e^{-gx} L^{2\gamma+10}_{\omega-\gamma}(2gx) \tag{8.24}$$

$$g = \frac{\mu\tau}{\sqrt{2}\left(\omega+\frac{11}{2}\right)}. \tag{8.25}$$

The normalization for the radial wave function is

$$\int x^{11} R_{\omega\gamma}(x) R_{\omega\gamma}(x) = 1. \tag{8.26}$$

Therefore, the radial solution for ground state $\omega = \gamma = 0$ and the fist excited state with $\omega = \gamma = 1$ are

$$R_{00}(x) = \sqrt{\frac{(2g_0)^{12}}{11!}} e^{-g_0 x} \tag{8.27}$$

$$R_{11}(x) = \sqrt{\frac{(2g_1)^{12}}{13!}}(2g_1 x) e^{-g_1 x}, \tag{8.28}$$

with $g_0 = \frac{\mu\tau}{\sqrt{2}\frac{11}{2}}$ and $g_1 = \frac{\mu\tau}{\sqrt{2}\frac{13}{2}}$ for the ground state and one orbital excited state, respectively.

8.3.2 Hyperangular equation

The hyperangular Schrödinger equation is given by

$$\begin{aligned}\Lambda^2(\Omega)Y_{[\gamma]}(\Omega) &= \left[-\frac{1}{(\cos\xi)^5(\sin\xi)^5}\frac{\partial}{\partial\xi}\left((\cos\xi)^5(\sin\xi)^5\frac{\partial}{\partial\xi}\right)+\frac{\Lambda_2^2(\Omega_2)}{(\cos\xi)^2}+\frac{\Lambda_1^2(\Omega_1)}{(\sin\xi)^2}\right]Y_{[\gamma]}(\Omega)\\ &= \gamma(\gamma+10)Y_{[\gamma]}(\Omega).\end{aligned} \tag{8.29}$$

Here there are two angular momentum operators in six-dimensions $\Lambda_1^2(\Omega_1)=\Lambda_1^2(\xi_1,\Omega_\rho,\Omega_\lambda)$ and $\Lambda_1^2(\Omega_2)=\Lambda_2^2(\xi_2,\Omega_\eta,\Omega_\zeta)$, fulfilling the eigenvalue equations

$$\Lambda_1^2(\Omega_1)Y_{[\gamma_1]}(\Omega_1) = \gamma_1(\gamma_1+4)Y_{[\gamma_1]}(\Omega_1) \tag{8.30}$$

$$\Lambda_2^2(\Omega_2)Y_{[\gamma_2]}(\Omega_2) = \gamma_2(\gamma_2+4)Y_{[\gamma_2]}(\Omega_2) \tag{8.31}$$

with $[\gamma_1]=\gamma_1,l_\rho,m_\rho,l_\lambda,m_\lambda$, and $[\gamma_2]=\gamma_2,l_\eta,m_\eta,l_\zeta,m_\zeta$. Because of the angular equation is separable in ξ, Ω_1 and Ω_2, the solution can be written as

$$Y_{[\gamma]}(\Omega)=A_\gamma(\xi)Y_{[\gamma_1]}(\Omega_1)Y_{[\gamma_2]}(\Omega_2) \tag{8.32}$$

With this form is obtained the differential equation in ξ

$$\left[-\frac{1}{(\cos\xi)^5(\sin\xi)^5}\frac{\partial}{\partial\xi}\left((\cos\xi)^5(\sin\xi)^5\frac{\partial}{\partial\xi}\right)+\frac{\gamma_1(\gamma_1+4)}{(\cos\xi)^2}+\frac{\gamma_2(\gamma_2+4)}{(\sin\xi)^2}-\gamma(\gamma+10)\right]A_{[\gamma]}(\xi)=0 \tag{8.33}$$

The solution of $A_{[\gamma]}(\xi)$ is given in terms of Jacobi polynomials as

$$A_\gamma(\xi)=(\cos\xi)^{\gamma_2}(\sin\xi)^{\gamma_1}P_n^{(\alpha,\beta)}(\cos2\xi)/\sqrt{\mathcal{N}_\gamma} \tag{8.34}$$

where

$$\begin{aligned}\alpha &= \gamma_1+2\\ \beta &= \gamma_2+2\\ n &= \frac{1}{2}(\gamma-\gamma_1-\gamma_2)\\ \mathcal{N}_\gamma &= \frac{\Gamma(n+\alpha+1)\Gamma(n+\beta+1)}{2(2n+\alpha+\beta+1)\Gamma(n+1)\Gamma(n+\alpha+\beta+1)}\end{aligned} \tag{8.35}$$

The equations for Ω_1 and Ω_2 satisfying Eqs. (8.30) and (8.31) are

$$\begin{aligned}\Lambda^2(\Omega_1)Y_{[\gamma_1]}(\Omega_1) &= \left[-\frac{1}{(\cos\xi_1)^2(\sin\xi_1)^2}\frac{\partial}{\partial\xi_1}\left((\cos\xi_1)^2(\sin\xi_1)^2\frac{\partial}{\partial\xi_1}\right)+\frac{L^2(\Omega_\lambda)}{(\cos\xi_1)^2}+\frac{L^2(\Omega_\rho)}{(\sin\xi_1)^2}\right]Y_{[\gamma_1]}(\Omega_1)\\ &= \gamma_1(\gamma_1+4)Y_{[\gamma_1]}(\Omega_1)\end{aligned} \tag{8.36}$$

$$\begin{aligned}\Lambda^2(\Omega_2)Y_{[\gamma_2]}(\Omega_2) &= \left[-\frac{1}{(\cos\xi_2)^2(\sin\xi_2)^2}\frac{\partial}{\partial\xi_2}\left((\cos\xi_2)^2(\sin\xi_2)^2\frac{\partial}{\partial\xi_2}\right)+\frac{L^2(\Omega_\lambda)}{(\cos\xi_2)^2}+\frac{L^2(\Omega_\rho)}{(\sin\xi_2)^2}\right]Y_{[\gamma_2]}(\Omega_2)\\ &= \gamma_1(\gamma_2+4)Y_{[\gamma_2]}(\Omega_2)\end{aligned} \tag{8.37}$$

in these case the four angular momentum operators $L^2(\Omega_\alpha)$ satisfies the following equations

$$L^2(\Omega_\rho)Y_{l_\rho m_\rho}(\Omega_\rho) = l_\rho(l_\rho+1)Y_{l_\rho m_\rho}(\Omega_\rho) \tag{8.38}$$

$$L^2(\Omega_\lambda)Y_{l_\lambda m_\lambda}(\Omega_\lambda) = l_\lambda(l_\lambda+1)Y_{l_\lambda m_\lambda}(\Omega_\lambda) \tag{8.39}$$

$$L^2(\Omega_\eta)Y_{l_\eta m_\eta}(\Omega_\eta) = l_\eta(l_\eta+1)Y_{l_\eta m_\eta}(\Omega_\eta) \tag{8.40}$$

$$L^2(\Omega_\zeta)Y_{l_\zeta m_\zeta}(\Omega_\zeta) = l_\zeta(l_\zeta+1)Y_{l_\zeta m_\zeta}(\Omega_\zeta) \tag{8.41}$$

again, both equations (8.36) and (8.37) are separable. The solutions can be written as

$$Y_{[\gamma_1]}(\Omega_1) = A_{\gamma_1}(\xi_1)Y_{l_\rho m_\rho}(\Omega_\rho)Y_{l_\lambda m_\lambda}(\Omega_\lambda) \tag{8.42}$$

$$Y_{[\gamma_2]}(\Omega_2) = A_{\gamma_2}(\xi_2)Y_{l_\eta m_\eta}(\Omega_\eta)Y_{l_\zeta m_\zeta}(\Omega_\zeta) \tag{8.43}$$

$$\tag{8.44}$$

then are obtained the differential equations in ξ_1 and ξ_2

$$\left[-\frac{1}{(\cos\xi_1)^2(\sin\xi_1)^2}\frac{\partial}{\partial\xi_1}\left((\cos\xi_1)^2(\sin\xi_1)^2\frac{\partial}{\partial\xi_1}\right)+\frac{l_\lambda(l_\lambda+1)}{(\cos\xi_1)^2}+\frac{l_\rho(l_\rho+1)}{(\sin\xi_1)^2}-\gamma_1(\gamma_1+4)\right]A_{\gamma_1}(\xi_1)=0 \quad (8.45)$$

$$\left[-\frac{1}{(\cos\xi_2)^2(\sin\xi_2)^2}\frac{\partial}{\partial\xi_2}\left((\cos\xi_2)^2(\sin\xi_2)^2\frac{\partial}{\partial\xi_2}\right)+\frac{l_\zeta(l_\zeta+1)}{(\cos\xi_2)^2}+\frac{l_\eta(l_\eta+1)}{(\sin\xi_2)^2}-\gamma_2(\gamma_2+4)\right]A_{\gamma_2}(\xi_2)=0 \quad (8.46)$$

$$(8.47)$$

and solutions are given in terms of Jacobi polynomials

$$A_{\gamma_1}(\xi_1) = (\cos\xi_1)^{l_\lambda}(\sin\xi_1)^{l_\rho}P_{n_1}^{(\alpha_1,\beta_1)}(\cos2\xi_1)/\sqrt{\mathcal{N}_{\gamma_1}} \quad (8.48)$$

$$A_{\gamma_2}(\xi_2) = (\cos\xi_2)^{l_\zeta}(\sin\xi_2)^{l_\eta}P_{n_2}^{(\alpha_2,\beta_2)}(\cos2\xi_2)/\sqrt{\mathcal{N}_{\gamma_2}} \quad (8.49)$$

where

$$\alpha_1 = l_\rho+\frac{1}{2} \qquad \alpha_2 = l_\eta+\frac{1}{2}$$

$$\beta_1 = l_\lambda+\frac{1}{2} \qquad \beta_2 = l_\zeta+\frac{1}{2}$$

$$n_1 = \frac{1}{2}(\gamma_1-l_\rho-l_\lambda) \qquad n_2 = \frac{1}{2}(\gamma_2-l_\eta-l_\zeta)$$

$$\mathcal{N}_{\gamma_i} = \frac{\Gamma(n_i+\alpha_i+1)\Gamma(n_i+\beta_i+1)}{2(2n_i+\alpha_i+\beta_i+1)\Gamma(n_i+1)\Gamma(n_i+\alpha_i+\beta_i+1)} \quad (8.50)$$

The quantum numbers for ground state and the first excited state are placed in Table 8.1

Table 8.1: Low lying quantum numbers for the hyperspherical harmonics with $\omega=\gamma=0$ and 1.

	γ	γ_1	γ_ρ	γ_λ	γ_2	l_η	l_ζ
$Y_{[0]}$	0	0	0	0	0	0	0
$Y_{[1]_\rho}$	1	1	1	0	0	0	0
$Y_{[1]_\lambda}$	1	1	0	1	0	0	0
$Y_{[1]_\eta}$	1	0	0	0	1	1	0
$Y_{[1]_\zeta}$	1	0	0	0	1	0	1

The hyperangular equation for ground state is

$$Y_{[0]}(\Omega) = \frac{2\sqrt{15}}{\pi^3} \quad (8.51)$$

and for the first excited states by

$$Y_{[1]_\rho}(\Omega) = \frac{4\sqrt{60}}{\pi^{5/2}}Y_{1m_\rho}(\Omega_\rho)\sin\xi\sin\xi_1 \quad (8.52)$$

$$Y_{[1]_\lambda}(\Omega) = \frac{4\sqrt{60}}{\pi^{5/2}}Y_{1m_\lambda}(\Omega_\lambda)\sin\xi\cos\xi_1 \quad (8.53)$$

$$Y_{[1]_\eta}(\Omega) = \frac{4\sqrt{60}}{\pi^{5/2}}Y_{1m_\eta}(\Omega_\eta)\cos\xi\sin\xi_2 \quad (8.54)$$

$$Y_{[1]_\zeta}(\Omega) = \frac{4\sqrt{60}}{\pi^{5/2}}Y_{1m_\zeta}(\Omega_\zeta)\cos\xi\cos\xi_2 \quad (8.55)$$

$$(8.56)$$

with the normalization

$$\int Y^*_{[0]}(\Omega)Y_{[0]}(\Omega)d\Omega = 1 \quad (8.57)$$

$$\int Y^*_{[1]_\alpha}(\Omega)Y_{[1]_\alpha}(\Omega)d\Omega = 1 \quad (8.58)$$

for $\alpha = \rho, \lambda, \eta, \zeta$.

Summarising, the total wave function for ground state and in general for one quantum of excitation in α are

$$\psi_{gs}(\vec{r}_1,\vec{r}_2,\vec{r}_3,\vec{r}_4,\vec{r}_5) = \left(\frac{a^2}{2a+3}\right)^{3/4} R_{00}(x)Y_{[0]}(\Omega)\frac{1}{(2\pi)^{\frac{3}{2}}}e^{-i\vec{K_{P_c}}\cdot\vec{R_{P_c}}}. \tag{8.59}$$

$$\psi_{exc,\alpha}(\vec{r}_1,\vec{r}_2,\vec{r}_3,\vec{r}_4,\vec{r}_5) = \left(\frac{a^2}{2a+3}\right)^{3/4} R_{11}(x)Y_{[1]_\alpha}(\Omega)\frac{1}{(2\pi)^{\frac{3}{2}}}e^{-i\vec{K_{P_c}}\cdot\vec{R_{P_c}}}. \tag{8.60}$$

with the normalization

$$\int\prod_{i=1}^{5} d^3r_i\psi^*_{gs}(\vec{r}_1,\vec{r}_2,\vec{r}_3,\vec{r}_4,\vec{r}_5)\psi_{gs}(\vec{r}_1,\vec{r}_2,\vec{r}_3,\vec{r}_4,\vec{r}_5) = 1 \tag{8.61}$$

and

$$\int\prod_{i=1}^{5} d^3r_i\psi^*_{exc,\alpha}(\vec{r}_1,\vec{r}_2,\vec{r}_3,\vec{r}_4,\vec{r}_5)\psi_{exc,\alpha}(\vec{r}_1,\vec{r}_2,\vec{r}_3,\vec{r}_4,\vec{r}_5) = 1. \tag{8.62}$$

The eigenfunctions for Hamiltonian of Eq. (8.15) are expressed in terms of the hyperradius x

$$\begin{aligned}\psi_{P_c}(\vec{x_1},\vec{x_2},\vec{x_3},\vec{x_4},\vec{x_5}) &= \frac{1}{(2\pi)^{\frac{3}{2}}}e^{-i\vec{K_{P_c}}\cdot\vec{R}}\phi_{P_c}(\vec{\rho},\vec{\lambda},\vec{\eta},\vec{\zeta}) \\ &= \left[\frac{(2g_0)^{12}}{11!}\right]^{\frac{1}{2}}\frac{2\sqrt{15}}{\pi^3}e^{-g_0x}\left(\frac{M_2^4m_3m_4m_5}{m_1^3m_2^3M_5}\right)^{\frac{3}{4}}\frac{1}{(2\pi)^{\frac{3}{2}}}e^{-i\vec{K}_{P_c}\cdot\vec{R}},\end{aligned} \tag{8.63}$$

where

$$g_0 = \frac{\tau\mu}{\sqrt{2}\frac{11}{2}}. \tag{8.64}$$

8.3.3 Confining potential

The hyperradial Schrödinger equation presented in Eq. (8.22) can be solved analytically only for two potentials; either for the twelve-dimensional harmonic oscillator or, as it was obtained in this section, for the twelve-dimensional hyper-Coulomb potential

$$V(x) = -\frac{\tau}{x}. \tag{8.65}$$

From several works based in different approaches and mainly in lattice QCD calculations [91], one expects a confining quark potential with an extra linear term for hadronic states, as follows

$$V(x) = -\frac{\tau}{x} + \epsilon\, x. \tag{8.66}$$

Nevertheless, this potential cannot be solved analytically, unless the linear term can be expanded in perturbation theory, provided that the parameter ϵ, real and positive, is small enough to consider the new term as a perturbation in the complete Hamiltonian. In fact this is a good approximation for the low-lying states in which we are interested on. *At first order in the perturbation theory [86], the solutions for both the proton and the pentaquark wave functions in this model remain exactly the same as we already obtain, and that is the reason why the wave functions in our derivation do not change if we consider the linear term in $V(x)$.*

8.4 Pentaquark Charge Radius

This observable is calculated using the previous pentaquark coordinates and also the ground state wave functions from The Hypercentral Model

$$\begin{aligned}\langle r^2_{ch}\rangle_{P_c} &= \int\prod_{i=1}^{5} d^3r_i\psi^*_{P_c}\sum_{j=1}^{5}\left(\vec{r_j}-\vec{R}\right)^2 e_j\psi_{P_c} \\ &= \frac{13}{4}\left(\frac{\frac{11}{2}\sqrt{2}}{\tau\mu}\right)^2\left(\frac{m_1m_2(2M_3^2+3m_4^2)}{M_2M_3m_4M_4}+\frac{m_1m_2(M_2^2+2m_3^2)}{M_2^2m_3M_3}\right. \\ &\qquad \left.-\frac{m_1m_2(2M_4^2-5m_5^2)}{M_2M_4m_5M_5}+\frac{m_1^2+m_2^2}{M_2^2}\right)e,\end{aligned} \tag{8.67}$$

here, the mass-dependent factor reduces to 6/5, when equal masses are taken. On the other hand, similarly to the harmonic oscillator, one can also simplify this results by talking the masses $m_1 = m_2 = m_3 = m$ for the light quarks, $m_4 = m_5 = m'$ for the heavy quarks with the definition of $a = m'/m$ to obtain

$$\langle r^2_{ch}\rangle_{P_c} = \frac{13}{4}\left(\frac{\frac{11}{2}\sqrt{2}}{\tau\mu}\right)^2 \frac{3(1+a)}{3+2a}e. \tag{8.68}$$

Finally, by using the effective masses $m_u = m_d = 320MeV$ for m and $m_c = m_{\bar{c}} = 1500MeV$ for m', respectively, and taking the same value of $\tau = 3.43$ as fitted to the proton in Eq. (8.10), then one obtains $\langle r_{ch}\rangle_{P_c} = 2.96fm$.

8.5 Overlap of the orbital part

8.5.1 Ground state

From making a Fourier Transform of the orbital overlap from the discussed Harmonic Oscillator formalism, we can obtain the form factor given the orbital contribution in the space of coordinates

$$\begin{aligned} F(k) &= \int\prod_{i=1}^{5} d^3x_i \int d^3x_0 \psi^*_p(\vec{x_1},\vec{x_2},\vec{x_3})\psi^{gs}_{P_c}(\vec{x_1},\vec{x_2},\vec{x_3},\vec{x_4},\vec{x_5}) \\ &\quad \delta^3(-\vec{x_4}+\vec{x_0})\delta^3(-\vec{x_5}+\vec{x_0})e^{-i\vec{k}\cdot\vec{x_0}}. \end{aligned} \tag{8.69}$$

Once the wave functions are placed into the integral, the above expression can be reduced to the next explicit integral

$$\begin{aligned} F_{gs}(k) &= \left(\frac{m_1^2 m_2^2 M_5}{M_2^2 M_3 m_4 m_5}\right)^{\frac{3}{4}} N_\zeta^{-\frac{3}{2}}(4\pi)^3\left[\frac{(2g_3)^6(2g_0)^{12}}{5!11!}\right]^{\frac{1}{2}}\frac{1}{\pi^{\frac{3}{2}}}\frac{2\sqrt{15}}{\pi^3}\frac{1}{q} \\ &\quad \int d\rho d\lambda d\eta \rho^2\lambda^2\eta\sin(q\eta)e^{-g_3\sqrt{\rho^2+\lambda^2}}e^{-g_0\sqrt{\rho^2+\lambda^2+\left(1+\frac{N_\eta}{N_\zeta}\frac{M_3^2}{M_4^2}\right)\eta^2}}, \end{aligned} \tag{8.70}$$

where q is defined as

$$q = \sqrt{N_\eta}\frac{m_5M_3 - m_4M_5 - M_3M_4}{M_4M_5}k. \tag{8.71}$$

The last integral can still be simplified by using a change of variables from ρ and λ to polar coordinates, where the angular part is solved immediately, and leaving us at the end with an integral in two variables. Unfortunately, this improper integral is hard to solve analytically, because of its asymptotic behaviour. That is the reason why we choose to solve it numerically.

Eq. (8.70) can be rewritten in terms of

$$m = m_1 = m_2 = m_3, \qquad \text{and} \qquad m' = m_4 = m_5, \tag{8.72}$$

again with

$$a \equiv \frac{m'}{m}. \tag{8.73}$$

$$\begin{aligned} F_{gs}(k) &= \left(\frac{2a+3}{3a^2}\right)^{\frac{3}{4}}\left(\frac{a(a+3)}{2a+3}\right)^{\frac{3}{2}}(4\pi)^2\left[\frac{(2g_3)^6(2g_0)^{12}}{5!11!}\right]^{\frac{1}{2}}\frac{1}{\pi^{\frac{3}{2}}}\frac{2\sqrt{15}}{\pi^3} \\ &\quad \int d\rho d\lambda d^3\eta\rho^2\lambda^2 e^{-i\vec{k}\cdot\vec{\eta}\frac{1}{\sqrt{2}}\sqrt{\frac{a+3}{3a}}}e^{-g_3\sqrt{\rho^2+\lambda^2}}e^{-g_0\sqrt{\rho^2+\lambda^2+\left(\frac{2(3+a)}{3+2a}\right)\eta^2}}, \end{aligned} \tag{8.74}$$

$$\begin{aligned} F_{gs}(k) &= \left(\frac{2a+3}{3a^2}\right)^{\frac{3}{4}}\left(\frac{a(a+3)}{2a+3}\right)^{\frac{3}{2}}(4\pi)^3\left[\frac{(2g_3)^6(2g_0)^{12}}{5!11!}\right]^{\frac{1}{2}}\frac{1}{\pi^{\frac{3}{2}}}\frac{2\sqrt{15}}{\pi^3} \\ &\quad \int d\rho d\lambda d\eta\rho^2\lambda^2\eta^2 j_0\left(-\frac{1}{\sqrt{2}}\sqrt{\frac{a+3}{3a}}k\eta\right)e^{-g_3\sqrt{\rho^2+\lambda^2}}e^{-g_0\sqrt{\rho^2+\lambda^2+\left(\frac{2(3+a)}{3+2a}\right)\eta^2}}. \end{aligned} \tag{8.75}$$

8.5.2 Pentaquark with one quantum of excitation in η and ζ

In virtue of previous definition of mass ratio, the proton wave function and pentaquark wave function with one quantum of excitation in η and ζ can be written as

$$\psi_B^*(\vec{x_1},\vec{x_2},\vec{x_3}) = \left[\frac{(2g_3)^6}{5!}\right]^{\frac{1}{2}} \frac{1}{\pi^{\frac{3}{2}}} e^{-g_3 x} \left(\frac{8}{3\sqrt{3}}\right)^{\frac{1}{2}} \frac{1}{(2\pi)^{\frac{3}{2}}} e^{-i\vec{K_{P_c}}\cdot\vec{R_{P_c}}}, \tag{8.76}$$

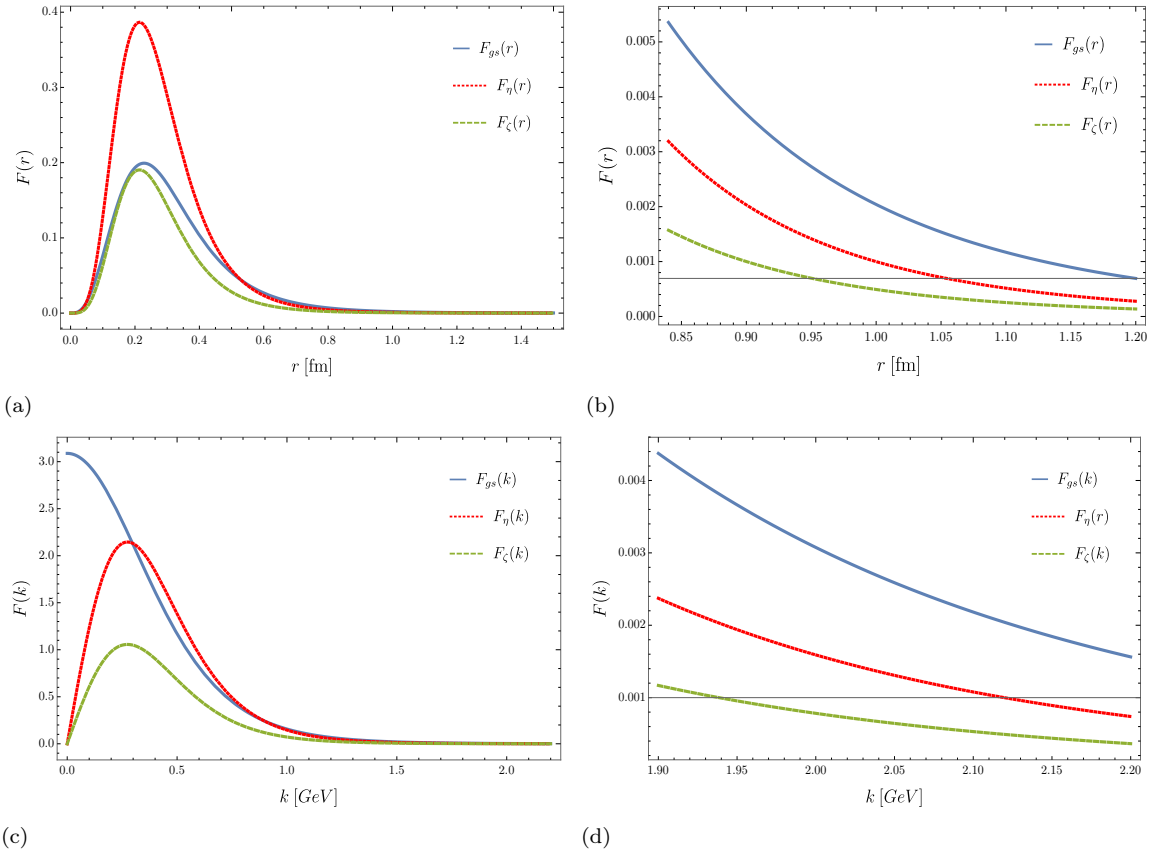

Fig. 8.1: Orbital contribution function to the photoproduction of ground and orbital excited pentaquaks $P_c(uudc\bar{c})$ in the Hypercentral Model. The upper plot (a) was calculated in terms of the pentaquark charge radius r, taken the momentum of the photon as $k = 2.1\,GeV$, whereas (c) is in terms of k, fixing $r = 1fm$. The graphs on the right hand side (b) and (d) are simply a zoom of the left ones. The analysis takes into account the orbital overlap with both excited modes, η and ζ.

$$\begin{aligned}\psi_{P_c,\eta}(\vec{x_1},\vec{x_2},\vec{x_3},\vec{x_4},\vec{x_5}) &= \left[\frac{(2g_1)^{14}}{13!}\right]^{\frac{1}{2}} \frac{8\sqrt{15}}{\pi^{\frac{5}{2}}} x_5 e^{-g_1 x_5} 8 \left(\frac{a^2}{3+2a}\right)^{\frac{3}{4}} Y_{1,m_\eta} cos(\xi) sin(\xi_2) \\ &\quad \frac{1}{(2\pi)^{\frac{3}{2}}} e^{-i\vec{K_{P_c}}\cdot\vec{R_{P_c}}},\end{aligned} \tag{8.77}$$

$$\begin{aligned}\psi_{P_c,\zeta}(\vec{x_1},\vec{x_2},\vec{x_3},\vec{x_4},\vec{x_5}) &= \left[\frac{(2g_1)^{14}}{13!}\right]^{\frac{1}{2}} \frac{8\sqrt{15}}{\pi^{\frac{5}{2}}} x_5 e^{-g_1 x_5} 8 \left(\frac{a^2}{3+2a}\right)^{\frac{3}{4}} Y_{1,m_\zeta} cos(\xi) cos(\xi_2) \\ &\quad \frac{1}{(2\pi)^{\frac{3}{2}}} e^{-i\vec{K_{P_c}}\cdot\vec{R_{P_c}}},\end{aligned} \tag{8.78}$$

respectively. Then, the orbital contributions for pentaquark with one quantum of excitation in η and ζ are

$$F_\eta(k) = i\left(\frac{(a+3)^2}{3(2a+3)}\right)^{\frac{3}{4}} 32\sqrt{15}\left[\frac{(2g_3)^6(2g_1)^{14}}{5!13!}\right]^{\frac{1}{2}} Y_{1,m_\eta}(\hat{k}) \int x^5 dx \eta^3 d\eta e^{-g_3 x} e^{-g_1\sqrt{x^2+\frac{2(3+a)}{3+2a}\eta^2}} j_1\left(-\frac{1}{\sqrt{2}}\sqrt{\frac{a+3}{3a}}k\eta\right), \tag{8.79}$$

$$F_\zeta(k) = i\left(\frac{2a+3}{3}\right)^{\frac{3}{4}}\left(\frac{3+a}{3}\right)^{\frac{3}{2}} 32\sqrt{15}\left[\frac{(2g_3)^6(2g_1)^{14}}{5!13!}\right]^{\frac{1}{2}} Y_{1,m_\zeta}(\hat{k}) \int x^5 dx \zeta^3 d\zeta e^{-g_3 x} e^{-g_1\sqrt{x^2+\frac{2(3+a)}{3}\zeta^2}} j_1\left(-\frac{1}{\sqrt{2}}\sqrt{\frac{(a+3)(3+2a)}{9a}}k\zeta\right). \tag{8.80}$$

Unlike the Harmonic Oscillator Model, here there are two excited states which in principle can be candidates to be photoproduced as pentaquark states. The above results together with the orbital function for the ground state, can be graphed in terms of the photon momentum and the pentaquark charge radius, Fig. 8.1.

8.6 Discussion of results

From the Hypercentral Model we observe a pretty similar behavior compared with the Harmonic Oscillator, since we have, qualitatively, the same shape of curves in each orbital function. Again, the photoproduction process is in essence ruled by, in this case, two decreasing exponentials inside the analytical expresions of the integrals, Eqs (8.75), (8.79) and (8.80). Nevertheless, in the present model there is a spherical Bessel function j_1 competing with the exponentials, where although $j_1(r)$ is a roughly like oscillating function, it has a decaying behaviour as r grows. The numerical solution shows that it is still preserved the fact that, after the function reaches its maximum, the larger the charge radius is, the much smaller the orbital factor becomes, as can be seen in charts from Fig. 8.1. An equivalent argument follows for $j_1(k)$.

Particularly, around $k = 2.1 GeV$ in chart (d) Fig. 8.1, one can observe that the r-dependent orbital factors are equal to or less than the order of 10^{-3} for both ground and excited states. The same order of magnitude keeps for the k-dependent orbital factors in chart (b). On the other hand, in Fig. 8.2, we obtain the radiative decay widths $\Gamma(P_c \to p + \gamma)$ in terms of the pentaquark charge radius. They mainly depend on the square modulus of the orbital overlaps, so around $1 fm$ we have an upper bound of the order of $\sim 10^{-2}$, as one could expect from Eq. (6.21), in comparison with the orbital functions. This result shows that although the orbital contribution, and therefore the electromagnetic width, is greater for the Hypercoulomb potential than for the Harmonic Oscillator, the photoproduction channel is still very suppressed.

Furthermore, one can compare results coming from the Hypercentral Model with results from the Harmonic Oscillator Model, in order to extract relevant information. For this purpose, we take the ground state pentaquark in each framework and graph both orbital functions $F_{gs}(k)$, Fig. 8.3. Even though the decay is smoother for the HC than for the HO, these functions decreased exponentially after they reach their maximum, where it is observed a gap between both graphs (a difference of roughly six orders of magnitude) at photon momentum $2.1\, GeV$ coming from the dynamical of the photoproduction process. Evidently, the orbital suppression of HO is higher than the HC for every value of k.

Of course, these conclusions together with those of the Harmonic Oscillator model were obtained under the hypothesis of a compact pentaquark structure. Such assumption was considered in the pentaquark classification of the wave function. There, we looked for configurations with hidden charm for $J^P = 3/2^-$, and flavor content $uudc\bar{c}$.

Hopefully, this study can provide insight in the understanding of the hidden charm pentaquark signals.

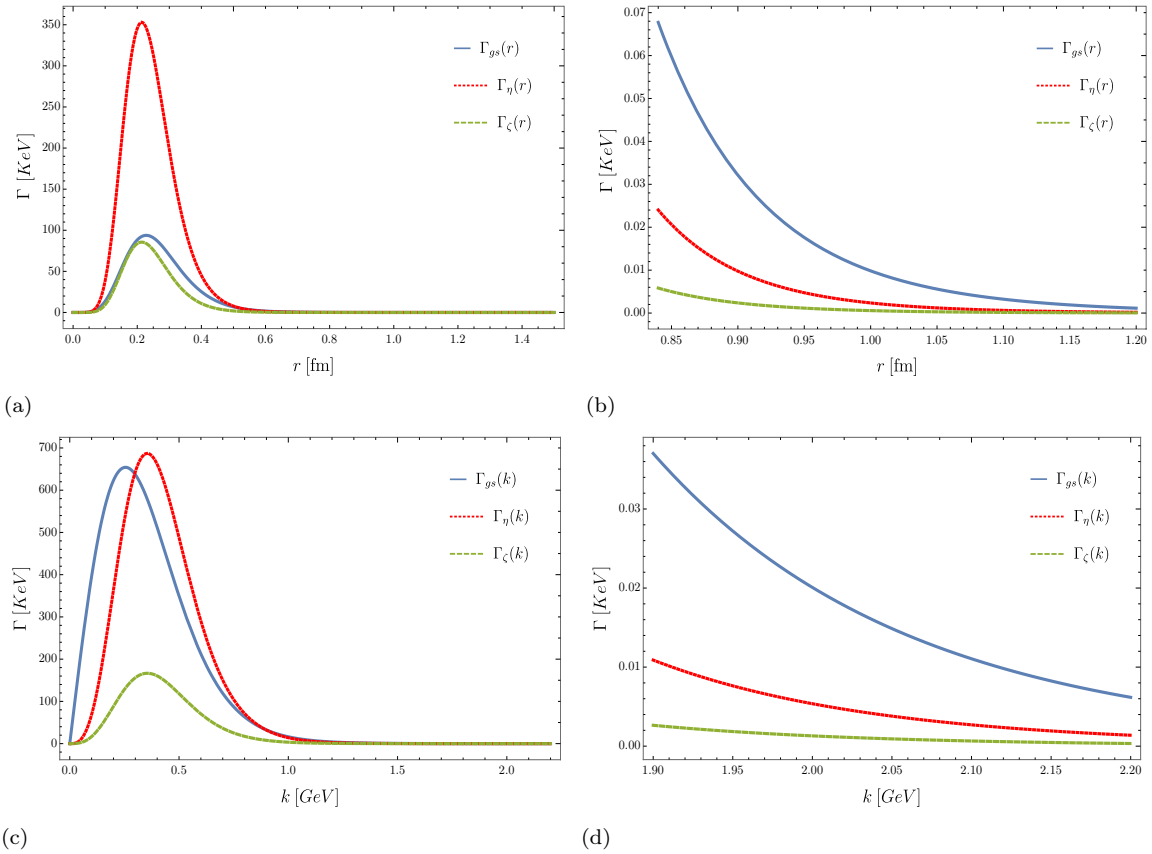

Fig. 8.2: Electromagnetic decay widths for the photoproduction of ground and orbital excited pentaquarks in the hypercentral model: $P_c^*(uudc\bar{c}) \to p + \gamma$. The widths are given in KeV units, and as a function of both the pentaquark charge radius and the momentum of the photon. In (b) and (d) are shown the zoom from (a) and (b) around the region of interest in 1 fm and $2.15\,GeV$, respectively.

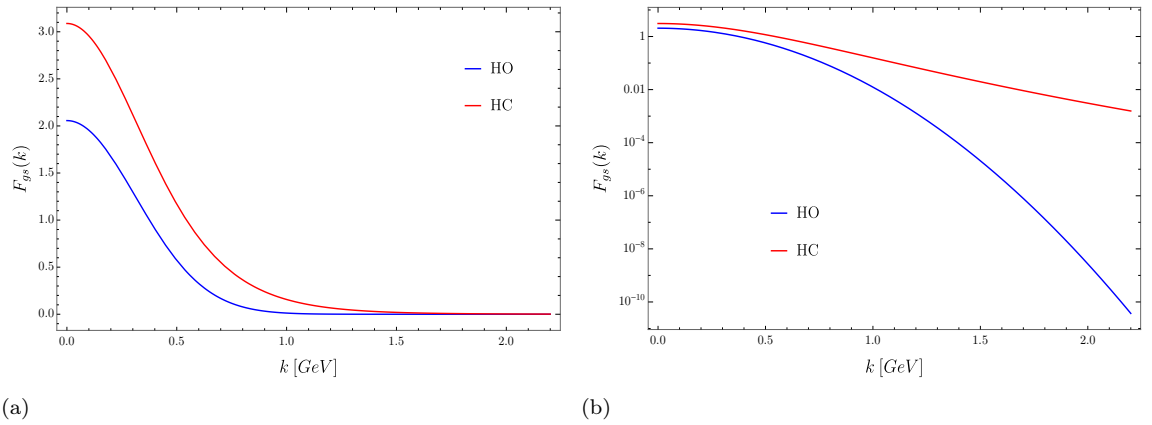

Fig. 8.3: Comparison between the Hypercentral Quark Model and the Harmonic Oscillator Quark Model. Both overlaps $F_{gs}(k)$ in (a) were done for ground state pentaquarks taking its charge radius fixed at $1fm$. Graph (b) is showed in logarithm scale.

Chapter 9

Summary and Conclusions

In this thesis I presented a study on multiquark systems with the heavy quarks. In particular, I focused on the singly-heavy quark baryons, and the hidden charm pentaquarks. Throughout the manuscript several process of current experimental interest were discussed and analyzed. Conclusions are presented below:

9.1 Heavy Baryons

- In the quark model singly-charm and singly-bottom baryons belong to either the flavor anti-triplet $\bar{\mathbf{3}}$ with spin and parity $S^P = 1/2^+$ or the flavor sextet $\mathbf{6}$ with $S^P = 1/2^+, 3/2^+$. For ground state baryons all states are S-wave states with $L^P = 0^+$ and $J^P = S^P$. P-wave baryons with $L^P = 1^-$ have negative parity and $|L - S| \leq J \leq L + S$. Furthermore, by using a mass rule which considers spin-orbit, isospin and flavor dependent contributions, we obtain the mass spectra. Our results are showed in Tables 2.2 and 2.3. As can be seen, there is a good agreement between our assignments and the experimental data for most of the heavy baryons. The only exceptions are a few resonances of the charm sector, specifically, $\Sigma_c(2800)$, $\Xi_c(2815)$ and $\Xi_c(3080)$, whose deviations are under 0.35%, while for $\Lambda_c(2595)$ and $\Lambda_c(2625)$ are less than 1.7%.

- By means of the Elementary-Meson Emission Model, we calculate all the strong decay widths allowed by the selection rules between singly heavy baryons. Each one of the contributions owing to individual isospin channels are listed from Table 3.4 to Table 3.9, whereas the total widths are presented in Tables 3.10 and 3.11. We found that with the exception of $\Xi_c(3080)$ and $\Omega_b(6340)$, all our theoretical results are consistently below the reported total decay widths. There are only a few works with a complete study on strong widths for heavy baryons. We compared our results with these approaches, and we observe that quark model is in better agreement with the current experimental data.

- We also obtained the radiative decay widths for baryons with one heavy quark c or b. Unlike the strong widths, for these decays there is not much experimental information. However, there are plenty of works with different approaches to compare with. Particularly, between ground states, Table 4.7, we observe a very close similarity from the Light cone QCD sum rules (LCQSR), hypercentral quark model (hCQM) and both the relativistic (RQM) and non-relativistic quark models (NRQM). For the bag model (BM) and the heavy hadron chiral perturbation theory (HHChPT) we observe widths slightly smaller than ours. On the other hand, we found a few discrepancies for the vector-meson dominance model (VDM) and the chiral quark model ($ChQM$). Furthermore, I report not only the electromagnetic widths for ground state but also for the orbital excited initial baryons, From Table 4.8 to Table 4.14.

- The signals $\Omega_c(3000)$, $\Omega_c(3050)$, $\Omega_c(3065)$, $\Omega_c(3090)$, $\Omega_c(3019)$ and $\Omega_c(3188)$ reported by either the LHCb or Belle Collaborations [8, 9] were interpreted as orbital excited states in the ρ and λ coordinates by considering an harmonic oscillator hamiltonian in [33]. Moreover, we calculate the strong decay widths within a $^3P_0$ model. In the same work, we give our predictions on new negative parity states and strong widths of the Ω_b states, which had not been reported experimentally at that time. Later in [10] the LHCb reported detection of four signals: $\Omega_b(6316)$, $\Omega_b(6330)$, $\Omega_b(6340)$ and $\Omega_b(6350)$ in the $\Xi_b^0 K^-$ mass spectrum, where these new data confirmed all our preceding assignments and strong widths.

- In a last study with the $^3P_0$ model [34], we also calculate the mass spectrum and strong widths of the single heavy baryons $\Xi_{c/b}$ and $\Xi'_{c/b}$. Here we proposed the identification of the new states reported by the LHCb and we found our results compatible with the current documented experimental data.

9.2 Pentaquarks

- First, I presented the classification of ground and orbital excited pentaquark states with total angular momentum and parity $J^P = 3/2^-$ for $qqqQ\bar{Q}$ configurations, which distinguishes between light and heavy quarks. For the radial part, two scenarios are considered, the harmonic oscillator model and the hypercentral model. Aside from obtaining the color-spin-flavor matrix elements, we also calculate the orbital transition matrix elements for the photoproduction channel of these states. As a result, we found that from a large number of pentaquark states, 5 for ground states and 19 for radially excited states, at the end of process there are contributions of only a few ones; 1 ground state, Eq. (5.40), and 2 radially excited states, Eqs. (5.48) and (5.53). This fact is due to the symmetry properties of the color wave functions and the orthogonality of the spin and flavor wave functions.
- When we investigate, with the HO, the behaviour of the orbital part $F(r)$ in the photoproduction of the three non vanishing pentaquarks, we observe only a very small contribution to the radiative decay width, at most of the order of $O(10^{-2})$. This happens for a short range of pentaquark charge radius r (roughly between $0.1 < r < 0.5\ fm$) and for a framework where the pentaquark is at rest having a photon momentum of $k = 2.1\ GeV$. After the function reaches its maximum, as r grows the orbital part starts to decrease monotonously and exponentially, as it was shown analytically in Eqs. (7.13) and (7.15). This fact can be seen in Fig. 7.3. Something equivalent occurs for $F(k)$, if we assume, as a matter of test, a pentaquark grater than the proton charge radius ($0.84\ fm$), and we choose to set r at for instance $1\ fm$, Fig. 7.3. The radiative decay widths presented in Fig. 7.4, also reflect the behavior of the form factor.
- Working in the HC model, we additionally were able to obtain reduced expressions for the orbital contribution to the photoproduction of pentaquarks $F(r)$, but in integral forms, Eqs. (8.75), (8.79) and (8.80). In such a case, besides all the integrands have two decreasing exponentials, they also depend on a continuous spherical Bessel functions $j_1(r)$, which has a roughly like decreasing oscillating behaviour as r grows. We solved numerically these integrals in terms of the r, Fig. 8.1, where we observe a pretty similar behavior compared with the HO. Indeed, when we studied the asymptotical behaviour of these solutions, we showed through a nonlinear fit that they decay as a decreasing exponential, so they rapidly approaches to zero as r grows. Again, we obtain an equivalent behavior for $F(k)$, as in the HO, Fig. 8.1. Moreover, in this case we obtain the radiative decay widths $\Gamma(r)$, Fig. 8.2, which in addition to reflect the same characteristics as $F(r)$, they show also the decaying trend. Naturally, this is due to $\Gamma(r)$ goes essentially as the square modulus of $F(r)$.
- Finally, under our hypothesis and considering all our results, we found that the photoproduction channel of pentaquark $p + \gamma \to P_c(uudc\bar{c})$ is highly suppressed, either in ground or excited states, and calculated with both the harmonic oscillator and the hypercentral models. For this reason we do not expect it to be feasible to experimentally reproduce the pentaquark state through the photoproduction process.
- The fact that, to date, the pentaquark has not been observed by the GlueX experiment [31] at Jefferson Lab does not exclude that the signals observed by LHCb belong to compact pentaquark states.

Appendix A

Conventions

Here are discussed the algebraic reductions to the formalism of the electromagnetic couplings, specially to the quark current, presented in Chapter 6. Along this thesis we choose to work in the conventional metric

$$g_{\mu\nu} = \begin{pmatrix} 1 & 0 & 0 & 0 \\ 0 & -1 & 0 & 0 \\ 0 & 0 & -1 & 0 \\ 0 & 0 & 0 & -1 \end{pmatrix} \tag{A.1}$$

The Dirac equation for fermions is given by

$$(i\gamma^{\mu}\partial_{\mu} - m)\psi = 0, \tag{A.2}$$

where ψ is the Dirac spinor and $\mu = \{0, 1, 2, 3\}$. The Dirac matrices satisfy the following algebraic relations

$$\{\gamma^{\mu}, \gamma^{\nu}\} = 2g_{\mu\nu} \tag{A.3}$$

$$\gamma^{0} = \begin{pmatrix} I & 0 \\ 0 & -I \end{pmatrix} \tag{A.4}$$

$$\gamma^{k} = \begin{pmatrix} 0 & \sigma^{k} \\ -\sigma^{k} & 0 \end{pmatrix} \tag{A.5}$$

where σ^{k} are Pauli matrices. The solution to Dirac Equation in a non-relativistic limit are Pauli Spinors.

Some useful definitions are presented in the following

$$v_s = \gamma^{5} u_s \tag{A.6}$$

$$\{\gamma^{\mu}, \gamma^{5}\} = 0 \tag{A.7}$$

$$(\gamma^{0})^2 = I_{4\times 4} \tag{A.8}$$

$$\gamma^{5} = \begin{pmatrix} 0 & I \\ I & 0 \end{pmatrix} \tag{A.9}$$

A.1 The non-relativistic limit of the electromagnetic quark current

In Chapter 6, Eq. 6.18 were presented the two relations between the quark current componentes in the covariant notation and the equivalents in a non-relativistic approximation

$$\begin{aligned}\bar{v}_{s'}(\vec{p'})\gamma^0 u_s(\vec{p}) &\rightarrow \chi^\dagger_{s'}\frac{\vec{\sigma}\cdot(\vec{p}+\vec{p'})}{2m}\chi_s \\ \bar{v}_{s'}(\vec{p'})\gamma^i u_s(\vec{p}) &\rightarrow \chi^\dagger_{s'}\sigma^i\chi_s. \end{aligned} \tag{A.10}$$

Here are calculated this relations explicitly. Starting with the zero component one has

$$\begin{aligned}\bar{v}_{s'}(\vec{p'})\gamma^0 u_s(\vec{p}) &= \bar{u}_s(\vec{p'})\gamma^5\gamma^0\gamma^\mu Q u_s(\vec{p}) \\ &= \bar{u}_s(\vec{p'})\gamma^\mu\gamma^5 Q u_s(\vec{p}) \\ &= \left(\frac{E'+m}{2m}\right)^{1/2}\left(\frac{E+m}{2m}\right)^{1/2}\begin{pmatrix}\chi^\dagger_{s'} & \chi^\dagger_{s'}\frac{\vec{\sigma}\cdot\vec{p'}}{E'+m}\end{pmatrix}\begin{pmatrix}0 & I\\ I & 0\end{pmatrix}Q\begin{pmatrix}\chi_s\\ \frac{\vec{\sigma}\cdot\vec{p}}{E+m}\chi_s\end{pmatrix}, \\ &= \left(\frac{E'+m}{2m}\right)^{1/2}\left(\frac{E+m}{2m}\right)^{1/2}\begin{pmatrix}\chi^\dagger_{s'} & \chi^\dagger_{s'}\frac{\vec{\sigma}\cdot\vec{p'}}{E'+m}\end{pmatrix}Q\begin{pmatrix}\frac{\vec{\sigma}\cdot\vec{p}}{E+m}\chi_s\\ \chi_s\end{pmatrix}, \\ &= \left(\frac{E'+m}{2m}\right)^{1/2}\left(\frac{E+m}{2m}\right)^{1/2}Q\left(\chi^\dagger_{s'}\frac{\vec{\sigma}\cdot\vec{p}}{E+m}\chi_s+\chi^\dagger_{s'}\frac{\vec{\sigma}\cdot\vec{p'}}{E'+m}\chi_s\right),\end{aligned} \tag{A.11}$$

and taking the non-relativistic limit, then the expression above is reduced to

$$\approx \quad Q\left(\chi^\dagger_{s'}\frac{\vec{\sigma}\cdot(\vec{p}+\vec{p'})}{2m}\chi_s\right) = Q\frac{\vec{\sigma}\cdot(\vec{p}+\vec{p'})}{2m}\delta_{s,s'}. \tag{A.12}$$

Now, for the spatial component one has

$$\begin{aligned}\bar{v}_{s'}(\vec{p'})\gamma^k u_s(\vec{p}) &= \bar{u}_s(\vec{p'})\gamma^k\gamma^5 Q u_s(\vec{p}) \\ &= \bar{u}_s(\vec{p'})\gamma^\mu\gamma^5 Q u_s(\vec{p}) \\ &= \left(\frac{E'+m}{2m}\right)^{1/2}\left(\frac{E+m}{2m}\right)^{1/2}\begin{pmatrix}\chi^\dagger_{s'} & \chi^\dagger_{s'}\frac{\vec{\sigma}\cdot\vec{p'}}{E'+m}\end{pmatrix}\gamma^0\gamma^k\gamma^5 Q\begin{pmatrix}\chi_s\\ \frac{\vec{\sigma}\cdot\vec{p}}{E+m}\chi_s\end{pmatrix}, \\ &= \left(\frac{E'+m}{2m}\right)^{1/2}\left(\frac{E+m}{2m}\right)^{1/2}\begin{pmatrix}\chi^\dagger_{s'} & \chi^\dagger_{s'}\frac{\vec{\sigma}\cdot\vec{p'}}{E'+m}\end{pmatrix}Q\begin{pmatrix}\sigma_k & 0\\ 0 & \sigma_k\end{pmatrix}\begin{pmatrix}\chi_s\\ \frac{\vec{\sigma}\cdot\vec{p}}{E+m}\chi_s\end{pmatrix}, \\ &= \left(\frac{E'+m}{2m}\right)^{1/2}\left(\frac{E+m}{2m}\right)^{1/2}\begin{pmatrix}\chi^\dagger_{s'} & \chi^\dagger_{s'}\frac{\vec{\sigma}\cdot\vec{p'}}{E'+m}\end{pmatrix}Q\begin{pmatrix}\sigma_k\chi_s\\ \sigma_k\frac{\vec{\sigma}\cdot\vec{p}}{E+m}\chi_s\end{pmatrix}, \\ &= \left(\frac{E'+m}{2m}\right)^{1/2}\left(\frac{E+m}{2m}\right)^{1/2}\left(\chi^\dagger_{s'}\sigma_k\chi_s+\chi^\dagger_{s'}\frac{\vec{\sigma}\cdot\vec{p'}}{E'+m}\sigma_k\frac{\vec{\sigma}\cdot\vec{p}}{E+m}\chi_s\right),\end{aligned} \tag{A.13}$$

and using non-relativistic limit we finally obtain

$$\approx \quad Q\left(\chi^\dagger_{s'}\sigma_k\chi_s\right).$$

Appendix B

Useful relations

In this Appendix are presented some mathematical tools, which are relevant for the evaluations of the transition matrix elements of many decay processes along this thesis.

B.1 Integrals

$$\begin{aligned}\int_0^\infty x^\mu e^{-\alpha^2 x^2} J_\nu(\beta x)dx &= \frac{\beta^\nu \Gamma(\frac{1}{2}(\mu+\nu+1))}{2^{\nu+1}\alpha^{\mu+\nu+1}\Gamma(\nu+1)}\ {}_1F_1\left(\frac{\nu+\mu+1}{2}, \nu+1, -\frac{\beta^2}{4\alpha^2}\right) \\ &= \frac{\beta^\nu}{2^{\nu+1}}\frac{\Gamma(\frac{\mu+\nu+1}{2})}{\alpha^{\mu+\nu+1}\Gamma(\nu+1)} e_1^{-\frac{\beta^2}{4\alpha^2}} F_1\left(\frac{\nu-\mu+1}{2}, \nu+1, \frac{\beta^2}{4\alpha^2}\right) \\ &= \left(\frac{\beta^2}{2\alpha}\right)^\nu \frac{\Gamma(\frac{\mu+\nu+1}{2})}{2\alpha^{\mu+1}\Gamma(\nu+1)} e_1^{-\frac{\beta^2}{4\alpha^2}} F_1\left(\frac{\nu-\mu+1}{2}, \nu+1, \frac{\beta^2}{4\alpha^2}\right) \qquad \text{(B.1)}\end{aligned}$$

where ${}_1F_1$ represent the hyper-geometrical confluent functions.

B.2 Bessel functions

$$j_l(kr) = \sqrt{\frac{\pi}{2kr}} J_{l+\frac{1}{2}}(kr) \qquad \text{(B.2)}$$

where $J_{l+\frac{1}{2}}(kr)$ are de Bessel functions and $j_l(kr)$ are de regular solutions (known as spherical Bessel functions) of the Bessel's equation used to solve the radial part of a free particle as a Central- Force problem with potential $V = 0$ and energy $E \geq 0$.

The plane waves $e^{i\vec{k}\cdot\vec{r}}$ and partial waves (or spherical waves) $j_l(kr)Y_{l,m}(\theta\phi)$ are a complete sets of eigenfunctions of the free particle Hamiltonian and both sets are equivalent. The expansion of plane waves in terms of partial waves is

$$e^{i\vec{k}\cdot\vec{r}} = 4\pi \sum_{l=0}^{+\infty} \sum_{m=-l}^{+l} i^l j_l(kr) Y_{l,m}(\hat{k}) Y^*_{l,m}(\hat{r}) \qquad \text{(B.3)}$$

B.3 Modified Bessel functions

Other important expansion is for cylindrical waves

$$e^{-\vec{k}\cdot\vec{r}} = 4\pi \sum_{l=0}^{+\infty} \sum_{m=-l}^{+l} (-1)^l i_l(kr) Y_{l,m}(\hat{k}) Y^*_{l,m}(\hat{r}) \qquad \text{(B.4)}$$

where

$$i_l(kr) = \sqrt{\frac{\pi}{2kr}} I_{l+\frac{1}{2}}(kr) \qquad \text{(B.5)}$$

These functions called the modified Bessel functions are defined in such way that are related to spherical Bessel ones as

$$i_l(kr) = i^{-l} j_l(kr) \tag{B.6}$$

B.3.1 Radial contribution of the baryon states

As previously derived in Eq. (2.9), the orbital wave function corresponding to the ground state is

$$\psi_{gs}^{rel} \equiv \psi_B^o(\vec{\rho},\vec{\lambda}) \quad = \quad \frac{\alpha_\rho^{\frac{3}{2}}}{\pi^{\frac{3}{4}}}\frac{\alpha_\lambda^{\frac{3}{2}}}{\pi^{\frac{3}{4}}} e^{-\frac{\alpha_\rho^2}{2}\rho^2} e^{-\frac{\alpha_\lambda^2}{2}\lambda^2} \tag{B.7}$$

and those corresponding to one quantum of excitation in ρ and λ are

$$\psi_\rho^{rel}(\vec{\rho},\vec{\lambda}) = \frac{1}{\sqrt{3\sqrt{3}}}\psi_{0,0,0}(\vec{\rho})\psi_{1,1,m_\rho}(\vec{\lambda}) = \frac{1}{\sqrt{3\sqrt{3}}}\sqrt{\frac{8}{3\sqrt{\pi}}} e^{-\rho^2\alpha_\rho^2/2}\rho\alpha_\rho^{5/2} Y_{1,m_\rho}(\hat{\rho})\frac{\alpha_\lambda^{\frac{3}{2}}}{\pi^{\frac{3}{4}}} e^{-\lambda^2\alpha_\lambda^2/2} \tag{B.8}$$

followed by

$$\psi_\lambda^{rel}(\vec{\rho},\vec{\lambda}) = \frac{1}{\sqrt{3\sqrt{3}}}\psi_{0,0,0}(\vec{\rho})\psi_{1,1,m_\lambda}(\vec{\lambda}) = \frac{1}{\sqrt{3\sqrt{3}}}\frac{\alpha_\rho^{\frac{3}{2}}}{\pi^{\frac{3}{4}}} e^{-\rho^2\alpha_\rho^2/2}\sqrt{\frac{8}{3\sqrt{\pi}}}\lambda\alpha_\lambda^{5/2} e^{-\lambda^2\alpha_\lambda^2/2} Y_{1,m_\lambda}(\hat{\lambda}) \tag{B.9}$$

respectively. The only non vanishing contribution in the overlap is for projections $m_\lambda = m_\rho = 0$, since the final state is the ground state.

Terms with a quantum of excitation in λ

First, it is illustrative to evaluate an integral (associated to orbital contributions of spin-flip amplitude) that contains a quantum of excitation in λ, and the coordinate $\vec{r}_3 = \vec{R} - \frac{\sqrt{6}m}{2m+m'}\vec{\lambda}$. Starting with

$$\begin{aligned} U_{\lambda,3} \quad &= \quad \langle\psi_{gs}|e^{-i\vec{k}\cdot\vec{r}_3}|\psi_\lambda\rangle = \frac{1}{\pi^{5/2}}\sqrt{\frac{8}{3}}\alpha_\rho^3\alpha_\lambda^4\int d^3\rho d^3\lambda e^{-\rho^2\alpha_\rho^2} e^{-\lambda^2\alpha_\lambda^2}\lambda e^{i\vec{k}\cdot\beta_3\vec{\lambda}} Y_{1,m_\lambda}(\hat{\lambda}) \\ &= \quad \frac{1}{\pi^{5/2}}\sqrt{\frac{8}{3}}\alpha_\rho^3\alpha_\lambda^4\left(\sqrt{\frac{\pi}{\alpha_\rho^2}}\right)^3\int d^3\lambda e^{-\lambda^2\alpha_\lambda^2}\lambda e^{i\vec{k}\cdot\beta_3\vec{\lambda}} Y_{1,m_\lambda}(\hat{\lambda}). \end{aligned}$$

for simplicity, here was defined $\beta_3 \equiv \frac{\sqrt{6}m}{2m+m'}$. Here is used the plane wave expansion in partial waves:

$$e^{i\vec{k}\cdot\beta_3\vec{\lambda}} = 4\pi\sum_{l=0}^{+\infty}\sum_{m=-l}^{+l} i^l j_l(\beta_3 k\lambda) Y_{l,m}(\hat{k}) Y_{l,m}^*(\hat{\lambda}) \tag{B.10}$$

where $j_l(x)$ are the spherical Bessel functions.

$$\begin{aligned} U_{\lambda,3} \quad &= \quad \frac{1}{\pi^{5/2}}\sqrt{\frac{8}{3}}\alpha_\lambda^4\sqrt{\pi}^3\int d^3\lambda e^{-\lambda^2\alpha_\lambda^2}\lambda 4\pi\sum_{l=0}^{+\infty}\sum_{m=-l}^{+l} i^l j_l(\beta_3 k\lambda) Y_{l,m}^*(\hat{\lambda}) Y_{l,m}(\hat{k}) Y_{1,m_\lambda}(\hat{\lambda}) \\ &= \quad \frac{4\pi}{\pi^{5/2}}\sqrt{\frac{8}{3}}\alpha_\lambda^4\sqrt{\pi}^3\int \lambda^2 d\lambda e^{-\lambda^2\alpha_\lambda^2}\lambda\sum_{l=0}^{+\infty}\sum_{m=-l}^{+l} i^l j_l(\beta_3 k\lambda) Y_{l,m}(\hat{k})\delta_{l,1}\delta_{m,m_\lambda} \\ &= \quad 4i\sqrt{\frac{8}{3}}\alpha_\lambda^4\int \lambda^2 d\lambda e^{-\lambda^2\alpha_\lambda^2}\lambda j_1(\beta_3 k\lambda) Y_{1,m_\lambda}(\hat{k}) \\ &= \quad 4i\sqrt{\frac{8}{3}}\alpha_\lambda^4 Y_{1,m_\lambda}(\hat{k})\int \lambda^3 d\lambda e^{-\lambda^2\alpha_\lambda^2}\sqrt{\frac{\pi}{2\beta_3 k}} J_{3/2}(\beta_3 k\lambda) \\ &= \quad 4i\sqrt{\frac{8}{3}}\alpha_\lambda^4\sqrt{\frac{\pi}{2\beta_3 k}} Y_{1,m_\lambda}(\hat{k})\int \lambda^{5/2} d\lambda e^{-\lambda^2\alpha_\lambda^2} J_{3/2}(\beta_3 k\lambda). \end{aligned}$$

where was used an identity to change the spherical Bessel function in terms of the cylindrical, $j_l(x) = \sqrt{\frac{\pi}{2x}} J_{l+1/2}(x)$. The last integral is known and it is equal to [92]:

$$\int_0^\infty x^\mu e^{-\alpha^2 x^2} J_\nu(\beta x) dx = \frac{\beta^\nu \Gamma(\frac{1}{2}(\mu+\nu+1))}{2^{\nu+1}\alpha^{\mu+\nu+1}\Gamma(\nu+1)}\, {}_1F_1\left(\frac{\nu+\mu+1}{2}, \nu+1, -\frac{\beta^2}{4\alpha^2}\right). \tag{B.11}$$

Now, in this case $\mu = 5/2$ and $\nu = 3/2$, also the momentum $\vec{k}$ of the photon with left-handed polarization is chosen along the z direction such that $\vec{k} = k\hat{z}$, so the previous integral becomes

$$\begin{aligned} U_{\lambda,3} &= 4i\sqrt{\frac{8}{3}}\alpha_\lambda^4\sqrt{\frac{\pi}{2\beta_3 k}}Y_{1,m_\lambda}(\hat{k})\frac{(\beta_3 k)^{\frac{3}{2}}\Gamma(\frac{5}{2})}{2^{5/2}\alpha_\lambda^5\Gamma(\frac{5}{2})}\,{}_1F_1\left(\frac{5}{2},\frac{5}{2},-\frac{\beta_3^2k^2}{4\alpha_\lambda^2}\right) \\ &= \frac{i}{2}\sqrt{\frac{8\pi}{3}}k\frac{\beta_3}{\alpha_\lambda}Y_{1,m_\lambda}(\hat{k})\,e^{-\frac{\beta_3^2k^2}{4\alpha_\lambda^2}}, \\ &= i\frac{\sqrt{3}m}{2m+m'}\frac{k}{\alpha_\lambda}e^{-\frac{3m^2k^2}{2\alpha_\lambda^2(2m+m')^2}}. \end{aligned} \tag{B.12}$$

where $Y_{1,m_\lambda}(\hat{k}) = \frac{1}{2}\sqrt{\frac{3}{\pi}}$. A similar calculation can be made for $\vec{r}_1 = \vec{R} + \frac{1}{\sqrt{2}}\vec{\rho} + \frac{\sqrt{\frac{3}{2}}m'}{2m+m'}\vec{\lambda}$ coordinate. The result is

$$U_{\lambda,1} = -i\frac{1}{2\alpha_\lambda}\frac{\sqrt{3}m'k}{2m+m'}e^{-\frac{k^2}{8\alpha_\rho^2}}e^{-\frac{3m'^2k^2}{8\alpha_\lambda^2(2m+m')^2}}. \tag{B.13}$$

Interestingly, the result is exactly the same for the missing term with $\vec{r}_2 = \vec{R} - \frac{1}{\sqrt{2}}\vec{\rho} + \frac{\sqrt{\frac{3}{2}}m'}{2m+m'}\vec{\lambda}$ coordinate, and is getting $U_{\lambda,2} = U_{\lambda,1}$. This can be seen from the fact that

$$\langle\psi_{gs}|e^{-i\vec{k}\cdot\vec{r}_1} - e^{-i\vec{k}\cdot\vec{r}_2}|\psi_\lambda\rangle = 0, \tag{B.14}$$

because ψ_λ is symmetric under interchange of the first two quarks.

Terms with a quantum of excitation in ρ

Can be demonstrated in an equivalent way that the integrals for the case of the terms with ρ excitation are

$$U_{\rho,3} = 0$$

and as before, a relation between terms $\vec{r}_1$ and $\vec{r}_2$ is getting

$$U_{\rho,1} = -U_{\rho,2} = -i\frac{k}{2\alpha_\rho}e^{-\frac{k^2}{8\alpha_\rho^2}}e^{-\frac{3}{8}\left(\frac{m'k}{\alpha_\lambda(2m+m')}\right)^2} \tag{B.15}$$

a similar argument is used to prove the above identity, since ψ_ρ is symmetric under interchange of the first two quarks

$$\langle\psi_{gs}|e^{-i\vec{k}\cdot\vec{r}_1} + e^{-i\vec{k}\cdot\vec{r}_2}|\psi_\rho\rangle = 0 \tag{B.16}$$

B.3.2 Spin-flavor contributions of the H_1 matrix elements

Evaluating the spin-flavor part is easier, since all the ingredients are available to perform the overlap of the states. Again, an example is useful to understand how the spin-flip operator affects the hyperons states and thus obtain the transition matrix elements. The only part of H_1 operator acting in the initial state to give a contribution is $e_j s_{j,-}$. Consider the ${}^2\rho(\Sigma_b^{*+}) \to \Sigma_b^+$ decay and the component $j = 1$, so the matrix element to be calculated in the spin-flavor basis (for helicity $\nu = 1/2$) is

$$\begin{aligned} \langle\Sigma_b^+; 1/2, \nu - 1/2|e_1 s_{1,-}|^2\rho(\Sigma_b^{*+}); J, \nu\rangle &= \langle uub\frac{1}{\sqrt{6}}(\downarrow\uparrow\downarrow + \uparrow\downarrow\downarrow - 2\downarrow\downarrow\uparrow)|e_1 s_{1,-}|uub\frac{1}{\sqrt{2}}(\uparrow\downarrow - \downarrow\uparrow)\uparrow\rangle \\ &= -\frac{1}{\sqrt{3}}e_u \end{aligned} \tag{B.17}$$

where the operator only affected fist component of the spin-flavor resonance lowering the spin projection and recording the charge of quark u. The result must be multiplied by their respective Clebsh-Gordan coefficient, in this case $\langle 10\frac{1}{2}\frac{1}{2}|J\frac{1}{2}\rangle$. In the same way, the rest of the spin-flip amplitudes can be calculated, either for helicity $\nu = 1/2$ or helicity $\nu = 3/2$. The results are shown in Tables **??** and 4.2. The Clebsch-Gordan factors are shown in Table (B.1).

Table B.1: Clebsch-Gordan coefficients for all the possible spin-angular momentum couplings.

CG	$J=\frac{1}{2}$	$J=\frac{3}{2}$	$J=\frac{5}{2}$
$\langle 10\frac{1}{2}\frac{1}{2}\vert J\frac{1}{2}\rangle$	$-\frac{1}{\sqrt{3}}$	$\sqrt{\frac{2}{3}}$	0
$\langle 10\frac{3}{2}\frac{1}{2}\vert J\frac{1}{2}\rangle$	$-\frac{1}{\sqrt{3}}$	$-\frac{1}{\sqrt{15}}$	$\sqrt{\frac{3}{5}}$
$\langle 11\frac{1}{2}-\frac{1}{2}\vert J\frac{1}{2}\rangle$	$\sqrt{\frac{2}{3}}$	$\frac{1}{\sqrt{3}}$	0
$\langle 11\frac{3}{2}-\frac{1}{2}\vert J\frac{1}{2}\rangle$	$\frac{1}{\sqrt{6}}$	$\sqrt{\frac{8}{15}}$	$\sqrt{\frac{3}{10}}$
$\langle 10\frac{3}{2}\frac{3}{2}\vert J\frac{3}{2}\rangle$	0	$-\sqrt{\frac{3}{5}}$	$\sqrt{\frac{2}{5}}$
$\langle 11\frac{1}{2}\frac{1}{2}\vert J\frac{3}{2}\rangle$	0	1	0
$\langle 11\frac{3}{2}\frac{1}{2}\vert J\frac{3}{2}\rangle$	0	$\sqrt{\frac{2}{5}}$	$\sqrt{\frac{3}{5}}$

Appendix C

Dynamical analysis for the strong and electromagnetic process

C.0.1 Four-momentum conservation in $P_c \to p + \gamma$ process

For three-momentum conservation we have the relation

$$\vec{K}_{P_c} = \vec{K_B} + \vec{k} \tag{C.1}$$
$$0 = \vec{K_B} + \vec{k} \tag{C.2}$$

where $\vec{K}_{P_c}$, $\vec{K}_B$ and $\vec{k}$ are the 3-momentum of the pentaquark, proton and the outgoing photon, respectively. **Choosing the reference frame of pentaquark at rest**, then $\vec{K}_{P_c} = 0$ and $\vec{K_B} = -\vec{k}$, i.e., $K_B = k$.

For energy conservation one has $E_{P_c} = m_B$, $E_B = \sqrt{m_B^2 + K_B^2}$ and k_0 are the energy of pentaquark, proton and photon, respectively, such that

$$\begin{aligned} E_{P_c} &= E_B + k_0 \\ m_{P_c} &= \sqrt{m_B^2 + K_B^2} + k_0 \\ m_{P_c} &= \sqrt{m_B^2 + k^2} + k_0 \end{aligned}$$

Therefore, if one calculates the square of the four-momentum $(k_0, \vec{k})$ of photon

$$Q^2 = Q^\mu Q_\mu = k_0^2 - k^2, \tag{C.3}$$

then one obtains

$$k^2 = \left(\frac{Q^2 - m_{P_c}^2 - m_B^2}{2m_{P_c}} \right)^2 - m_B^2. \tag{C.4}$$

and because the squared mass of photon $Q^2 = 0$, the previous equation is reduced to

$$k = \frac{m_{P_c}^2 - m_B^2}{2m_{P_c}} \tag{C.5}$$

By using the effective values of proton, $m_B = 0.938\ GeV$, and pentaquark, $m_{P_c} = 4.450\ GeV$, in the above equation, one obtains the momentum of photon for the photoproduction channel as, $k = 2.12\ GeV$.

C.0.2 Four-momentum conservation in $B \to B' + M$ process

In the rest frame of the decaying baryon, the energy for each one of hadron involve in process are

$$\begin{aligned} E_B &= m_B \\ E_{B'} &= \sqrt{m_{B'}^2 + p_{B'}^2} \\ E_M &= \sqrt{m_M^2 + k^2} \end{aligned}$$

Energy conservation implies

$$\begin{aligned} E_B &= E'_B + E_M \\ m_B &= \sqrt{m^2_{B'} + p^2_{B'}} + \sqrt{m^2_M + k^2} \\ m_B &= \sqrt{m^2_{B'} + k^2} + \sqrt{m^2_M + k^2} \end{aligned} \tag{C.6}$$

Where in the last line was used the momentum conservation $\vec{p_B} = \vec{p_{B'}} + \vec{k}$, i.e. $\vec{p_{B'}} = -\vec{k}$. Solving Eq. (C.6) for k^2 of emitted meson

$$k^2 = -m^2_M + \frac{(m^2_B - m^2_{B'} + m^2_M)^2}{4m^2_B}. \tag{C.7}$$

C.0.3 Four-momentum conservation in $B \to B' + \gamma$ process

In the rest frame of the decaying baryon, the energy for initial and final baryons, and photon are

$$\begin{aligned} E_B &= m_B \\ E_{B'} &= \sqrt{m^2_{B'} + p^2_{B'}} \\ E_\gamma &= k \end{aligned}$$

Energy conservation implies

$$\begin{aligned} E_B &= E'_B + E_\gamma \\ m_B &= \sqrt{m^2_{B'} + p^2_{B'}} + k \\ m_B &= \sqrt{m^2_{B'} + k^2} + k \end{aligned} \tag{C.8}$$

Where in the last line was used the momentum conservation $\vec{p_B} = \vec{p_{B'}} + \vec{k}$, i.e. $\vec{p_{B'}} = -\vec{k}$. Solving Eq. (C.6) for k of emitted meson

$$k = \frac{m^2_B - m^2_{B'}}{2m_B} \tag{C.9}$$

Bibliography

[1] R. Aaij *et al.* (LHCb Collaboration), Phys. Rev. Lett. **122**, 012001 (2019).

[2] R. Aaij *et al.* (LHCb Collaboration), Phys. Rev. Lett. **124**, 222001 (2020).

[3] R. Aaij *et al.* (LHCb Collaboration), Phys. Rev. Lett. **114**, 062004 (2015).

[4] R. Aaij *et al.* (LHCb Collaboration), Phys. Rev. Lett. **113**, 242002 (2014).

[5] R. Aaij *et al.* (LHCb Collaboration), Phys. Rev. D **99**, 052006 (2019).

[6] R. Aaij *et al.*, Journal of High Energy Physics **2016**, 161 (2016).

[7] R. Aaij *et al.* (LHCb Collaboration), Phys. Rev. Lett. **121**, 072002 (2018).

[8] R. Aaij *et al.* (LHCb Collaboration), Phys. Rev. Lett. **118**, 182001 (2017).

[9] Y. Yelton *et al.* (Belle Collaboration), Phys. Rev. D **97**, 051102 (2018).

[10] R. Aaij *et al.* (LHCb Collaboration), Phys. Rev. Lett. **124**, 082002 (2020).

[11] R. Aaij *et al.* (LHCb), Phys. Rev. Lett. **115**, 072001 (2015), arXiv:1507.03414 [hep-ex] .

[12] R. Aaij *et al.* (LHCb), Phys. Rev. Lett. **117**, 082002 (2016), arXiv:1604.05708 [hep-ex] .

[13] R. Aaij *et al.* (LHCb Collaboration), Phys. Rev. Lett. **122**, 222001 (2019).

[14] F.-K. Guo, U.-G. Meißner, W. Wang, and Z. Yang, Phys. Rev. **D92**, 071502 (2015), arXiv:1507.04950 [hep-ph] .

[15] X.-H. Liu, Q. Wang, and Q. Zhao, AIP Conference Proceedings **1735**, 060004 (2016), https://aip.scitation.org/doi/pdf/10.1063/1.4949440 .

[16] U.-G. Meißner and J. A. Oller, Phys. Lett. **B751**, 59 (2015), arXiv:1507.07478 [hep-ph] .

[17] H.-X. Chen, W. Chen, X. Liu, T. G. Steele, and S.-L. Zhu, Phys. Rev. Lett. **115**, 172001 (2015), arXiv:1507.03717 [hep-ph] .

[18] L. Roca, J. Nieves, and E. Oset, Phys. Rev. **D92**, 094003 (2015), arXiv:1507.04249 [hep-ph] .

[19] J. He, Phys. Lett. **B753**, 547 (2016), arXiv:1507.05200 [hep-ph] .

[20] Q.-F. Lü and Y.-B. Dong, Phys. Rev. **D93**, 074020 (2016), arXiv:1603.00559 [hep-ph] .

[21] S. G. Yuan, K. W. Wei, J. He, H. S. Xu, and B. S. Zou, Eur. Phys. J. **A48**, 61 (2012), arXiv:1201.0807 [nucl-th] .

[22] L. Maiani, A. D. Polosa, and V. Riquer, Phys. Lett. **B749**, 289 (2015), arXiv:1507.04980 [hep-ph] .

[23] R. F. Lebed, Phys. Lett. **B749**, 454 (2015), arXiv:1507.05867 [hep-ph] .

[24] A. Mironov and A. Morozov, JETP Lett. **102**, 271 (2015), [Pisma Zh. Eksp. Teor. Fiz.102,no.5,302(2015)], arXiv:1507.04694 [hep-ph] .

[25] E. Santopinto and A. Giachino, Phys. Rev. **D96**, 014014 (2017), arXiv:1604.03769 [hep-ph] .

[26] Z. Meziani *et al.* (Hall A), *E12-12-006: Near Threshold Electroproduction of J/ψ at 11 GeV* (2012).

[27] S. Stepanyan *et al.* (Hall B), *E12-12-001A Near Threshold J/ψ Photoproduction and Study of LHCb Pentaquarks with CLAS12* (2017).

[28] Z. E. Meziani *et al.* (Hall C), *E12-16-007: A Search for the LHCb Charmed 'Pentaquark' using Photo-Production of J/ψ at Threshold in Hall C at Jefferson Lab* (2016) arXiv:1609.00676 [hep-ex] .

[29] L. Robison (GlueX), in *2017 Fall Meeting of the APS Division of Nuclear Physics. Pittsburgh, Pennsylvania, October 25-28, 2017* (2017).

[30] D. Winney, C. Fanelli, A. Pilloni, A. N. H. Blin, C. Fernández-Ramírez, M. Albaladejo, V. Mathieu, V. I. Mokeev, and A. P. Szczepaniak (Joint Physics Analysis Center), Phys. Rev. D **100**, 034019 (2019).

[31] A. Ali *et al.* (GlueX Collaboration), Phys. Rev. Lett. **123**, 072001 (2019).

[32] E. Ortiz-Pacheco, R. Bijker, and C. Fernández-Ramírez, (2018), arXiv:1808.10512 [nucl-th] .

[33] E. Santopinto, A. Giachino, J. Ferretti, H. García-Tecocoatzi, M. A. Bedolla, R. Bijker, and E. Ortiz-Pacheco, The European Physical Journal C **79**, 1012 (2019).

[34] R. Bijker, H. García-Tecocoatzi, A. Giachino, E. Ortiz-Pacheco, and E. Santopinto, "Masses and decay widths of $\xi_{c/b}$ and $\xi'_{c/b}$ baryons," (2020), arXiv:2010.12437 [hep-ph] .

[35] F. Stancu, *Group theory in subnuclear physics*, Vol. 19 (Oxford Stud. Nucl. Phys., 1996).

[36] G. E. Baird and L. C. Biedenharn, J. Math. Phys. **4**, 1449 (1963).

[37] E. M. Haacke, J. W. Moffat, and P. Savaria, J. Math. Phys. **17**, 2041 (1976).

[38] R. Bijker, F. Iachello, and A. Leviatan, Annals of Physics **284**, 89 (2000).

[39] J. D. Bjorken and S. L. Glashow, Phys. Lett. **11**, 255 (1964).

[40] S. L. Glashow, J. Iliopoulos, and L. Maiani, Phys. Rev. **D2**, 1285 (1970).

[41] M. K. Gaillard, B. W. Lee, and J. L. Rosner, Rev. Mod. Phys. **47**, 277 (1975).

[42] A. De Rujula, H. Georgi, and S. L. Glashow, Phys. Rev. **D12**, 147 (1975).

[43] M. Tanabashi *et al.* (Particle Data Group), Phys. Rev. **D98**, 030001 (2018).

[44] A. Hosaka, M. Takayama, and H. Toki, Nucl. Phys. **A678**, 147 (2000), arXiv:hep-ph/9910469 [hep-ph] .

[45] N. Isgur and G. Karl, Phys. Rev. D **18**, 4187 (1978).

[46] E. Ortiz-Pacheco, R. Bijker, H. García-Tecocoatzi, A. Giachino, and E. Santopinto, Journal of Physics: Conference Series **1610**, 012011 (2020).

[47] P. Zyla *et al.* (Particle Data Group), PTEP **2020**, 083C01 (2020).

[48] M. Padmanath, "Heavy baryon spectroscopy from lattice qcd," (2019), arXiv:1905.10168 [hep-lat] .

[49] R. A. Briceño, H.-W. Lin, and D. R. Bolton, Phys. Rev. D **86**, 094504 (2012).

[50] Z. S. Brown, W. Detmold, S. Meinel, and K. Orginos, Phys. Rev. D **90**, 094507 (2014).

[51] P. Mohanta and S. Basak, Phys. Rev. D **101**, 094503 (2020).

[52] M. Padmanath and N. Mathur, Phys. Rev. Lett. **119**, 042001 (2017).

[53] C. Alexandrou and C. Kallidonis, Phys. Rev. D **96**, 034511 (2017).

[54] P. Pérez-Rubio, S. Collins, and G. S. Bali, Phys. Rev. D **92**, 034504 (2015).

[55] C. Alexandrou, V. Drach, K. Jansen, C. Kallidonis, and G. Koutsou, Phys. Rev. D **90**, 074501 (2014).

[56] Y. Namekawa, S. Aoki, K.-I. Ishikawa, N. Ishizuka, K. Kanaya, Y. Kuramashi, M. Okawa, Y. Taniguchi, A. Ukawa, N. Ukita, and T. Yoshié (PACS-CS Collaboration), Phys. Rev. D **87**, 094512 (2013).

[57] L. Liu, H.-W. Lin, K. Orginos, and A. Walker-Loud, Phys. Rev. D **81**, 094505 (2010).

[58] H. Bahtiyar, K. U. Can, G. Erkol, P. Gubler, M. Oka, and T. T. Takahashi (TRJQCD Collaboration), Phys. Rev. D **102**, 054513 (2020).

[59] R. Aaij *et al.* (LHCb Collaboration), Phys. Rev. Lett. **109**, 172003 (2012).

[60] A. Le Yaouanc, L. Oliver, O. Pene, and J. C. Raynal, *Hadron Transitions in the Quark Model* (Gordon and Breach, New York, NY, USA, 1988).

[61] R. Koniuk and N. Isgur, Phys. Rev. D **21**, 1868 (1980).

[62] S.-H. Lee *et al.* (Belle Collaboration), Phys. Rev. D **89**, 091102 (2014).

[63] R. Mizuk *et al.* (Belle Collaboration), Phys. Rev. Lett. **94**, 122002 (2005).

[64] B. Aubert *et al.* (BABAR Collaboration), Phys. Rev. D **78**, 112003 (2008).

[65] R. Aaij *et al.* (LHCb Collaboration), Phys. Rev. D **103**, 012004 (2021).

[66] K.-L. Wang, Y.-X. Yao, X.-H. Zhong, and Q. Zhao, Phys. Rev. D **96**, 116016 (2017).

[67] T. M. Aliev, K. Azizi, and A. Ozpineci, Phys. Rev. D **79**, 056005 (2009).

[68] T. M. Aliev, K. Azizi, and H. Sundu, The European Physical Journal C **75**, 14 (2015).

[69] T. M. Aliev, T. Barakat, and M. Savc ı, Phys. Rev. D **93**, 056007 (2016).

[70] A. Bernotas and V. Šimonis, Phys. Rev. D **87**, 074016 (2013).

[71] T. M. Aliev, M. Savci, and V. S. Zamiralov, Modern Physics Letters A **27**, 1250054 (2012).

[72] A. Majethiya, B. Patel, and P. C. Vinodkumar, The European Physical Journal A **42**, 213 (2009).

[73] G.-J. Wang, L. Meng, and S.-L. Zhu, Phys. Rev. D **99**, 034021 (2019).

[74] M. A. Ivanov, J. G. Körner, V. E. Lyubovitskij, and A. G. Rusetsky, Phys. Rev. D **60**, 094002 (1999).

[75] K. Gandhi, Z. Shah, and A. K. Rai, International Journal of Theoretical Physics **59**, 1129 (2020).

[76] K. Gandhi, Z. Shah, and A. K. Rai, The European Physical Journal Plus **133**, 512 (2018).

[77] Z. Shah, K. Thakkar, A. K. Rai, and P. C. Vinodkumar, Chinese Physics C **40**, 123102 (2016).

[78] K.-L. Wang, L.-Y. Xiao, X.-H. Zhong, and Q. Zhao, Phys. Rev. D **95**, 116010 (2017).

[79] D. Gamermann, C. E. Jiménez-Tejero, and A. Ramos, Phys. Rev. D **83**, 074018 (2011).

[80] T. M. Aliev *et al.*, The European Physical Journal C **79**, 437 (2019).

[81] A. Ali *et al.* (GlueX Collaboration), Phys. Rev. Lett. **123**, 072001 (2019).

[82] E. Ortiz-Pacheco, R. Bijker, and C. Fernández-Ramírez, Journal of Physics G: Nuclear and Particle Physics **46**, 065104 (2019).

[83] L. A. Copley, G. Karl, and E. Obryk, Nucl. Phys. **B13**, 303 (1969).

[84] F. E. Close, *An Introduction to Quarks and Partons* (Academic Press, London, UK, 1979).

[85] A. O. Barut and Y. Kitagawara, Journal of Physics A: Mathematical and General **15**, 117 (1982).

[86] E. Santopinto, F. Iachello, and M.M. Giannini, Eur. Phys. J. A **1**, 307 (1998).

[87] R. Bijker, F. Iachello, and E. Santopinto, Journal of Physics A Mathematical General **31**, 9041 (1998), arXiv:nucl-th/9801051 [nucl-th] .

[88] M. M. Giannini and E. Santopinto, "The hypercentral constituent quark model and its application to baryon properties," (2015), arXiv:1501.03722 [nucl-th] .

[89] J. Ballot and M. Fabre de la Ripelle, Annals of Physics **127**, 62 (1980).

[90] F. T. Smith, Phys. Rev. **120**, 1058 (1960).

[91] M. Campostrini, K. Moriarty, and C. Rebbi, Phys. Rev. D **36**, 3450 (1987).

[92] I. S. Gradshteyn and I. M. Ryzhik, *Table of integrals, series, and products*, seventh ed. (2007).